

CONTRACT NAS 9-12387
DRL NO. T-750
LINE ITEM NO. 2
DRD NO. MA-129T
FILE NO. 71-228 NAS

EVALUATION OF LAMINATED ALUMINUM PLATE
FOR SHUTTLE APPLICATIONS

FINAL REPORT
8 MARCH 1973

PREPARED FOR
NATIONAL AERONAUTICS AND SPACE ADMINISTRATION
MANNED SPACECRAFT CENTER
HOUSTON, TEXAS 77058

Details of illustrations in
this document may be better
studied on microfiche

PREPARED BY


M. J. MARTIN
STUDY MANAGER

APPROVED BY


W. LUDWIG
SHUTTLE RESEARCH & TECHNOLOGY MANAGER

GRUMMAN AEROSPACE CORPORATION
BETHPAGE, NEW YORK 11714

DISTRIBUTION LIST

- | | | |
|----|--|------------------|
| 1. | NASA Manned Spacecraft Center
Research & Technology Procurement Branch
Attn: Ted Lapko, Mail Code BC 731 (33)
Houston, TX 77058 | One copy |
| 2. | NASA Manned Spacecraft Center
Technical Library Branch
Attn: Retha Shirkey, Mail Code JM 6
Houston, TX 77058 | Four copies |
| 3. | NASA Manned Spacecraft Center
Management Services Divison
Attn: John T. Wheeler, Mail Code JM 7
Houston, TX 77058 | One copy |
| 4. | NASA Manned Spacecraft Center
SMD - Materials Technology
Attn: R. E. Johnson, Mail Code ES 5
Houston, TX 77058 | Seventeen copies |

ABSTRACT

Flaw growth behavior in roll diffusion bonded and adhesive bonded 2219-T87 aluminum alloy was compared to that in monolithic 2219-T87. Based on tests at 40 KSI cyclic stress, for equivalent cyclic life, an .004 interlayer laminate can tolerate a surface flaw twice as wide as in monolithic material, or provide an 8% weight saving by operating at higher stress for the same initial flaw.

Roll diffusion bonded material with three structural plies of 2219-T87 and two interlayers of 1100 aluminum was prepared with interlayer thicknesses of .004, .007 and .010 in. Total laminate thickness was .130 in. The .004 interlayer laminate was most effective and gave better results than monolithic material at 40 and 48 KSI. Flaws in roll diffusion bonded material grow to become through-the-thickness flaws.

Adhesive bonded specimens were fabricated of three sheets of 2219-T87 aluminum alloy bonded with METLBOND 329 adhesive. Adhesive bonded specimens gave longer lives to failure than diffusion bonded specimens at 40 KSI but at 48 KSI the diffusion bonded material was superior. Flaws initiated in one ply of the laminate grew to the edges of the specimen in that ply but did not propagate into adjacent plies.

CONTENTS

Section	Page
1 INTRODUCTION	1-1
2 PROGRAM PLAN	2-1
3 MATERIALS FABRICATION	3-1
Roll Diffusion Bonding	3-1
Adhesive Bonding	3-1
4 MATERIALS EVALUATION	4-1
Specimen Fabrication	4-1
Material Properties Determination	4-4
Phase I Testing	4-4
Phase II Testing	4-10
Phase III Testing	4-12
Adhesive Bonded Specimens	4-20
Summary	4-20
Nondestructive Tests	4-23
Shear Wave Ultrasonics	4-23
Surface Wave Ultrasonics	4-23
Conventional Eddy Currents	4-25
Deep-Penetration Eddy Current	4-25
Visual Observations	4-30
Summary	4-30
Fabricability	4-32
Weight Comparison of Shuttle Orbiter Tanks	4-32
Fabrication of Large Adhesive Bonded Tanks	4-49
Bonding Pre-Treatment Investigation	4-54
Welding of Laminated Plate	4-64
Forming of Laminated Plate	4-71
Weight/Reliability Analysis	4-74
Reliability Comparison	4-74
Weight Comparison	4-74
5 CONCLUSIONS AND RECOMMENDATIONS	5-1
6 BIBLIOGRAPHY	6-1

CONTENTS (Continued)

Appendixes		Page
A	Flaw Growth Rate Tables	A-1
B	Curves of Specimen Surface Flaw Width Versus Cycles	B-1

ILLUSTRATIONS

Figure		Page
3-1	Defects Found by Ultrasonics - Location of Defects (Approximate Dimensions)	3-2/3
3-2	Defects Found by Ultrasonics - Contaminant at Interlayer	3-4/5
3-3	Defects Found by Ultrasonics - Interlayer Delamination	3-4/5
3-4	Coordinates for Thickness Measurements	3-9
3-5	Voids Indications on First 2219-T87 Adhesive Bonded Laminated Panel	3-11
3-6	Location of Thickness Measurements on Chem-Milled 2219-T87 Sheet for Second 2219 Adhesive Bonded Panel	3-15
3-7	Ultrasonic Resonance Test Results, Second 2219-T87 Adhesive Bonded Panel	3-17
4-1	Specimen Design	4-2
4-2	Dimensions of Semi-Circular "Elox" Starter Flaw	4-2
4-3	Small Specimen - 1/2 Thickness Flaw-Depth Test	4-3
4-4	Flaw Width Measurement Setup - Binocular Instrument	4-5
4-5	Flaw Width Measurement Setup - "Telescope" Instrument	4-5
4-6	Partial Phase I Specimens; Envelopes of Flaw Growth Curves, Surface Crack Length vs Cycles to Breakthrough.	4-9
4-7	Envelopes of Flaw Growth Curves, Surface Crack Length vs. Cycles	4-9
4-8	Fracture Surface of Specimen No. 353492-1A	4-13
4-9	Fracture Surface of Specimen No. 353492-2A	4-13
4-10	Surface Flaw Width vs Flaw Depth for Small Specimen	4-15
4-11	Fracture Surface of Specimen No. 353492-8A - Elox Notch at Center of Upper Edge	4-18
4-12	Fracture Surface of Specimen No. 353492-8A - Nine Times Magnification Under White Light	4-18

ILLUSTRATIONS (Continued)

Figure		Page
4-13	Fracture Surface of Specimen No. 353492-8A - Nine Times Magnification Under Ultraviolet Light	4-19
4-14	Fracture Surface of Specimen No. 353492-10A - Elox Notch at Center of Upper Edge	4-19
4-15	Ultrasonic Indication vs Surface Crack Length; Shear Wave Technique	4-24
4-16	"Leakage" Detector Unit	4-27
4-17	Eddy Current Probe Assembly	4-28
4-18	Vacuum Leak Detector Unit	4-29
4-19	MRA Probe	4-29
4-20	C2 Orbiter Integral Tank Configuration - Structural Arrangement	4-33
4-21	Orbiter Design C2F, Min-Max Limit Design Pressures (ΔP) . .	4-35
4-22	Orbiter Design C2F, Limit Load-Intensity Envelope at Top of Tank	4-36
4-23	Orbiter Design C2F Limit Load-Intensity Envelope at Bottom of Tank	4-37
4-24	Orbiter Design C2F, Limit Load-Intensity Envelope at Tank Center	4-38
4-25	Orbiter Design C2F, Limit Shear-Intensity Envelope at Tank Center	4-39
4-26	Orbiter Design C2F, Ultimate Load-Intensity Envelope at Top of Tank	4-40
4-27	Orbiter Design C2F, Ultimate Load-Intensity Envelope at Bottom of Tank	4-41
4-28	Orbiter Design C2F, Ultimate Load-Intensity Envelope at Tank Center	4-42
4-29	Orbiter Design C2F, Ultimate Shear-Intensity Envelope at Tank Center	4-43
4-30	C2F Orbiter Monolithic Liquid Oxygen Tank	4-44
4-31	C2F Monolithic LH ₂ Tank	4-45
4-32	C2F Laminated Liquid Oxygen Tank	4-46
4-33	C2F Laminated LH ₂ Tank	4-47
4-34	Proposed Splices, Adhesive Bonded Laminated Tanks	4-50
4-35	Splice Concepts	4-51
4-36	Laminating Methods	4-52

ILLUSTRATIONS (Continued)

Figure		Page
4-37	Laminating Methods	4-53
4-38	Assembly Procedures	4-55
4-39	Assembly Procedures	4-56
4-40	Weld in 0.008 In. Interlayer Laminated Aluminum Plate (20X Magnification)	4-70
4-41	Photomicrograph (200X Magnification) Showing Fusion Line of Weld in 0.008 In. Interlayer Laminated Aluminum Plate	4-70
4-42	Three by Three Foot Adhesive Bonded Panel Formed to 50 In. Radius.	4-72
4-43	One-Inch Wide Adhesive Bonded Strip Formed to Eight-Inch Radius	4-72
4-44	Photomicrographs of Longitudinal and Transverse Specimens . .	4-73

TABLES

No.		Page
2-1	Test Matrix for Laminated Aluminum Composites	2-2
3-1	Ultrasonic Technique for Inspection of As-Received Laminated Plate	3-2/3
3-2	Thickness of Individual Elements of Roll Diffusion Bonded Laminated Plates	3-6
3-3	Material Properties, Tension, As-Received and Chem-Milled 2219-T87 Sheet	3-7
3-4	Sheet Thickness After Chem-Milling, Adhesive Bonded Specimens	3-10
3-5	Material Properties, Tension, As Received and Chem-Milled 2219-T87 Sheet After Exposure to Metlbond 329 Curing Cycle . .	3-12
3-6	Material Properties, Tension, 2219-T87 Aluminum Sheet, As-Received and After Chem-Milling and Exposure to Metlbond 329 Curing Cycle	3-13
3-7	Thickness Measurements of Chem Milled 2219-T87 Sheet for Second Adhesive Bonded Test Panel	3-16
3-8	Bondline Thickness Measurements, Adhesive Bonded Specimens .	3-18
4-1	Phase I Flaw Growth Test Results Summary	4-7
4-2	Summary of Phase I Test Results, Cycles begin with .090 In. Surface Flaw Width	4-8

TABLES (Continued)

No.		Page
4-3	Phase I Specimens, Comparison of Cycles to Breakthrough . . .	4-11
4-4	Approximate Flaw Depths for Laminated Specimens	4-14
4-5	Phase II Specimens, 1/2 t Flaws, 40 KSI	4-16
4-6	Phase III Testing, 1/3 t Flaws, 48 KSI	4-17
4-7	Phase III Testing, 1/2 t Flaws, 48 KSI	4-21/22
4-8	Adhesive Bonded Specimens	4-21/22
4-9	Detection Points During Cyclic Flaw Growth, Cycles	4-26
4-10	MRA Results	4-31
4-11	Weight Comparison, Monolithic and Laminated Design Concepts .	4-48
4-12	Room Temperature Lap Shear Test Results, Bonding Pre-Treatment Investigation	4-58
4-13	Lap Shear Test Results, Four Days Aging at 350 ^o F and 30-Day Exposure to 98% Relative Humidity, Bonding Pre-Treatment Investigation	4-59
4-14	Lap Shear Test Results, 30-Day Exposure to 98% Relative Humidity, Bonding Pre-Treatment Investigation	4-60
4-15	Lap Shear Test Results, 30-Day Salt Spray Exposure, Bonding Pre-Treatment Investigation	4-61
4-16	Lap Shear Test Results, Two Weeks Aging at 350 ^o F, Bonding Pre-Treatment Investigation	4-62
4-17	Lap Shear Test Results Summary, Bonding Pre-Treatment Investigation	4-63
4-18	Tensile Test Results, Butt Weld in .004 Interlayer Laminated 2219-T87 Aluminum Plate, 2319 Filler Wire	4-65
4-19	Tensile Test Results, Butt Weld in .008 Laminated 2219-T87 Plate, 2319 Filler Wire	4-66
4-20	Tensile Test Results, Butt Weld in .012 Interlayer Laminated 2219-T87 Aluminum Plate, 2319 Filler Wire	4-67
4-21	Tensile Test Results, Diffusion Bonded Laminated 2219-T87 Aluminum Plate	4-68
4-22	Tensile Test Data Summary, Welded and Unwelded 2219-T87 Diffusion Bonded Laminated Plate, Butt Welded, 2319 Filler Wire .	4-69
4-23	Flaw Size Calculations for Equivalent Life to Breakthrough . . .	4-75
4-24	Flaw Width Ratios	4-76
4-25	Specimen Comparison, Phases I and III	4-78
4-26	Weight Comparison, of Monolithic and Roll Diffusion Bonded Laminate	4-79

SUMMARY

A prime consideration in the design of tankage for space vehicles is the requirement to prevent leakage or failure during the tank service life. Previous work has established that soft interlayers tend to blunt crack fronts and thus lower cyclic flaw growth rates.

In this program, roll-diffusion bonded laminated material and adhesive bonded laminated material both showed superior performance in cyclic life as compared to monolithic high-strength aluminum alloy material. The two laminates behaved differently in the presence of flaws. A flaw initiated in one layer of a diffusion bonded specimen grew to become a through-the-thickness flaw, while in the adhesive bonded material, the flaw grew in depth only to the thickness of the layer in which it was initiated and then grew to the edges of the test specimen.

The application to design of these two materials would require very different methods of fabrication. Designs and manufacturing procedures for adhesive bonded tanks were investigated. The feasibility of welding diffusion bonded material was demonstrated, welded specimens having strengths approaching the typical weld strength of monolithic material.

For equivalent cyclic life to leakage, a roll diffusion bonded laminated specimen can tolerate a surface flaw approximately twice as long as in a monolithic specimen. Again for equivalent cyclic life, starting with the same initial flaw, due to the higher stress that the roll diffusion laminate can tolerate, a weight saving of 8% over a monolithic tank is preliminarily estimated.

The first steps toward a quantitative assessment of the relative merits of laminated and monolithic structural systems have been accomplished. Further work along lines indicated by the results of this program is recommended.

Section 1

INTRODUCTION

This final report was prepared by Grumman Aerospace Corporation for NASA-MSC Contract NAS 9-12387, Evaluation of Laminated Aluminum Plate for Shuttle Applications. The report covers the period 8 February 1972 to 8 March 1973. Mr. R. E. Johnson is the NASA Technical Monitor.

The requirement for safe life for tankage for space vehicles, coupled with the need for minimizing structural weight, presents a formidable problem to the spacecraft designer. Inspection and test procedures designed to detect flaws larger than a specified minimum size, in combination with fracture mechanics analytical techniques to predict flaw growth based on the service environment, are the tools he uses to optimize tanks fabricated of monolithic materials. With the aid of data accumulated in many previous tankage test programs, the designer may specify tank life with reasonable accuracy.

One method of reducing tank weight would be to find a material that has similar strength-to-weight properties and the same resistance to service environments as the monolithic material we might consider, but one that would provide a lower cyclic flaw growth rate. The present study, which is in support of Manned Spacecraft Center's fracture control efforts, investigates the effects on flaw growth rates of soft aluminum and adhesive interlayers in laminated aluminum material.

It will be attempted to provide a quantitative comparison between flaw growth rates in monolithic and laminated materials. The interlayers may slow flaw growth rate but add enough structural weight to offset the advantage in cyclic life. A weight comparison of monolithic and laminated tanks designed for the same cyclic life will illustrate a weight advantage for either system.

Fabrication and inspection of roll diffusion bonded tanks are assumed to be similar to monolithic tanks. Bonded construction requires additional weight in splices and attachments but offers structural redundancy. Inspection techniques for bonded construction are quite different from those used for monolithic tanks and are considered to be more complex. Fabrication methods for the two different types of construction will be studied. Inspection procedures that might be applied will be used during the testing phase of this program. Shear wave and surface wave ultrasonics and eddy current devices will be tried on the laminated specimens.

The contributions of the following personnel are gratefully acknowledged: B. Aleck and T. Taglarine (Advanced Development), H. Pallmeyer and S. Leinoff (Design), P. Donohue, J. Mahon, R. Micich and O. Paul (Materials and Processes), R. Chance and E. Mastik (Quality Control) and F. Hettinger (Structural Mechanics).

Section 2

PROGRAM PLAN

The activities of this program are divided into two main tasks: Materials Fabrication and Materials Evaluation. Subtasks under these headings define the work in greater detail.

MATERIALS FABRICATION

Monolithic material, roll diffusion bonded material and adhesive bonded material will be tested in this program. The roll diffusion bonded and adhesive bonded materials are specially prepared for this program.

Roll Diffusion Bonding

Roll diffusion bonded material will consist of three structural plies of 2219-T87 aluminum alloy and two interlayers of 1100 aluminum. Three interlayer thicknesses, .004 in., .008 in., and .012 in. will be supplied for this program. The roll diffusion bonded material is supplied by ALCOA in the form of .130 in. thick, 13 in. by 62 in. plates.

Adhesive Bonding

An adhesive bonded panel is to be fabricated at Grumman. Three .040 in. thick 2219-T87 sheets will be bonded using METLBOND 329 adhesive. This panel will be large enough to provide the number of specimens required for this program, approximately 3 ft. by 3 ft.

MATERIALS EVALUATION

The two laminated materials specified for this program will be evaluated to assess their applicability to space vehicle tankage. Their behavior at moderately high stresses in the presence of flaws will be determined experimentally. Fabricability studies will be mostly analytical, while weight and reliability studies will use data generated in the program tests.

Specimen Fabrication

A standard specimen configuration is to be used with both monolithic and laminated materials. This specimen is designed to minimize edge effects in the program data. Program specimens will be machined from the monolithic, roll diffusion bonded and adhesive bonded plates. Initial flaws will be produced by the ELOX process.

Material Properties Determination

Roll diffusion bonded laminated material will be compared with monolithic material in a three-phase test program. Phase I will compare three different interlayer thickness laminates with monolithic material at a cyclic stress of 40 KSI and with initial flaws one-third of the thickness deep. The best performing laminate will be selected for further testing in Phases II and III in which one-half thickness cracks and cyclic stress levels of 48 KSI will also be studied. Adhesive bonded specimens will be tested with one-third thickness cracks at stress levels of 40 and 48 KSI. Table 2-1 lists the specimen quantity and conditions for each group of test specimens. Flaw growth will be measured throughout the life of the specimen. Growth of a flaw to a through-the-thickness crack will be noted.

TABLE 2-1 TEST MATRIX FOR LAMINATED ALUMINUM COMPOSITES

Test Phase	Interlayer Thickness, In.	Number of Spec.	Precrack Flaw Depth	Cyclic Stress	Data Required
<u>Diffusion Bonded</u>					
I	0.004	6	1/3 thickness ⁽¹⁾	0-40 ksi	Flaw growth rate and cycles-to-leak
	0.008	6	1/3 thickness	0-40 ksi	
	0.012	6	1/3 thickness	0-40 ksi	
	None	6	1/3 thickness	0-40 ksi	
II	To be determined from I	6	1/2 thickness	0-40 ksi	Same
	None	6	1/2 thickness	0-40 ksi	
III	Same as II	3	1/3 thickness	0-48	Same
	Same as II	3	1/2 thickness	0-48	
	None	3	1/3 thickness	0-48	
	None	3	1/2 thickness	0-48	
<u>Adhesive Bond</u>					
	3 plys				
	.040" thick	3	1/3 thickness ⁽²⁾	0-40 ksi	Same
	each	3	1/3 thickness	0-48 ksi	

(1) Total specimen thickness = 0.130" for diffusion bonded specimens. Flaw depth shown is that obtained after sharpening of "elox" flaw. All specimens will have semi-circular shaped flaws.

(2) Total specimen thickness to be measured after bonding.

Nondestructive Tests

Various methods of flaw detection will be evaluated during the flaw growth testing of the specimens. Surface wave ultrasonics, shear wave ultrasonics, and eddy current techniques will be used on the monolithic and laminated specimens. Attempts will be made to provide a quantitative measurement of flaw depth.

Fabricability

The methods of fabricating tanks for space vehicles from laminated material will be studied in this subtask. Analytical efforts will be supported by pre-treatment evaluation of bonding methods, weld strength tests of diffusion bonded material, and formability investigations of adhesive bonded and diffusion bonded material. Weight calculations of proposed space vehicle tanks are presented for monolithic and laminated designs.

Weight/Reliability Analysis

Data collected in this program will attempt to confirm a longer cyclic life for laminated material compared to monolithic material. If this is true then the laminated material could tolerate a larger initial flaw than monolithic material for the same cyclic life or for the same flaw size, operate at a higher cyclic stress. Estimates of the larger flaw size (reliability) or higher stress level (weight) benefits will be made.

Section 3

MATERIALS FABRICATION

ROLL DIFFUSION BONDING

Roll diffusion bonded aluminum plate for this program was fabricated by the Aluminum Company of America (ALCOA). Nominal interlayer thicknesses of .004 in., .008 in., and .012 in. were requested. Structural plies were of 2219-T87 material and the interlayers of 1100 aluminum.

Ultrasonic inspection, using an immersion technique described in Table 3-1, was performed on the laminated material. Local defects were indicated in two areas of one plate of the .004 interlayer material (Figure 3-1). The defects were sectioned and examined metallurgically. Figure 3-2 shows a contaminant at an interface between the 1100 and 2219-T87 plies. Figure 3-3 shows a delamination at an interface between the 1100 and 2219-T87 plies. After examination at Grumman, the sectioned defects were sent to ALCOA for their study. ALCOA's reply stated: "... the results of our metallographic examination indicate that the discontinuities at the faying surfaces were the result of highly worked metal oxides from the scratch brushing operation used prior to rolling. These oxide stringers can be more readily identified in the unetched condition. It is entirely possible that these unbonded regions would be detected ultrasonically. "

No defects were discovered in the .008 in. or .012 in. interlayer plates. In fabricating specimens from the .004 in. interlayer material, areas of ultrasonic indication were avoided.

Four 13 in. by 62 in. plates of each nominal interlayer thickness laminate were received. The thicknesses of each individual element of each plate were measured and recorded. Table 3-2 shows the results of these measurements. All plates had an overall thickness of .130 in. This means that additional interlayer thickness was obtained at the cost of structural material. The desired nominal interlayer thicknesses were .004, .008 and .012 in. As can be seen from Table 3-2, the actual interlayer thicknesses produced were .004, .007 and .010 in. For convenience, in this report, the interlayers will be referred to by their nominal designations.

ADHESIVE BONDING

Adhesive bonded panels required in this program were to be three layers of .040 in. 2219-T87 aluminum bonded with METLBOND 329 adhesive. Panel size was to be 3 ft by 3 ft.

Early in the program difficulty was encountered in obtaining .040 in. 2219-T87 sheet. A stock of .050 in. 2219-T87 was located and the decision to chem-mill this material to .040 in. thickness was made after discussion with Materials and Processes personnel failed to indicate any objectionable factors in bonding or fatigue life due to the chem-milling.

To establish that there were no detrimental effects on the 2219-T87 sheet stock due to chem-milling, tensile specimens were prepared from the as received and the chem-milled sheet. No degradation of the properties, as shown in Table 3-3, was noted.

TABLE 3-1 ULTRASONIC TECHNIQUE FOR INSPECTION OF AS-RECEIVED LAMINATED PLATE

A. Transducer

Short focus type with focal point set for the center of the laminated plate; frequency is 15 Hz.

B. Gain Settings (in terms of the % loss of the average return signal from reflector plate)

Scan 1 (low gain): 50% loss of back reflection

Scan 2 (high gain): 75% loss of back reflection

C. Water Travel = 2.23 in.

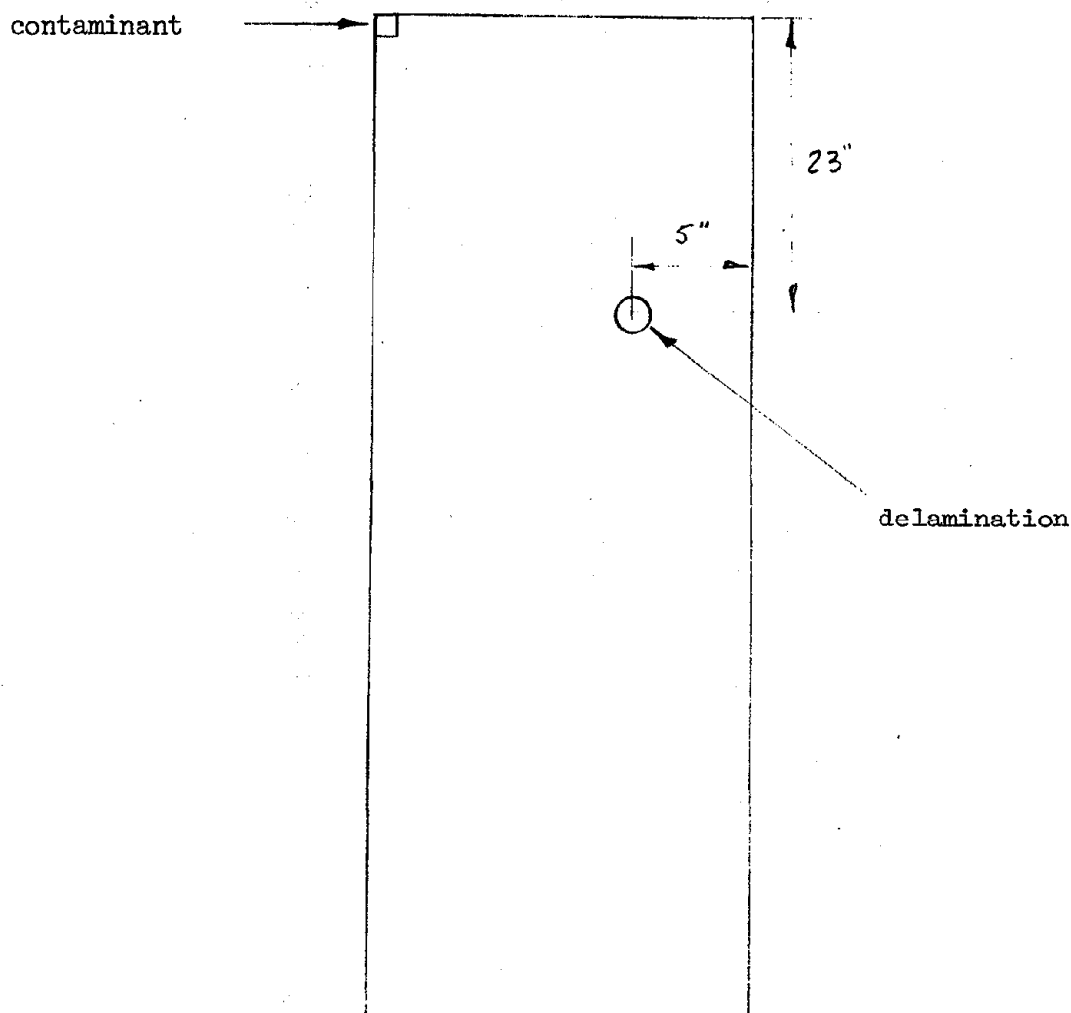
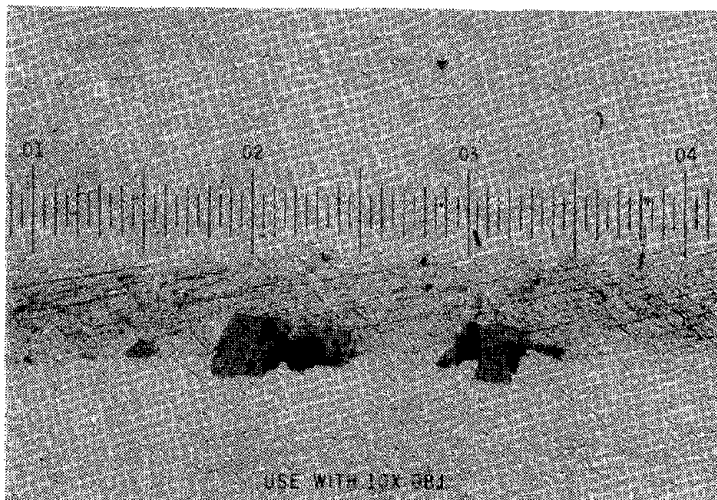
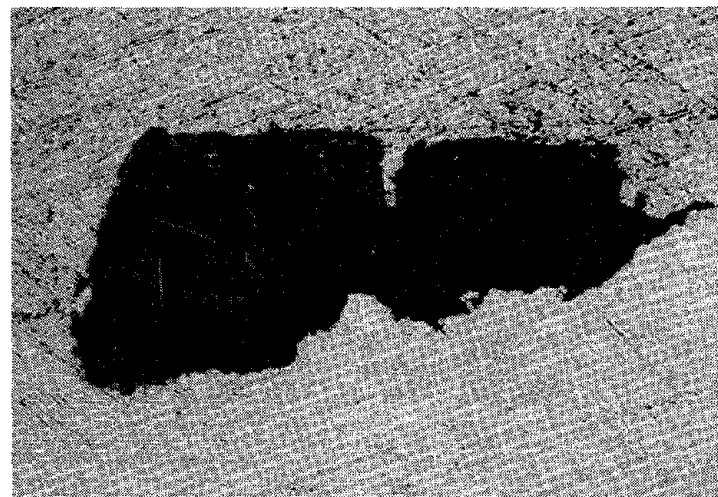


Figure 3-1 Defects Found by Ultrasonics - Location of Defects (Approximate Dimensions)

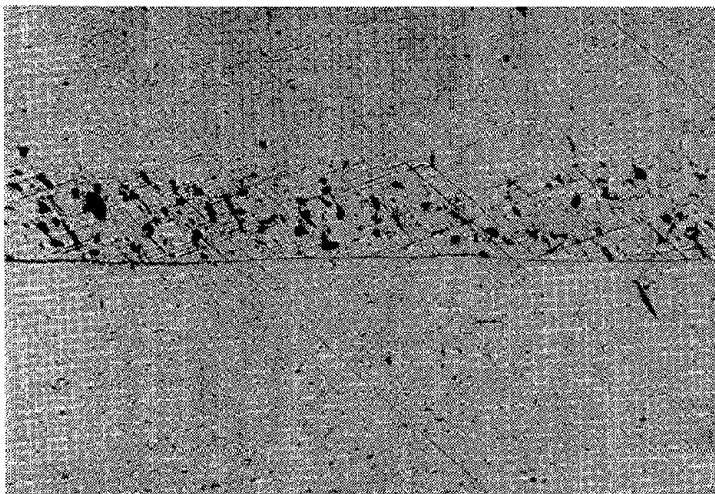


100X Magnification

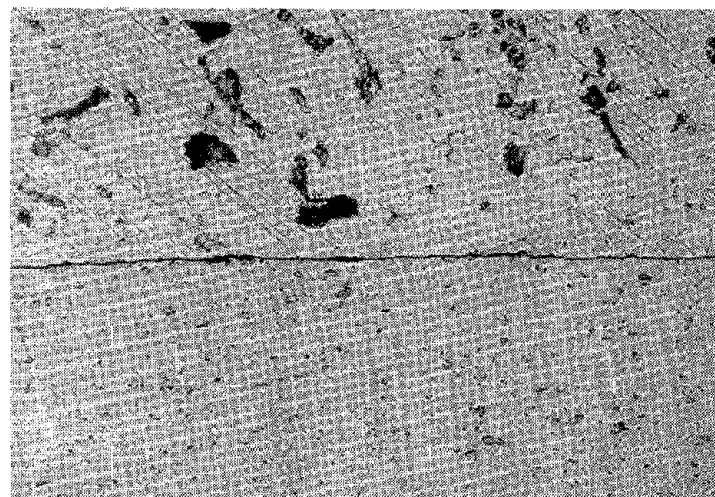


400X Magnification

Figure 3-2 Defects Found by Ultrasonics - Contaminant at Interlayer



100X Magnification

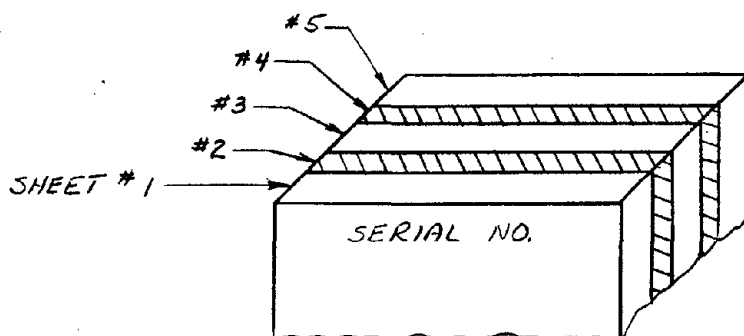


400X Magnification

Figure 3-3 Defects Found by Ultrasonics - Interlayer Delamination

Reproduced from
best available copy.

TABLE 3-2 THICKNESSES OF INDIVIDUAL ELEMENTS OF ROLL
DIFFUSION BONDED LAMINATED PLATES



THICKNESSES MEASURED AT ONE CORNER

(LAMINATED PLATE #)

	353492-1	-2	-3	-4	Diagonally Opposite Corner -1
Sheet #1	.040	.043	.041	.041	.040
#2	.004	.004	.0035	.004	.004
#3	.042	.041	.042	.042	.042
#4	.004	.004	.004	.004	.004
#5	.040	.038	.041	.040	.039
	353493-1	-2	-3	-4	Diagonally Opposite Corner -1
Sheet #1	.038	.041	.040	.039	.039
#2	.007	.007	.007	.007	.007
#3	.037	.036	.037	.036	.036
#4	.008	.007	.007	.007	.007
#5	.039	.040	.039	.038	.038
	353494-1	-2	-3	-4	Diagonally Opposite Corner -1
Sheet #1	.035	.036	.038	.038	.037
#2	.009	.010	.010	.010	.010
#3	.037	.037	.037	.036	.036
#4	.010	.009	.010	.010	.010
#5	.037	.037	.036	.035	.036

TABLE 3-3 MATERIAL PROPERTIES, TENSION, AS-RECEIVED
AND CHEM-MILLED 2219-T87 SHEET

	AS-RECEIVED		CHEM-MILLED		
Specimen Number	AR-2	AR-4	CM-2	CM-3	CM-4
Grain Direction	L	L	L	L	L
Test Section	.051 x .494	.051 x .497	.044 x .493	.044 x .492	.044 x .494
Initial Gage Length	2	2	2	2	2
Test Temperature	RT	RT	RT	RT	RT
Strain Rate to Yield (in/in/min)	.005	.005	.005	.005	.005
Ultimate Load, lb	1725	1735	1465	1480	1470
Yield Load, 0.2% Off-Set	1350	1350	1175	1183	1170
Gage Length After Failure	2.20	2.19	2.19	2.19	2.19
Initial Specimen Area	.0252	.0253	.0217	.0216	.0217
Ultimate Stress, psi	68,450	68,580	67,510	68,520	67,740
Yield Stress, psi	53,570	53,360	54,150	54,770	53,920
% Elongation	10.0	9.5	9.5	9.5	9.5
E x 10 ⁶ psi	10.32	10.38	10.36	10.41	10.78

After the .050 in. panels were chem-milled, thickness measurements were taken across each of the panels. Locations at which thickness measurements were taken are shown in Figure 3-4. Thicknesses of each of the three chem-milled sheets are shown in Table 3-4.

The initial attempt to produce a 4 ft by 3 ft adhesive bonded panel was unsuccessful. Using the chem-milled 2219-T87 sheet described previously, a three-ply layup was fabricated according to Grumman manufacturing procedures applicable to METLBOND 329 adhesive. After curing, the panel was inspected ultrasonically by a Reflectoscope (pulse-echo instrument) and large areas of delamination were indicated. (See Figure 3-5.) Areas of defective bond were then examined by a Fokker "Bondtester" and again "poor bond" or "no bond" was indicated. The panel was then sectioned and the delamination indications were confirmed. Since the areas of poor bond indications from the Fokker "Bondtester" covered approximately 30% of the panel, provisions were made for bonding a second 2219-T87 panel.

Sheet material in the as-received condition and the chem-milled condition was exposed to the bonding cycle of the METLBOND 329 adhesive to determine the effect of the bonding cycle on material properties. Results of tension tests on the as-received and chem-milled sheet, shown in Table 3-5, indicate a reduction in "% elongation" in the chem-milled specimens as the only significant difference in properties.

Table 3-6 includes the average material properties of the as-received sheet, chem-milled sheet and both sheets exposed to the bonding cycle of the METLBOND 329 adhesive. Again, a reduction in "% elongation" of the chem-milled-and-bonded specimens from 9.5 to 7.5 is the most significant change. All other changes are on the order of 2%.

Before proceeding with a second 2219-T87 panel, a bonded panel using .040 in. thick 2024-T3 sheet was fabricated to verify the bonding procedure used. The finished three layer 4 ft by 3 1/2 ft panel was nondestructively tested using both ultrasonic resonance and pulse echo methods, and no voids were indicated. An important difference in the manufacture was the placing of a 0.250 in. thick aluminum plate on top of the panel layup before vacuum bagging. On the first attempt to bond a 4 ft by 3 1/2 ft panel, it seemed that the edges of the panel sealed before all the air trapped at irregularities at the center of the panel could escape. Placing the plate on top of the layup assures that the autoclave pressure will be uniformly distributed across the surface of the bonded panel.

The following procedure was used:

1. The aluminum sheet was cleaned per Grumman standard GSS-7022, in which a sulfuric acid/sodium dichromate solution is specified.
2. No primer was applied.
3. The film adhesive was cut and put in place.
4. The panel layup was bagged to the autoclave table, the bag seal was vacuum checked and then the table was transferred into the autoclave.
5. A vacuum of 20 in. of Hg minimum was drawn on the part.
6. The autoclave was pressurized to 45 psi using CO₂ and then the bag vacuum was reduced to atmospheric pressure.
7. Heat to 330°-350°F was applied in 45-60 minutes.

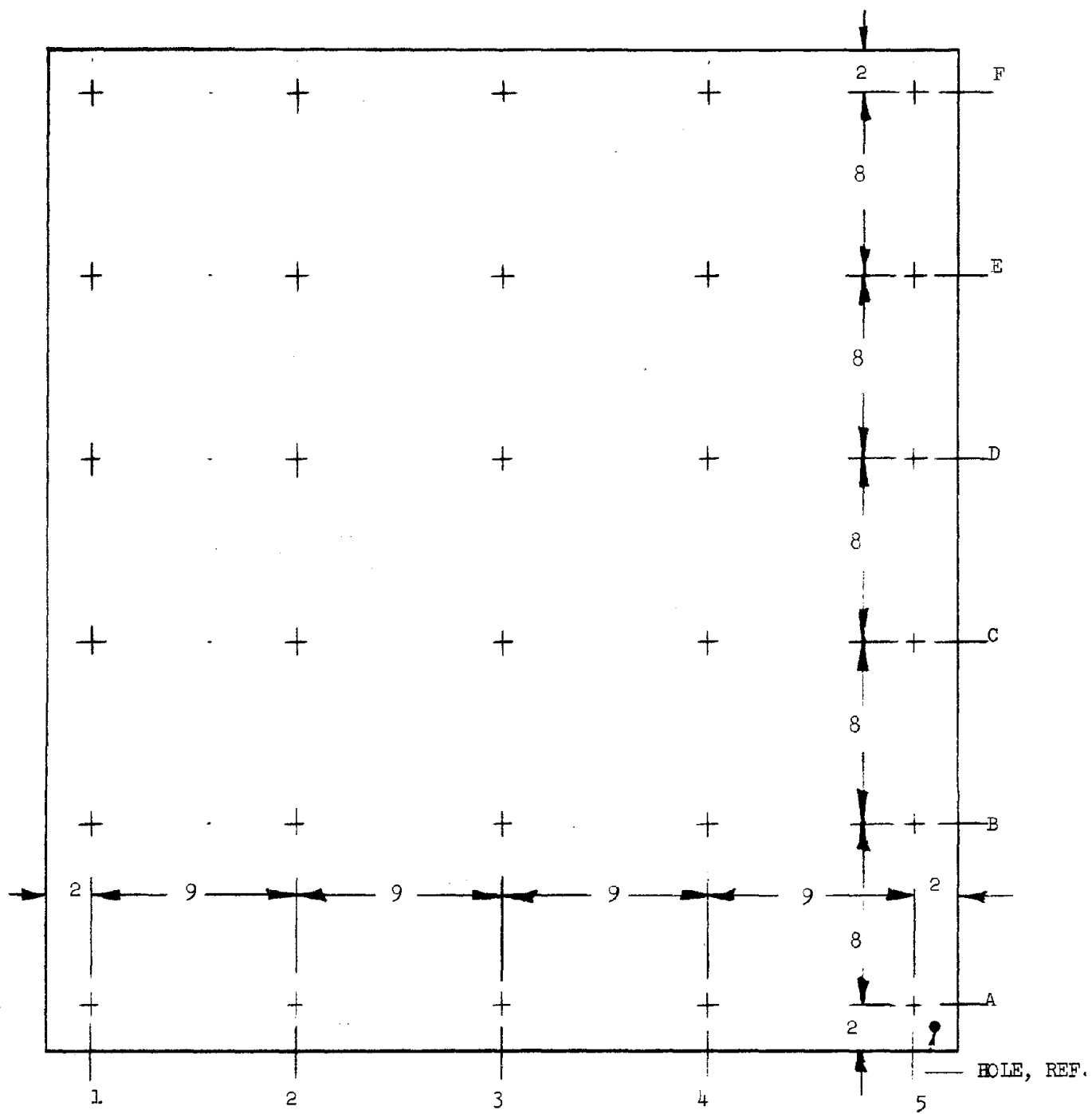


Figure 3-4 Coordinates for Thickness Measurements

TABLE 3-4 SHEET THICKNESS AFTER CHEM-MILLING, ADHESIVE BONDED SPECIMENS

Sheet Thickness, in.							
Sheet No.	COORDINATES*						
		A	B	C	D	E	F
1	1	.0430	.0434	.0435	.0438	.0436	.0434
	2	.0428	.0432	.0434	.0436	.0435	.0434
	3	.0425	.0428	.0430	.0434	.0433	.0431
	4	.0426	.0430	.0432	.0435	.0435	.0433
	5	.0427	.0430	.0432	.0435	.0434	.0433
2	1	.0427	.0432	.0432	.0434	.0433	.0430
	2	.0429	.0432	.0433	.0435	.0433	.0431
	3	.0430	.0433	.0434	.0435	.0434	.0432
	4	.0431	.0434	.0436	.0438	.0436	.0433
	5	.0432	.0435	.0437	.0439	.0437	.0435
3	1	.0431	.0434	.0436	.0438	.0436	.0433
	2	.0429	.0432	.0434	.0436	.0434	.0432
	3	.0429	.0433	.0434	.0435	.0434	.0432
	4	.0429	.0433	.0435	.0436	.0435	.0433
	5	.0430	.0434	.0436	.0438	.0437	.0434
*Layout of coordinates for thickness measurements is shown in Figure 3-4							

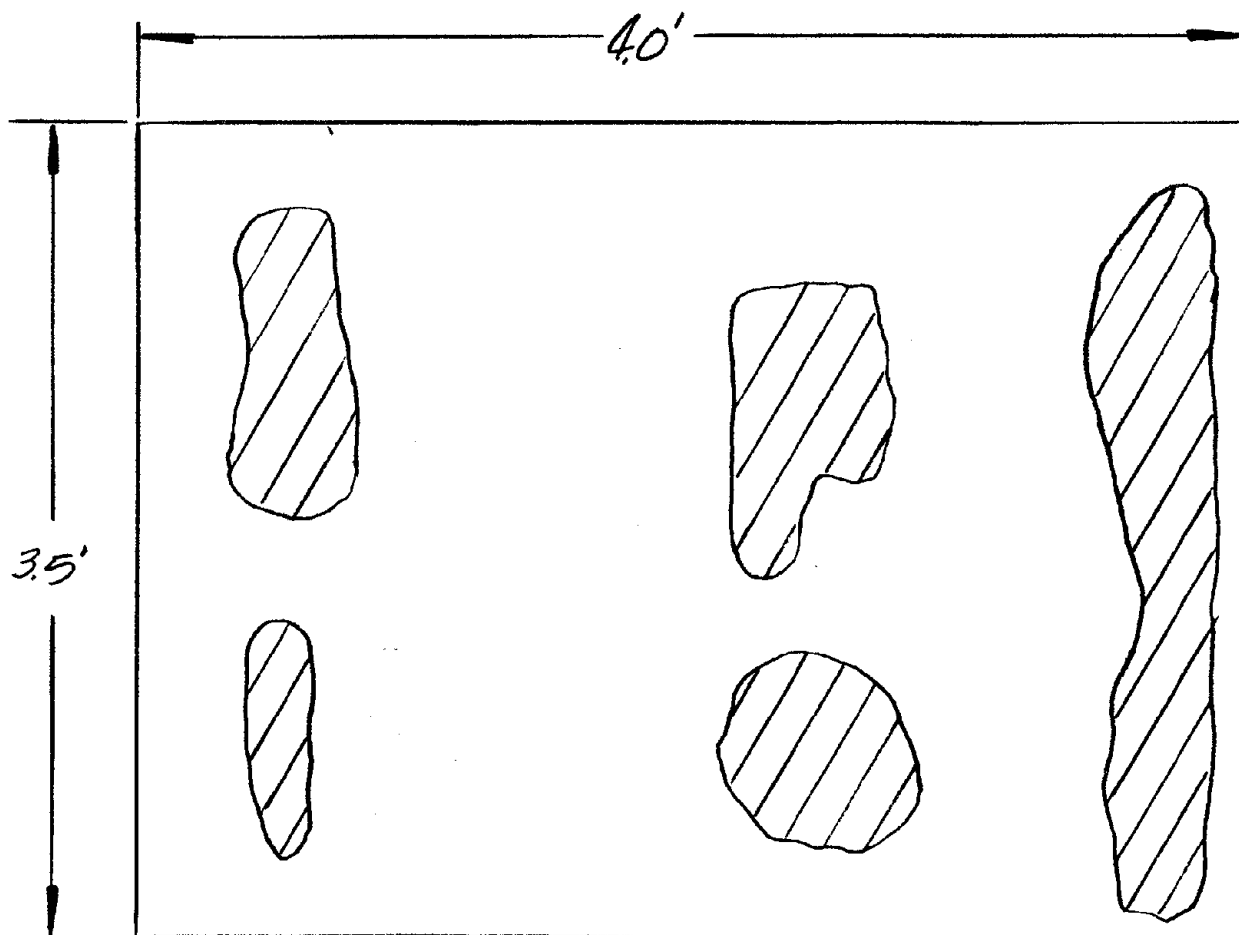


Figure 3-5 Void Indications on First 2219-T87 Adhesive Bonded Laminated Panel

TABLE 3-5 MATERIAL PROPERTIES, TENSION, AS-RECEIVED AND
CHEM-MILLED 2219-T87 SHEET AFTER EXPOSURE TO
METLBOND 329 CURING CYCLE

	As- Received	Chem-milled		
Specimen Number	AR*	CM-1*	CM-2*	CM-3*
Test Section	.0505 x .506	.0438 x .501	.0438 x .503	.0439 x .498
Initial Gage Length	2.00	2.00	2.00	2.00
Test Temperature	RT	RT	RT	RT
Ultimate Load, lb.	1735	1500	1510	1492
Yield Load, 0.2% Off-Set, lb.	1409	1212	1221	1208
Gage Length after Failure	2.19	2.15	2.15	2.15
Initial Specimen Area	.0256	.0219	.0220	.0218
Ultimate Stress, psi	67,800	68,500	68,600	68,400
Yield Stress, psi	55,000	55,300	55,500	55,400
% Elongation	9.5	7.5	7.5	7.5
E (x 10 ⁶ psi)	10.5	10.7	10.6	10.4

TABLE 3-6 MATERIAL PROPERTIES, TENSION, 2219-T87 ALUMINUM SHEET, AS-RECEIVED AND AFTER CHEM-MILLING AND EXPOSURE TO METLBOND 329 CURING CYCLE

	AVERAGE VALUES			
	As Received	Chem-Milled	As-Received Exp. Bond Cyc.	Chem-Milled Exp. Bond Cyc.
No. of Specimens	2	3	1	3
Test Temperature	RT	RT	RT	RT
Ult. Stress, psi	68,500	67,900	67,800	68,500
Yield Stress, psi	53,500	54,300	55,000	55,400
% Elongation	9.75	9.5	9.5	7.5
E ($\times 10^6$) psi	10.35	10.52	10.5	10.6

8. The heat was held at 340°-360°F for 60 ± 10 minutes. Cooled to 140°-150°F in not less than 60 minutes, maintaining 45 psi pressure on the part.

9. Removed from autoclave and allowed to cool.

Additional .050 in. thick 2219-T87 sheet was chem-milled to a nominal .040 in. thickness for fabrication of the test panel. Sheet thicknesses were measured across the three structural sheets as before. Figure 3-6 shows the locations of points chosen for thickness measurements. Table 3-7 lists the individual thickness measurements recorded. Average sheet thickness was approximately .043 in.

Cleaning, bonding and curing of the 2219-T87 panel followed the procedure given for the 2024-T3 panel, which is the Grumman standard procedure for bonding with METLBOND 329.

Ultrasonic resonance inspection of the panel indicated one small void area on one side of the panel. (See Figure 3-7.) Small areas of "heavy" bond lines, which would result in reduced adhesive strength, were also noted and are shown in Figure 3-7.

Test standards were fabricated for use in inspecting the adhesive bonded panel. The skins were 2024 aluminum and the adhesive was METLBOND 329. A two-step bonding process was used, and the thickness of the standard was measured before and after each bond cycle. Shims were used to obtain various bondline thicknesses.

The resonant frequency of the skin alone (.040 in. thick) was determined. This simulates a void condition. When testing a known bondline thickness of .006 in., a frequency shift of 35,000 cycles is observed. When the bondline thickness is increased to .009 in. the frequency shift decreased to 30,000 cycles. Further increasing the bondline thickness to .014 in. reduced the frequency shift to 10,000 cycles.

All bonded areas with a frequency shift of over 25,000 cycles were considered satisfactory. All areas with a frequency shift of 10,000 cycles to 25,000 cycles were reported as areas of heavy bondline. All areas with frequency shifts of 0 to 10,000 cycles were reported as void areas.

After machining the adhesive bonded specimens from the 4 ft by 3 1/2 ft panel, the adhesive bond line thickness was measured optically using a "profile projector" at 10x magnification. These measurements, shown in Table 3-8, indicate bond line thicknesses varying from .010 to .012 in. If we accept these measurements, and the total specimen thicknesses measured, this would call for total metal thicknesses (three sheets) varying from .1305 in. to .133 in. Summing the thickness measurements of the chem-milled sheets in Table 3-7 in the area B through E and 2 through 4, from which the specimens were cut, gives a range of .1295 to .1305 for total metal thickness. This would mean that the bond line thickness varied from .011 to .013 in. Greater confidence is given to the .011 in. to .013 in. bondline thickness estimate.

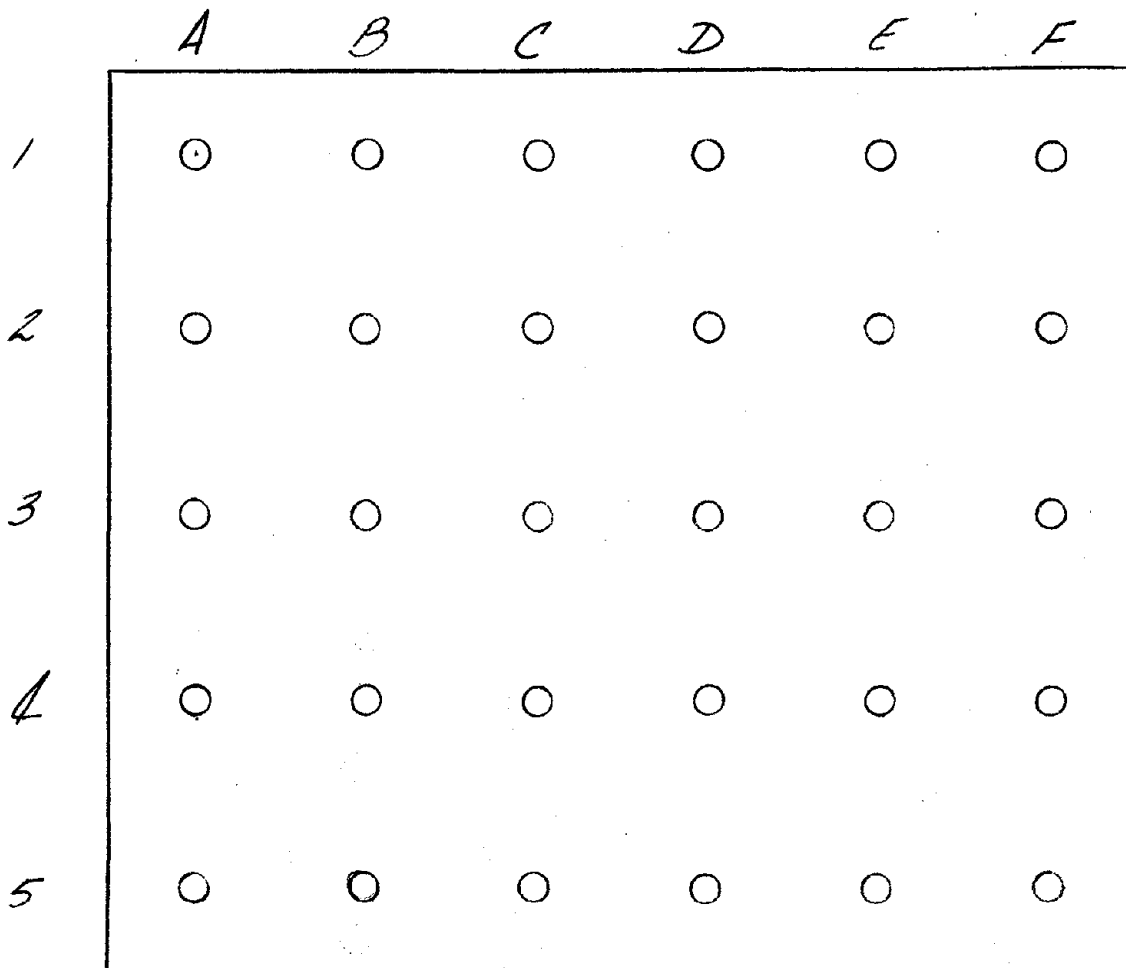


Figure 3-6 Location of Thickness Measurements on Chem-Milled 2219-T87 Sheet for Second 2219 Adhesive Bonded Panel

TABLE 3-7 THICKNESS MEASUREMENTS OF CHEM-MILLED 2219-T87
SHEET FOR SECOND ADHESIVE BONDED TEST PANEL

SHEET No. 1						
	A	B	C	D	E	F
1	.0431	.0435	.0437	.0436	.0434	.0434
2	.0435	.0440	.0441	.0439	.0436	.0435
3	.0435	.0440	.0441	.0439	.0436	.0433
4	.0436	.0443	.0442	.0442	.0439	.0435
5	.0439	.0443	.0442	.0441	.0438	.0435

SHEET No. 2						
	A	B	C	D	E	F
1	.0434	.0435	.0436	.0433	.0436	.0432
2	.0431	.0435	.0435	.0435	.0433	.0431
3	.0431	.0435	.0433	.0435	.0434	.0430
4	.0431	.0433	.0435	.0434	.0432	.0430
5	.0434	.0434	.0434	.0436	.0433	.0432

SHEET No. 3						
	A	B	C	D	E	F
1	.0424	.0427	.0430	.0433	.0435	.0430
2	.0424	.0425	.0426	.0426	.0425	.0455
3	.0426	.0427	.0428	.0431	.0428	.0455
4	.0426	.0429	.0430	.0431	.0431	.0413
5	.0428	.0429	.0432	.0432	.0433	.0428

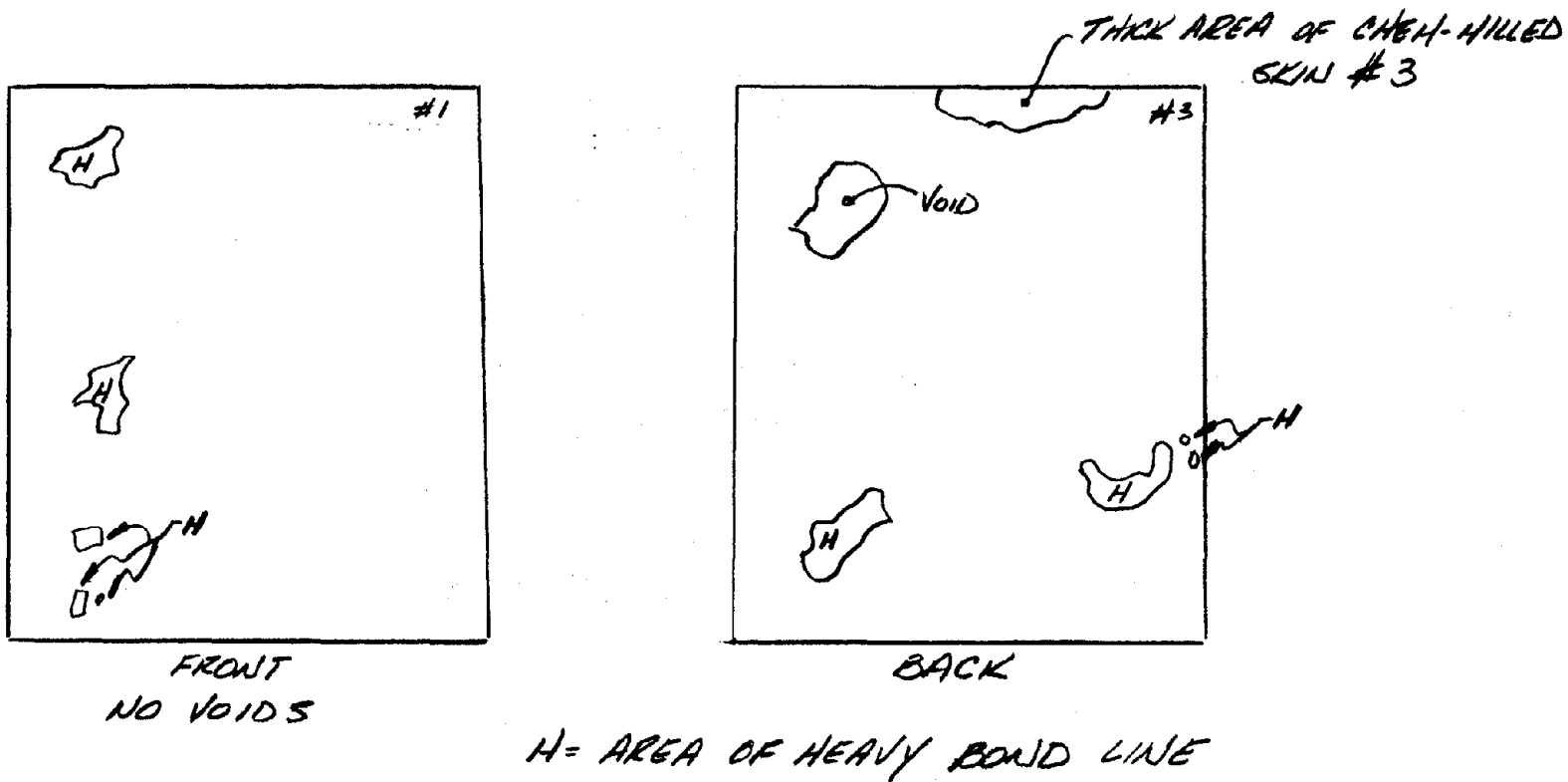


Figure 3-7 Ultrasonic Resonance Test Results, Second 2219-T87 Adhesive Bonded Panel

TABLE 3-8 BONDLINE THICKNESS MEASUREMENTS, ADHESIVE BONDED SPECIMENS

SPECIMEN NO.	TOTAL THICKNESS, in.	BOND LINE #1, in.	BOND LINE #2, in.	TOTAL BOND t, in.	TOTAL METAL t, in.
1	.155	.011	.011	.022	.133
2	.153	.010	.010	.020	.133
3	.155	.012	.012	.024	.131
4	.153	.011	.0115	.0225	.1305
5	.156	.012	.011	.023	.133
6	.152	.0105	.011	.0215	.1305

Section 4

MATERIALS EVALUATION

SPECIMEN FABRICATION

A total of 54 specimens was scheduled for testing in this program. Eighteen specimens were machined from monolithic 2219-T87 material, thirty were machined from the different interlayer thickness roll diffusion bonded laminates, and six specimens were machined from an adhesive bonded laminated panel.

Details of the fabrication of the roll diffusion bonded and adhesive bonded laminates are given in Section 3. For the monolithic specimens, .125 in. thick 2219-T37 plate was heat treated to the -T87 condition.

Test specimen configuration is shown in Figure 4-1. The 2.5 in. width was chosen to minimize end effects in the area of flaw-growth. Figure 4-2 shows the dimensions of the ELOX starter flaw, which was initiated in each specimen.

Care was taken to assure that the laminated specimens were flaw-free in the test area before the ELOX notch was initiated. The ultrasonic inspection of the roll diffusion bonded laminates described in Section 3 was repeated in the test section of each specimen after machining and before "eloxing." No defects were observed in this inspection. Similarly, the ultrasonic inspection of the adhesive bonded specimen was repeated after machining. In this case, one specimen, No. 3, contained three small (1/8 in. dia., 1/4 in. dia., and 3/16 in. by 1/2 in.) questionable areas of possible bond line porosity. It was decided to proceed with the test of this specimen, and it gave representative results.

During the course of the program, difficulty was encountered in producing sharpened flaws to a depth of one-half the specimen thickness in roll diffusion bonded specimens. Additional small specimens of the .004 interlayer thickness laminate were machined to the configuration shown in Figure 4-3. Tests on these specimens showed that an elox notch of .110 wide by .055 deep permitted controlled growth to 1/2 specimen thickness. Roll diffusion bonded laminates for Phase II and Phase III testing, which required 1/2 thickness flaws, were eloxed to the .110 wide by .055 deep configuration.

MATERIAL PROPERTIES DETERMINATION

All material properties determination tests were performed at room temperature. Cyclic stress levels and initial flaw configurations were in accordance with the objectives of the program test plan as discussed in Section 2. All testing will be done with stress ratio R (= minimum cyclic stress/maximum cyclic stress) = 0.05.

A record of surface flaw width vs number of cycles was kept for each program specimen. Flaw width was measured optically (Figures 4-4 and 4-5). The number of cycles at which the flaw grew to become a through-the-thickness flaw ("breakthrough") was also recorded. Breakthrough was noted either through observing a surface flaw on the back face of the specimen or by an instrument called a leak detector unit. The leak detector unit will be more fully described in Nondestructive Tests on page 4-25. The tests were concluded by failure of the specimens. Nondestructive testing was conducted concurrently with flaw growth testing. Tables of flaw growth for each specimen are given in Appendix A. Curves of surface flaw width vs cycles for each specimen are given in Appendix B.

Phase I Testing

Phase I testing was designed to give a relative evaluation of the three laminate interlayer thicknesses and provide a comparison with monolithic material. All Phase I specimens were to have initial flaw depths of one-third the thickness. Since it is not possible to measure flaw depth directly, an approximate surface-width-to-depth ratio of 2.18 to 1, noted in previous 2219-T87 tests at Grumman, was used to estimate flaw depth. Based on this relationship surface flaw widths of .090 in., ($\frac{125}{3} \times 2.18 = .091$), were produced in the Phase I monolithic specimens. A one-third thickness flaw represents a depth of approximately .042 in. If the range of outer ply thicknesses of the laminated plates is examined (Table 3-2), it can be seen that an .042 in. deep flaw would penetrate into the interlayer in most cases. Outer ply thicknesses varied from .035 in. to .043 in. If the interlayer's purpose is to provide a flaw growth delay mechanism, this effect would not be noted if the initial flaw were to extend into or through the interlayer. To observe this delay, initial flaws in the laminate were limited to .032 in. in depth or, $.032 \times 2.18 = .070$ in. in width.

Initial flaws were started with ELOX notches and then, by applying cyclic stresses, grown to the desired depth. ELOX notches in Phase I specimens were semicircular and approximately .020 in. deep (Figure 4-2).

The ELOX notch was "sharpened" to the desired depth using a cyclic stress of 36 KSI. Ideally, a stress level significantly below the level at which growth stress will be measured would be used for flaw sharpening. In this program a sharpening stress of 20 KSI was selected initially. However, 100,000 cycles at this stress level produced no flaw growth. Previous work had found 36 KSI to be an acceptable level for flaw growth, but this was quite close to the program stress of 40 KSI. A compromise solution was tried in which 36 KSI was applied for a small number of cycles to insure that a flaw did, in fact, grow from the elox notch, then followed by cycling at 20 KSI. In this method, 1000 cycles at 36 KSI approximately doubled the surface flaw width, but the subsequent 33,000 cycles at 20 KSI resulted in no additional growth. The decision to use 36 KSI as the sharpening stress was made at this point.

A post-test examination of monolithic specimens was conducted but accurate determination of the initial flaw depth was not possible. Because the sharpening stress (36 KSI) and the growth stress (40 KSI) are so close, it was very difficult to differentiate between growth at the sharpening stress and growth at the program growth stress. Since initial flaw depth verification is quite desirable, alternate means were sought. A fluorescent dye was injected into several specimens at the conclusion of the sharpening cycles. In some specimens

Reproduced from
best available copy.

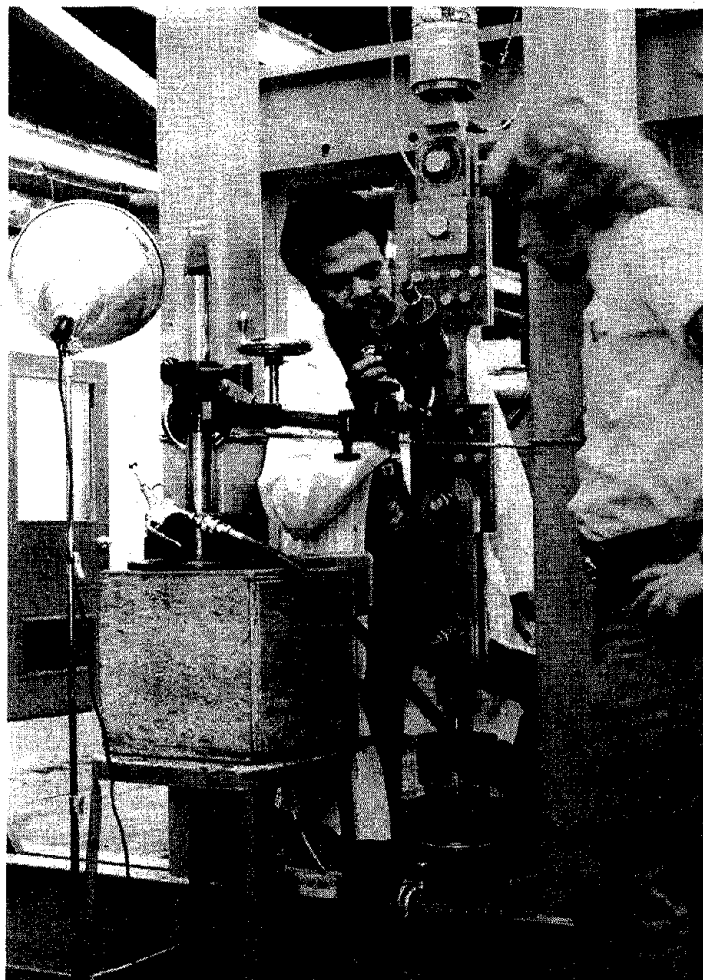


Figure 4-4 Flaw Width Measurement Setup-
Binocular Instrument

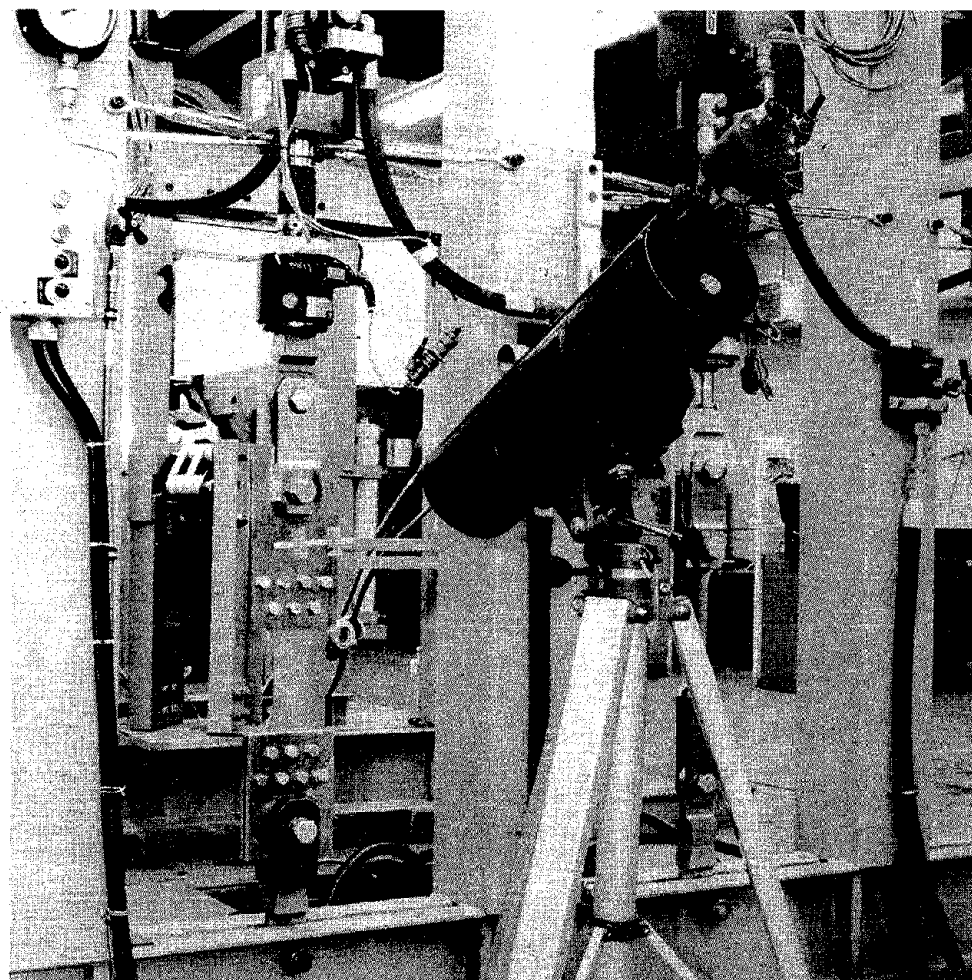


Figure 4-5 Flaw Width Measurement Setup-
"Telescope" Instrument

results appeared excellent but in others the dye did not dry properly and ran into the flaw growth area, and in others did not penetrate the crack at all. The dye marking procedure was, at best, unreliable for measurement of initial flaw depth.

The method of dye marking included the following steps:

1. Dye (Tracer-Tech P-135) was swabbed onto the specimen while it was undergoing cycling at 1 cps for 10-15 cycles.
2. Air dried for 15-20 minutes.
3. Developer (Spot-Check) was sprayed on while the specimen was undergoing cycling at 1 cps for 10-15 cycles.
4. Air dried for 15-20 minutes.
5. Testing continued.

Six monolithic specimens and six specimens of each of the three interlayer thickness materials were tested in Phase I. Since there is a variation in initial flaw width, .070 in. for the laminated specimens and .090 in. for the monolithic specimens, for purposes of comparison cyclic life was assumed to begin with a surface flaw .090 in. wide. Table 4-1 lists cycles to breakthrough and failure for each of the Phase I specimens. A summary of data is given in Table 4-2. It can be clearly seen that the .004 laminate displayed superior performance in both life-to-leakage and life-to-failure. The .004 laminate shows a 96% increase in cycles to breakthrough over monolithic material and 73% in cycles to failure. The .008 laminate also displayed better cyclic life than the monolithic material, showing an increase in cycles-to-breakthrough of 47% and an increase of 31% in cycles to failure. Monolithic material outperformed the .012 laminate in both breakthrough and failure life. It should be recognized that all specimens were subjected to a cyclic stress of 40 KSI on the gross cross-section, so that the structural material in the .012 laminate was operating at a considerably higher stress than in the monolithic material. The optimum material then is the laminate with the maximum structural material and just enough of the interlayer material to be effective in the flaw growth delay action. The results of this program show that a .004 interlayer can certainly perform this function.

Based on the results shown in Tables 4-1 and 4-2, the .004 laminate was chosen for testing in Phase II and Phase III. Greater confidence is lent to this choice by the lack of scatter in the data. Envelopes of the flaw growth curves of each class of specimen are shown in Figures 4-6 and 4-7. The clear separation between the materials reinforces the choice of the .004 laminate.

A question was raised as to the effect of the difference in initial flaw size between the laminated and monolithic specimens. Another difference is that the basic specimen size of the monolithic specimens was .125 in. while the laminated specimens were all .130 in. thick. An analytic effort was undertaken to resolve the question resulting from these differences. Using data from the Phase I monolithic specimens and stipulating a semicircular flaw shape, an expression was obtained for flaw growth rate in the monolithic specimens. The number of cycles to grow from .0321 in. flaw depth (.070 in. width) to .0413 in. depth (.090 width) was calculated as was the number of cycles to grow from .125 in. to .130 in. Using the expression:

TABLE 4-1

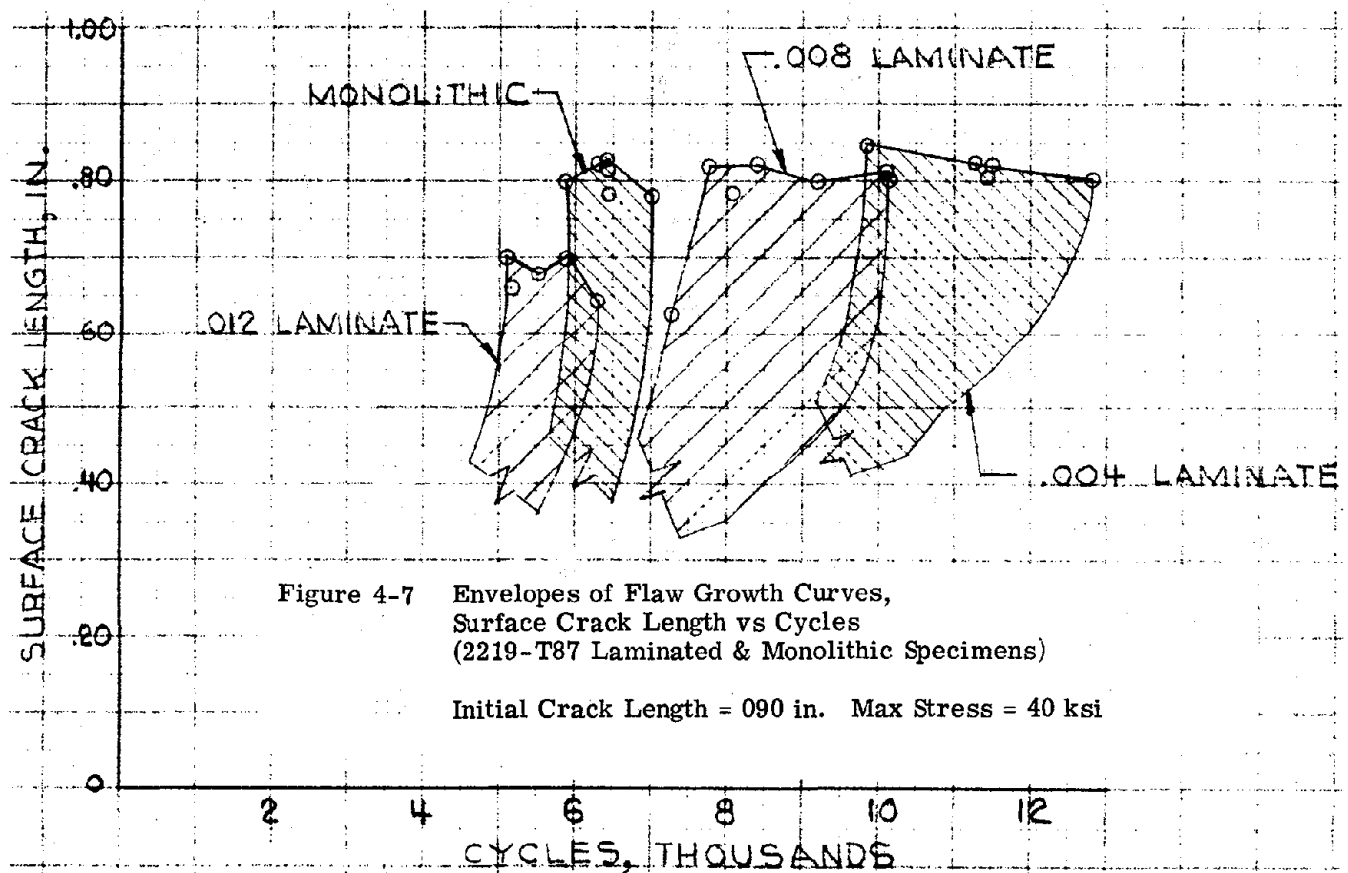
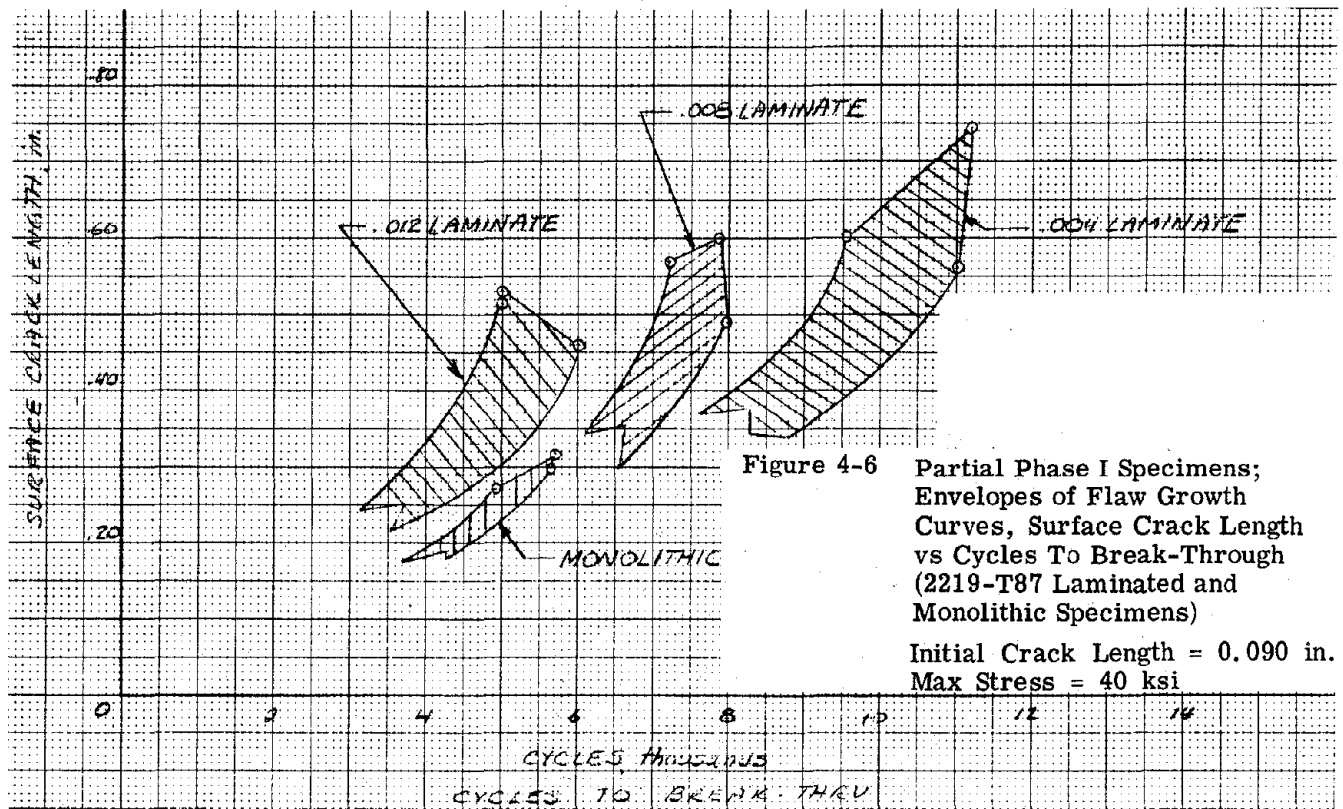
PHASE I FLAW GROWTH TEST RESULTS SUMMARY

(GROWTH STRESS: 40 KSI; CYCLES BEGIN WITH .090 IN. SURFACE FLAW WIDTH)

Specimen		Cycles				
Type	Number	Breakthrough	Failure	High	Low	Average
Monolithic	1	5670	6497			
Monolithic	3	5500	6460			
Monolithic	5	5720	6475			
Monolithic	7	4900	5915			
Monolithic	9	6160	7015			
Monolithic	11	5330	6366			
Monolithic, Cycles to Breakthrough				6160	4900	5547
Monolithic, Cycles to Failure				7015	5915	6455
.004 Laminate	353492-1	11,100	11,430			
.004 Laminate	353492-2	11,000	11,450			
.004 Laminate	353492-3	12,550	12,900			
.004 Laminate	353492-4	9585	9850			
.004 Laminate	353492-5	9800	10,120			
.004 Laminate	353492-6	11,200	11,300			
.004 Laminate, Cycles to Breakthrough				12,550	9585	10,873
.004 Laminate, Cycles to Failure				12,900	9850	11,175
.008 Laminate	353493-1	7900	8050			
.008 Laminate	353493-2	8000	8330			
.008 Laminate	353493-3	8700	9200			
.008 Laminate	353493-4	9688	10,100			
.008 Laminate	353493-5	7500	7820			
.008 Laminate	353493-6	7260	7345			
.008 Laminate, Cycles to Breakthrough				9688	7260	8175
.008 Laminate, Cycles to Failure				10,100	7345	8474
.012 Laminate	353494-1	5687	5960			
.012 Laminate	353494-2	6061	6300			
.012 Laminate	353494-3	5318	5598			
.012 Laminate	353494-4	5000	5145			
.012 Laminate	353494-5	Accidentally overloaded to Failure				
.012 Laminate	353494-6	5000	5150			
.012 Laminate, Cycles to Breakthrough				6061	5000	5413
.012 Laminate, Cycles to Failure				6300	5145	5631

TABLE 4-2 SUMMARY OF PHASE I TEST RESULTS, CYCLES BEGIN
WITH .090 IN. SURFACE FLAW WIDTH

Specimen Description	No. of Specimens	Number of Cycles					
		Break Through			Failure		
		High	Low	Avg.	High	Low	Avg.
Monolithic	6	6160	4900	5547	7015	5915	6455
.004 Laminate	6	12,550	9585	10,873	12,900	9850	11,175
.008 Laminate	6	9688	7260	8175	10,100	7345	8474
.012 Laminate	5	6061	5000	5413	6300	5145	5631



$$n = \frac{3.38 \times 10^9}{B^{2.135}} \left[\begin{matrix} -1.135 & -1.135 \\ A_o & -A_f \end{matrix} \right] \quad (4-1)$$

where n = number of cycles for a flaw to progress from an initial depth A_o , to a final depth A_f .

$$B = \frac{1.21 \pi (\Delta\sigma)^2}{Q}$$

$$Q = \Phi^2 - 0.212 \left(\frac{\Delta\sigma}{\sigma_y} \right)^2$$

$\Delta\sigma$ = cyclic stress range, KSI

σ_y = material yield stress, KSI

Φ^2 = 2.46 for a semicircular flaw

the number of cycles to grow from .032 in. to .041 in. was 2705, and 101 cycles was required to grow from .125 in. to .130 in. Reviewing the data for the monolithic specimens, the average number of cycles to breakthrough is 5448 for specimens No. 1, 3, 5 and 7 which had initial flaws .090 in. wide. Adding the calculated number of cycles to account for differences in flaw size and specimen size, 2806, the equivalent cycles to breakthrough is 8254. This compares to an average of 12,130 cycles to breakthrough for the .004 laminate based on the five specimens which had initial flaws .070 in. wide. This represents an increase of 47% rather than the 96% increase in life based on starting both specimens at .090 in. surface flaws. Two monolithic specimens were tested with initial flaws .070 in. wide. The average cycles-to-breakthrough for these two specimens was 7245 cycles. Comparing them to the five .004 laminates with .070 initial flaws, and accounting for specimen thickness, the laminate showed a 65% increase in cyclic life. This data is summarized in Table 4-3. The conclusion is evident that the laminated material provides a substantial increase in cyclic life over the monolithic material at the same gross stress.

Phase II Testing

Phase II testing specified one-half thickness flaws and a cyclic stress of 40 KSI. Based on the previously mentioned flaw width to depth ratio, monolithic specimens were sharpened to $(\frac{.125}{2} \times 2.18 = .136)$.135 in. surface flaw width.

Initial attempts to produce one-half thickness flaws in .004 laminate were unsuccessful. Based on the flaw growth records of Phase I specimens, it was assumed that a surface flaw of .300 in. would represent an approximately one-half thickness flaw. Accordingly, starting from the elox notch used in Phase I, two specimens, 353492-1A and -2A, were sharpened to produce .290 in. wide surface flaws. Specimen 1A failed after 7040 cycles at 40 KSI and specimen 2A failed after 2750 cycles at 40 KSI. Dye penetrant was applied to the surface of both specimens near the conclusion of the sharpening cycles. Inspection of specimen 2A after test showed that the dye had penetrated to the third layer of material. The dye did not penetrate into the flaw in specimen 1A. It was not possible to discriminate between growth which occurred at the sharpening stress, 36 KSI, and growth at the program stress, 40 KSI. Results of the Phase I testing had quite limited scatter so that the results of specimens 1A and 2A infer that the testing began with different depth flaws. The conclusion was reached that flaw depth in the laminate cannot be accurately predicted from the surface width beyond the first interlayer.

TABLE 4-3

PHASE I SPECIMENS, COMPARISON OF CYCLES TO BREAKTHROUGH

MATERIAL	No. of Specimens	INITIAL FLAW SIZE IN.	CYCLES TO BREAKTHROUGH	% INC. OVER MONOLITHIC
All Specimens began at .090 in. initial flaw				
Monolithic	6	.090	5547	96
.004 Laminate	6	.090	10873	
Calculate Δ Cyc for Mono. from .070 to .090 and for increased t				
Monolithic	4	.090	5448	47
		Calculated Cycles	<u>2806</u>	
			Σ 8254	
.004 Lam.	5	.070	12130	
Monolithics began at .070 initial flaw, add Δ cyc for increased t				
Monolithic	2	.070	7245	65
		Δ cyc for t=.125 to t = .130	<u>101</u>	
			Σ 7346	
.004 Lam.	5	.070	12130	

Photographs of the fracture surfaces of specimens 1A and 2A are shown in Figures 4-8 and 4-9. The lighter colored areas adjacent to the elox notches are the regions of flaw growth. It appears that the flaw changes from an initial semicircular shape to separate rectangles in each layer of the laminate, the flawed surface being the widest and the rear face the narrowest.

Due to the lack of success in predicting flaw depth from surface flaw width, an alternative procedure to produce one-half thickness flaws was sought. It was suggested that if the elox notch was to penetrate the first interlayer, a relationship between flaw width and depth could be demonstrated. To verify this, six small .004 laminate specimens (Figure 4-3) were machined. Semicircular elox notches $.053 \pm \begin{smallmatrix} .000 \\ -.005 \end{smallmatrix}$ in. deep were introduced into the specimens. Maximum thickness of an outer ply and the adjacent interlayer is .047 in. based on the data of Table 3-2. These specimens were to be cycled at the sharpening stress of 36 KSI until it was judged that a one-half thickness flaw was produced. The edges of the specimen were then saw-cut and the specimen was failed in tension. Post-test examination of the specimen shows the actual flaw depth. Repeated trials would indicate the proper surface flaw width for a one-half thickness flaw.

Test results of the small specimens showed that surface flaws of .145 in. to .150 in. width grown from .100 in. wide by .050 deep semicircular notches give one-half thickness depth flaws in the .004 laminate. Table 4-4 lists these results. A plot of the surface flaw width versus flaw depth for the small specimens is given in Figure 4-10. Based on these tests, Phase II .004 laminated specimens were eloxed as noted above to insure penetration into the second ply, and then sharpened to approximately .145 in. surface flaw width.

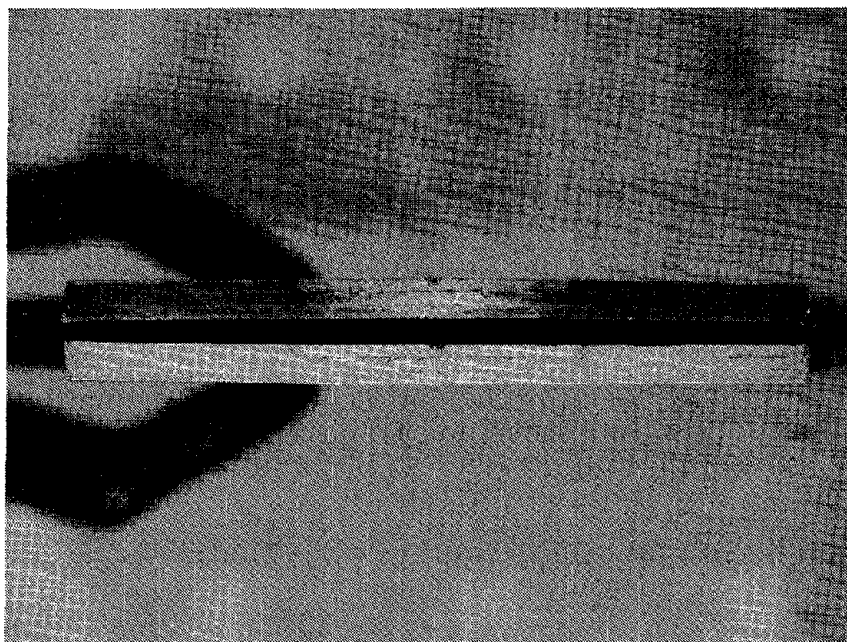
Results of the Phase II specimens are shown in Table 4-5. Monolithic specimens averaged 3023 cycles to breakthrough. The four .004 laminate specimens that had the larger elox notches averaged 4671 cycles to breakthrough, which represents a 54% increase in cyclic life to leakage. At failure, the monolithic specimens averaged 3892 cycles, while the .004 laminate averaged 4849 or an increase of 25%.

Phase III Testing

All Phase III testing was to be conducted at 48 KSI. Three monolithic and three .004 laminate specimens were to be tested with one-third thickness flaws and an additional three of each material with one-half thickness flaws.

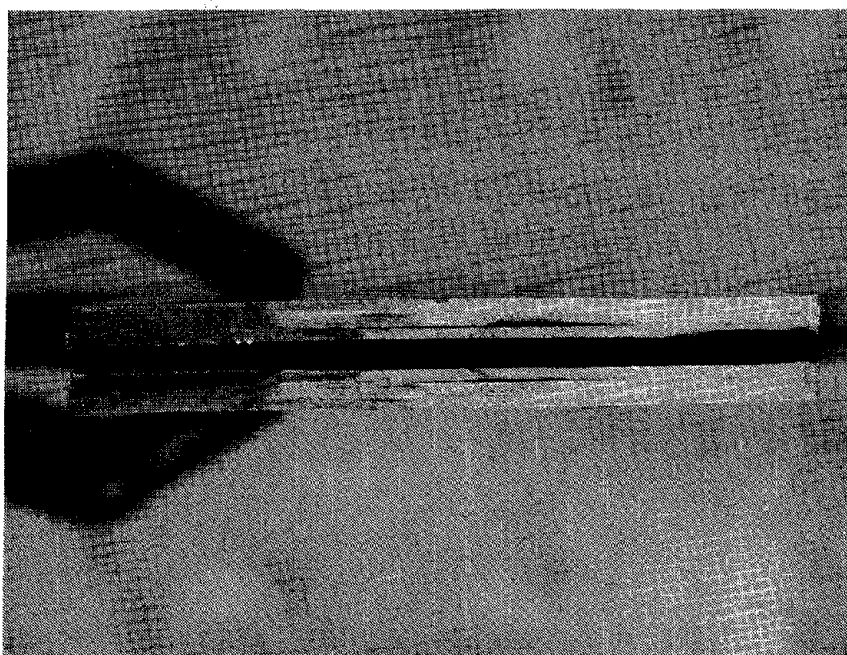
Elox notches similar to those used in the Phase I testing were used for the specimens that were to be tested with one-third thickness flaws. All laminated specimens had initial surface flaw widths of .070 in. Two of the three monolithic specimens also had .070 in. initial flaws; the third had an initial flaw width of .090 in. Results of these tests are shown in Table 4-6. The two monolithic specimens that had initial surface flaws of .070 in. averaged 3842 cycles to breakthrough and 3965 cycles to failure. At 40 KSI cyclic stress, breakthrough occurred approximately 1000 cycles before failure. The laminated material reached breakthrough and failure simultaneously at an average of 8052 cycles.

Photographs of the fracture surface of specimen 353492-8A are shown in Figures 4-11, 4-12 and 4-13. Figure 4-11 particularly well illustrates the flaw growth pattern in the roll diffusion bonded laminate. Figure 4-12 shows the fracture surface of the same specimen at higher magnification under white light. Fluorescent dye had been injected into the flaw toward the end of the sharpening cycles. When viewed under ultraviolet light, the dyed area is seen and approximates the one-third thickness flaw depth called for in the program (Fig. 4-13).



Reproduced from
best available copy.

Figure 4-8 Fracture Surface of Specimen No. 353492-1A



Note Elox notch at center of upper edge; also delamination between second and third plies (down from Elox surface)

Figure 4-9 Fracture Surface of Specimen No. 353492-2A

TABLE 4-4

APPROXIMATE FLAW DEPTHS FOR LAMINATED SPECIMENS
(RESULTS OF SMALL SPECIMEN TESTS)

Specimen No.	Flaw Width	Flaw Depth
353492-1X	.120	Not distinguishable
" -2X	.130	.059
" -3X	.145	.066
" -4X	.132	.059
" -5X	.150	.072
" -6X	.192	.090

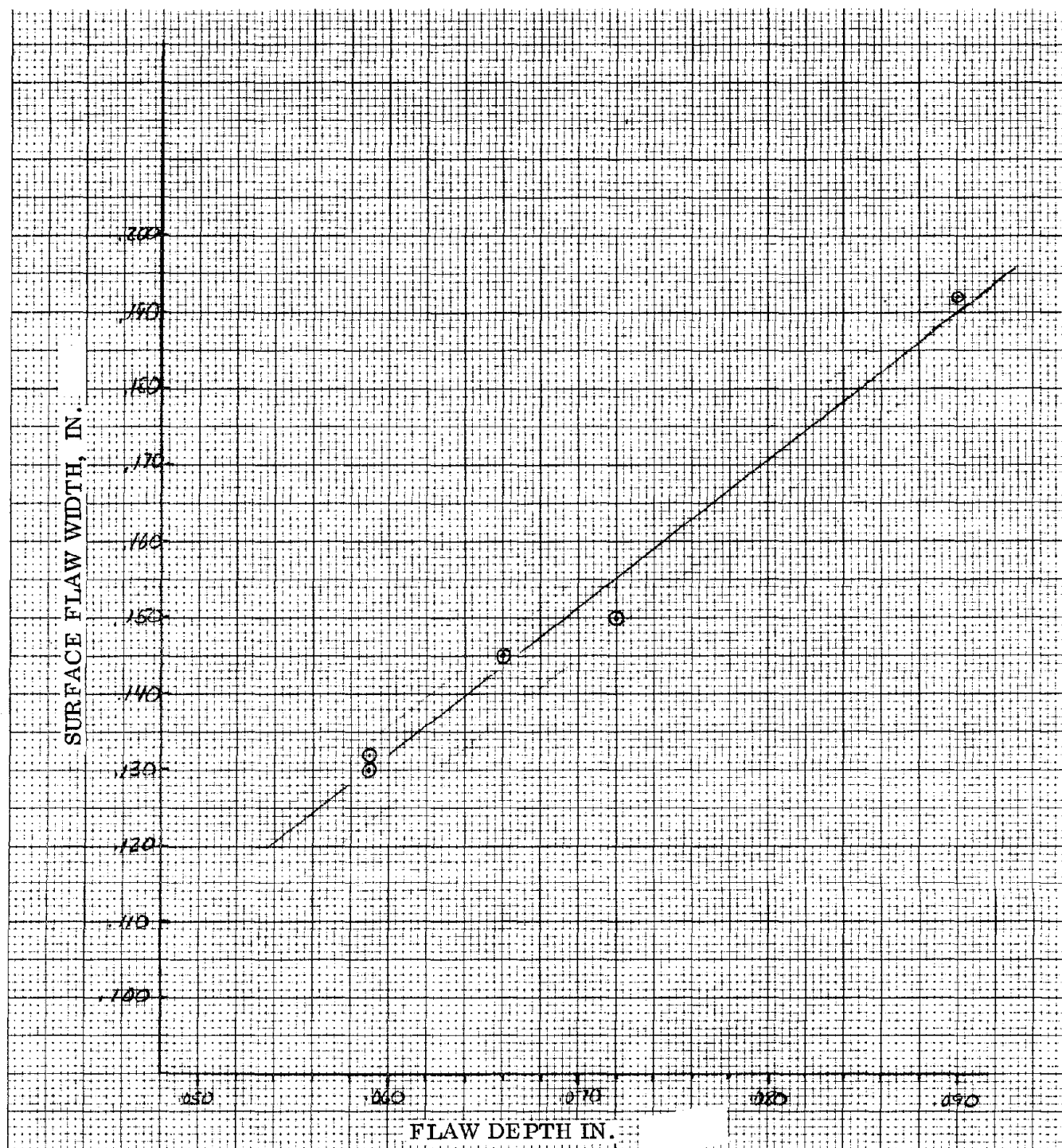


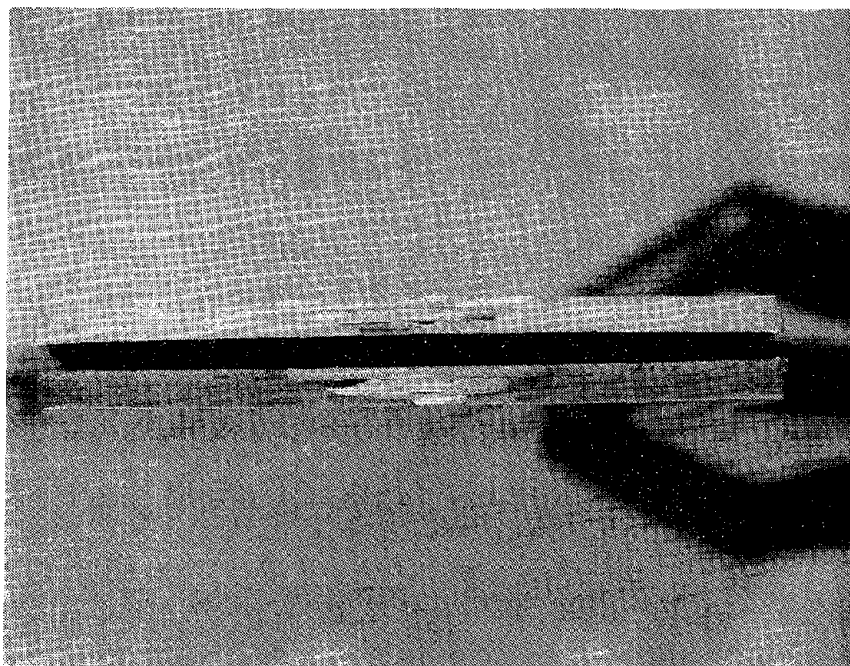
Figure 4-10 Surface Flaw Width vs Flaw Depth for Small Specimen

TABLE 4-5 PHASE II SPECIMENS, 1/2 t FLAWS, 40 KSI

Material	Specimen No.	Elox	SFC Flaw Width	Flaw Depth	CYC To Breakthru	Cycles To Failure
Monolithic	2	.020 x .040	.135	.062 - .072	4019 Hi	4972 Hi
Monolithic	4	.022 x .040	.135	.062 - .072	3078	3985
Monolithic	6	.023 x .040	.135	.062 - .072	2740 Lo	3521 Lo
Monolithic	8	.023 x .040	.135	.062 - .072	2745	3645
Monolithic	10	.024 x .040	.135	.062 - .072	2769	3680
Monolithic	12	.024 x .040	.135	.062 - .072	2786	3550
					Avg 3023	Avg 3892
.004 Laminate	353492-1A	.018 x .050	.290		7000	7040
.004 Laminate	353492-2A	.016 x .050	.290		-	2750
.004 Laminate	353492-3A	.053 x .110	.145	~.067	4180	4300
.004 Laminate	353492-4A	.053 x .110	.145	~.067	4690	4930
.004 Laminate	353492-5A	.048 x .110	.145	~.067	5685 Hi	5930 Hi
.004 Laminate	353492-6A	.059 x .110	.150	~.069	4130 Lo	4235 Lo
					Avg (4) 4671	Avg (4) 4849

TABLE 4-6 PHASE III TESTING,
1/3 t FLAWS, 48 KSI

Specimen Description	Specimen No.	Initial Flaw Width, in.	Cycles To Breakthrough	Cycles To Failure
Monolithic	13	.090	2572	2810
Monolithic	15	.070	4000	4130
Monolithic	17	.070	3683	3800
Avg. (Spec. With .070 Initial Flaw)			3842	3965
.004 Laminate	353492-7A	.070	-	8175
	353492-8A	.070	-	7750
	353492-9A	.070	-	8230
	Avg.			8052



Reproduced from
best available copy.

Note growth pattern, wide in layer with Elox flaw,
narrower in second ply

Figure 4-11 Fracture Surface of Specimen No. 353492-8A - Elox Notch
at Center of Upper Edge

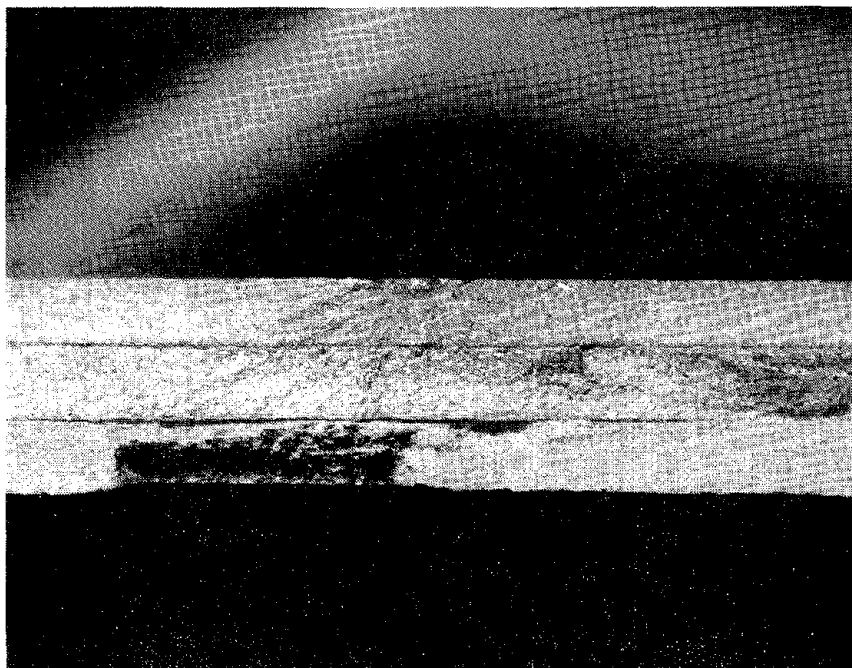
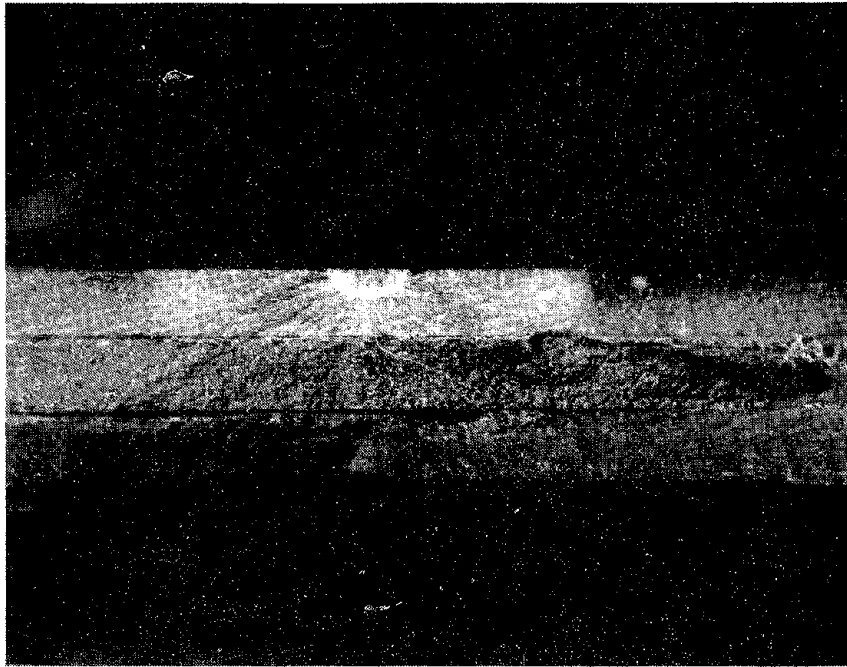


Figure 4-12 Fracture Surface of Specimen No. 353492-8A - Nine Times
Magnification Under White Light



Note that dye applied at end of sharpening cycles appears to have penetrated one layer only

Figure 4-13 Fracture Surface of Specimen No. 353492-8A - Nine Times Magnification Under Ultraviolet Light

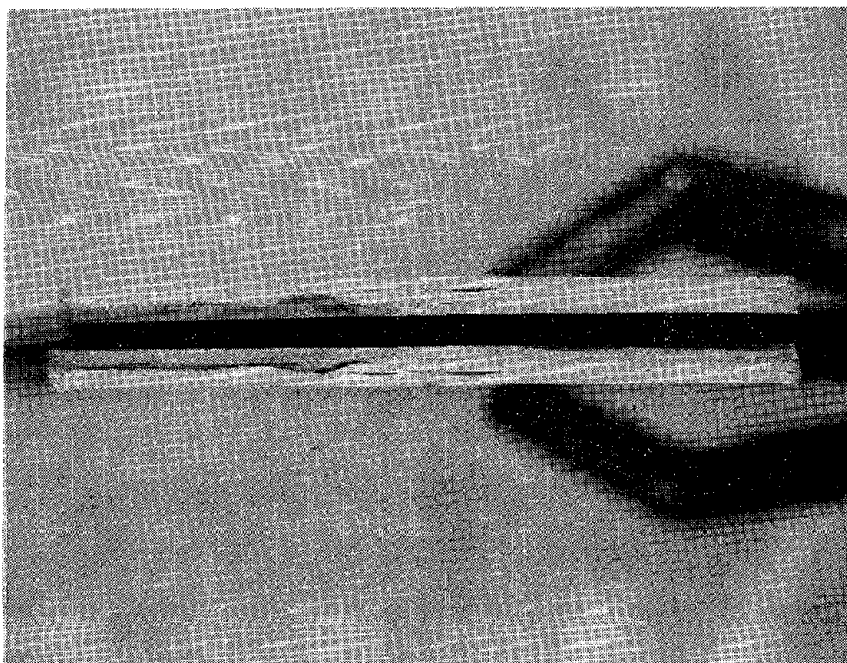


Figure 4-14 Fracture Surface of Specimen No. 353492-10A - Elox Notch at Center of Upper Edge

Monolithic specimens which were to be tested with one-half thickness flaws were sharpened to produce .135 in. wide surface flaws as in Phase II testing. One .004 laminated specimen, 353492-10A, was sharpened to a surface flaw width of .320 in. to obtain a one-half thickness flaw. When this method of producing one-half thickness flaws was shown to be unreliable, the remaining two specimens were given the large elox notch, .050 deep, as discussed in Phase II testing, and sharpened to .145 in. surface flaw width. Post-test examination of specimen 10A showed that dye injected at the end of the sharpening cycles had penetrated to the third structural layer. This specimen had failed after 600 cycles at 48 KSI. A photograph of the fracture surface of specimen 10A is shown in Figure 4-14.

Results of the one-half thickness flaw testing are shown in Table 4-7. The monolithic specimens averaged 1364 cycles to breakthrough and 1467 cycles to failure. The 100 cycle delay between leakage and failure is similar to that found in the one-third thickness - 48 KSI tests. Again, for the .004 laminate specimens, leakage and failure occurred simultaneously at an average value of 1890 cycles for the two specimens with the large elox notch.

Adhesive Bonded Specimens

Six adhesive bonded test specimens were prepared from the adhesive bonded panel described in Section 3. All specimens were to be tested with one-third thickness flaws. As with the diffusion bonded specimens, an effort was made to keep the flaw in the first structural ply. Accordingly, an elox notch similar to that used for Phase I specimens was called for, and the specimens were sharpened at 36 KSI to produce nominal .070 in. wide surface flaws. Three specimens were tested at 40 KSI and three at 48 KSI. In each case, a flaw initiated in an outer ply grew to the full specimen width in that ply. Flaw growth in an outer ply did not appear to propagate into adjacent plies. Failure of the remaining two plies was usually removed from the location of the flaw in the outer surface. No indication could be noted in the remaining plies of any flaw growth beyond the outer layer.

Results of the adhesive bonded specimen testing are shown in Table 4-8. The specimens tested at 40 KSI show the longest lives to failure of any specimens tested in this program. For example, the lowest specimen in this group failed after 16,630 cycles while the longest life Phase I .004 laminate specimen failed after 13,900 cycles. However, at 48 KSI the picture seems reversed. The best adhesive bonded specimen failed after 5135 cycles, while the lowest life .004 laminate specimen failed after 7750 cycles. The adhesive bonded specimens, however, still appear superior to the monolithic specimens whose longest life was 4130 cycles to failure.

Summary

In all cases the .004 laminate provided superior cyclic life to the monolithic material. Adhesive bonded specimens showed long cyclic lives to failure at 40 KSI cyclic stress. In the monolithic specimens the flaw appeared to have maintained its approximately semicircular shape right up to breakthrough. Flaws in the laminated material appeared to propagate laterally and through the depth so as to give a rectangular appearance in a particular layer. The relation of flaw depth-to-cycles could not be determined, and no relation between flaw width and depth could be established.

TABLE 4-7 PHASE III TESTING,
1/2 t FLAWS, 48 KSI

Specimen Description	Specimen No.	Initial flaw Width, in.	Cycles To Breakthrough	Cycles To Failure
Monolithic	14	.135	1500	1520
Monolithic	16	.135	1350	1530
Monolithic	18	.135	1241	1350
		Average	1364	1467
.004 Laminate	353492-10A	.320	-	600
	353492-11A	.145	-	2055
	353492-12A	.145	-	1725
	Average (-11A & -12A)		-	1890

TABLE 4-8 ADHESIVE BONDED SPECIMENS

Specimen No.	Initial Flaw, in.	Cyclic Stress, KSI	Cycles To Full Width Crack	Cycles To Failure
1	.080	40	12,500	16,875
2	.070	40	12,600	18,830
3	.070	40	14,550	16,630
4	.070	48	5100	5135
5	.080	48	4880	4980
6	.080	48	4555	4575

NONDESTRUCTIVE TESTS

Four nondestructive test methods were used during the cyclic flaw growth studies to demonstrate capabilities in detecting and sizing cracks. Program specimen loading was approximately 13,000 lb (40 KSI stress level) and 15,000 lb (48 KSI stress level). In most cases NDT evaluations were made with the specimens in the test fixture, not being cycled, but supporting approximately 8000 lb. The NDT instruments were all applied to the back surfaces of the specimens to simulate more realistic conditions for crack detection.

The methods evaluated were: shear wave ultrasonics, surface wave ultrasonics, conventional eddy currents and a custom-designed, deep-penetration, eddy-current device. Where possible, indications from these techniques were checked by visual means. The most sensitive method was found to be shear wave ultrasonics, while the most practical for large area coverage appears to be surface wave ultrasonics.

Shear Wave Ultrasonics

Shear wave ultrasonics was used to monitor quantitatively the propagation of the flaw from its inception as an elox notch, through sharpening and growth until a dimple is visible on the rear face. A 5 MHz - 45° shear wave transducer was employed with a Branson ultrasonic instrument. The transducer was placed on the rear face and moved until the elox notch was detected. The transducer was then located to maximize the signal, and the gain control on the instrument was adjusted for a half-scale reading of five units. The position of the transducer was then carefully marked.

As the flaw grows, its area increases, and it reflects a greater portion of the incident beam, causing an increase in the signal displayed on the instrument screen. The reflected signal increases quite rapidly as the crack propagates until it is off-scale. To bring the reading back on scale, the received signal is attenuated a known amount and then converted into the original scale. This method allows the use of the high sensitivity needed to monitor the initial sharpening, as well as permitting one to draw a continuous curve of surface flaw width vs signal strength. The original gain settings need not be altered at any time during the test.

The received signal was found to vary linearly with increased crack surface length. (See Figure 4-15.) In the monolithic specimens, surface length is assumed to be related to depth in the proportion $S.L. = 2.18D$, but no such relation has been established for the diffusion bonded specimens. The ratio for the monolithic specimens holds until the plastic deformation zone preceding the crack reaches the rear face, at which time the factor 2.18 increases rapidly.

Transducer placement is quite critical as slight linear or angular displacement of the transducer will cause large changes in signal strength. The transducer must be carefully placed in the identical position after each group of fatigue cycles.

The results of the shear wave investigation show that signal strength varies linearly with surface length, and that consistent results are attainable with similar specimen configurations. With proper standards, quantitative measurements of flaw size should be possible. The sensitivity of this method is apparent from its ability to detect the sharpened elox flaw, which is .030 to .040 in. deep.

Surface Wave Ultrasonics

Surface wave ultrasonic methods were developed in an effort to gain wide area sensitivity, conceding, however, a corresponding loss of depth sensitivity. A 2 MHz transducer, which yields a depth sensitivity of one wavelength or approximately .050 in., was employed. Defects

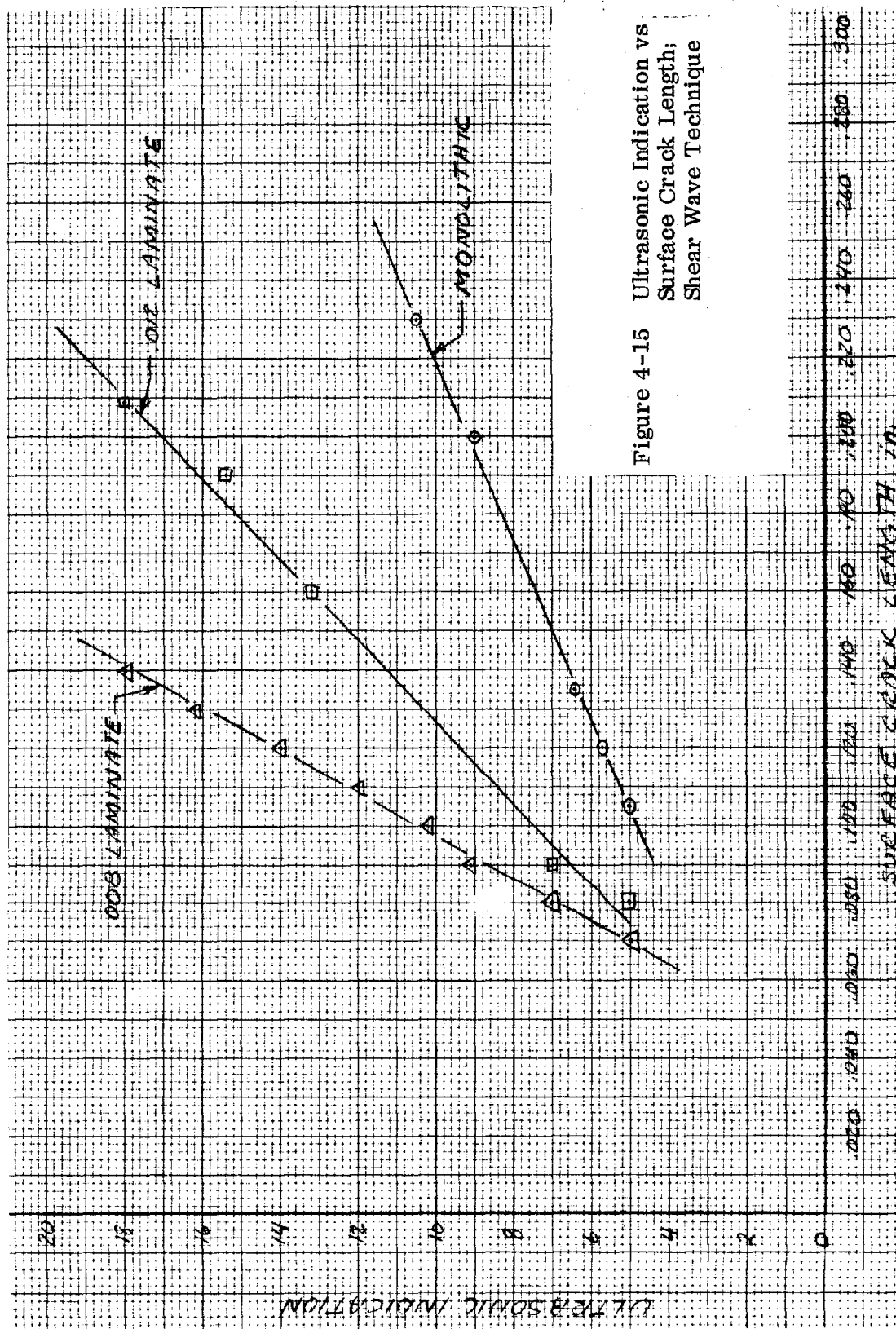


Figure 4-15 Ultrasonic Indication vs
Surface Crack Length;
Shear Wave Technique

were detectable prior to reaching .050 in. from the transducer because of the plastic zone that precedes the flaw by approximately .025 in. This plastic zone represents an acoustic mismatch that will reflect an incident signal.

Results indicate that defects are detectable prior to dimpling of the rear face and a large number of cycles before breakthrough. Using the geometric relation mentioned earlier for monolithic specimens, detection of the flaw occurs at a distance of .060 in. from the rear face, indicating the sensitivity of the transducer to the plastic zone preceding the flaw. The diffusion bonded sensitivity levels are difficult to assess because crack depth vs surface width relations are not known. Crack detection was possible, however, prior to dimpling. Table 4-9 shows the relative times of ultrasonic indication, dimpling and crack-through.

Surface wave ultrasonics did not detect flaws until they were approximately .060 in. from the back face. This was still a minimum of 500 cycles before visual evidence of a flaw's presence was detectable, (dimpling) and 1500 cycles before leakage.

Conventional Eddy Currents

Conventional eddy-current techniques were employed using the Nortec NDT-4. This instrument is an amplitude sensitive impedance bridge that monitors the change in impedance of a coil in the proximity of a defect.

A preliminary theoretical analysis was performed to optimize frequency and probe selection. For the instrument to detect a subsurface flaw, the defect width must be approximately equal to one-half the probe diameter. At the same time, the depth of penetration, which determines sensitivity limits to cracks below the surface, decreases with increasing frequency. Since the diameter of the probe that is to be used also decreases with higher frequencies, it can be seen that high sensitivity (high frequency and small diameter) and deep penetration (low frequency and large diameter) are difficult to achieve. Fortunately, the probes can be operated at frequencies other than their normal rating without critical loss of sensitivity.

To determine the best combination of frequency and probe, the assumed defect geometry was examined. In the monolithic specimens, the flaw shape is approximately semi-circular. One can see that the crack must propagate considerably beyond the standard depth of penetration of the instrument before the width of the flaw at that depth is equal to one-half the diameter of, say, a 1/4 in. probe. It was determined that best results should be obtained by operating at 10 KHz with a 1/4 in. diameter probe designed for 50 KHz. The depth of penetration at this frequency is .050 in. From geometry we find that the crack must be .032 in. from the probe for detection.

Based on its apparent poorer sensitivity than ultrasonic methods, only a limited evaluation of this method was made. Two specimens were evaluated, and the results are shown in Table 4-9. These results suggest that this method is even less sensitive than the calculations indicate. This effect is possibly due to operating the probe at other than its rated frequency.

Deep-Penetration Eddy Current

A unit was designed that could be attached to the test specimens which would incorporate leak detection and deep-penetration, eddy-current methods. A sketch of the unit, referred to as a leakage detector unit, is shown in Figure 4-16. An assembly drawing of the eddy-current probe and leak detector is shown in Figure 4-17. Figure 4-18 is a photo of the unit in operation.

The leak detection method is based on having an "O"-ring sealed chamber in which a vacuum of 50 to 100 microns was drawn during cycling. A leak, indicating a through-the-thickness crack, was noted by a sudden loss of vacuum, which is shown on a precision gage.

TABLE 4-9
DETECTION POINTS DURING CYCLIC FLAW GROWTH, CYCLES

Specimen No.	Shear Wave Ultrasonics	Surface Wave Ultrasonics	Conventional Eddy Current	Visual (Dimpling)	Break-through
353492-1 (.004 Lam.)	0	5500	7000	7500	12,100
353492-1A* (.004 Lam.)	0	-	-	1000	7000
353492-2 (.004 Lam)	0	10,000	-	11,000	12,000
353492-3 (.004 Lam)	0	5500	7000	8500	13,550
353493-2 (.008 Lam)	0	7500	-	8000	9000
353494-6 (.012 Lam)	0	4500	-	5000	6000
3 (Mono)	-	3500	-	4000	5500
* Phase II Specimen, All Others Phase I					

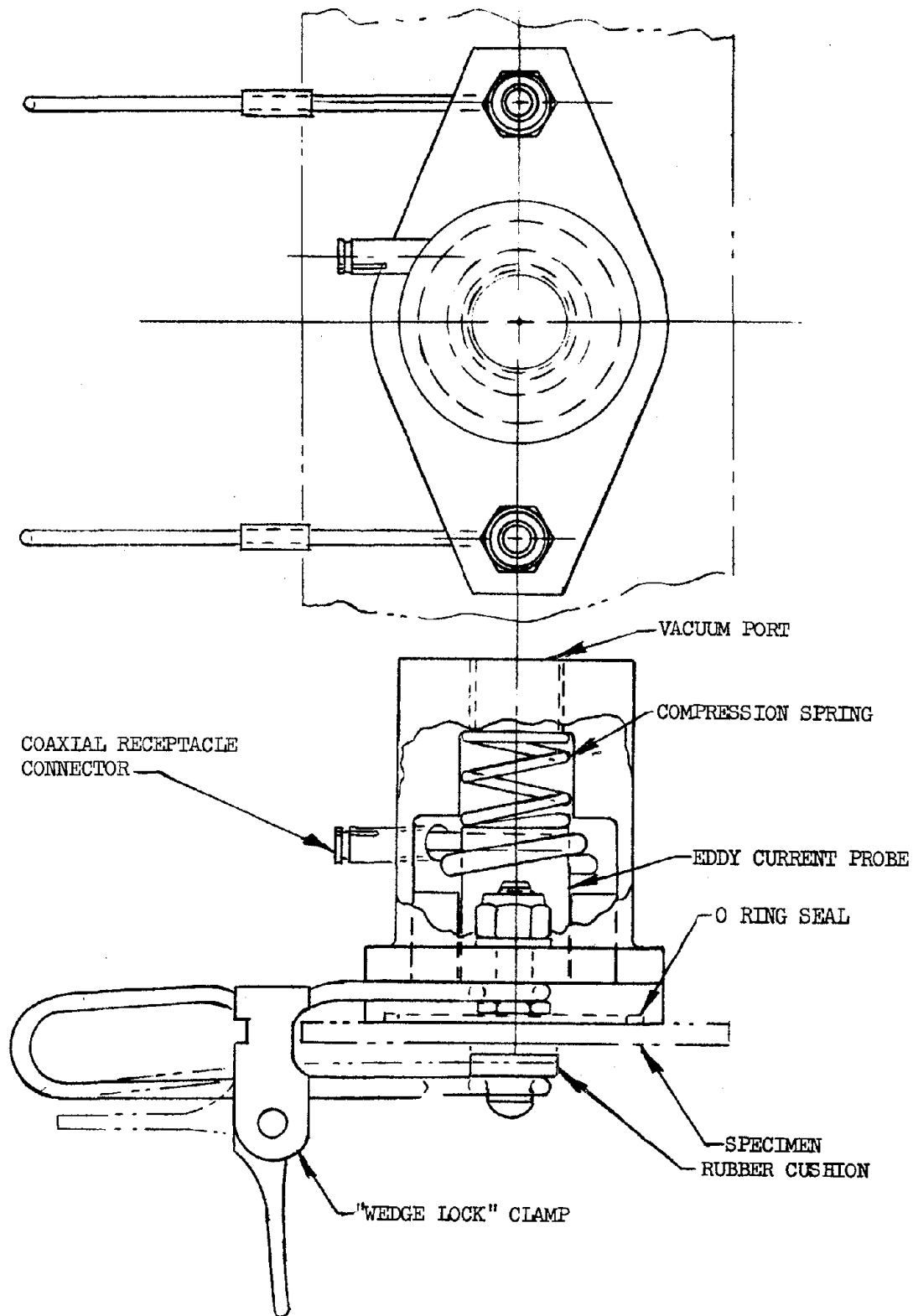


Figure 4-16 "Leakage" Detector Unit

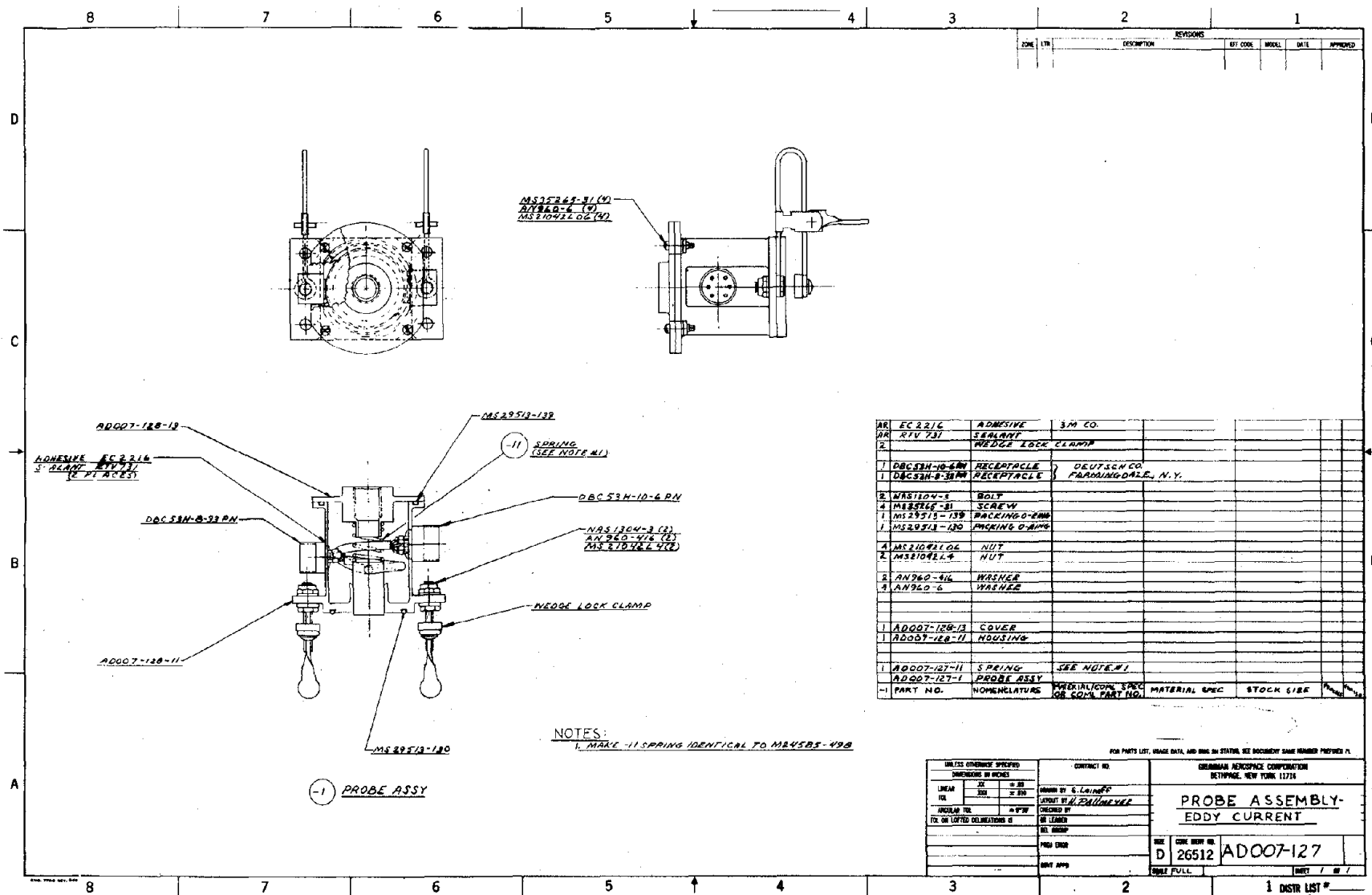


Figure 4-17 Eddy Current Probe Assembly

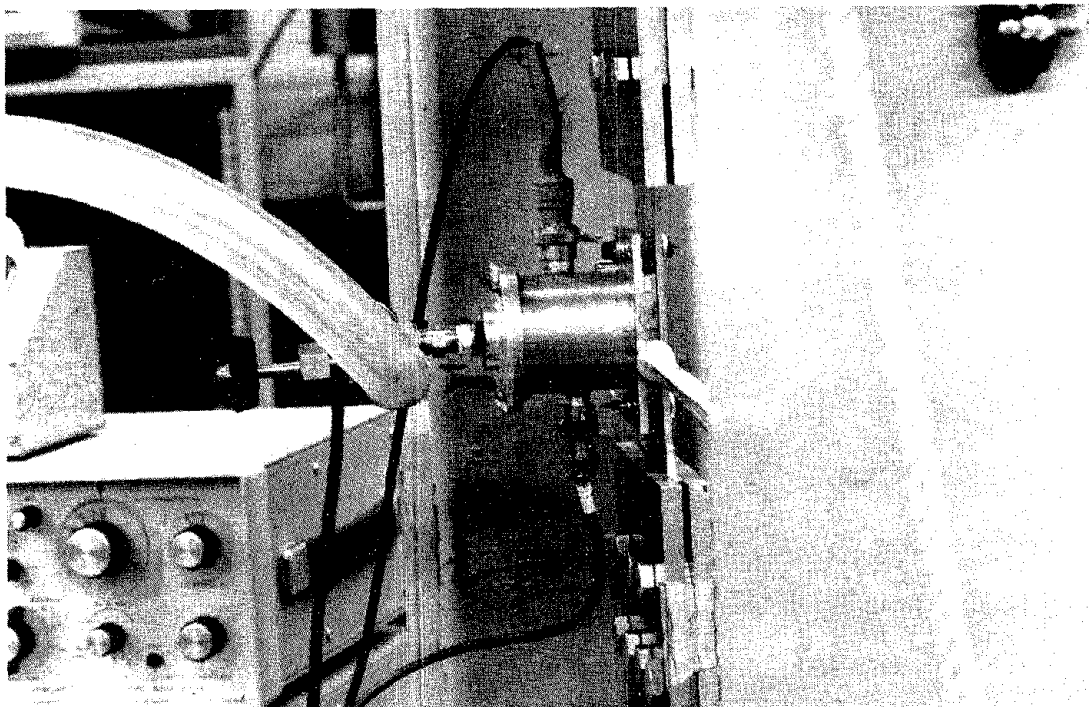


Figure 4-18 Vacuum Leak Detector Unit

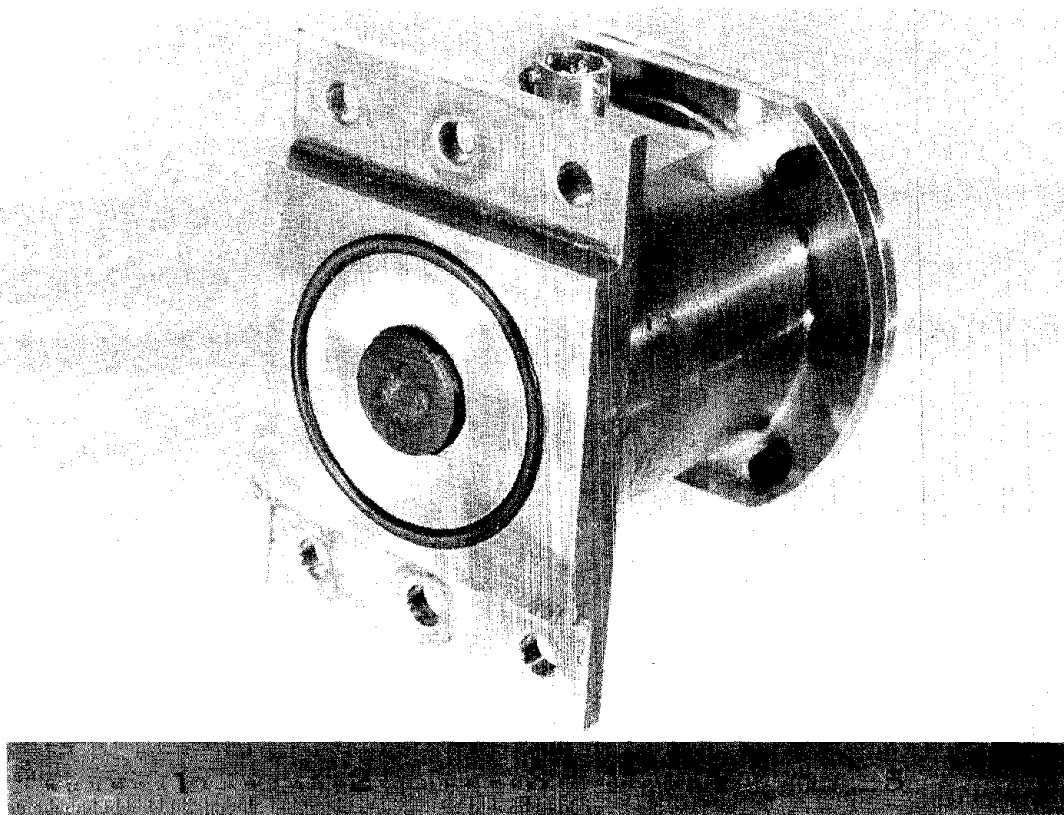


Figure 4-19 MRA Probe

The deep-penetration, eddy-current method was selected over conventional eddy-current methods because of their depth-sensitivity limitations. The deep-penetration method employs a Magnetic Reaction Analyzer (MRA) system that uses an eddy-current coil to generate a field in the specimen and a Hall device to detect minor variations in the field. By using the Hall device, greater depth sensitivity is possible since it is not necessary to detect minute field changes in large eddy-current coils, which are necessary in standard instruments to achieve sufficient penetration. A custom-made probe meeting frequency, effective area, and dimensional specifications was required for the tests planned for this program. Figure 4-19 is a photograph of the custom probe. Referred to as an MRA Differential Probe, it was manufactured by F. W. Bell, Inc. of Columbus, Ohio. The coil consists of 40 turns of No. 26 wire on 1/2 in. diameter. It is designed to operate in a differential mode at an operating frequency of 2000 Hz.

The leak detector unit was designed to be attached to the test specimens prior to flaw growth cycling and to remain on the specimen until crack-through is detected. This procedure made it impossible to collect correlating data for other NDT methods on the same specimens. The sensitivity of the MRA probe seems quite good, detecting the presence of the flaw slightly after the completion of the sharpening cycles on the Phase I specimens. The results of MRA testing are shown in Table 4-10. Relative to conventional eddy current methods the MRA probe is quite sensitive, detecting flaws at approximately .045 in. depth.

Visual Observations

In earlier testing the appearance of a dimple on the back face of a cyclic flaw growth specimen was noted significantly earlier than crack-through. This dimple is associated with the plastic zone which develops in front of a propagating crack. The effect is enhanced by polishing the surface with fine grit emery paper prior to flaw growth cycling. The appearance of the dimple was noted on the test specimens in this program, for which the leak detector was not used. This data provided a check of the sensitivity of NDT methods by confirming the proximity of the crack to the back face.

Conclusions

Shear wave ultrasonics provided the most sensitive detection of flaws in the program specimens, picking up flaws which were .030 in. to .040 in deep. The deep penetration MRA instrument also provided good results, detecting flaws approximately .045 in deep. Surface wave ultrasonics did not detect flaws until they were more than halfway through the specimen depth (0.70 in.). Conventional eddy currents provided the poorest sensitivity, detecting cracks only after they were three-quarters through the depth (.095 in.).

The MRA method does not require coupling to the article being examined as does the shear wave method, but both require 100% scanning of suspected areas. Only surface wave ultrasonics offers area scanning.

TABLE 4-10 MRA RESULTS

Specimen No.	Cycles	Crack Data		MRA Meter Reading Microamps
		Front Surface Width, in.	Back Surface Width, in.	
353493-3	1500*	.090	-	11.0
	4000	.145	-	12.5
	4500	.160	-	15.0
	6000	.205	-	17.0
	7500	.270	-	24.0
	8000	.300	-	27.0
353493-5	1000*	.085	-	8.0
	2000	.105	-	12.0
	3500	.135	-	13.0
	4000	.150	-	13.0
	5000	.190	-	14.0
	6000	.225	-	14.5
	7000	.290	-	15.0
	8500	.460	-	23.0
	8750**	.510	.080	48.0
353494-1	1000*	.105	-	5.5
	2000	.130	-	15.5
	3000	.160	-	16.0
	4000	.200	-	28.0
	5000	.245	-	36.0
	6000	.360	-	38.0
	6312**	.460	.080	>100.0
* First Point Detectable ** Leak Detector Indication				

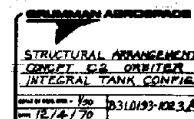
FABRICABILITY

Construction methods for laminated tanks have been studied. Tank weights have been developed for monolithic and laminated tanks. The problems related to manufacturing adhesive bonded tanks have been examined in some detail. An investigation to determine the best preparation methods and procedures for adhesive bonding of 2219-T87 was conducted. Weld strength of diffusion bonded plate was determined. Formability of adhesive bonded and roll diffusion laminates was studied.

Weight Comparison of Shuttle Orbiter Tanks

Stress analysis and weight calculations have been performed for monolithic and adhesive bonded laminated tanks for the C2F Orbiter configuration. Tank geometry is shown in Figure 4-20. The criteria and ground rules for this investigation are summarized below:

- The designs shall provide zero leakage for both the LO₂ and LH₂ tanks during the design life and after any predicted crack growth.
- Maximum system tank pressure:
LH₂ 39 PSIA; LO₂ 49 PSIA
- Negative pressure shall not be a design condition
- For the laminated design the tank structure shall meet all mission requirements with limited flaw growth. In addition it shall withstand limit design loads after the loss of a single primary structural member (such as a stringer).
- Crack length in one of the skins of the laminated design is assumed small so that the resulting secondary stresses in the adjacent skins are negligible. No extensive delamination is assumed.
- The ultimate factor of safety of the initial laminated structural design is to be no less than 1.5.
- The LH₂ and LO₂ tanks shall be separated (no common bulkhead). End domes are to be $1/\sqrt{2}$ ellipses.
- Tank material is to be 2219-T87 aluminum alloy.
- Factors of safety for the monolithic tanks will be based on fracture mechanics analyses.
- Material yield shall not occur at proof pressure.
- For the flaw growth study, the vehicle life shall be defined as 110 orbital flights (100 mission flights and 10 additional flights to account for preflight checkout). A scatter factor of four is assumed so that fracture mechanics calculations are made for 440 cycles.
- Only three-skin construction shall be considered in the laminated tank design.
- All-welded construction is to be used for LH₂ and LO₂ monolithic designs.
- All stiffeners are external to the tank for both the monolithic and laminated designs.



4-33

FOLDOUT FRAME 2

FOLDOUT FRAME /

Limit design pressures are shown in Figure 4-21. Critical design load envelopes are presented in Figures 4-22 thru 4-29 for limit and ultimate load intensity values. These design envelopes are based on an assumed ultimate factor of safety of 1.5 for compression and shear, and 1.75 for principal tension stress. For the monolithic designs these loads are used directly for tank sizing. For the laminated design, the ultimate tensile load envelopes were reduced by a factor of 1.5/1.75. These loads were then used for sizing the laminated skin-stringer structure.

Monolithic design concepts for the LO₂ and LH₂ tanks are shown in Figures 4-30 and 4-31, respectively. Both tanks are integrally machined from 2219-T87 plate. Wall thicknesses and stiffener dimensions are established by tensile, compressive and fracture mechanics considerations. Wall thicknesses are then increased by 10% to account for secondary stresses in the walls resulting from restraints by the frames and stringers. Final wall thicknesses and stringer sections are shown in Figures 4-30 and 4-31.

Laminated design concepts for the LO₂ and LH₂ tanks are shown in Figures 4-32 and 4-33. Wall thicknesses are determined from pressure and dynamic loading conditions. Hat section stiffeners are assumed for compression analysis. Having obtained a required wall thickness and stiffener configuration, the failure of one stiffener is assumed and the section checked for limit loads with ultimate allowables. Wall thicknesses are then increased 10% to account for secondary stresses as in the monolithic design. The inner skin of the LO₂ tank is welded to prevent LO₂ from coming in contact with the adhesive. The middle skin of both the LO₂ and LH₂ tanks is of constant thickness, and the inner and outer skins are chem-milled to meet net thickness requirements. Skin splices are staggered to reduce load peaking and maximize path lengths in order to minimize chances of leakage.

Weights of the monolithic and adhesive bonded tanks are shown in Table 4-11. The weight of the METLBOND 329 adhesive is assumed to be 0.075 lb/ft². This includes an allowance for scrim cloth. The use of scrim cloth is currently considered essential to manufacturing feasibility and to the control of bond line thickness. This comparison covers only the basic LO₂ and LH₂ skin-stringer tank structure and does not include attachment point bulkheads, frames, Y-rings, or skirts.

For purposes of analysis, the designs were sized at the top, bottom and middle of the tank, and the sections thus obtained were considered to be typical for the quadrant of the tank.

The weight of the monolithic tanks allows for an initial proof test. Proof test requirements, to the extent dictated by a fracture mechanics approach, are not considered applicable to the laminated tank concept.

The laminated tank designs of Figures 4-32 and 4-33 show a frame detail consisting of a formed zee or channel bonded to a tee clip which, in turn, is bonded to the tank wall. If the outer laminate of the three wall tank is machined from a plate of sufficient thickness to provide a vertical leg for attachment of the frame, similar to the detail shown for the monolithic tanks, a weight saving of 331.9 lb per Orbiter can be achieved.

Summarizing Table 4-11, the monolithic LO₂ tank weighs 1760.0 lb and the Metlbond 329 laminated LO₂ tank weighs 1916.7 lb. The monolithic LO₂ tank is thus 156.7 lb or 12% lighter than the laminated LO₂ tank. The monolithic LH₂ tank weighs 4040.3 lb and the Metlbond 329 laminated tank weighs 4720.8 lb. The advantage again is in favor of the monolithic LH₂ tank which is 680.5 lb or 14% lighter than the laminated LH₂ tank. If the integrally machined frame attachment is used the advantage for the monolithic tanks is reduced from approximately 14% to 10%.

- LOAD CONDITIONS:
1. END BOOST
 2. MAX GN (-)
 3. MAX GN (+)
 4. MAX GN (+)
 5. TROD PT LANDING

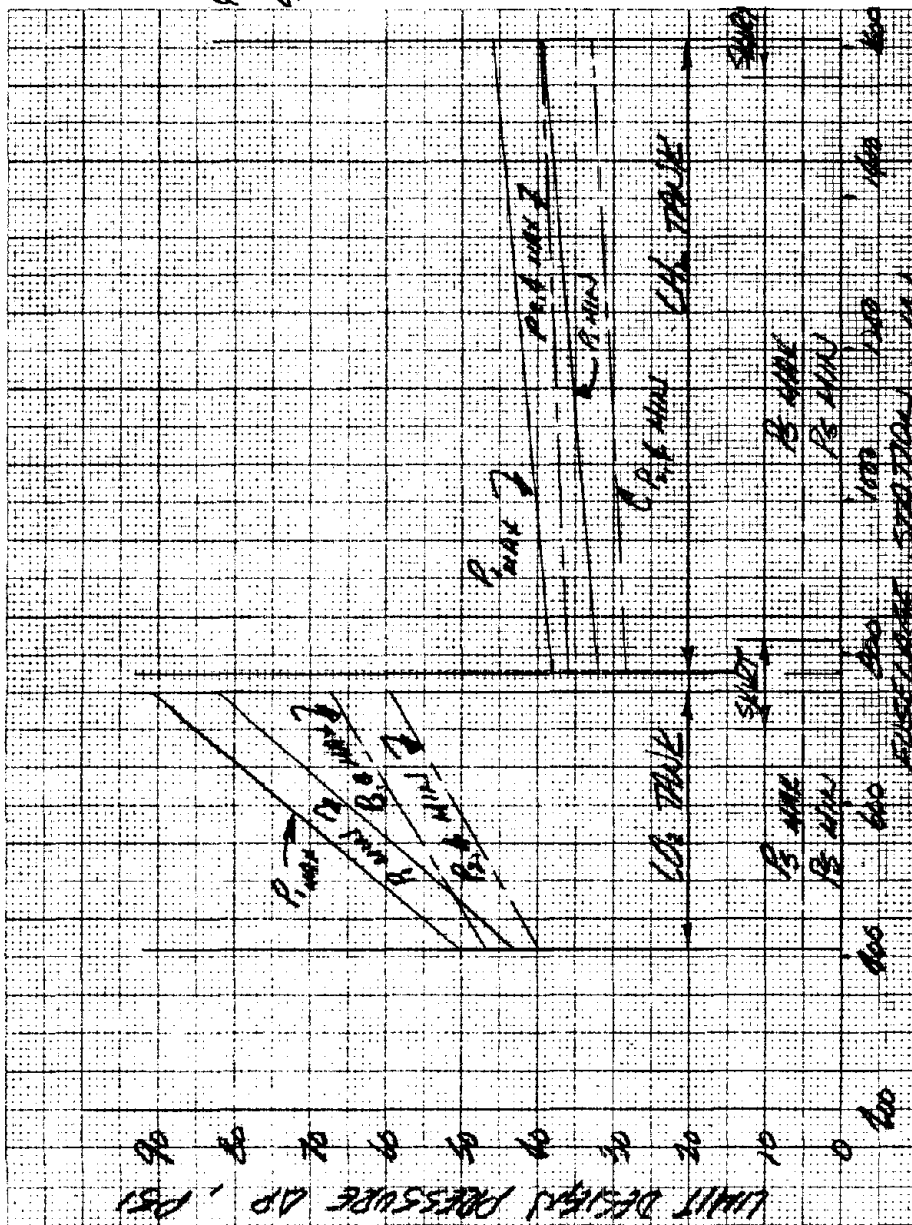


Figure 4-21 Orbiter Design C2F, Min-Max Limit Design Pressures (ΔP)

1. END BOOST
2. MAX GA'(-)
4. MAX GA(+)
5. TWO PT LANDING.

$$N_0 = \text{Hoop Load}$$

N_{ϕ} = LONGITUDINAL LOAD

$$= \frac{1}{2} \left(\frac{P_{TOT}}{2\pi R} - \frac{M_{TOT}}{\pi R^2} \right) + \frac{P_D}{2}$$

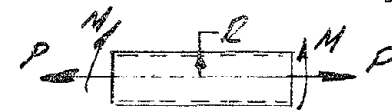


Figure 4-22 Orbiter Design C2F, Limit Load-Intensity Envelope at Top of Tank

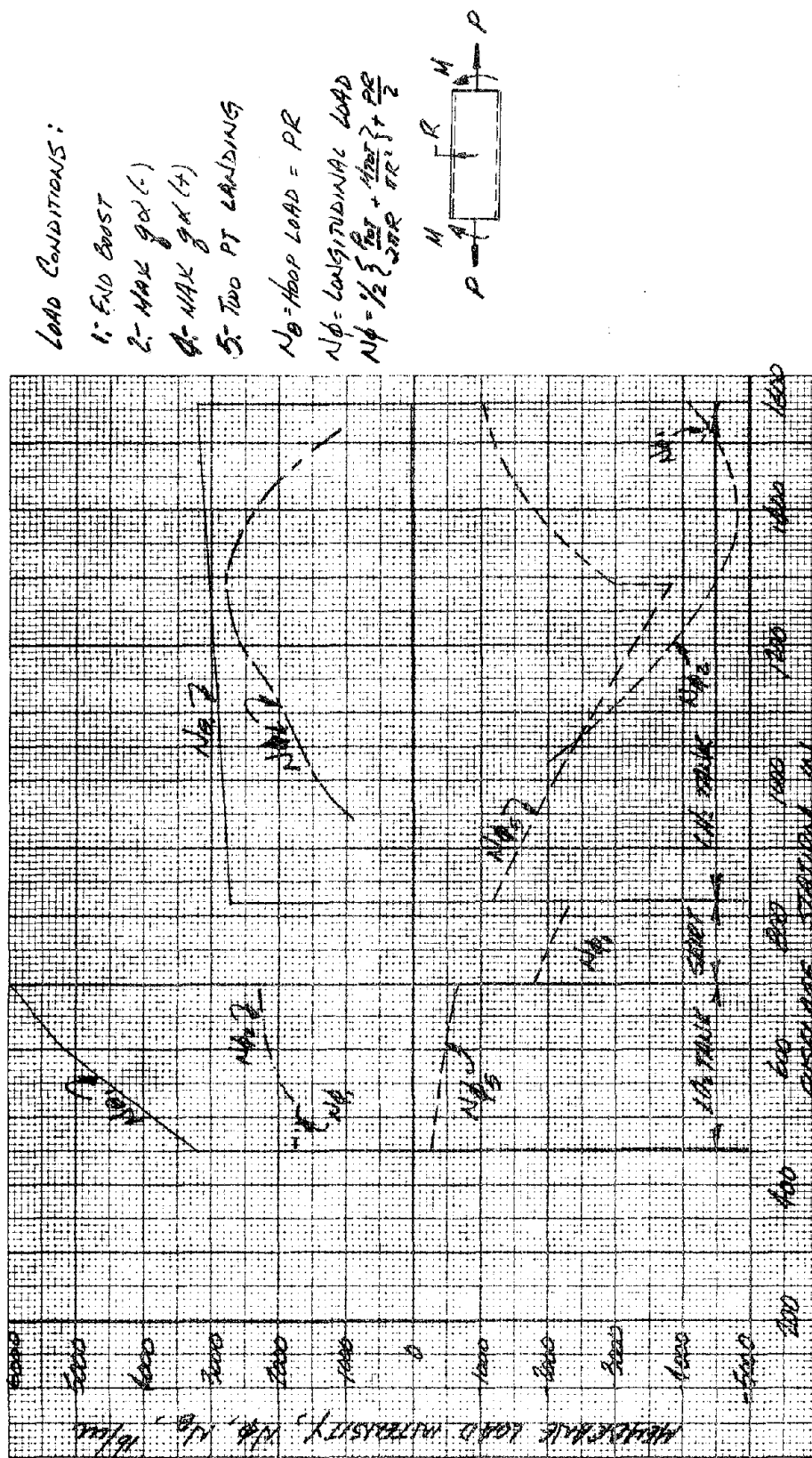


Figure 4-23 Orbiter Design C2F, Limit Load-Intensity Envelope at Bottom of Tank

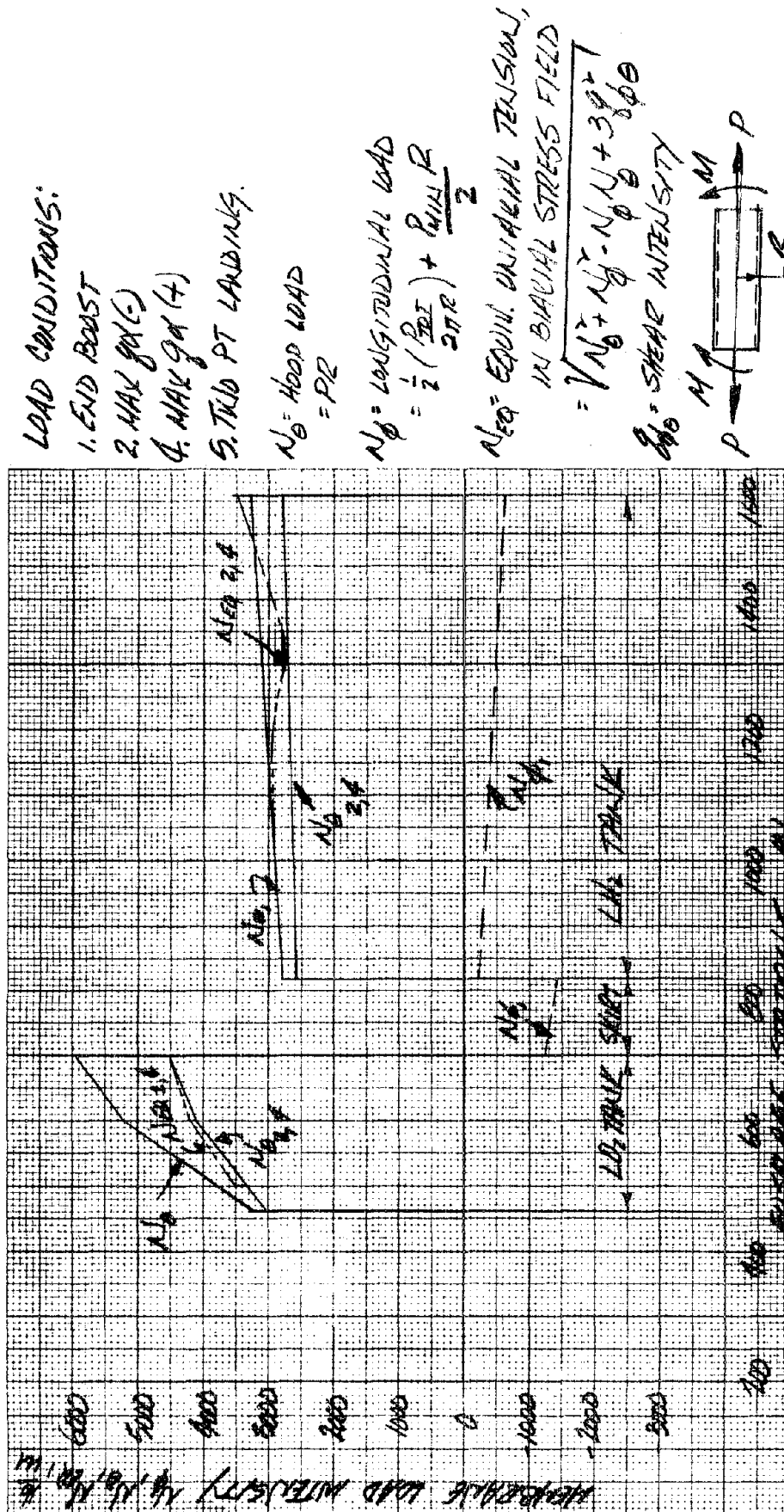


Figure 4-24 Orbiter Design C2F, Limit Load-Intensity Envelope At Tank Center

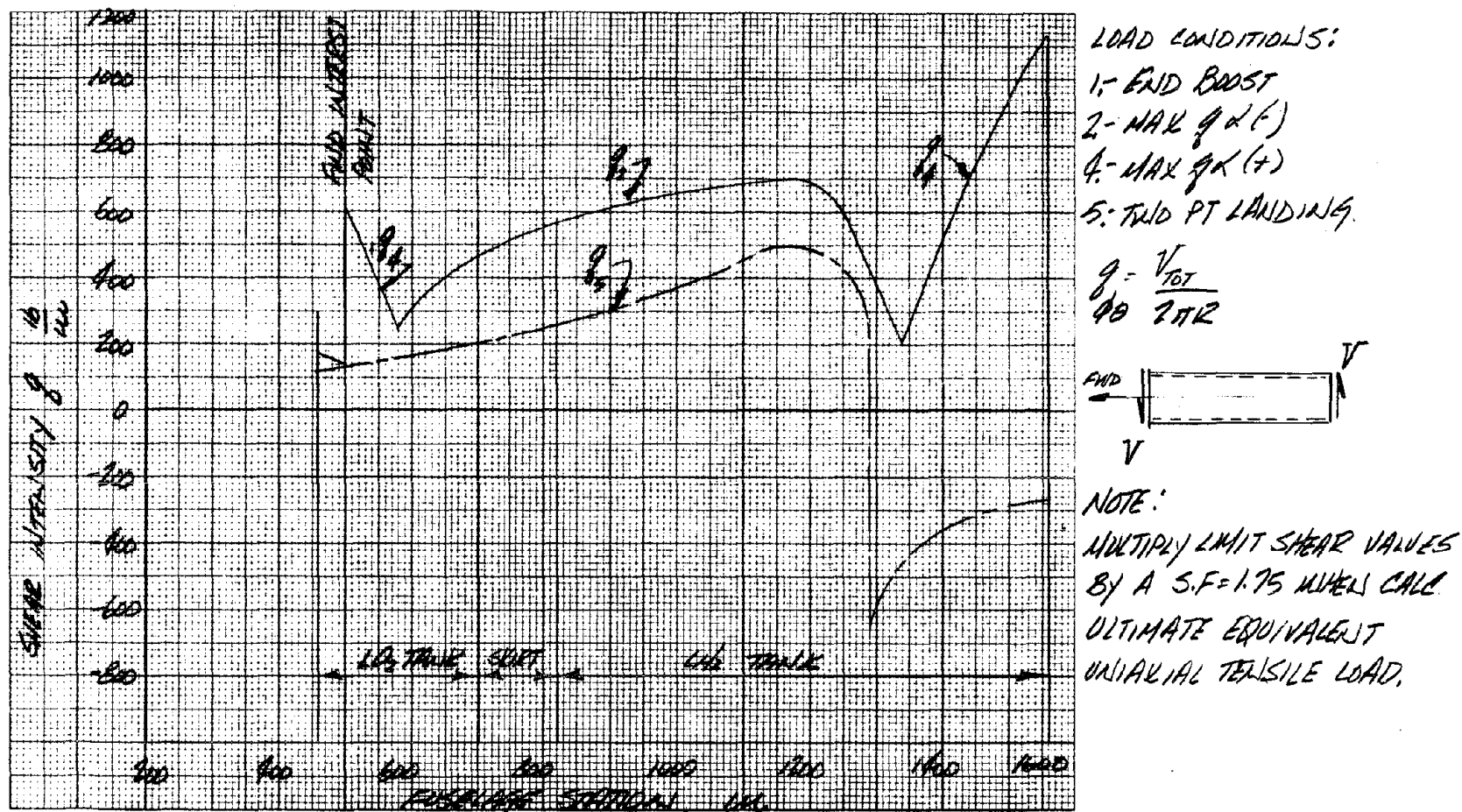
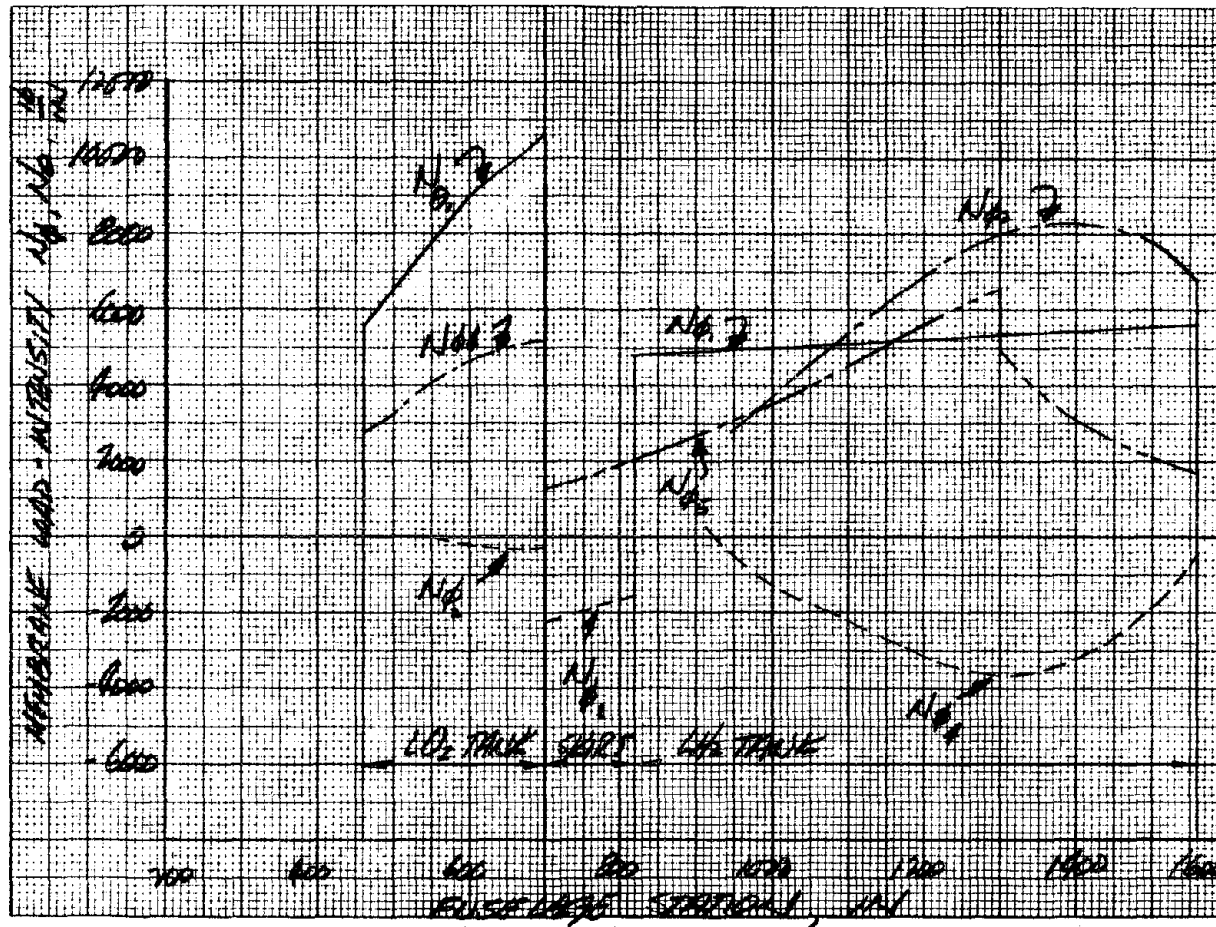


Figure 4-25 Orbiter Design C2F, Limit Shear-Intensity Envelope at Tank Center



LOAD CONDITIONS:

1. END BOOST
2. MAX $g_X(-)$
3. MAX $g_X(+)$
4. MAX $g_X(+)$
5. TWO PT LANDING.

TENSION: (S.F. = 1.75)

N_θ = HOOP LOAD
= 1.75 (PR)

N_ϕ = LONGITUDINAL LOAD

$$= 1.75 \left[\frac{1}{2} \left(\frac{P_{TOT}}{2\pi R} - \frac{M_{TOT}}{\pi R^2} \right) + \frac{P_{MAX} R}{2} \right]$$

COMPRESSION: (S.F. = 1.5)

$$N_\phi = 1.5 \left[\frac{1}{2} \left(\frac{P_{TOT}}{2\pi R} - \frac{M_{TOT}}{\pi R^2} \right) + \frac{P_{MIN} R}{2} \right]$$



Figure 4-26 Orbiter Design C2F, Ultimate Load-Intensity Envelope at Top of Tank



LOAD CONDITIONS:

1. END BOOST
2. MAX $g_x (-)$
3. MAX $g_x (+)$
4. MAX $g_x (+)$
5. TWO PT LANDING

TENSION: (S.F. = 1.75)

$$N_{\theta} = \text{HOOP LOAD} \\ = 1.75 (PR)$$

$$N_{\phi} = \text{LONGITUDINAL LOAD} \\ = 1.75 \left[\frac{1}{2} \left(\frac{P_{DT}}{2\pi R} + \frac{M_{DT}}{\pi R^2} \right) + \frac{P_{MAX} R}{2} \right]$$

COMPRESSION: (S.F. = 1.5)

$$N_{\phi} = 1.5 \left[\frac{1}{2} \left(\frac{P_{DT}}{2\pi R} + \frac{M_{DT}}{\pi R^2} \right) + \frac{P_{MIN} R}{2} \right]$$

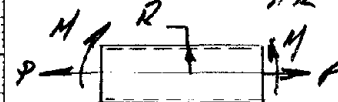
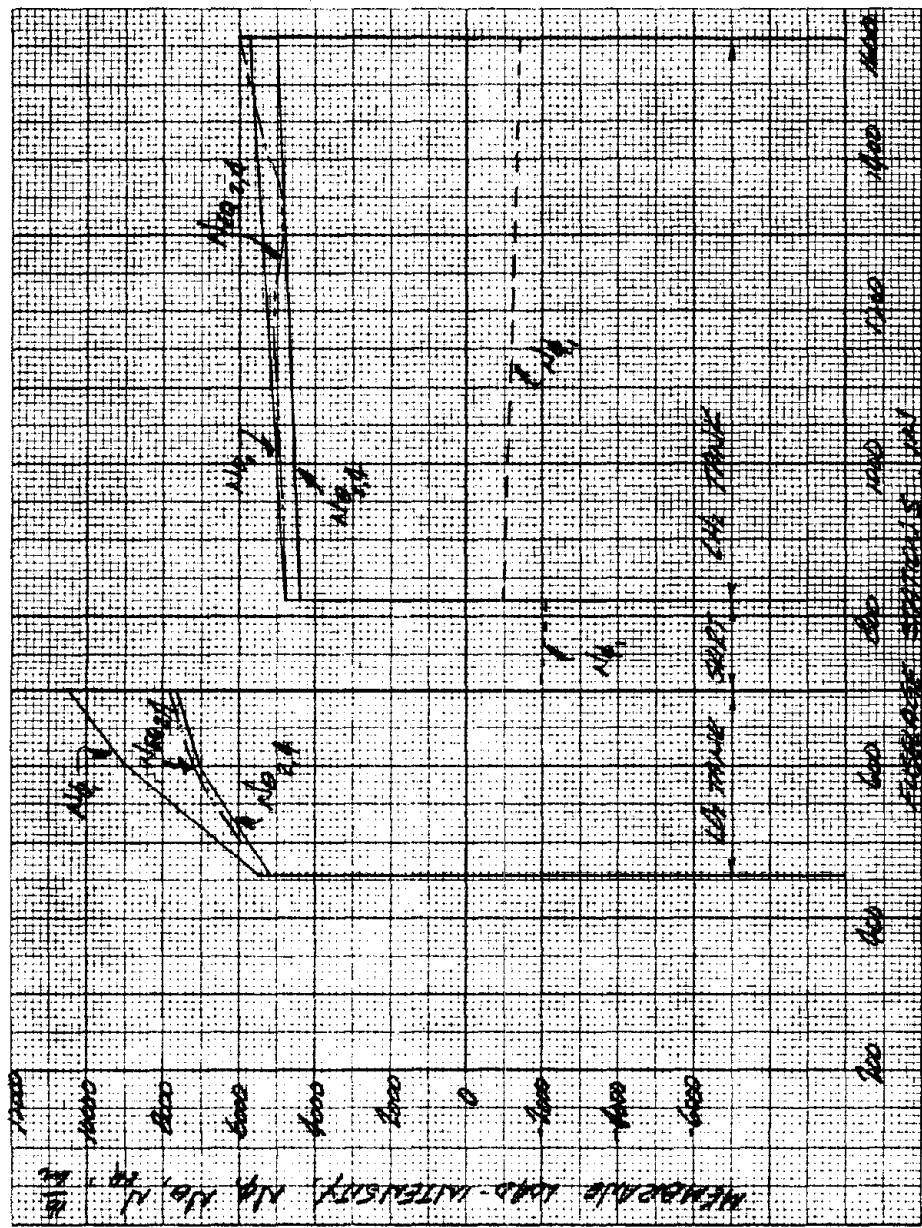


Figure 4-27 Orbiter Design C2F, Ultimate Load-Intensity Envelope at Bottom of Tank

Reproduced from
best available copy.



LOAD CONDITIONS:

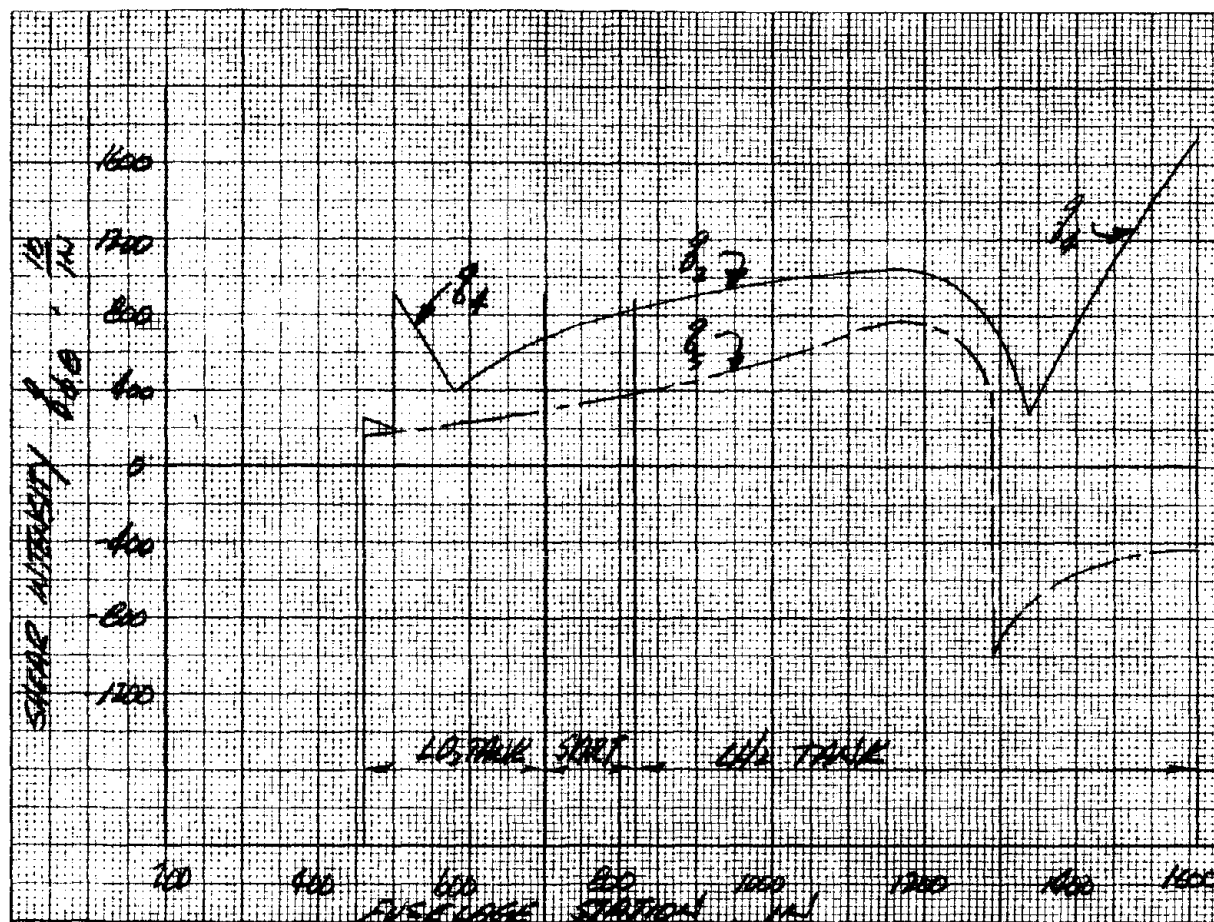
1. END BOOST
 2. MAX g_A (+)
 3. MAX g_A (-)
 4. MAX g_A (+)
 5. TILD BY RANDOMLY
- N_D - HOOP LOAD = 1.75 (PR) S.F.
- N_L - LONGITUDINAL LOAD
- $N_{\phi} = 1.5 \left[\frac{1}{2} \left(\frac{P_{OT}}{2TR} \right) \right] + \frac{P_{INT} R}{2}$
- N_{EQ} - EQUILIBRIUM TENSION, IN BIAXIAL STRESS FIELD (S.F. = 1.75)

$$N_{EQ} = 1.75 \sqrt{N_D^2 + N_L^2 - N_D N_L + 3 g_A^2}$$

g_A - SHEAR INTENSITY



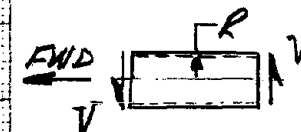
Figure 4-28 Orbiter Design C2F, Ultimate Load-Intensity Envelope at Tank Center



LOAD CONDITIONS:

1. END BOOST
2. MAX $g_x (-)$
3. MAX $g_x (+)$
5. TWO PT LANDING

$$g_{\phi} = 1.5 \left[\frac{V_{TOT}}{2TR} \right]$$



NOTE:

SEE NOTE 11.1 FIG 4-25
FOR ULT. UNIAXIAL
TENSILE LOADS.

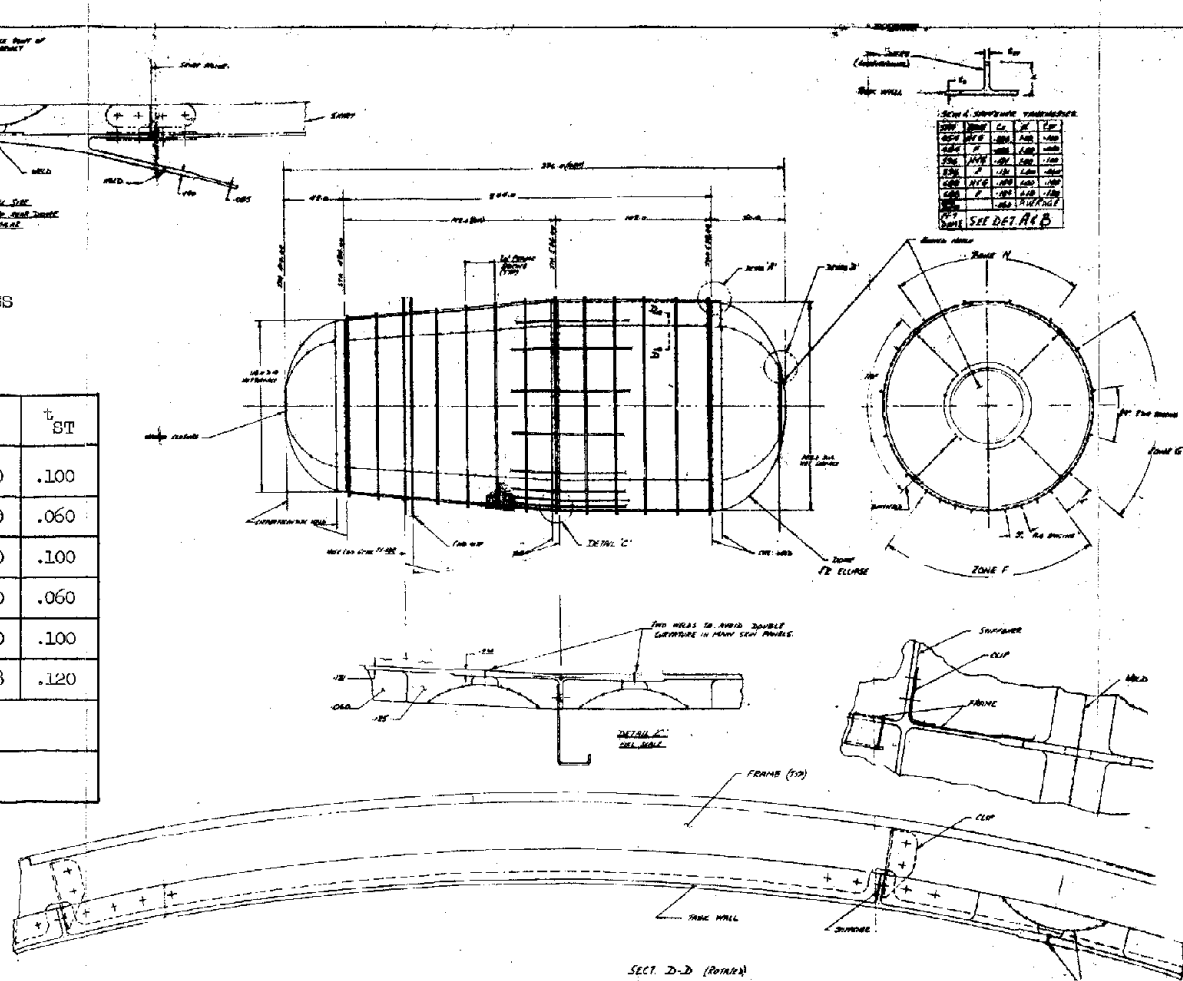
Reproduced from
best available copy.

Figure 4-29 Orbiter Design C2F, Ultimate Shear-Intensity Envelope at Tank Center

Reproduced from
best available copy.

SKIN & STIFFENER THICKNESS

STA	ZONE	t _s	d	t _{ST}
454	H & G	.086	1.00	.100
454	F	.086	1.00	.060
596	H & G	.131	1.00	.100
596	F	.131	1.00	.060
688	H & G	.154	1.00	.100
688	F	.154	1.18	.120
FWD DOME		.060 AVERAGE		
AFT DOME	SEE DETAIL A & B			



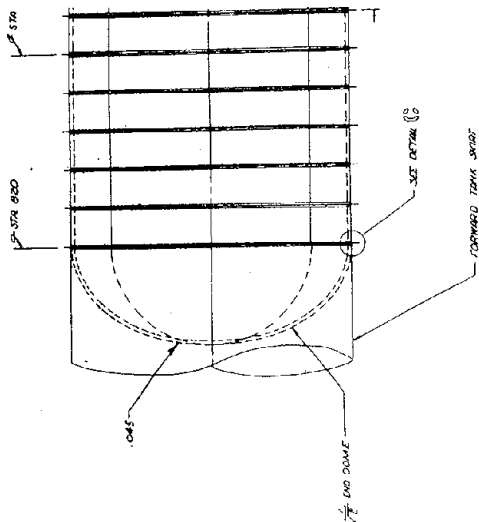
- NOTES:
1. MAX. ALLOW. STRESS: 25,000 PSI (TENSILE)
STRESSING: 25,000 PSI (TENSILE)
25,000 PSI
 2. ALL SURFACES: 25,000 PSI (TENSILE)
 3. MAX. ALLOW. STRESS: 1/2 MAX. ALLOW. STRESS
 4. FOLDOUTS: 25,000 PSI (TENSILE)
(FOLDOUTS: 25,000 PSI (TENSILE)
NOT TENSILE. To be made in special
direction.)

Figure 4-30. C2F Orbiter Monolithic Liquid Oxygen Tank

FOLDOUT FRAME /

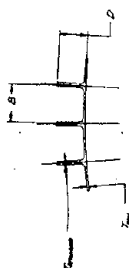
4-44

FOLDOUT FRAME 2



TANK LOWER DIMENSIONS				TANK JOST DIMENSIONS			
STA	B	D	T _{max}	T _{min}	B	D	T _{max}
850	090	244	1.60	0.75	090	372	1.00
900	090	244	1.60	0.70	090	372	1.00
950	090	244	1.60	0.65	090	372	1.00
1000	090	244	1.60	0.60	090	372	1.00
1050	090	244	1.60	0.55	090	372	1.00
1100	090	244	1.60	0.50	090	372	1.00
1150	090	244	1.60	0.45	090	372	1.00
1200	090	244	1.60	0.40	090	372	1.00
1250	090	244	1.60	0.35	090	372	1.00
1300	090	244	1.60	0.30	090	372	1.00
1350	090	244	1.60	0.25	090	372	1.00
1400	090	244	1.60	0.20	090	372	1.00
1450	090	244	1.60	0.15	090	372	1.00
1500	090	244	1.60	0.10	090	372	1.00
1550	090	244	1.60	0.05	090	372	1.00
1600	090	244	1.60	0.00	090	372	1.00

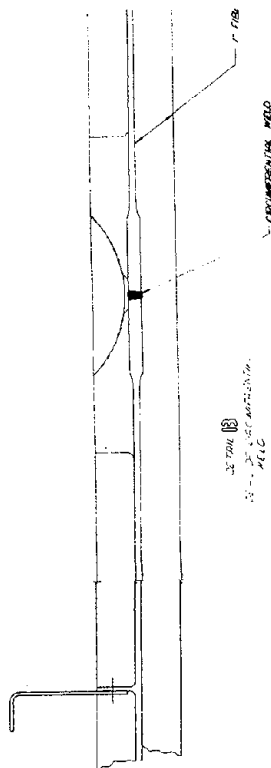
TANK WEL AND STIFFNESS GEOMETRY



FORWARD END DOME

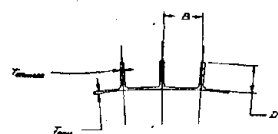


DETAIL 8
V-RING JOINT AT FORWARD
SHOT AND END DOME



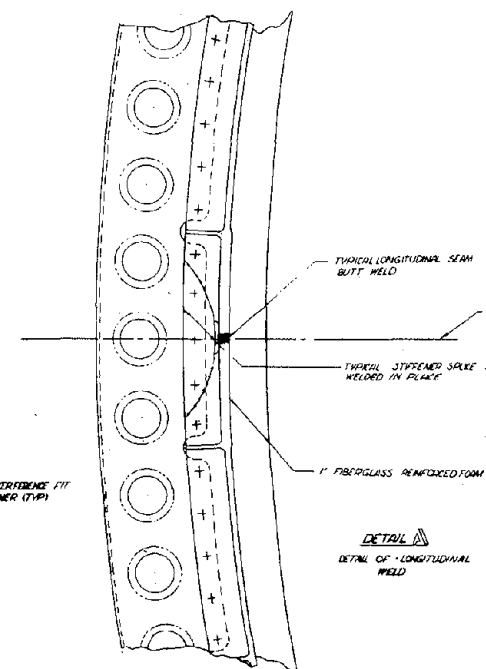
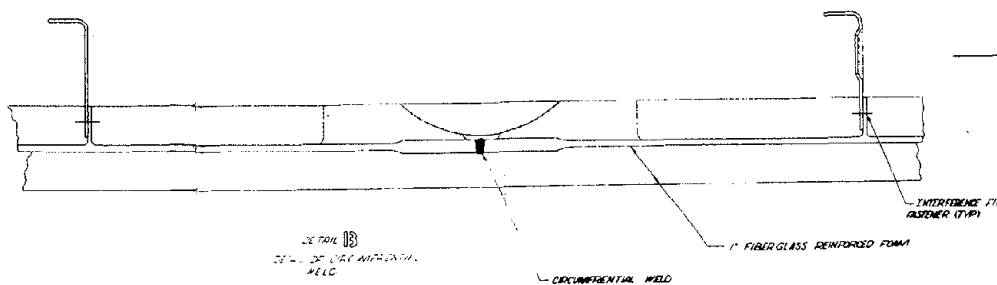
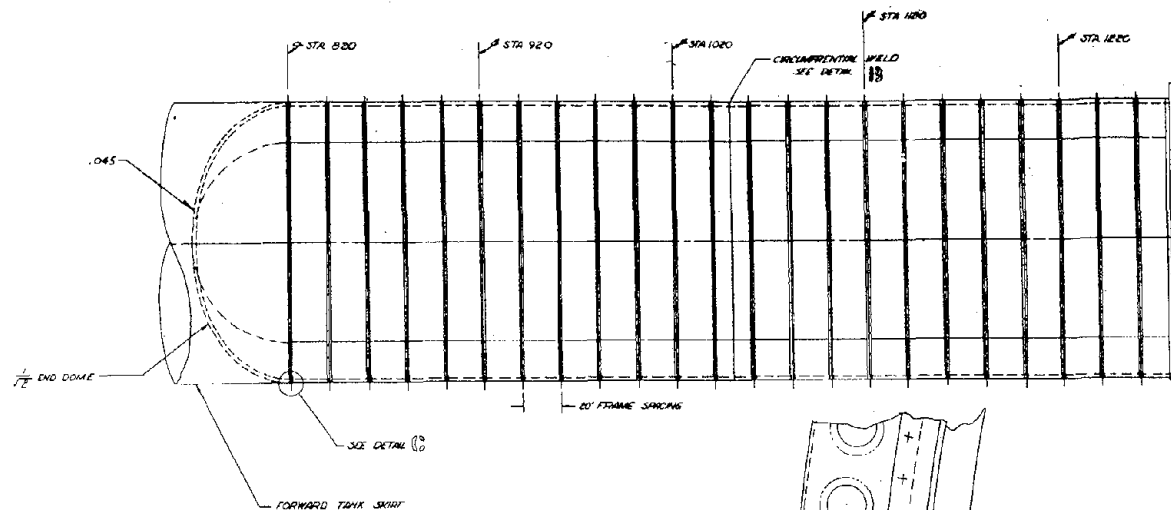
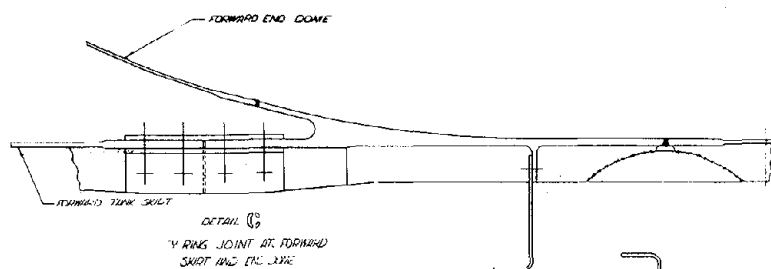
DETAIL 8
V-RING JOINT AT FORWARD
SHOT AND END DOME

FOLDOUT FRAME /



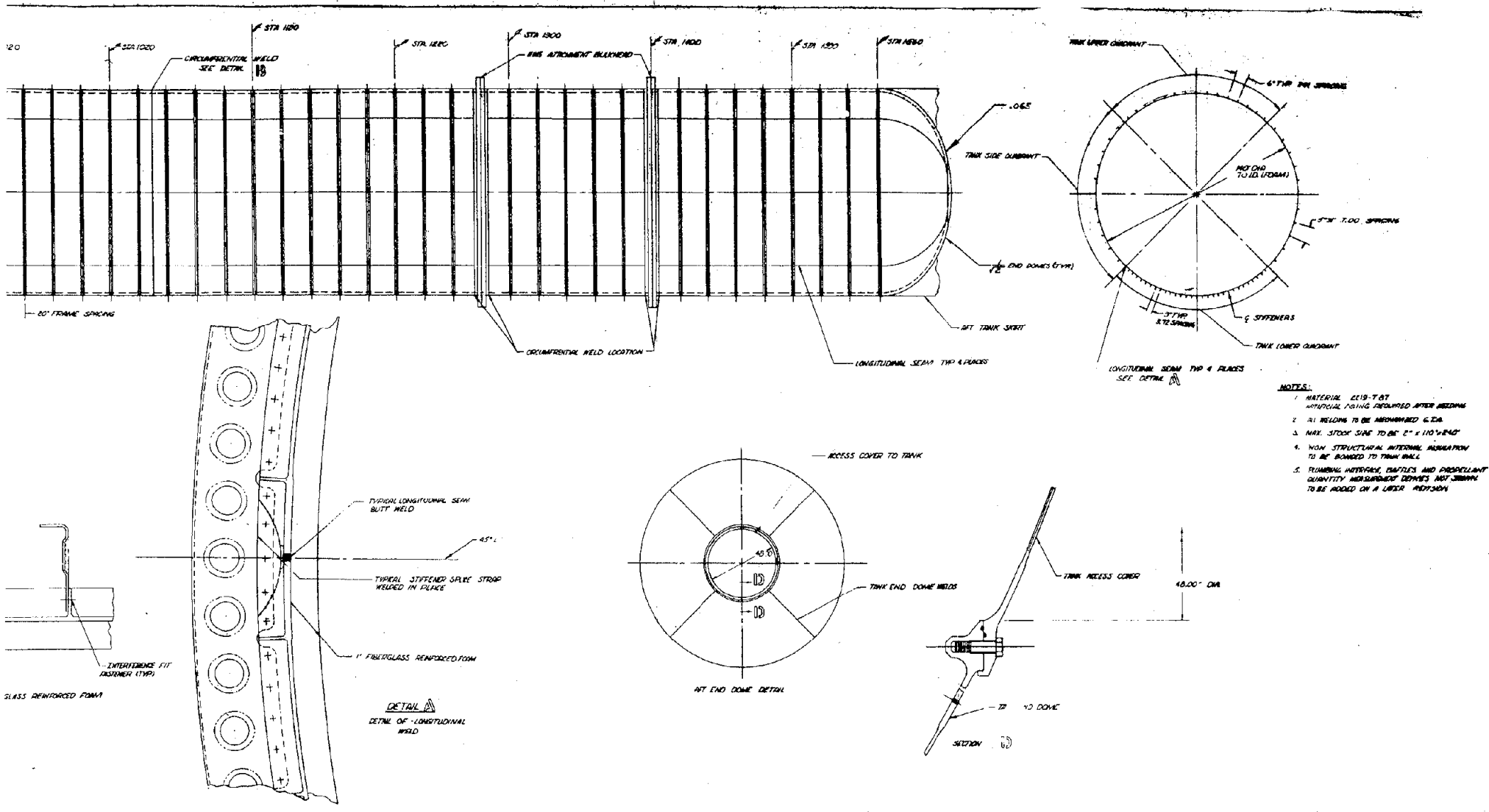
TANK UPPER QUADRANT				TANK LOWER QUADRANT				TANK SIDE QUADRANT				
STA	T _{max}	B	D	T _{max}	B	D	T _{max}	T _{max}	B	D	T _{max}	
820	.090	7.44	1.80	.070	.090	3.72	1.00	.059	.090	7.00	1.00	.074
900	.090	7.44	1.80	.070	.090	3.72	1.40	.069	.090	7.00	1.00	.074
1000	.090	7.44	1.80	.070	.090	3.72	1.40	.084	.090	7.00	1.00	.074
1100	.090	7.44	1.80	.090	.090	3.72	1.40	.096	.090	7.00	1.00	.074
1200	.090	7.44	1.80	.090	.090	3.72	1.70	.124	.090	7.00	1.00	.074
1300	.090	7.44	1.80	.110	.090	3.72	1.70	.113	.090	7.00	1.00	.074
1400	.090	7.44	1.80	.110	.090	3.72	1.70	.125	.090	7.00	1.00	.074
1500	.090	7.44	1.80	.117	.110	3.72	1.70	.165	.090	7.00	1.00	.074
1550	.090	7.44	1.80	.110	.090	3.72	1.70	.165	.090	7.00	1.00	.074

TANK WALL AND STIFFENER GEOMETRY



FOLDDOUT FRAME 1

FOLDDOUT FRAME 2

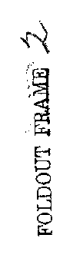


FOLDOUT FRAME 2

FOLDOUT FRAME 3

Figure 4-31 GEF Monolithic LH₂ Tank

FOLDOUT FRAME 4



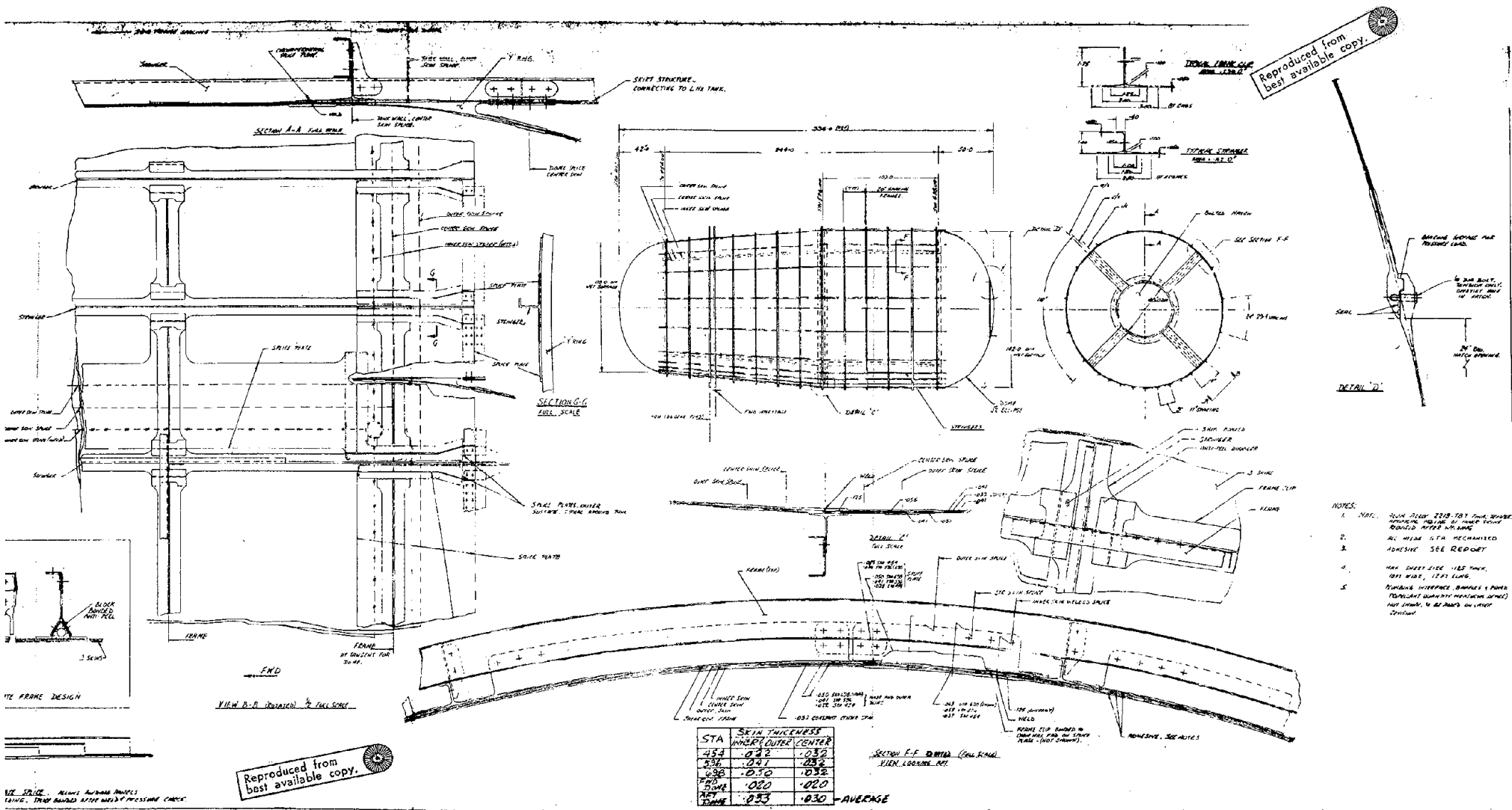
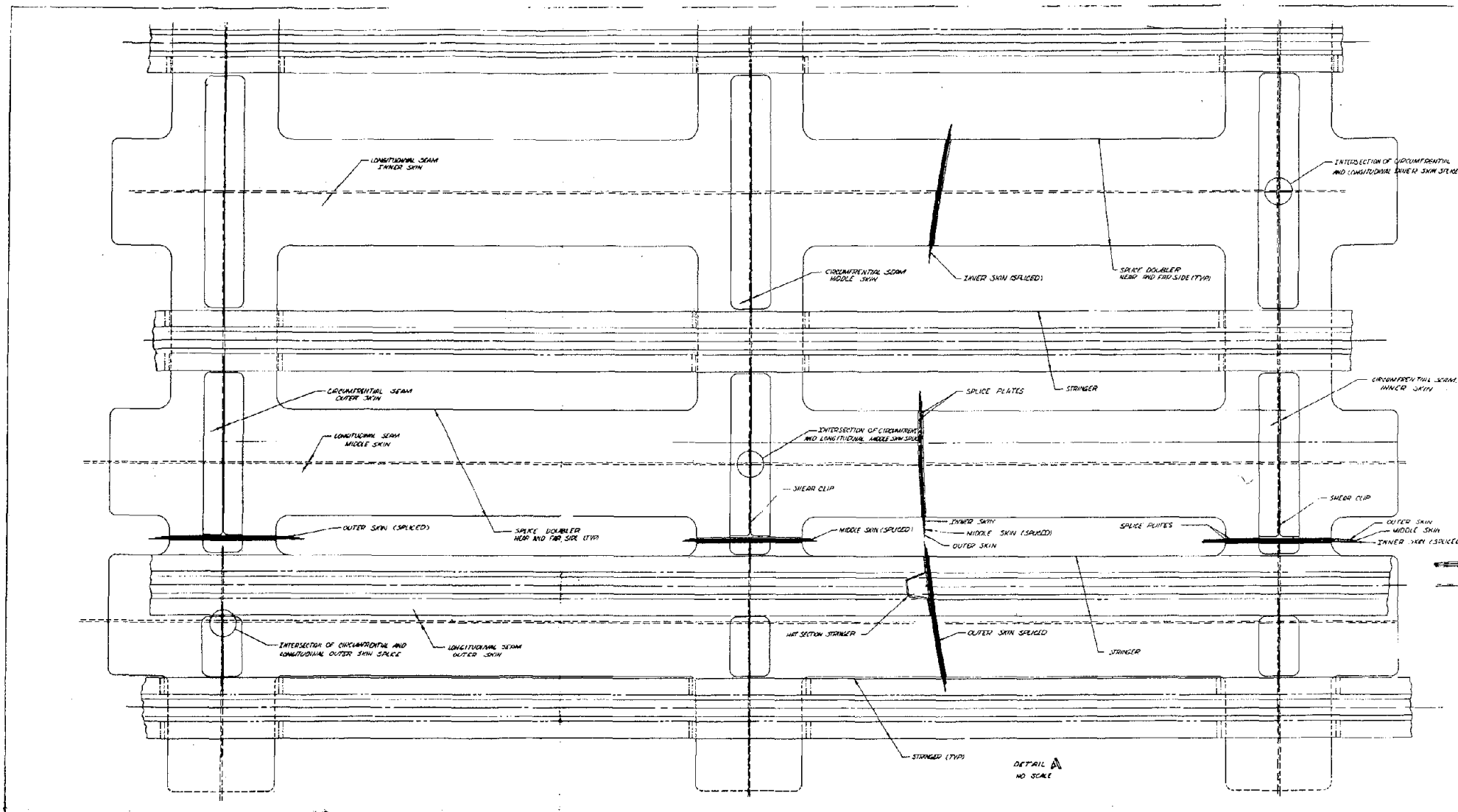


Figure 4-32 C2F Laminated Liquid Oxygen Tank

FOLDOUT FRAME 2

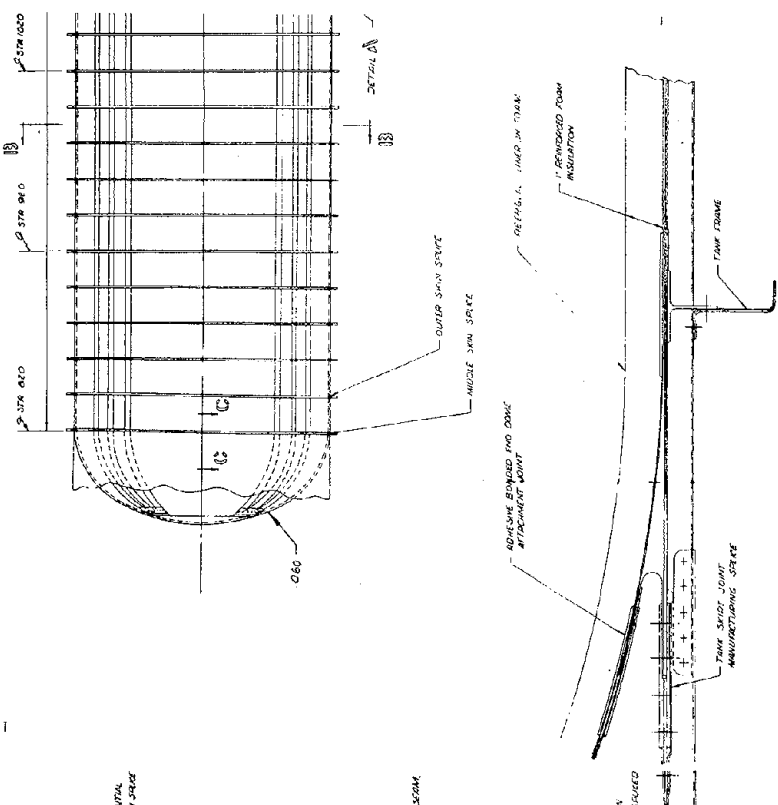
4-46

FOLDOUT FRAME 3



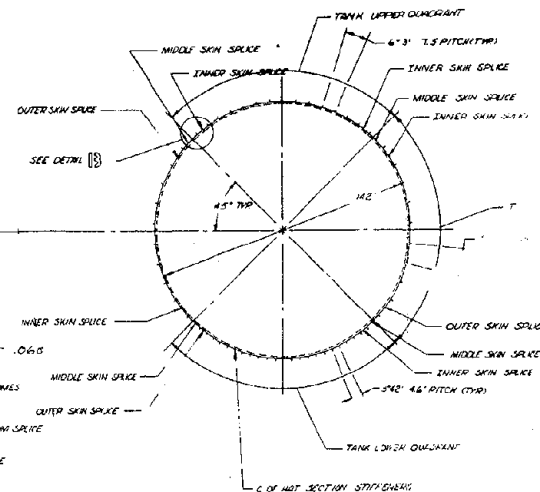
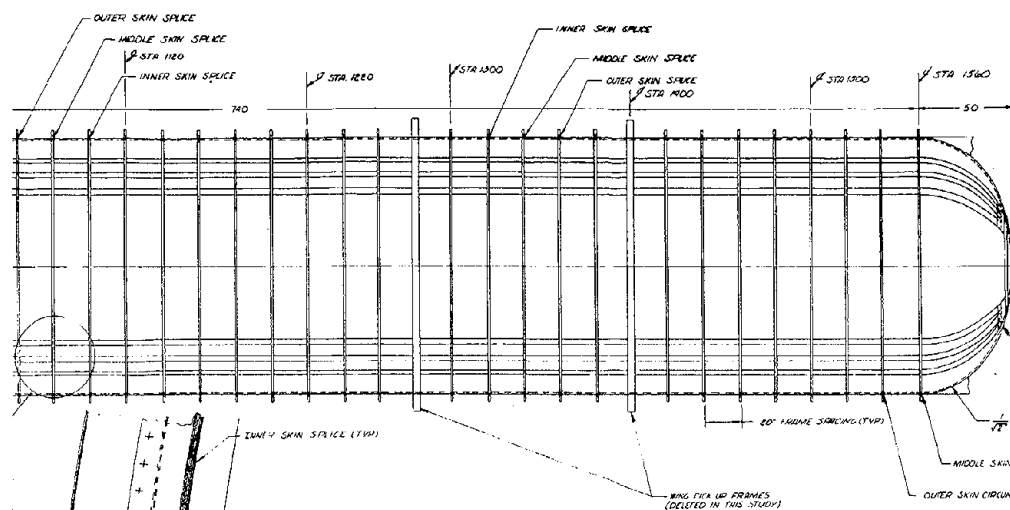
FOLDOUT FRAME /

FOLDOUT FRAME 2

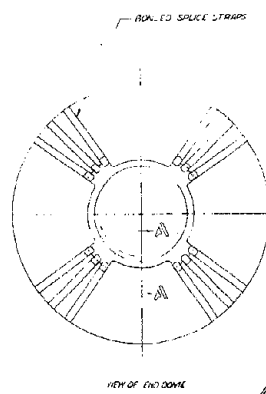
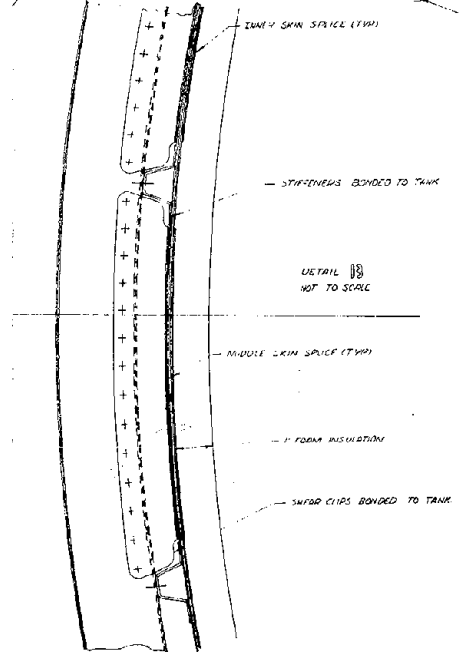


FOLDOUT FRAME³

5



SECTION B-B
1/4" FIBER INSULATION



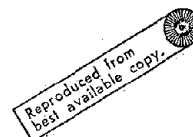
SECTION A-A
(FROM JEE)

STA	TANK UPPER QUADRANT			TANK LOWER QUADRANT			TANK SIDE QUADRANT		
	T _{max}	B	R _{max}	T _{max}	B	R _{max}	T _{max}	B	R _{max}
870	.078	7.5	.068	.090	4.6	.069	.078	7.00	.084
920	.078	7.5	.068	.090	4.6	.069	.078	7.00	.084
1000	.078	7.5	.068	.090	4.6	.069	.078	7.00	.084
1100	.078	7.5	.068	.090	4.6	.069	.078	7.00	.084
1200	.078	7.5	.068	.090	4.6	.069	.078	7.00	.084
1300	.078	7.5	.068	.090	4.6	.069	.078	7.00	.084
1400	.078	7.5	.068	.090	4.6	.069	.078	7.00	.084
1500	.078	7.5	.068	.090	4.6	.069	.078	7.00	.084
1560	.078	7.5	.068	.090	4.6	.069	.078	7.00	.084

TANK WALL AND STIFFENER DIMENSIONS

FOLDOUT FRAME 4

FOLDOUT FRAME 5



Tank

4-47

TABLE 4-11 WEIGHT COMPARISON, MONOLITHIC AND LAMINATED
DESIGN CONCEPTS

	Weight, lbs. (1)			
	Monolithic Design		Laminated Design Metlbond 329 Adhesive	
	IO ₂ Tank	LH ₂ Tank	IO ₂ Tank	LH ₂ Tank
<u>Aluminum (2219-T87) Material Per Tank:</u>				
Tank Walls and Stringers	1362.0	3649.7	1200.0	3390.4
Forward End Dome Skins	77.0	95.0	107.0 ⁽³⁾	154.5 ⁽³⁾
Aft End Dome Skins	221.0	112.0	190.0	154.5 ⁽³⁾
Splices	100.0	183.6	150.6	268.0
Frame Attachments (Per Figures 4 & 5)			93.9	238.0
<u>Aluminum Total</u>	1760.0	4040.3	1741.5	4205.4
<u>Bond Material Per Tank with Scrim Cloth (2)</u>				
Tank Walls			108.0	342.0
End Domes			45.6	53.8
Stringers and Frames			10.5	51.1
Splices			11.1	68.5
<u>Bond Total</u>			175.2	515.4
<u>Tank Total</u>			1916.7	4720.8
<u>One IO₂ Tank Plus One LH₂ Tank</u>	5800.3		6637.5	
<u>Combined Tank Weight Per Orbiter</u>	11,600.6		13,275.0	
<u>Weight Difference Per Orbiter</u>			+1674.4	
<u>Weight Saving with Integrally Machined Frame Attachment per Orbiter</u>			331.9	
<u>Total Weight Difference Per Orbiter with Integral Frame Attachment</u>			+1342.5	
NOTES:				
(1) Frames, y-rings, end dome hatches, and skin tolerances are not included in the weight comparison				
(2) Bond weight: Metlbond 329, wt = 0.075 lb/ft ²				
(3) Established by minimum sheet thickness of 0.020 in. per laminate				

Fabrication Of Large Adhesive Bonded Tanks

In the manufacture of large laminated tanks, a major problem is the manner in which the segments of the tank will be joined to form a tank assembly. Several alternate methods of splicing subassemblies are shown schematically in Figures 4-34 and 4-35.

Constraints will be placed on fabrication procedures both by the size of the final article and by material availability sizes. Diameters of both tanks are 140 in. The cylindrical section of the LH₂ tank is 740 in. long. If it is desired to bond and cure the entire LH₂ cylinder in one operation, existing autoclaves could contain the cylinders. Bonding with METLBOND 329 is done using 45 psi autoclave pressure at 350°F. Bonded panels for the L-1011 Tri Star airliner are fabricated in a 22 ft. (264 in.) by 66 ft (792 in.) autoclave capable of operating at 600°F temperature and pressures of 150 psi (Ref. 1) Information received from ALCOA indicates a maximum sheet size in .040 in. gage of 84 in. x 420 in. for 2219-T87.

Figures 4-34 and 4-35 show various methods of fabrication being considered based upon the available stock size of the 2219-T87. Methods 1A, B and C of Figure 4-34 show sheets rolled into cylindrical sections with longitudinal splices closing the cylinders. Based on 84 in. sheet width, nine such cylinders are required to complete the 740 in. cylinder length. These cylinders would be spliced as shown in Figure 4-35. (J).

The tank circumference, 440 in., is just 20 in. longer than the maximum sheet length of 420 in. Method A of Figure 4-34 uses two splices, 180° apart, of equal length sheet. Method B makes use of the full-length stock size and adds a small local piece, still using only two splices. Method C is similar to Method B but offsets splice locations to decrease possibility of leakage. Method D combines adhesive bonding with welding. The material would be rolled into short cylinders with edge members inserted and joined as in Figure 4-35 (M).

If it is desired to orient the sheets with the longitudinal direction along the axis of the tank, Method E of Figure 4-34 may be used. Six longitudinal splices are required to close the cylinder. The two cylindrical sections are joined as shown in Figure 4-35 (L). Method F combines the longitudinal orientation with the welded joint of Method D. In this case the two long cylinders would be joined by a circumferential weld, Figure 4-35 (K).

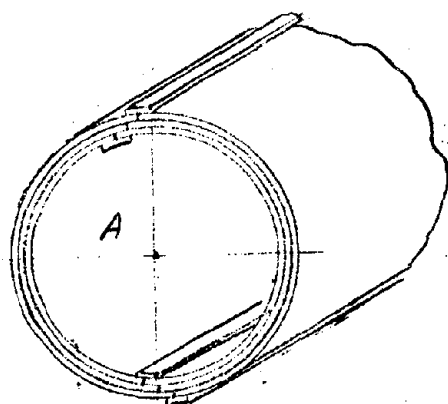
The concepts shown in Figures 4-34 and 4-35 are illustrated only schematically. Practical designs would include thickened areas at welds and adhesive splice areas.

All of these methods allow panels to be bonded and cured in the flat. After curing, the panels can be rolled to the required radius. If it is desired to roll the sheets before bonding, curved mandrel tooling would be required for curing.

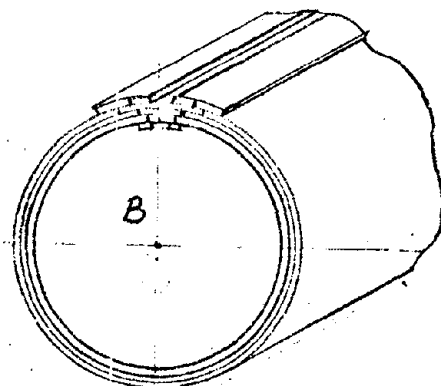
Laminated sheets must be oriented and held in position during curing. Provisions must be made to assure the required lap splice area is available for each sheet. Several methods of meeting this requirement are shown in Figures 4-36 and 4-37.

- Method A: Sheets of equal size are laminated such that equal offsets are made on two adjacent edges. When rolled, the lapped edges of one panel will match with a similar panel.

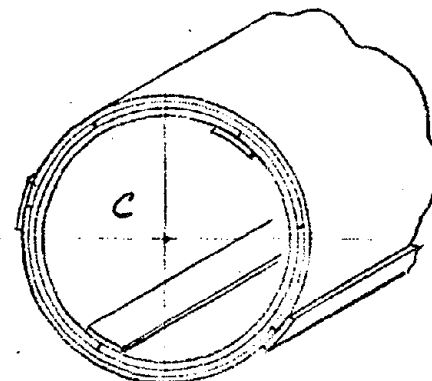
Ref. 1 "Materially Speaking", (Thiokol, Chemical Division) No. 13, May 1971, p. 27



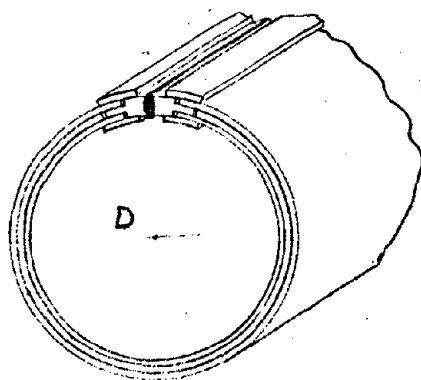
METHOD A



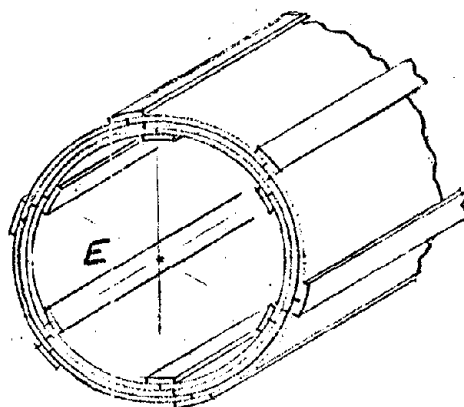
METHOD B



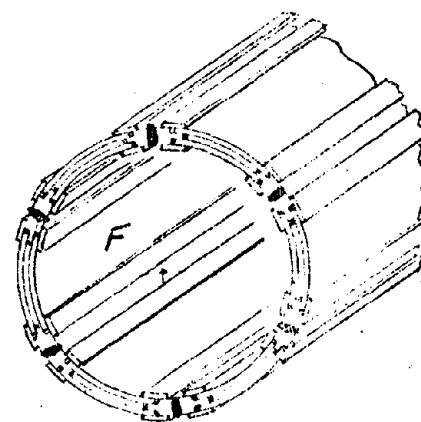
METHOD C



METHOD D



METHOD E



METHOD F

Figure 4-34 Proposed Splices, Adhesive Bonded Laminated Tanks

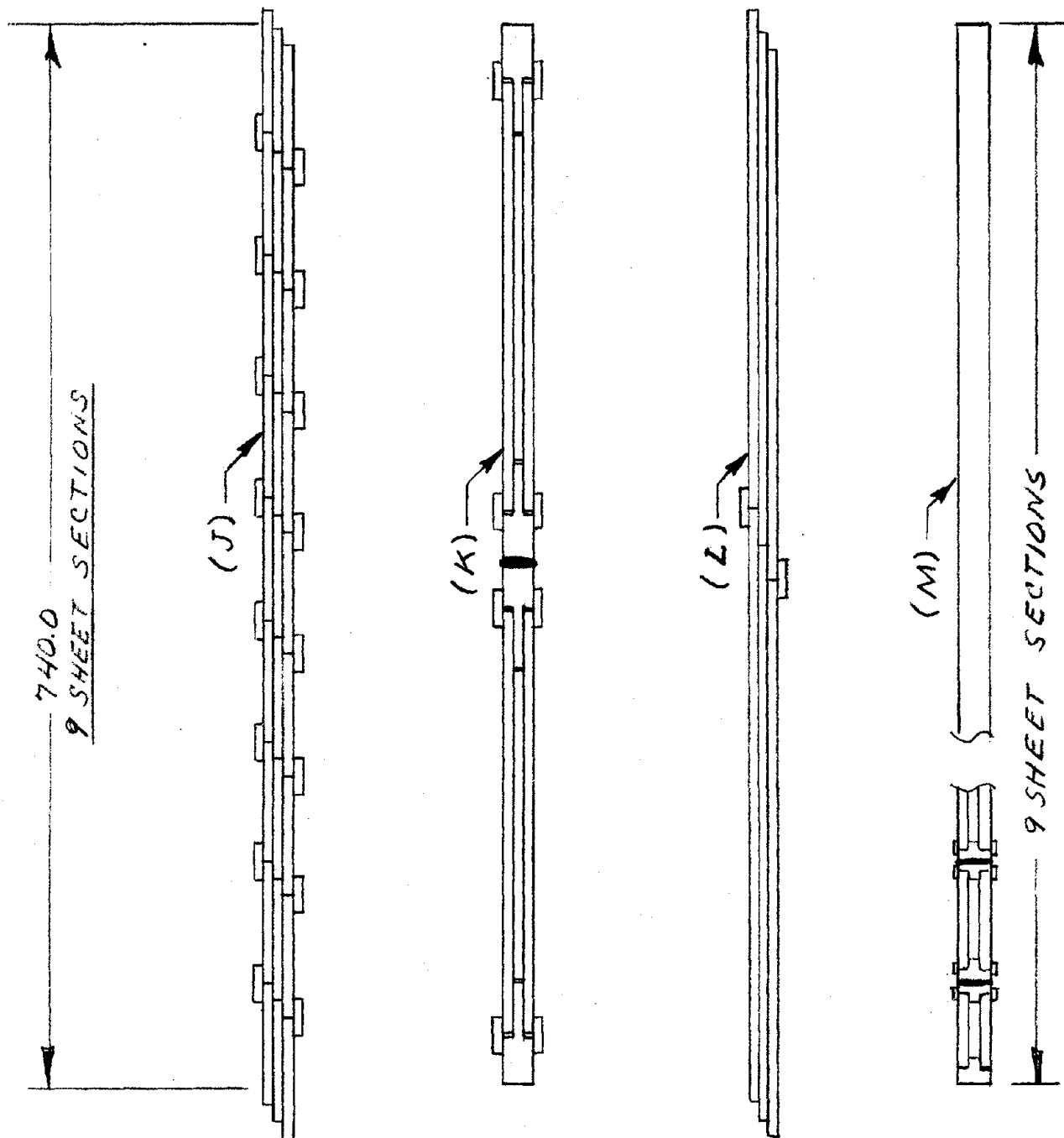


Figure 4-35 Splice Concepts

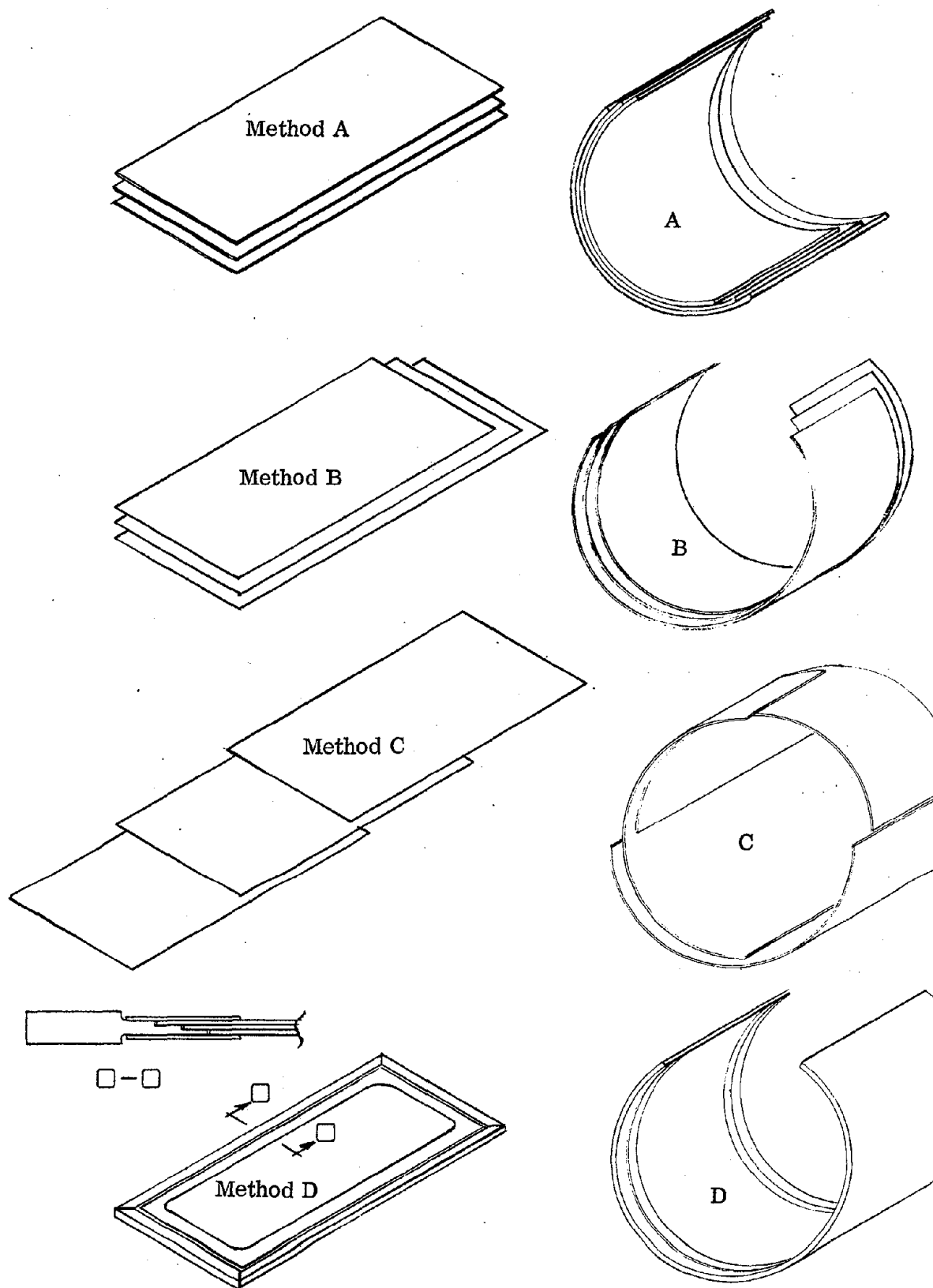


Figure 4-36 Laminating Methods

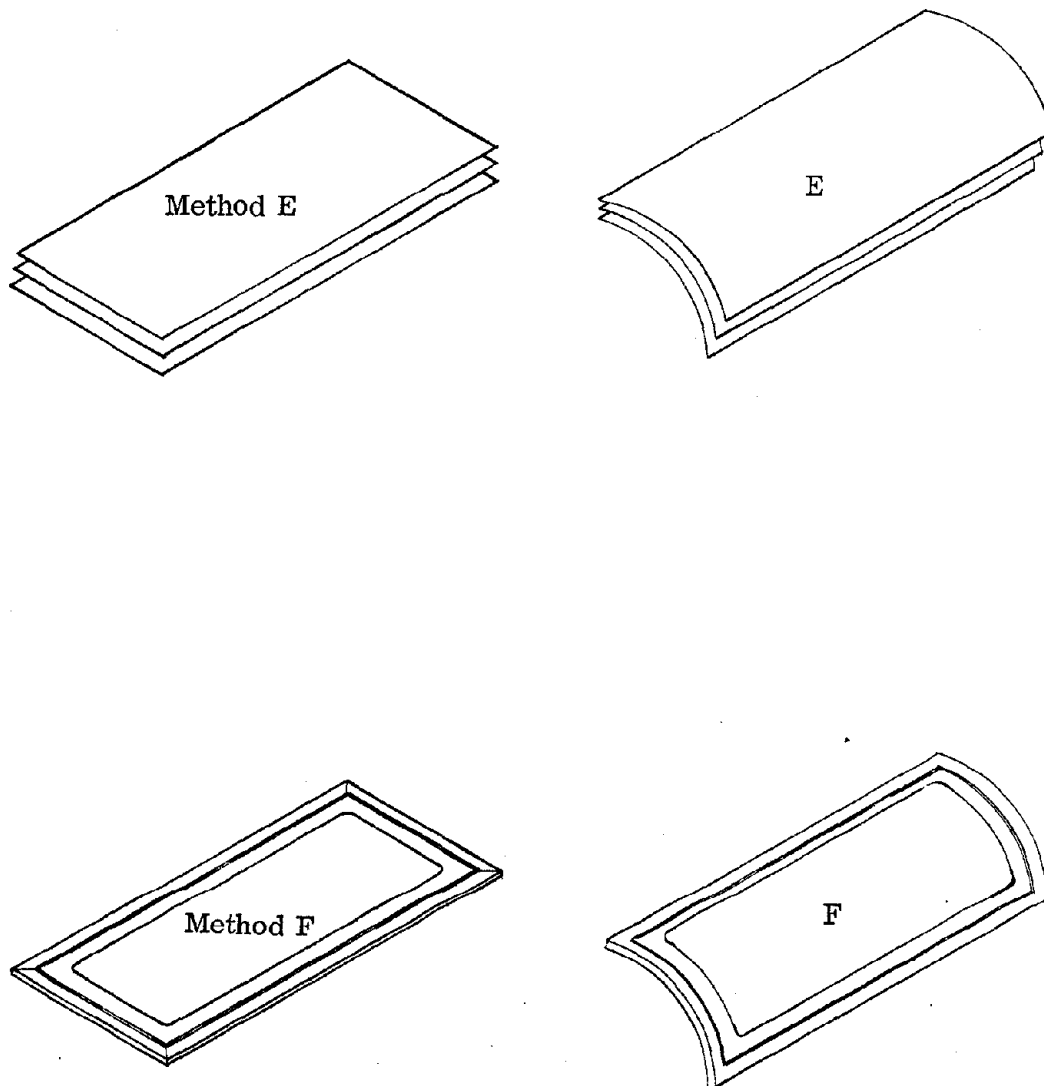


Figure 4-37 Laminating Methods

- Method B: Starting with the largest size sheet practical, each additional sheet is smaller in length and width by twice the required bond lap width. By alternately rolling with the large sheet first inside and then outside, mating splices can be made in both the circumferential and longitudinal directions.
- Method C: This method is similar to Method A except that the splice length is much longer. If the splices of the laminates are staggered by 90° a sheet size of 84 by 440 inches would be required.
- Methods D and F: Both methods use a picture frame of monolithic weldable material which is then bonded into the edges of the laminate. Method D varies from F in the width of the frame pieces and the direction of rolling.
- Method E: This method is identical to A except for the orientation of the laminate for rolling.

Final assembly of the tank cylinder will require accurate alignment tools for all of the methods shown. Rolled laminated sections may be joined longitudinally using a press. The sections to be joined and the splice plates are held in place in the press after the adhesive has been applied. Pressure and temperature required for curing may then be supplied by the press. Cylindrical splices may better be made in an autoclave using vacuum bagging. An internal mandrel is required to position the segments, and assure a true diameter and concentricity of the segments being joined. Suggested assembly procedures for Methods A through F are shown in Figures 4-38 and 4-39.

The optimum assembly setup would hold all the sections to be joined and their splice plates in a single aligning and clamping fixture. The entire assembly could be placed in an autoclave, vacuum bagged and cured in one operation. The two methods requiring welding, D and F, will be able to make use of conventional aligning and expanding tools. Care must be exercised in providing adequate chilling at the weld to prevent degradation of the bond by exposure to high temperature.

Bonding Pre-Treatment Investigation

One of the factors that will ultimately affect a decision to use adhesive bonded tank structure is its ability to withstand the service environment. To evaluate processing parameters for various conditions simulating the service environment, lap shear specimens were exposed to humidity, high temperature and salt spray. Results of the lap shear tests were used to select effective pretreatments for bonding 2219-T87 aluminum with METLBOND 329 adhesive.

The processing parameters which were investigated are: molding pressure, cleaning method and primer.

Two molding pressures were considered:

1. 45 psi - noted by symbol 4
2. Atmospheric - noted by symbol A

Two cleaning methods were considered:

1. Per GSS-7022 (sulfuric acid/sodium dichromate solution) noted by symbol 7
2. Vapor degrease and Oakite rinse noted by symbol 0

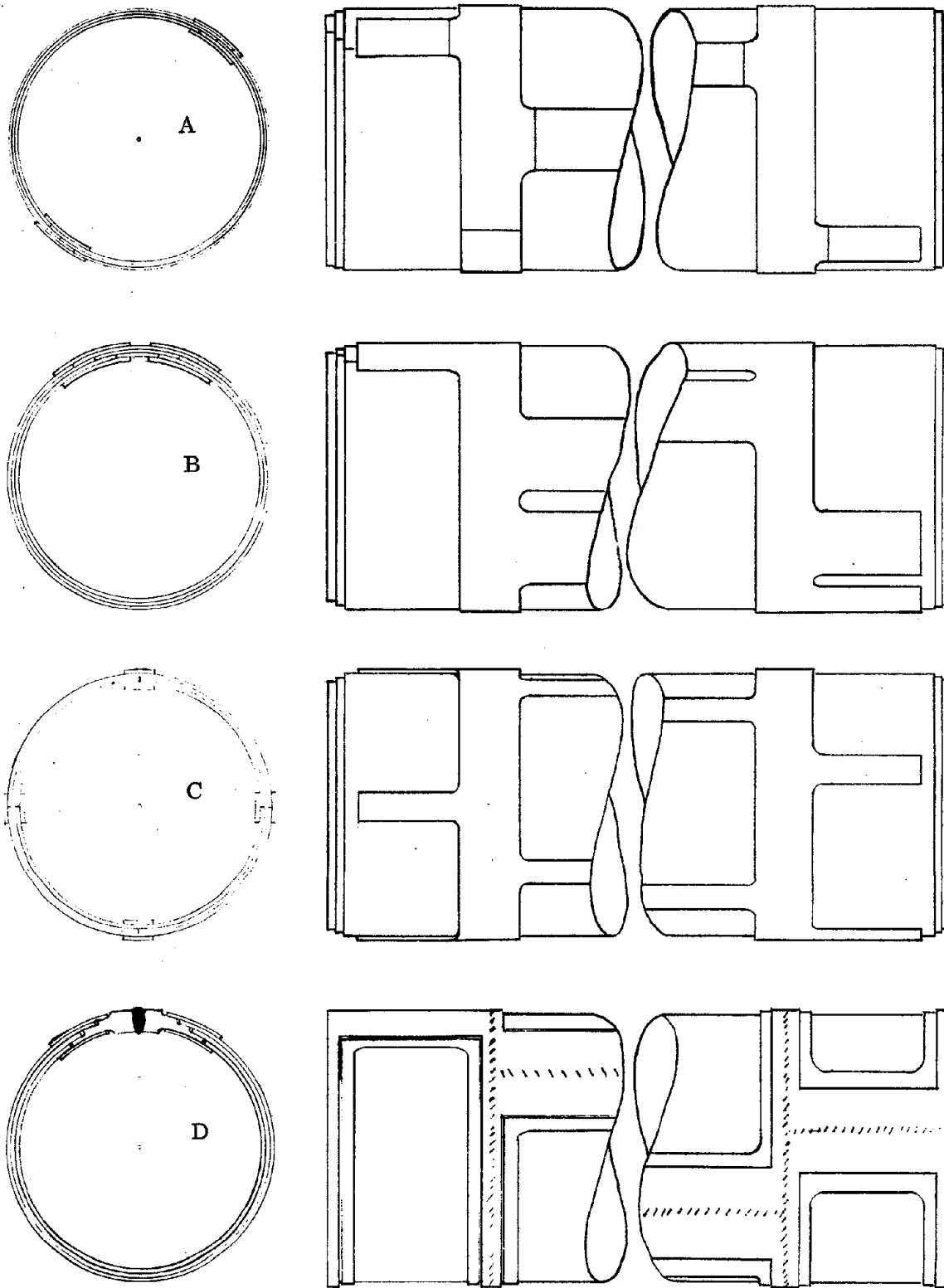


Figure 4-38 Assembly Procedures

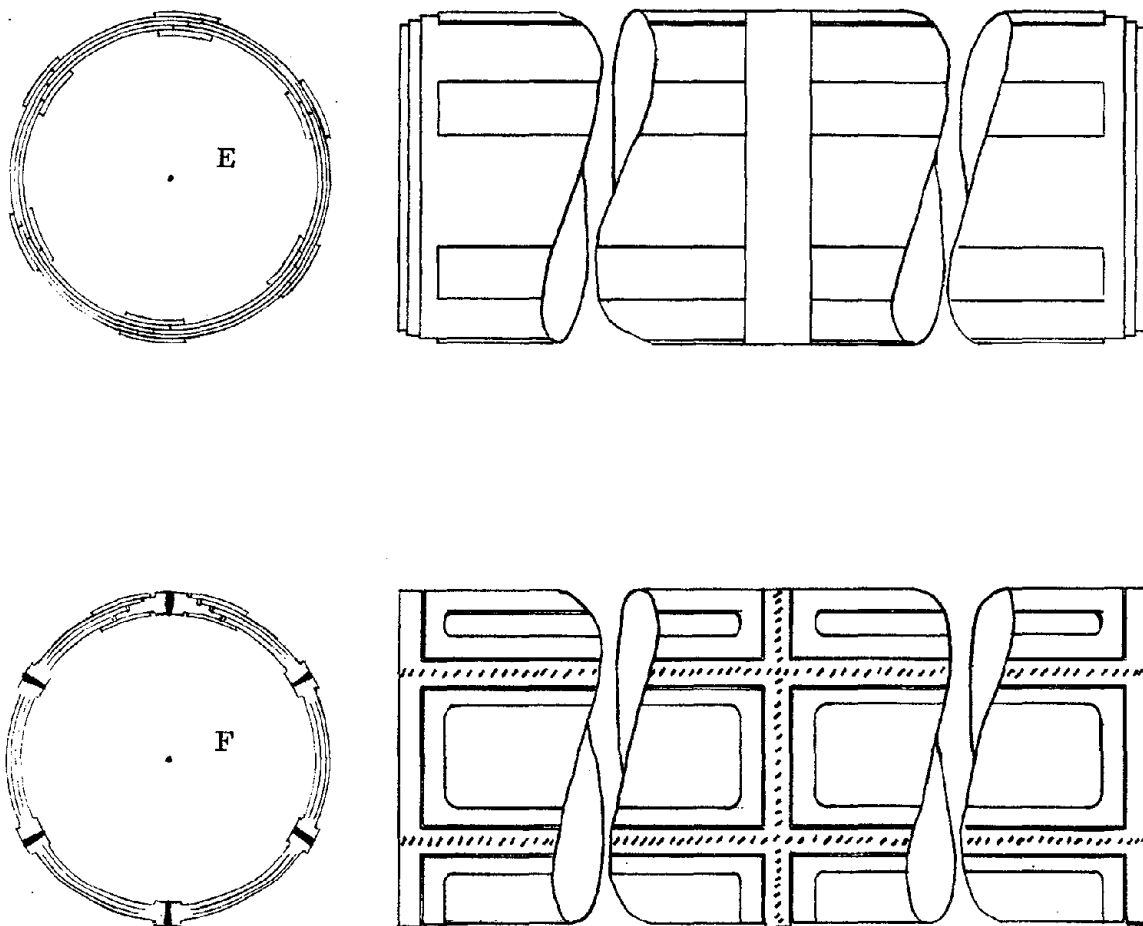


Figure 4-39 Assembly Procedures

Three primer conditions were considered:

1. EC 2333 noted by symbol E
2. No primer, noted by symbol N
3. METLBOND 329 primer, noted by symbol M

Five testing conditions were used:

1. Tensile shear at room temperature
2. Tensile shear at room temperature after 4 days at 350°F and 30 days at 98% relative humidity
3. Tensile shear at room temperature after 30 days at 98% relative humidity
4. Tensile shear at room temperature after 30 day salt spray
5. Tensile shear at room temperature after two weeks aging at 350°F

A specimen designated A-7-E-3 then, is bonded at atmospheric pressure, cleaned per Grumman specification GSS-7002, using EC-2333 primer and tested at room temperature following 30 days exposure to 98% relative humidity.

The following combinations of processing parameters were tested:

A-7-E	4-7-E
A-7-M	4-7-M
A-7-N	4-7-N
A-0-E	4-0-E

Each combination was tested for all five testing conditions. Three specimens of each group were tested at each condition. Test results are reported in Tables 4-12 through 4-16. Room temperature results are given in Table 4-12. Results after exposure to a four-day aging at 350°F and 30 days at 98% relative humidity are shown in Table 4-13. Specimens exposed to 30 days at 98% relative humidity are reported on in Table 4-14. Results after a 30-day salt spray are shown in Table 4-15. Specimens given a two-week aging at 350°F are reported on in Table 4-16. A summary of the behavior of the eight different combinations of processing parameters to the five different test conditions is given in Table 4-17.

Average values for the three specimens tested at each condition varied from a high of 2860 psi to a low of 1890 psi. For purposes of evaluation, values above 2300 psi were rated good, and those below 2200 psi were rated poor. On this basis, the best performer was group A-7-M whose values exceeded 2300 psi in four test conditions and reached 2290 psi for two weeks aging at 350°F. Groups 4-7-N and A-7-N were almost as good, exceeding 2300 psi in four conditions and recording 2270 psi and 2245 psi respectively for 30 days at 98% relative humidity. Group 4-7-E also had four values above 2300 psi and 2210 psi for two weeks aging at 350°F.

TABLE 4-12 ROOM TEMPERATURE LAP SHEAR TEST RESULTS,
BONDING PRE-TREATMENT INVESTIGATION

Specimen Group	Test Temp, °F	Specimen No.	Width in.	Overlap in.	Bondline Thickness, in.	Bond Area sq in.	Failure Load, lb.	Stress psi	Failure Type
A-7-E-1	Rm Temp	1	1.007	.58	.008	.58	1255	2130	Adhesive
	Rm Temp	2	1.008	.60	.007	.60	1315	2190	Adhesive
	Rm Temp	3	1.010	.62	.007	.63	1305	2070	Adhesive
	Average							2130	
A-7-N-1	Rm Temp	1	1.005	.64	.007	.64	1651	2520	Adhesive
	Rm Temp	2	1.008	.61	.006	.61	1775	2910	Adhesive
	Rm Temp	3	1.012	.60	.006	.61	1410	2310	Adhesive
	Average							2580	
A-7-M-1	Rm Temp	1	1.011	.63	.007	.63	1585	2520	Adhesive
	Rm Temp	2	1.009	.63	.007	.63	1350	2140	Adhesive
	Rm Temp	3	1.009	.62	.007	.62	1510	2430	Adhesive
	Average							2365	
A-O-E-1	Rm Temp	1	1.010	.62	.006	.62	1455	2340	Adhesive
	Rm Temp	2	1.010	.62	.006	.62	1610	2600	Adhesive
	Rm Temp	3	1.007	.61	.007	.61	1330	2180	Adhesive
	Average							2375	
4-7-E-1	Rm Temp	1	1.007	.61	.006	.61	1440	2360	Adhesive
	Rm Temp	2	1.009	.61	.006	.61	1495	2450	Adhesive
	Rm Temp	3	1.009	.61	.006	.61	1375	2260	Adhesive
	Average							2355	
4-7-M-1	Rm Temp	1	1.013	.62	.006	.63	1535	2440	Adhesive
	Rm Temp	2	1.015	.60	.006	.61	1360	2240	Adhesive
	Rm Temp	3	1.015	.62	.006	.63	1450	2300	Adhesive
	Average							2325	
4-7-N-1	Rm Temp	1	1.019	.61	.006	.62	1435	2310	Adhesive
	Rm Temp	2	1.017	.62	.006	.63	1455	2310	Adhesive
	Rm Temp	3	1.015	.64	.006	.65	1495	2300	Adhesive
	Average							2305	
4-O-E-1	Rm Temp	1	1.014	.61	.006	.62	1270	2040	Adhesive
	Rm Temp	2	1.013	.60	.006	.61	1205	1975	Adhesive
	Rm Temp	3	1.013	.60	.006	.61	1325	2170	Adhesive
	Average							2060	

TABLE 4-13 LAP SHEAR TEST RESULTS, FOUR DAYS AGING AT 350°
AND 30-DAY EXPOSURE TO 98% RELATIVE HUMIDITY,
BONDING PRE-TREATMENT INVESTIGATION

Specimen Group	Test Temp, °F	Specimen No.	Width in.	Overlap in.	Bondline Thickness, in.	Bond Area sq in.	Failure Load lb.	Stress psi	Failure Type
A-7-E-2	Rm Temp	1	1.01	.60	.008	.61	1482	2430	Adhesive
	Rm Temp	2	1.01	.60	.007	.61	1468	2400	Adhesive
	Rm Temp	3	1.01	.60	.007	.61	1496	2450	Adhesive
	Average							2430	
A-7-M-2	Rm Temp	1	1.01	.60	.008	.61	1548	2540	Adhesive
	Rm Temp	2	1.01	.60	.008	.61	1536	2520	Adhesive
	Rm Temp	3	1.01	.60	.009	.61	1456	2390	Adhesive
	Average							2480	
A-7-N-2	Rm Temp	1	1.01	.60	.008	.61	1568	2570	Adhesive
	Rm Temp	2	1.01	.60	.007	.61	1628	2670	Adhesive
	Rm Temp	3	1.01	.60	.007	.61	1628	2670	Adhesive
	Average							2640	
A-O-E-2	Rm Temp	1	1.01	.60	.008	.61	1360	2230	Adhesive
	Rm Temp	2	1.01	.60	.008	.61	1392	2280	Adhesive
	Rm Temp	3	1.01	.60	.007	.61	1306	2140	Adhesive
	Average							2220	
4-7-E-2	Rm Temp	1	1.01	.60	.007	.61	1502	2460	5% Cohesive-95%
	Rm Temp	2	1.01	.60	.007	.61	1448	2370	Adhesive
	Rm Temp	3	1.01	.60	.007	.61	1504	2470	Adhesive
	Average							2430	
4-7-M-2	Rm Temp	1	1.01	.60	.007	.61	1484	2430	Adhesive
	Rm Temp	2	1.01	.60	.007	.61	1504	2470	Adhesive
	Rm Temo	3	1.01	.60	.006	.61	1482	2430	Adhesive
	Average							2440	
4-7-N-2	Rm Temp	1	1.01	.60	.007	.61	1720	2820	Adhesive
	Rm Temp	2	1.01	.60	.008	.61	1804	2960	Adhesive
	Rm Temp	3	1.01	.60	.008	.61	1714	2810	Adhesive
	Average							2860	
4-O-E-2	Rm Temp	1	1.01	.60	.007	.61	1570	2570	Adhesive
	Rm Temp	2	1.01	.60	.007	.61	1512	2480	Adhesive
	Rm Temp	3	1.01	.60	.007	.61	1528	2500	Adhesive
	Average							2520	

**TABLE 4-14 LAP SHEAR TEST RESULTS, 30-DAY EXPOSURE TO 98%
RELATIVE HUMIDITY, BONDING PRE-TREATMENT
INVESTIGATION**

Specimen Group	Test Temp, °F	Specimen No.	Width, in.	Overlap, in.	Bondline Thickness, in.	Bond Area, sq in.	Failure Load, lb.	Stress psi	Failure Type
A-7-E-3	Rm Temp	1	1.007	.60	.008	.61	1320	2160	Adhesive
	Rm Temp	2	1.006	.60	.006	.61	1345	2210	Adhesive
	Rm Temp	3	1.009	.60	.007	.61	1340	2200	Adhesive
							Average	2190	
A-7-M-3	Rm Temp	1	1.008	.61	.007	.61	1655	2710	Adhesive
	Rm Temp	2	1.005	.60	.007	.60	1505	2510	Adhesive
	Rm Temp	3	1.008	.61	.007	.61	1590	2610	Adhesive
							Average	2610	
A-7-N-3	Rm Temp	1	1.007	.61	.007	.61	1420	2330	Adhesive
	Rm Temp	2	1.005	.62	.007	.62	1390	2240	Adhesive
	Rm Temp	3	1.008	.61	.007	.61	1325	2170	Adhesive
							Average	2245	
A-0-E-3	Rm Temp	1	1.009	.62	.006	.63	1210	1920	Adhesive
	Rm Temp	2	1.008	.62	.006	.63	1210	1920	Adhesive
	Rm Temp	3	1.008	.62	.007	.63	1155	1835	Adhesive
							Average	1890	
4-7-E-3	Rm Temp	1	1.010	.60	.006	.61	1380	2260	Adhesive
	Rm Temp	2	1.006	.60	.006	.60	1440	2400	Adhesive
	Rm Temp	3	1.006	.61	.006	.60	1545	2570	Adhesive
							Average	2410	
4-7-M-3	Rm Temp	1	1.01	.62	.007	.63	1400	2220	Adhesive
	Rm Temp	2	1.02	.62	.007	.63	1490	2360	Adhesive
	Rm Temp	3	1.02	.62	.007	.63	1446	2290	Adhesive
							Average	2290	
4-7-N-3	Rm Temp	1	1.02	.61	.008	.62	1438	2320	Adhesive
	Rm Temp	2	1.01	.62	.008	.63	1460	2320	Adhesive
	Rm Temp	3	1.01	.62	.008	.63	1372	2180	Adhesive
							Average	2270	
4-0-E-3	Rm Temp	1	1.02	.60	.007	.61	1230	2160	Adhesive
	Rm Temp	2	1.01	.60	.007	.61	1640	2670	Adhesive
	Rm Temp	3	1.01	.60	.007	.61	1372	2250	Adhesive
							Average	2360	

TABLE 4-15 LAP SHEAR TEST RESULTS, 30-DAY SALT SPRAY
EXPOSURE, BONDING PRE-TREATMENT INVESTIGATION

Specimen Group	Test Temp, °F	Specimen No.	Width, in.	Overlap, in.	Bond Area sq in.	Failure Load lb.	Stress, psi	Failure Type
A-7-E-4	Rm Temp	1	1.00	.60	.60	1498	2500	Adhesive
	Rm Temp	2	1.00	.60	.60	1628	2710	Adhesive
	Rm Temp	3	1.00	.60	.60	1422	2370	Adhesive
						Average	2530	
A-7-M-4	Rm Temp	1	1.00	.60	.60	1670	2780	Adhesive
	Rm Temp	2	1.00	.60	.60	1744	2910	Adhesive
	Rm Temp	3	1.00	.60	.60	1704	2840	Adhesive
						Average	2840	
A-7-N-4	Rm Temp	1	1.00	.60	.60	1382	2300	Adhesive
	Rm Temp	2	1.00	.60	.60	1406	2340	Adhesive
	Rm Temp	3	1.00	.60	.60	1430	2380	Adhesive
						Average	2340	
A-O-E-4	Rm Temp	1	1.00	.60	.60	1160	1930	Adhesive
	Rm Temp	2	1.00	.60	.60	1174	1960	Adhesive
	Rm Temp	3	1.00	.60	.60	1172	1950	Adhesive
						Average	1950	
4-7-E-4	Rm Temp	1	1.00	.60	.60	1314	2190	Adhesive
	Rm Temp	2	1.00	.60	.60	1680	2800	Adhesive
	Rm Temp	3	1.00	.60	.60	1602	2670	Adhesive
						Average	2550	
4-7-M-4	Rm Temp	1	1.00	.60	.60	1498	2500	Adhesive
	Rm Temp	2	1.00	.60	.60	1434	2390	Adhesive
	Rm Temp	3	1.00	.60	.60	1452	2420	Adhesive
						Average	2440	
4-7-N-4	Rm Temp	1	1.00	.60	.60	1450	2420	Adhesive
	Rm Temp	2	1.00	.60	.60	1496	2490	Adhesive
	Rm Temp	3	1.00	.60	.60	-	-	Adhesive
						Average	2460	
4-O-E-4	Rm Temp	1	1.00	.60	.60	1300	2170	Adhesive
	Rm Temp	2	1.00	.60	.60	1288	2150	Adhesive
	Rm Temp	3	1.00	.60	.60	1298	2160	Adhesive
						Average	2160	

TABLE 4-16 LAP SHEAR TEST RESULTS, TWO WEEKS AGING AT 350°F,
BONDING PRE-TREATMENT INVESTIGATION

Specimen Group	Test Temp, °F	Specimen No.	Width, in.	Overlap, in.	Bondline Thickness, in.	Bond Area, sq in.	Failure Load, lb.	Stress, psi	Failure Type
A-7-E-5	Rm Temp	1	1.01	.62	.009	.63	1438	2280	Adhesive
	Rm Temp	2	1.01	.60	.009	.61	1464	2400	Adhesive
	Rm Temp	3	1.00	.60	.009	.60	1410	2350	Adhesive
							Average	2340	
A-7-N-5	Rm Temp	1	1.01	.60	.008	.61	1420	2330	Adhesive
	Rm Temp	2	1.01	.60	.008	.61	1466	2400	Adhesive
	Rm Temp	3	1.01	.60	.009	.61	1390	2280	Adhesive
							Average	2340	
A-7-M-5	Rm Temp	1	1.01	.60	.009	.61	1440	2360	Adhesive
	Rm Temp	2	1.01	.60	.009	.61	1378	2260	Adhesive
	Rm Temp	3	1.01	.60	.009	.61	1382	2260	Adhesive
							Average	2290	
A-O-E-5	Rm Temp	1	1.01	.60	.008	.61	1254	2060	Adhesive
	Rm Temp	2	1.01	.60	.008	.61	1238	2030	Adhesive
	Rm Temp	3	1.01	.60	.008	.61	1200	1970	Adhesive
							Average	2020	
4-7-E-5	Rm Temp	1	1.01	.62	.008	.63	1384	2200	Adhesive
	Rm Temp	2	1.01	.62	.007	.63	1368	2170	Adhesive
	Rm Temp	3	1.01	.64	.008	.65	1462	2250	Adhesive
							Average	2210	
4-7-N-5	Rm Temp	1	1.01	.62	.008	.63	1534	2440	Adhesive
	Rm Temp	2	1.02	.62	.008	.63	1584	2520	Adhesive
	Rm Temp	3	1.02	.62	.009	.63	1566	2480	Adhesive
							Average	2480	
4-7-M-5	Rm Temp	1	1.02	.60	.008	.61	1308	2140	Adhesive
	Rm Temp	2	1.01	.60	.007	.61	1286	2110	Adhesive
	Rm Temp	3	1.01	.60	.007	.61	1290	2120	Adhesive
							Average	2120	
4-O-E-5	Rm Temp	1	1.01	.60	.008	.61	1330	2180	Adhesive
	Rm Temp	2	1.01	.60	.007	.61	1330	2180	Adhesive
	Rm Temp	3	1.02	.60	.007	.61	1290	2110	Adhesive
							Average	2160	

TABLE 4-17 LAP SHEAR TEST RESULTS SUMMARY, BONDING PRE-TREATMENT INVESTIGATION

Specimen Group	Average Room Temperature Lap Shear Stress				
	Room Temperature	4 Days at 350°F, 30 Days at 98% RH	30 Days at 98% Rel. Hum	30 Day Salt Spray	2 Weeks at 350°F
A-7-E	2130	2430	2190	2530	2340
A-7-M	2365	2480	2610	2840	2290
A-7-N	2580	2640	2245	2340	2340
A-O-E	2375	2220	1890	1950	2020
4-7-E	2355	2430	2410	2250	2210
4-7-M	2325	2440	2290	2440	2120
4-7-N	2305	2860	2270	2460	2480
4-O-E	2060	2520	2360	2160	2160

A slightly lower level of performance was recorded for groups 4-7-M and A-7-E. Each group had 3 values over 2300 psi but also had one group just slightly above 2100 psi. The lowest level of performance is indicated for groups 4-0-E and A-0-E.

Preliminary conclusions from this data indicate that:

- Molding pressures of 45 psi (4), and atmospheric pressure (A) such as is used in vacuum bag molding, both produce acceptable bonds.
- Specimens cleaned per GSS-7022 (7), in general gave good results, while those cleaned by vapor degreasing and an Oakite rinse (0), gave the poorest result of all combinations tested.
- Good results were obtained using the METLBOND 329 primer or no primer. EC 2333 primer gave good results when used with 45 psi molding pressure.

Welding of Laminated Plate

Tensile specimens were machined from butt-welded samples of the three different roll diffusion bonded plates. Straight butt welds were made between twelve inch long, six inch wide pieces along the twelve inch edge. Specimens were TIG fusion welded using 2319 filler wire. No post-welding heat treatment was performed. Six specimens of each interlayer thickness were prepared. Three specimens were tested in the as-welded condition, and three had the weld ground flush. Test results for the three interlayer thickness materials are given in Tables 4-18 through 4-20.

Since the specimens were of constant thickness, it is to be expected that the material with the thickest interlayers would give the lowest strength.

In general, the test results followed this relationship.

To assess weld efficiency in the laminated plate, tensile specimens were prepared from unwelded laminated material and tested under the same conditions as the welded specimens. Results of the tensile tests on the unwelded laminated material are shown in Table 4-21.

A summary of the weld test strengths for the three laminated materials and the strength of the unwelded material is shown in Table 4-22. Ultimate weld strengths for the three laminates are all greater than 40,000 psi in the "as-welded" condition. Typical "as-welded" properties for monolithic 2219-T87 material are: yield strength 30 KSI and ultimate strength, 41 ksi (Ref. 2). The ultimate strengths of the welded laminate are very close to the typical data but the yield strengths show a reduction of approximately 2.5 KSI for the .004 and .008 laminates and 4.5 KSI for the .012 laminate in the "as-welded" condition. The actual interlayer thickness in the nominal .012 laminate is .010 in., so that approximately 85% of the specimen is structural material. This would indicate that the structural material is behaving essentially as typical monolithic material ($.85 \times 30 \text{ KSI} = 25.5 \text{ KSI}$) with no apparent degradation of the structural material due to the presence of the 1100 alloy interlayer.

Photographs were taken of a section through the weld in the laminated plate. Figure 4-40 shows the weld with the bead on at 20x magnification. The fusion zone is in the center of the picture, the darker areas to either side of the fusion zone are the heat affected zone and at the edge of the picture is the parent material. Note that the 1100 interlayer extends into the fusion zone. The melting range of the 1100 aluminum is 1190 to 1215°F while the melt-

Ref 2: Alcoa Green Letter, Aluminum Alloy 2219, June 1967

TABLE 4-18 TENSILE TEST RESULTS, BUTT WELD IN .004 INTER-LAYER LAMINATED 2219-T87 ALUMINUM PLATE, 2319 FILLER WIRE

	As Welded			Machined Flush		
Specimen No.	92-4-B-1	92-4-B-2	92-4-B-3	92-4-F-1	92-4-F-2	92-4-F-3
Test Section	.499x.132	.491x.131	.500x.131	.500x.131	.497x.123	.495x.125
Initial Gage Length, in.	2.00	2.00	2.00	2.00	2.00	2.00
Strain Rate to Yield in./in./min.	.005	.005	.005	.005	.005	.005
Ultimate Load, Lb.	2730	2710	2660	2500	2470	2420
Yield Load, lb. (0.2% offset)	1840	1830	1930	1720	1800	1780
Gage Length After Failure, in.	2.05	2.07	2.04	2.06	2.06	2.06
Initial Specimen Area, in. ²	.0659	.0643	.0655	.0655	.0611	.0619
Ultimate Stress psi	41,400	42,100	42,300	38,200	40,400	39,100
Yield Stress, psi	27,900	28,500	29,500	26,300	29,400	28,800
% Elongation	2.5	3.5	2.0	3.0	3.0	3.0
Modulus of Elasticity psi x 10 ⁶	11.2	11.1	11.9	10.5	9.6	11.7

TABLE 4-19 TENSILE TEST RESULTS, BUTT WELD IN .008
LAMINATED 2219-T87 PLATE, 2319 FILLER WIRE

	AS WELDED			MACHINED FLUSH		
Specimen Number	B-1	B-2	B-3	F-1	F-2	F-3
Test Section	.1285 x .503	.128 x .498	.128 x .481	.121 x .489	.121 x .490	.120 x .494
Strain Rate to Yield in/in/ min	.005	.005	.005	.005	.005	.005
Ultimate Load, lb.	2580	2585	2525	2300	2320	2290
Yield Load, lb. (0.2% Offset)	1790	1800	1810	1560	1450	1400
Gage Length After Failure	2.05	2.06	2.06	2.08	2.09	2.07
Initial Specimen Area	.0646	.0637	.0616	.0591	.0593	.0593
Ultimate Stress, psi	39,900	40,600	41,000	38,900	39,100	38,600
Yield Stress, psi	27,700	28,200	29,400	26,400	24,500	23,600
% Elongation	2.5	3.0	3.0	4.0	4.5	3.5
Mod. of Elasticity psi x 10 ⁶	10.9	11.1	9.9	11.5	10.8	10.9

TABLE 4-20 TENSILE TEST RESULTS, BUTT WELD IN .012
INTERLAYER LAMINATED 2219-T87 ALUMINUM PLATE,
2319 FILLER WIRE

	As Welded			Machined Flush		
Specimen No.	94-4-B-1	94-4-B-2	94-4-B-3	94-4-F-1	94-4-F-2	94-4-F-3
Test Section	.507x.130	.487x.130	.504x.131	.505x.129	.504x.129	.488x.127
Initial Gage Length, in.	2.00	2.00	2.00	2.00	2.00	2.00
Strain Rate to Yield, in./in./min.	.005	.005	.005	.005	.005	.005
Ultimate Load, lb.	2720	2610	2670	2360	2360	2370
Yield Load, lb. (0.2% offset)	1675	1640	1650	1560	1540	1650
Gage Length After Failure, in.	2.06	2.07	2.07	2.07	2.07	2.07
Initial Specimen Area, Sq. In.	.0659	.0633	.0660	.0651	.0650	.0620
Ultimate Stress psi	41,300	41,200	40,400	36,200	36,300	38,200
Yield Stress, psi	25,400	25,900	25,000	23,900	23,700	26,600
% Elongation	3.0	3.5	3.5	3.5	3.5	3.5
Modulus of Elasticity	11.3	---	10.6	9.5	9.8	10.7

TABLE 4-21 TENSILE TEST
RESULTS, DIFFUSION
BONDED LAMINATED
2219-T87 ALUMINUM
PLATE

	.004 Interlayer			.008 Interlayer			.012 Interlayer		
Specimen Number	92-4-AR-1	92-4-AR-2	92-4-AR-3	93-4-AR-1	93-4-AR-2	93-4-AR-3	94-4-AR-1	94-4-AR-2	94-4-AR-3
Test Section	.131 x .499	.132 x .496	.132 x .499	.128 x .493	.128 x .496	.129 x .491	.129 x .501	.130 x .509	.130 x .503
Initial Gage Length, In.	2.00	2.00	2.00	2.00	2.00	2.00	2.00	2.00	2.00
Strain Rate To Yield In./In./Min.	.005	.005	.005	.005	.005	.005	.005	.005	.005
Ultimate Load, lb.	4350	4230	4250	3890	3890	3880	3830	3900	3880
Yield Load, lb. (0.2% offset)	3520	3510	3550	3250	3250	3230	3200	3260	3230
Gage Length After Failure, In..	2.23	2.23	2.23	2.24	2.20	2.24	2.21	2.20	2.21
Initial Specimen Area Sq. In.	.0654	.0655	.0659	.0631	.0635	.0633	.0646	.0662	.0654
Ultimate Stress, psi	66,500	64,600	64,500	61,600	61,300	61,300	59,300	58,900	59,300
Yield Stress, psi	53,800	53,600	53,900	51,500	51,200	51,000	49,500	49,300	49,400
% Elongation	11.5	11.5	11.5	12.0	10.0	12.0	10.5	10.0	10.5
Modulus of Elasticity psi x 10 ⁶	9.98	10.13	9.69	9.51	9.45	10.08	8.76	8.80	9.44

FOLDOUT FRAME 1

FOLDOUT FRAME 2

TABLE 4-22 TENSILE TEST DATA SUMMARY, WELDED AND UNWELDED
2219-T87 DIFFUSION BONDED LAMINATED PLATE, BUTT
WELDED, 2319 FILLER WIRE

Laminate Description	As-Received Plate (Not Welded)		As Welded (Bead On)		Welded and Machined Flush	
	Yield, KSI	Ultimate, KSI	Yield, KSI	Ultimate, KSI	Yield, KSI	Ultimate, KSI
.004 Interlayer	53.8	65.2	28.6	41.9	28.2	39.2
.008 Interlayer	51.2	61.4	28.4	40.5	24.8	38.9
.012 Interlayer	49.4	59.3	25.4	41.0	24.7	36.9
Typical, as welded, 2219-T87 ⁽¹⁾ Butt Welds (2319 Filler Wire) Suggested Minimums ⁽¹⁾ (1) Alcoa Green Letter, Aluminum Alloy 2219, June 1967			30	41 35		

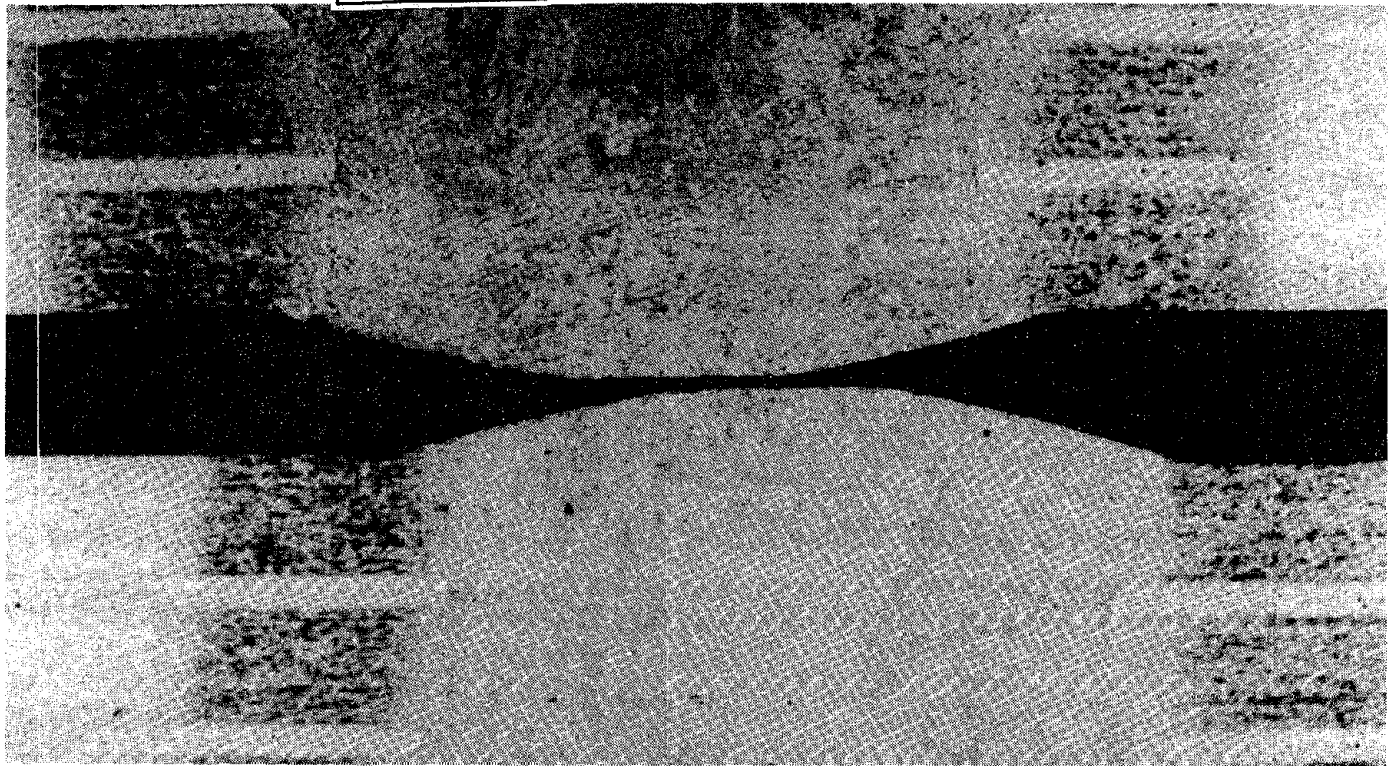


Figure 4-40 Weld in 0.008 In. Interlayer Laminate Aluminum Plate (20X Magnification)

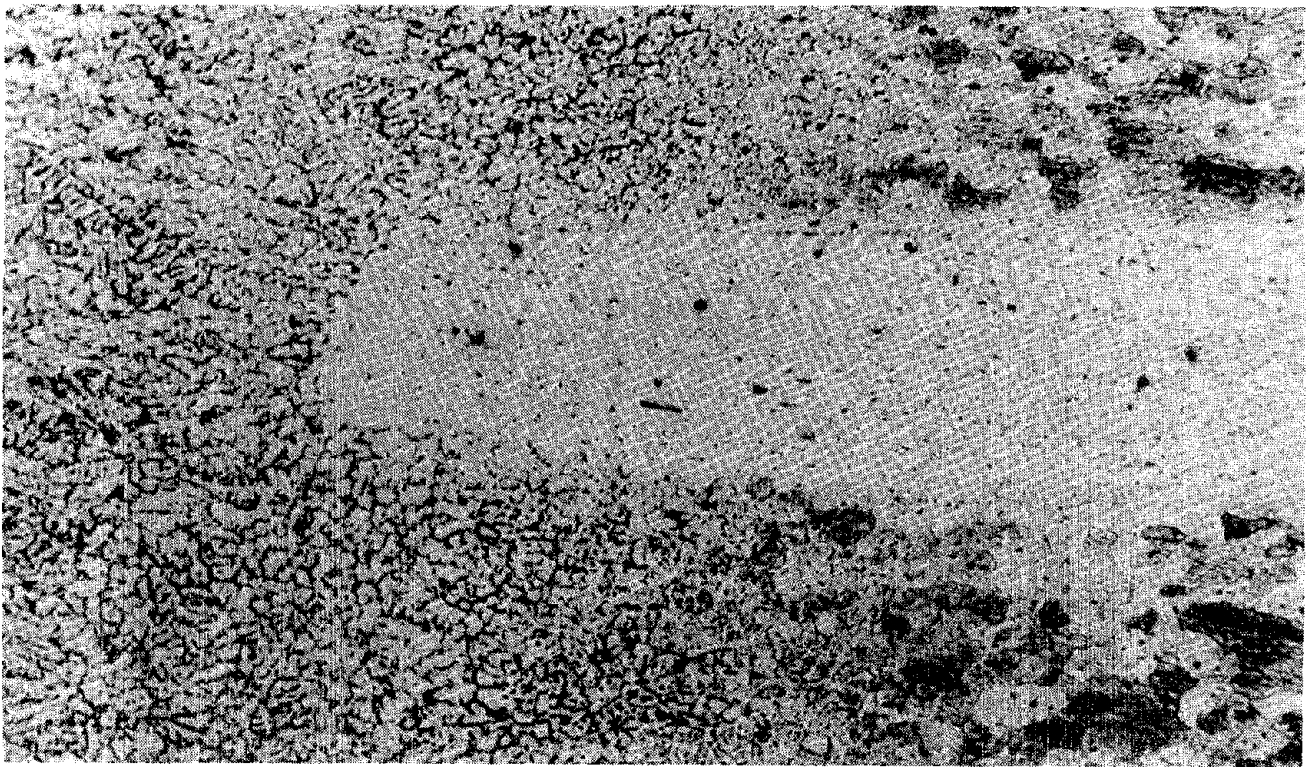


Figure 4-41 Photomicrograph (200X Magnification) Showing Fusion Line of
Weld in 0.008 In. Interlayer Laminated Aluminum Plate

ing range of 2219 alloy is 1010 to 1090°F, which offers an explanation for the interlayer maintaining its identity while the surrounding alloy has melted. Figure 4-41 shows the end of the interlayer in the fusion zone at higher magnification. The interface between the fusion zone and the heat affected zone is called the fusion line. It can be identified in Figure 4-41 as the line of demarcation between the large grain structure in the heat affected zone, to the right, and the small grain structure in the fusion zone, to the left.

Forming of Laminated Plate

The 2024-T3 panel, described in Section 3, which was produced to verify bonding procedure, was used to demonstrate the formability of an adhesive panel. Inspection of this panel after bonding and curing showed no defects. A three ft by three ft section of the panel was formed to a 50 in. radius (Figure 4-42) by rolling at room temperature. After the rolling operation the panel was reinspected to see if any separation had occurred at the bond lines. No defects were found in this inspection either. A one-inch wide strip from the original panel was successfully formed to an 8 in. radius (Figure 4-43). NDT inspection and visual checks of the exposed bond lines gave no indication of defects in the bond.

Similarly, one-inch wide strips were taken from the longitudinal and transverse directions of each thickness interlayer roll diffusion bonded plate and rolled to a 50 in. radius. No cracks were detected on any specimen on examination in the 20-40x range. Photomicrographs of the longitudinal and transverse specimens from the .008 laminate are shown in Figure 4-44.

Reproduced from
best available copy.

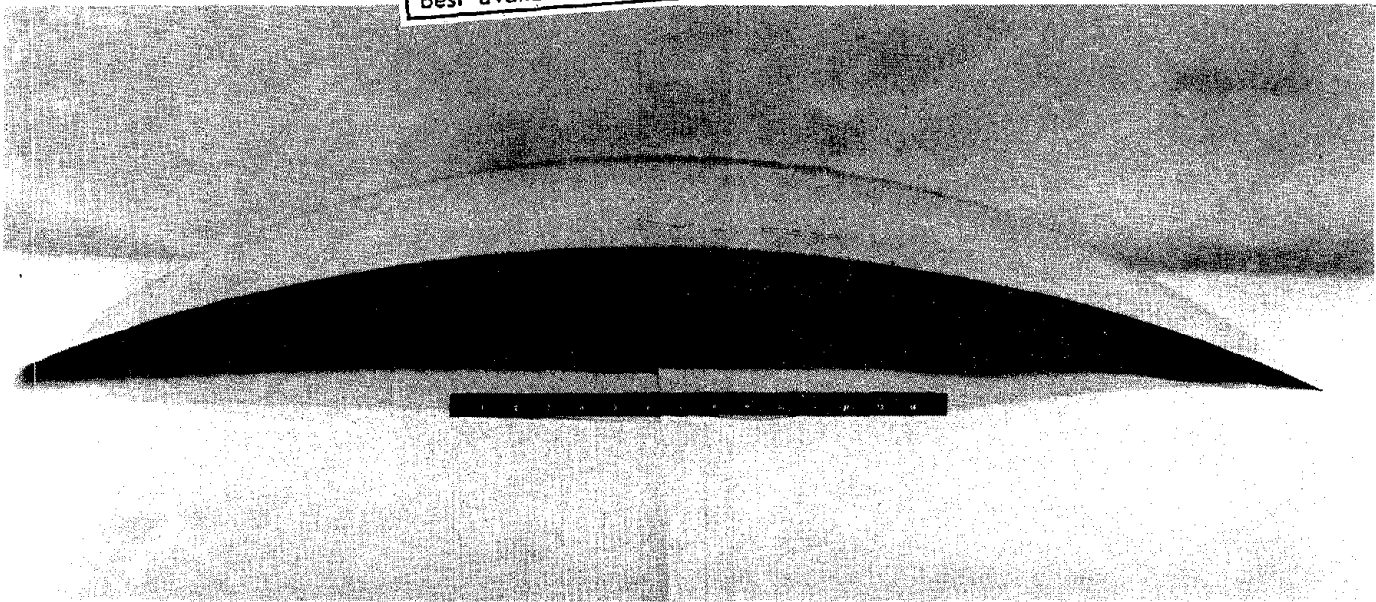


Figure 4-42 Three by Three Foot Adhesive Bonded
Panel Formed to 50 In. Radius

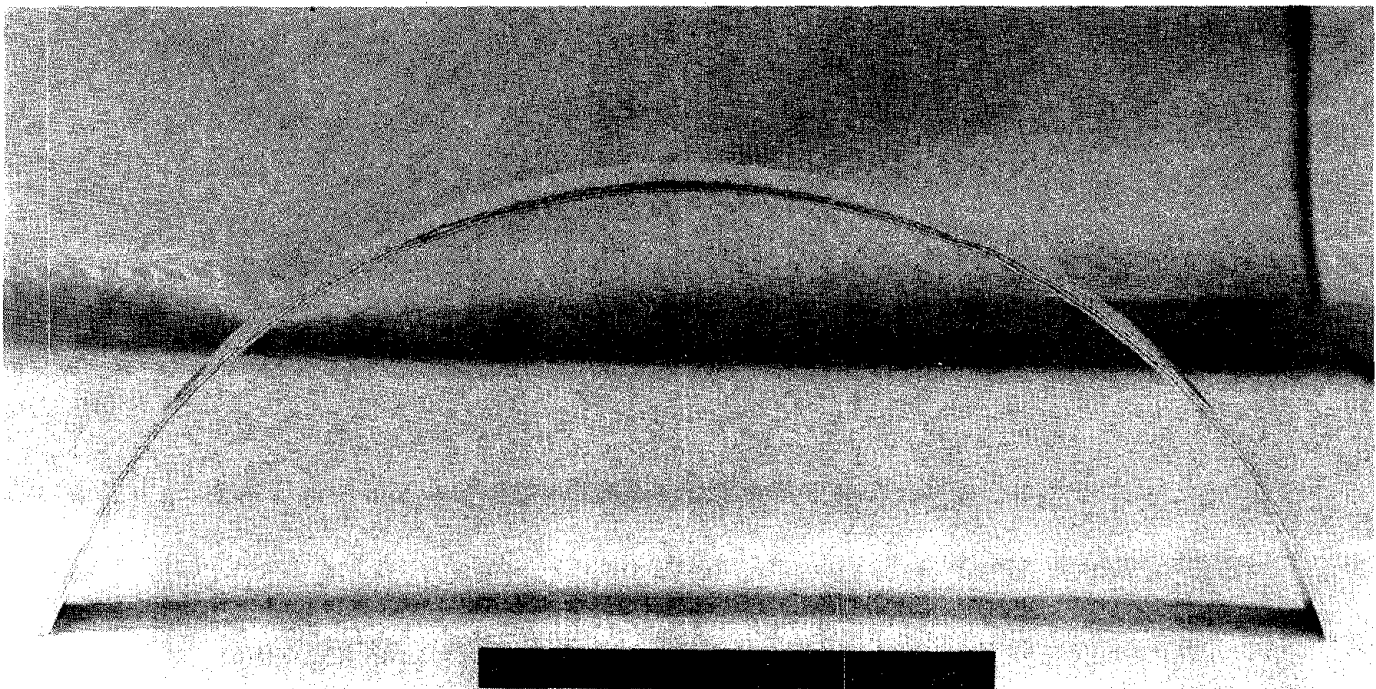
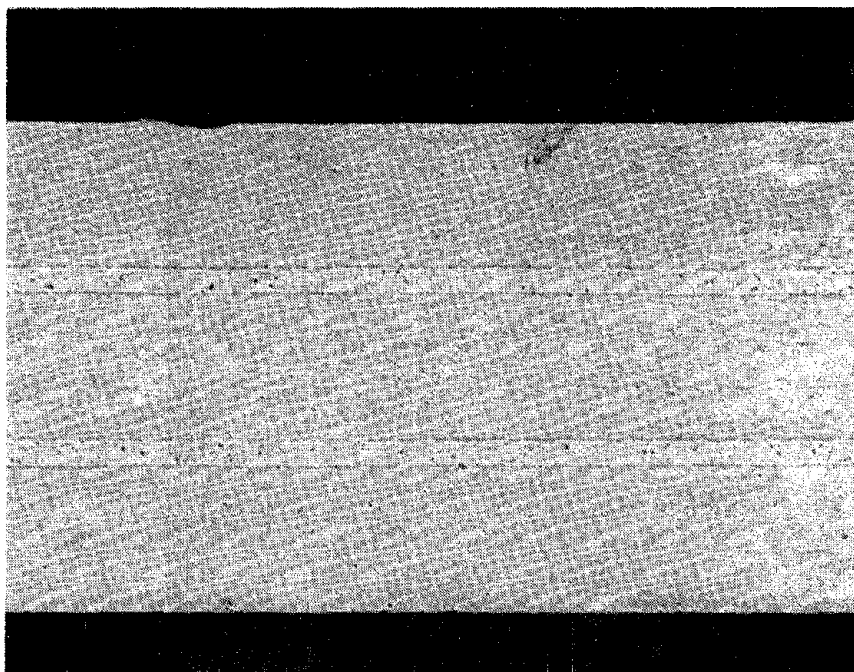
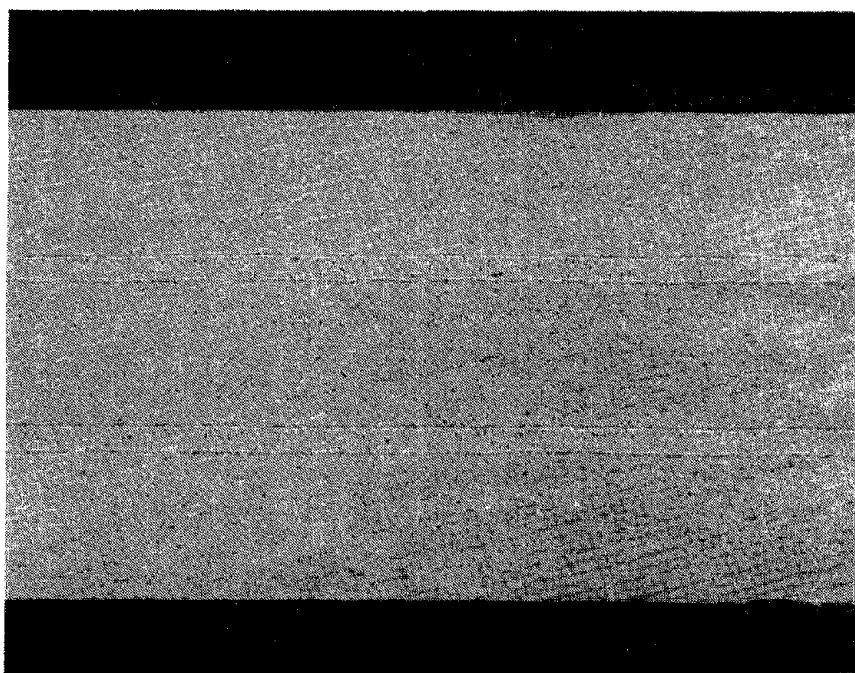


Figure 4-43 One-Inch Wide Adhesive Bonded Strip
Formed to Eight-Inch Radius

Reproduced from
best available copy.



A. Longitudinal



B. Transverse

Figure 4-44 Photomicrographs of Longitudinal and Transverse Specimens

WEIGHT/RELIABILITY ANALYSIS

Reliability Comparison

In the design of the monolithic tanks, whose weight is reported on in the paragraph entitled "Weight Comparison of Shuttle Orbiter Tanks" on page 4-32, the ratio of the final flaw depth, a_f , to wall thickness, t , varies from 0.5 to 0.77. These tanks are designed for flaws whose width is five times their depth ($a/2c = 0.2$). If semicircular flaws are considered in the analysis, the ratio a_f/t may approach 0.9. For monolithic tanks the ratio of flaw width to depth, starting with a semicircular flaw, is reasonably well known. However, for laminated plate no such relationship has been determined. It is not possible, therefore, to provide a direct comparison of flaw depth vs cycles between monolithic and laminated material. Measurements of surface flaw width vs cycles were obtained for each specimen tested in this program, and a comparison on the basis of surface flaw widths may be made.

The range of a_f/t from 0.5 to 0.9 was examined. It was assumed that a semicircular flaw remained semicircular through this range, and surface flaw widths were calculated for each 0.1 interval. The monolithic specimens of Phase I were examined to determine their flaw growth behavior. The Phase I specimens were chosen because the stress level was similar to that which resulted from the tank analysis and to give the greatest range of data. Cycles-to-breakthrough were tabulated for each of the Phase I monolithic specimens. The surface flaw widths for a_f/t from 0.5 to 0.9 are .125 in., .150 in., .175 in., .200 in. and .225 in. The number of cycles required for the flaw to grow to a through-the-thickness-flaw starting from each surface flaw width was determined for each monolithic specimen. Average and maximum number of cycles to leak from each flaw width are shown in Table 4-23.

Using the cyclic lives determined for each flaw size from the monolithic data, a flaw size for an equivalent number of cycles before leak in the .004 interlayer laminated specimens were determined. Flaw sizes were determined for the average and maximum number of cycles found for the monolithic specimens. These flaw sizes are also shown in Table 4-23.

A comparison of the average flaw size in a laminated specimen for equivalent life in a monolithic specimen with a specified surface flaw width is shown in Table 4-24. It can be seen that the ratio of surface flaw widths for equivalent cyclic lives ranges from 2.3 to 2.6 times larger flaws in the laminated specimens. If the maximum number of cycles to breakthrough in the monolithic is compared to the average laminate value, the ratio varies from 2.2 to 2.5 times larger flaws in the laminate.

It seems safe to assume an approximate 2:1 surface flaw width relation. That is, for the same number of cycles to leak, the starting surface flaw width in the laminated specimen is twice as long as the starting flaw in the monolithic specimen at typical design stress.

Weight Comparison

Since the laminated material displays greater cyclic life in the presence of a specified flaw, for equivalent cyclic life to a monolithic structure, the laminated structure should be able to operate at a higher cyclic stress. Having been unable to determine the flaw depth vs cycle relation for the laminated material it was not possible to calculate the increased stress level in the laminate directly. Instead, the average cyclic life of the laminated specimen was tabulated and a reduced stress level sought in the monolithic specimen to provide an equivalent cyclic life.

TABLE 4-23 FLAW SIZE CALCULATIONS FOR EQUIVALENT LIFE TO BREAK-THROUGH

AVERAGE AND MAXIMUM NUMBER OF CYCLES TO BREAK-THROUGH FROM SPECIFIED SURFACE FLAW WIDTHS
PHASE I MONOLITHIC SPECIMENS

Specimen No.	CYC To Brkthru	CYC To .125 in	Δ CYC	CYC To .150 in	Δ c	CYC To .175 in	Δ c	CYC To .200 in	Δ c	CYC To .225 in	Δ c
1	5670	2250	3420	3270	2400	4125	1545	4612	1058	4895	775
3	5500	2167	3333	3000	2500	3750	1750	4333	1167	4687	813
5	5720	2250	3470	3250	2470	4000	1720	4358	1362	4750	970
7	4900	2167	2733	3000	1900	3555	1345	4071	829	4430	470
9	7660	4250	3410	5333	2327	6083	1577	6500	1160	6916	744
11	6830	3875	2955	4500	2330	5333	1497	5750	1080	6071	759
Avg			3220		2321		1572		1109		755
Max			3470		2500		1750		1362		970

FLAW SIZE IN LAMINATED SPECIMENS

FLAW WIDTH BASED ON AVERAGE NO. OF CYCLES FROM MONOLITHIC TEST DATA

Specimen No.	CYC To Brkthru	-3220 CYC	Flaw Size	-2321 CYC	Flaw Size	-1572 CYC	Flaw Size	-1109 CYC	Flaw Size	-755 CYC	Flaw Size
353492-1	12,100	8880	.333	9779	.388	10,528	.442	10,991	.479	11,345	.521
" -2	12,000	8780	.286	9679	.334	10,428	.393	10,891	.422	11,245	.463
" -3	13,550	10,330	.393	11,229	.429	11,978	.497	12,441	.544	12,795	.580
" -4	10,085	6865	.289	7764	.345	8513	.391	8976	.428	9330	.463
" -5	10,800	7580	.283	8479	.338	9228	.403	9691	.453	10,045	.497
" -6	12,200	8980	.389	9879	.455	10,628	.509	11,091	.549	11,445	.602
Avg			.329		.382		.439		.479		.521

FLAW SIZE IN LAMINATED SPECIMENS

FLAW WIDTH BASED ON MAXIMUM NO. OF CYCLES FROM MONOLITHIC TEST DATA

Specimen No.	CYC To Brkthru	-3470 CYC	Flaw Size	-2500 CYC	Flaw Size	-1750 CYC	Flaw Size	-1362 CYC	Flaw Size	-970 CYC	Flaw Size
353492-1	12,100	8630	.318	9600	.368	10,350	.428	10,738	.459	11,130	.496
" -2	12,000	8530	.280	9500	.320	10,250	.377	10,638	.407	11,030	.434
" -3	13,550	10,080	.383	11,050	.422	11,800	.476	12,188	.519	12,580	.558
" -4	10,085	6615	.269	7585	.335	8335	.380	8723	.408	9915	.441
" -5	10,800	7330	.273	8300	.324	9050	.385	9438	.424	9830	.470
" -6	12,200	8730	.374	9700	.448	10,450	.496	10,838	.524	11,230	.567
Avg			.316		.370		.424		.457		.494

TABLE 4-24 FLAW WIDTH RATIOS
A. AVERAGE DATA FOR MONOLITHIC AND LAMINATED SPECIMENS

A_f/t	Flaw Width, in		Fl. Wd. Lam./ Flaw Wd. Mono.
	Mono.	.004 Lam.	
.5	.125	.329	2.63
.6	.150	.382	2.54
.7	.175	.439	2.50
.8	.200	.479	2.39
.9	.225	.521	2.32

B. MAXIMUM NO. OF CYCLES FOR MONOLITHIC SPECIMEN,
AVERAGE DATA FOR LAMINATED SPECIMENS

A_f/t	Flaw Width, in		Fl. Wd. Lam./ Flaw Wd. Mono.
	Mono.	.004 Lam.	
.5	.125	.316	2.52
.6	.150	.370	2.46
.7	.175	.424	2.42
.8	.200	.457	2.28
.9	.225	.494	2.19

Two comparisons were made. First, the Phase I .004 laminated specimens were examined. These specimens were tested with a cyclic stress range of 38,000 psi. Starting with an 0.070 in. surface flaw, an average cyclic life of 11,844 cycles-to-leak was measured. Assuming a semicircular flaw, a stress level for equivalent life in the monolithic material was determined as follows:

$$N = \frac{13.3254 \times 10^8}{(\Delta\sigma)^{4.27}} \left[44.9245 - \left(\frac{\Delta\sigma}{4.94} \right)^{1.135} \right]$$

N = cycles

$\Delta\sigma$ = cyclic stress, KSI

Q is assumed to be 2.46

This expression is reached by assuming that the product of stress and thickness must remain constant to support the applied load. By iteration an approximate stress level of 35,200 psi is determined for the monolithic material, so that a 8% weight decrease might be assumed for the laminated material.

A comparison was also made based on the Phase III laminated specimens with one-third thickness flaws. These specimens were tested with a cyclic stress increment of 45,600 psi and recorded an average cyclic-life-to-leak of 8052 cycles. In this comparison, a cyclic stress of 38,700 psi was determined for equivalent life in the monolithic specimen, or a weight advantage of 18% for the laminated material.

The results of the iteration procedure are shown in Table 4-25.

The tank weights previously discussed in Section 4 are based on stress levels of approximately 40,000 psi, so that a 8% weight saving for using laminated material will be used to arrive at a weight comparison. If we assume that the weld allowable strength is equal to that used in the monolithic material, 35 KSI, then the weight saving in the LO₂ tank is 141 lb and in the LH₂ tank, 323 lb. (Refer to Table 4-26).

It is possible that some deleterious effects may be experienced in the weld due to the presence of the interlayer material. In an effort to account for this possibility, weight calculations were repeated using a weld allowable strength of 28 KSI. The weight of weld lands in the tanks was estimated at 8% of the total tank weight. In this case net savings of 106 lb for the LO₂ tank and 242 lb for the LH₂ tank were computed. This means that a reduction in weld allowable from 35 KSI to 28 KSI decreases the tank weight saving from 8% to 6%.

TABLE 4-25 SPECIMEN COMPARISON, PHASES I AND III

● PHASE I

$$Q = 2.46$$

$$\Delta N = \frac{13.3254 \times 10^8}{(\Delta \sigma)^{4.27}} \left[44.9245 - \left(\frac{\Delta \sigma}{4.94} \right)^{1.135} \right]$$

$\Delta \sigma$, KSI	ΔN , Cycles
38	8,323
36	10,667
35	12,132
35.5	11,371
35.4	11,512
35.3	11,675
35.2	11,827

● PHASE III

$$Q = 2.46$$

$$\Delta N = \frac{13.3254 \times 10^8}{(\Delta \sigma)^{4.27}} \left[44.9245 - \left(\frac{\Delta \sigma}{5.928} \right)^{1.135} \right]$$

$\Delta \sigma$, KSI	ΔN , Cycles
42	5573
39	7806
38	8782
38.6	8179
38.8	7990
38.7	8084

TABLE 4-26 WEIGHT COMPARISON,
MONOLITHIC AND ROLL DIFFUSION BONDED LAMINATE

A. LAMINATE WELD ALLOWABLE 35 KSI

Tank	Weight lb	% Saving	Wt. Saving, lb
LO ₂	1760	8	141
LH ₂	4040.3	8	323

B. LAMINATE WELD ALLOWABLE 28 KSI

Tank	Weight, lb	Weld Wt, lb	Increased Weld Wt, lb	% Wt. Saving	Weight Saving, lb	Net Weight Saving, lb
LO ₂	1760	141	176	8	141	106
LH ₂	4040.3	323	404	8	323	242

Section 5

CONCLUSIONS AND RECOMMENDATIONS

CONCLUSIONS

Material Properties: Roll diffusion bonded and adhesive bonded laminated material showed much greater cyclic life, in the presence of a flaw, than monolithic material. Best results for the roll diffusion bonded laminate were indicated for material with arc .004 in. inter-layer thickness. Flaws in the roll diffusion bonded material grew to become through-the-thickness flaws while in the adhesive bonded specimens, a flaw initiated in a surface ply grew to the edges of the specimen in that ply but did not affect the adjacent ply. No relation between flaw depth in the roll diffusion bonded material and number of test cycles was determined.

Nondestructive Test: Shear wave ultrasonics and deep penetration eddy current methods detected flaws on the order of one-third the specimen thickness. Shear wave signal strength was found to vary linearly with surface flaw width in both monolithic and diffusion bonded specimens. Surface wave ultrasonics was able to predict the appearance of a back face dimple some 500 to 1000 cycles in advance in monolithic material. Less reliable results were obtained on diffusion bonded specimens. A vacuum leak detector unit, constructed to aid in determining the number of cycles to breakthrough, gave almost immediate response.

Fabricability: Tank designs and fabrication methods for large adhesive bonded laminated tanks showed the feasibility of this concept. LO₂ and LH₂ tank designs for a particular Orbiter configuration and loading showed a weight penalty of 10 to 14% for adhesive bonding compared to monolithic construction. Construction and inspection are considered more complex for adhesive bonded tanks than for monolithic tanks. Fabrication with roll diffusion bonded material seems similar to monolithic procedures. Ultimate weld strength of the .004 laminate was higher than the typical weld strength of monolithic material. Forming of diffusion bonded and adhesive bonded material to a 50 in. radius caused no defects. A pre-treatment investigation for bonding with METLBOND 329 adhesive showed that properly cleaned specimens, primed and unprimed, can demonstrate acceptable strength after over-aging, 30 day exposure at high humidity and 30 day salt spray tests.

Weight: Based on the program test results, a weight saving of 8% is projected for diffusion bonded tanks over monolithic tanks assuming a similar initial flaw and equivalent cyclic lives to leakage at a 40 KSI operating stress. Since flaws in adhesive bonded specimens did not grow through the thickness, a direct comparison on the basis of leakage was not possible for the adhesive bonded tank. The adhesive bonded specimens tested at 40 KSI gave greater life than the best diffusion bonded specimen, so that despite the 10 to 14% weight penalty mentioned earlier, the advantages of longer life and resistance to leakage make adhesive bonded construction a very effective concept.

Reliability: At operating stresses of 40 KSI, for the same number of cycles to leak, the starting flaw in laminated material is more than twice as wide as the starting flaw in monolithic material.

RECOMMENDATIONS FOR FUTURE WORK

In this program the thinnest interlayer laminate provided the best results. Reducing the interlayer still further may provide even better results.

Only semicircular flaws were tested in this program. The effect of flaw shape on the behavior of roll diffusion bonded laminates should be investigated.

If resources permit, specimens should be cycled, saw-cut and failed in tension to help with the determination of flaw shape at various stages of flaw growth in the laminated specimens.

All specimens in this program were machined from the "L" direction of the material. Verification of the properties in the "W" direction should be demonstrated.

Standard fatigue testing of the optimum laminate should be undertaken. Cyclic load programs for many type missions are available.

In sections through the weld in laminated plate, it was noted that the soft interlayer projects into the heat-affected zone. Since most weld failures occur in the HAZ, the presence of the interlayer may prove beneficial in halting flaw growth in this area. If testing can show that a delay does occur, this would be a most interesting result.

BIBLIOGRAPHY

1. Fracture Toughness of 7075-T6 and -T651 Sheet, Plate and Multilayered Adhesive-Bonded Panels, J. G. Kaufman, Aluminum Company of America, Journal of Basic Engineering, Trans. ASME, September 1967
2. Improved Fracture Toughness of Ti-6Al-4V Through Controlled Diffusion Bonding, D. Cox and A. S. Tetelman, Failure Analysis Associates, AFML-TR-71-264
3. The Fracture of Mild Steel Laminates, J. D. Embury, N. J. Petch, A. E. Wraith, and E. S. Wright, Transactions of the Metallurgical Society of AIME, Vol 239, January 1967
4. "Preliminary Test Results: Fatigue Crack Growth Evaluation of Laminated/Monolithic Construction" GAC IOM B35-196MO-8, 22 December 1970
5. "Status Report: Fatigue Crack Growth Evaluation of Laminated/Monolithic Construction", GAC IOM B34-196MO-25, 27 July 1971
6. "Status Report: Fatigue Crack Growth Evaluation of Laminated/Monolithic Construction", GAC IOM B34-196MO-59, 16 November 1971

Appendix A

FLAW GROWTH RATE TABLES

Tabular flaw growth records for each program test specimen are presented in this Appendix. Specimen records are ordered to coincide with the Program Test Plan, Table A-1. The specimen numbers which correspond to a particular test condition as called out in Table A-1, are listed in Table A-2.

TABLE A-1 TEST MATRIX FOR LAMINATED ALUMINUM COMPOSITES

Test Phase	Interlayer Thickness, In.	Number of Spec.	Precrack Flaw Depth	Cyclic Stress	Data Required
<u>Diffusion Bonded</u>					
I	0.004	6	1/3 thickness ⁽¹⁾	0-40 ksi	Flaw growth rate and cycles-to-leak
	0.008	6	1/3 thickness	0-40 ksi	
	0.012	6	1/3 thickness	0-40 ksi	
	None	6	1/3 thickness	0-40 ksi	
II	To be determined from I	6	1/2 thickness	0-40 ksi	Same
	None	6	1/2 thickness	0-40 ksi	
III	Same as II	3	1/3 thickness	0-48	Same
	Same as II	3	1/2 thickness	0-48	
	None	3	1/3 thickness	0-48	
	None	3	1/2 thickness	0-48	
<u>Adhesive Bond</u>					
	3 plys				
	.040" thick	3	1/3 thickness ⁽²⁾	0-40 ksi	Same
	each	3	1/3 thickness	0-48 ksi	

TABLE A-2 SPECIMEN IDENTIFICATION NUMBER

Phase	Fabrication	Interlayer t	Flaw Depth	Cyclic Stress	Specimen No.					
					1	2	3	4	5	6
I	Monolithic	-	1/3	40,000	1	3	5	7	9	11
I	Diffusion Bond.	.004	1/3	40,000	353492-1	353492-2	353492-3	353492-4	353492-5	353492-6
I	Diffusion Bond.	.008	1/3	40,000	353493-1	353493-2	353493-3	353493-4	353493-5	353493-6
I	Diffusion Bond.	.012	1/3	40,000	353494-1	353494-2	353494-3	353494-4	353494-5	353494-6
II	Monolithic	-	1/2	40,000	2	4	6	8	10	12
II	Diff. Bonded	.004	1/2	40,000	353492-1A	353492-2A	353492-3A	353492-4A	353492-5A	353492-6A
III	Monolithic	-	1/3	48,000	13	15	17			
III	Monolithic	-	1/2	48,000	14	16	18			
III	Diff'n Bond.	.004	1/3	48,000	353492-7A	353492-8A	353492-9A			
III	Diff'n. Bond.	.004	1/2	48,000	353492-10A	353492-11A	353492-12A			
	Adhesive Bonded	-	1/3	40,000	1	2	3			
	Adhesive Bonded	-	1/3	48,000	4	5	6			

Appendix A (Continued)

PHASE I SPECIMENS

TABLE A-3 FLAW GROWTH RECORD

SPECIMEN #1		TYPE: MONOLITHIC		ELOX: .020 x .040	
SHARPENING STRESS 20 KSI, RATE 5CPS		GROWTH STRESS 40 KSI, RATE 5CPS			
CYCLES	SURFACE LENGTH	CYCLES	FRONT FACE	REAR FACE	REMARKS
0	.040 (ELOX)	0	.090		
100,000	.040 (NO GROWTH)	500	.100		
RAISED STRESS TO 36 KSI		1000	.1075		
1000	.075	2000	.120		
DROPPED STRESS TO 20 KSI		3000	.140		
33,000	.075 (NO GROWTH)	4000	.170		
RAISED STRESS TO 36 KSI		4500	.190		
1000	.080	4950	.230		DIMPLE ON REAR FACE
1750	.085	5000	.235		DIMPLE ON REAR FACE
2200	.090	5500	.280		"DECIDED" DIMPLE ON REAR FACE
		5670	.300	.06	CRACK THRU
		6000	.360	.285	
		6250	.440	.420	
		6350	.500	.515	
		6400	.550	.550	
		6450	.620	.660	
		6497	.820	.840	FAILURE

TABLE A-4 FLAW GROWTH RECORD

Specimen No. 3 (1)		Type: Monolithic		ELOX: .021 x .040	
Sharpening Stress: 36 KSI Rate: 5 cps		Growth Stress: 40 KSI Rate: 5 cps			
Cycles	Surface Length, in.	Cycles	Front Face, in.	Rear Face, in.	Remarks
0	.040 (ELOX)	0	.090		
13,000	.055	500	.100		
13,500	.060	1000	.105		
14,000	.065	1500	.115		
14,500	.070	2000	.120		
15,000	.075	2500	.135		
15,500	.080	3000	.150		
16,000	.085	3500	.170		Ultrasonic Indication
16,250	.085				Dimple on
16,500	.0875	4000	.180		Rear Face
16,750	.0875				
17,000	.090	4500	.210		
		5000	.250		
		5500	.340	.080	Crack Thru
		6000	.400	.300	
		6250	.500	.500	
		6350	.600	.600	
		6450	.770	.800	
		6460	.820	.840	Failure

(1) Surface Wave Ultrasonics Used Intermittently

TABLE A-5 FLAW GROWTH RECORD

SPECIMEN #5		TYPE: MONOLITHIC		ELOX: .022 x .040	
SHARPENING STRESS: 36 KSI RATE: 5CPS			GROWTH STRESS: 40 KSI RATE: 5CPS		
CYCLES	SURFACE LENGTH	CYCLES	FRONT FACE	REAR FACE	REMARKS
0	.040 (ELOX)	0	.090		
10,000	.065	500	.095		
11,000	.075	1000	.100		
12,000	.085	1500	.110		
12,500	.0875	2000	.120		
12,750	.090	2500	.130		
		3000	.140		
		3500	.160		
		4000	.175		
		4500	.210		SLIGHT DIMPLE
		5000	.240		DECIDED DIMPLE
		5500	.290		DECIDED DIMPLE
		5720	.315	.190	CRACK THRU
		6000	.380	.335	
		6250	.480	.460	
		6350	.550	.580	
		6400	.600	.625	
		6450	.760	.720	
		6475	.780	.820	FAILURE

TABLE A-6 FLAW GROWTH RECORD

Specimen #7		Type: MONOLITHIC		ELOX: .023 x .040	
Sharpening Stress: 36 KSI Rate: 5 cps		Growth Stress: 40 KSI Rate: 5 cps			
Cycles	Surface Length, in.	Cycles	Front Face, in.	Rear Face, in.	Remarks
0	.040 (ELOX)	0	.090		
7,500	.050	1000	.100		
8,000	.055	2000	.120		
9,000	.060	3000	.150		
10,000	.070	3700	—		Dimple on Rear Face
11,000	.075				
11,500	.080	4000	.195		
12,000	.085	4500	.230		
12,500	.0875	4900	—	.060	Crack Thru
12,750	.089	5500	.370	.220	
13,000	.090	5915	.800	.800	Failure

TABLE A-7 FLAW GROWTH RECORD

Specimen No. 9 ⁽¹⁾		Type: Monolithic		ELOX: .024 x .040	
Sharpening Stress: 36 KSI Rate: 5 cps		Growth Stress: 40 KSI Rate: 5 cps			
Cycles	Surface Length, in.	Cycles	Front Face: in.	Rear Face, in.	Remarks
0	.040 (ELOX)	0	.070		
13,250	.065	500	.080		
14,100	.070	1000	.085		
		1500	.090		
		2000	.095		
		2500	.100		
		3000	.105		
		3500	.110		
		4000	.120		
		4500	.130		
		5000	.140		
		5500	.155		
		6000	.170		
		6500	.200		Dimple on Rear Face
		7000	.230		
		7500	.280		
		7660	.300	.060	Leak Detector Indication
		8000	.360	.200	
		8500	.740	.740	
		8515	.780	.780	Failure

(1) Vacuum Leak Detector Used Throughout Test

TABLE A-8 FLAW GROWTH RECORD

Specimen No. 11 ⁽¹⁾		Type: Monolithic		ELOX: .024 x .040	
Sharpening Stress: 36 KSI Rate: 5 cps		Growth Stress: 40 KSI Rate: 5 cps			
Cycles	Surface Length, in.	Cycles	Front Face, In.	Rear Face, in.	Remarks
0	.040 (ELOX)	0	.070		
10,460	.065	1000	.080		
11,000	.070	1500	.090		
		2000	.095		
		2500	.100		
		3000	.105		
		3500	.110		
		4000	.130		
		4500	.150		
		5000	.165		
		5500	.180		
		6000	.220		
		6500	.255		
		6830	.300	.060	Leak Detector Indication
		7000	.320	.080	
		7250	.370	.280	
		7500	.450	.360	
		7866	.830	.830	Failure

(1) Vacuum Leak Detector Used Throughout Test

TABLE A-9 FLAW GROWTH RECORD

Specimen No. 353492-1		Type: .004 Laminate		ELOX: .018 x .040	
Sharpening Stress: 36 KSI Rate: 5 cps		Growth Stress: 40 KSI Rate: 5 cps			
Cycles	Surface Length, in.	Cycles	Front Face, in.	Rear Face, in.	Remarks
0	.040 (ELOX)	0	.070		
13,400	.050	500	.080		
14,000	.060	1000	.090		
16,000	.070	1500	.100		
		2000	.110		
		2500	.120		
		3000	.130		
		3500	.140		Dye Injected
		4000	.150		
		4500	.160		
		5000	.170		
		5500	.190		Surface Wave Ultrasonic Indication
		6000	.210		
		6500	.230		
		7000	.250		Eddy Current Indication
		7500	.270		Dimple on Rear Face
		8000	.290		
		8500	.310		
		9000	.340		
		9500	.360		
		10,000	.400		
		10,500	.440		
		11,000	.480		
		11,500	.540		
		12,000	.600		
		12,100	.630	.080	Crack Thru
		12,430	.820	.820	Failure

(1) Surface Wave Ultrasonic and Eddy Current Readings Taken Throughout Test

TABLE A-10 FLAW GROWTH RECORD

Specimen No. 353492-2		Type: .004 LAMINATE		ELOX: .023 x .040	
Sharpening Stress: 36 KSI Rate: 5 cps		Growth Stress: 40 KSI Rate: 5 cps			
Cycles	Surface Length, in.	Cycles	Front Face, in.	Rear Face, in.	Remarks
0	.040 (ELOX)	0	.070		
9,000	.060	500	.080		
10,000	.070	1000	.090		
		1500	.100		
		2000	.110		
		2500	.120		
		3000	.130		
		3500	.140		
		4000	.150		
		4500	.160		
		5000	.170		
		5500	.180		
		6000	.200		
		6500	.220		
		7000	.240		
		7500	.250		
		8000	.260		
		8500	.280		
		9000	.290		
		9500	.320		
		10,000	.360		
		10,300	.380		
		10,500	.400		
		10,800	.415		
		11,000	.430		Dimple On Rear Face
		11,300	.470		
		11,500	.490		
		11,800	.520		
		12,000	.560	.080	Crack Thru
		12,300	.620	.360	
		12,450	.800	.800	Failure

TABLE A-11 FLAW GROWTH RECORD

Specimen No. 353492-3 ⁽¹⁾		Type: .004 Laminate		ELOX: .018 x .040	
Sharpening Stress: 36 KSI Rate: 5 cps		Growth Stress: 40 KSI Rate: 5 cps			
Cycles	Surface Length, in.	Cycles	Front Face, in.	Rear Face, in.	Remarks
0	.040 (ELOX)	0	.070		
9000	.050	500	.080		
10,000	.060	1000	.090		
11,800	.070	1500	.095		
		2000	.110		
		2500	.120		
		3000	.130		
		3500	.137		
		3800	.140		
		4000	.142		Dye Injected
		4500	.160		
		5000	.180		
		5500	.190		Surface Wave Ultrasonic Indication
		6000	.210		
		6500	.230		
		7000	.250		Eddy Current Indication
		7500	.270		
		8000	.290		
		8500	.310		Dimple on Rear Face
		9000	.330		
		9500	.350		
		10,000	.380		
		10,500	.400		
		11,000	.420		
		11,500	.440		
		12,000	.500		
		12,500	.550		
		13,000	.600		
		13,500	.660		
		13,550	.680	.08	Crack-Thru Failure
		13,900	.800	.700	

(1) Surface Wave Ultrasonic and Eddy Current Readings Taken Throughout Test

TABLE A-12 FLAW GROWTH RECORD

Specimen No. 353492-4		Type: .004 LAMINATE		ELOX: .022 x .040	
Sharpening Stress: 36 KSI Rate: 5 cps		Growth Stress: 40 KSI Rate: 5 cps			
Cycles	Surface Length, in.	Cycles	Front Face, in.	Rear Face, in.	Remarks
0	.040 (ELOX)	0	.080		
14,000	.080	500	.090		
		1,000	.100		
		1,500	.110		
		2,000	.120		
		2,500	.130		
		3,000	.140		
		3,500	.150		
		4,000	.170		
		4,500	.190		
		5,000	.205		
		5,500	.220		
		6,000	.240		
		6,500	.260		
		7,000	.300		Dimple On Rear Face
		7,500	.330		
		8,000	.360		
		8,500	.390		
		9,000	.430		
		9,500	.480		
		10,000	.580		
		10,085	.600	.100	Crack Thru
		10,200	.640	.320	
		10,300	.700	.540	
		10,350	.840	.800	Failure

TABLE A-13 FLAW GROWTH RECORD

Specimen No. 353492-5		Type: .004 Laminate		ELOX: .020 x .040	
Sharpening Stress: 36 KSI Rate: 5 cps		Growth Stress: 40 KSI Rate: 5 cps			
Cycles	Surface Length, in.	Cycles	Front Face, in.	Rear Face, in.	Remarks
0	.040 (ELOX)	0	.070		
10,000	.060	500	.080		
11,500	.070	1000	.090		
		1500	.100		
		2000	.110		
		2500	.120		
		3000	.130		
		3500	.150		
		4000	.160		
		4500	.170		
		5000	.190		
		5500	.210		
		6000	.230		Dye Injected
		6500	.245		
		7000	.260		
		7500	.280		
		8000	.300		Dimple on Rear Face
		8500	.340		
		9000	.380		
		9500	.430		Dye Repeated
		10,000	.490		
		10,800	.620	.080	Crack thru
		10,900	.650	.240	
		11,000	.680	.400	
		11,120	.800	.780	Failure

TABLE A-14 FLAW GROWTH RECORD

Specimen No. 353492-6		Type: .004 LAMINATE		ELOX: .027 x .040	
Sharpening Stress: 36 KSI Rate: 5 cps		Growth Stress: 40 KSI Rate: 5 cps			
Cycles	Surface Length, in.	Cycles	Front Face, in.	Rear Face, in.	Remarks
0	.040 (ELOX)	0	.070		
9500	.070	500	.085		
		1,000	.090		
		1,500	.100		
		2,000	.110		
		2,500	.115		
		3,000	.125		
		4,000	.170		
		5,000	.195		
		6,000	.225		
		7,000	.275		
		7,500	.300		
		8,000	.330		
		8,500	.360		
		9,000	.390		
		9,500	(.440) ?		Dimple On Rear Face
		10,000	.460		
		10,500	.500		
		11,000	.535		
		11,500	.610		
		11,750	.640		
		12,000	.680		
		12,200	.740	.200	Crack Thru
		12,300	.820	.820	Failure

TABLE A-15 FLAW GROWTH RECORD

Specimen No. 353493-1		Type: .008 LAMINATE		ELOX: .021 x .040	
Sharpening Stress: 36 KSI Rate: 5 cps		Growth Stress: 40 KSI Rate: 5 cps			
Cycles	Surface Length, in.	Cycles	Front Face, in.	Rear Face, in.	Remarks
0	.040 (ELOX)	0	.070		
8,000	.060	1,000	.090		
8,500	.070	2,000	.110		
		2,500	.120		
		3,500	.165		
		4,000	.180		
		4,500	.205		
		5,000	.225		
		5,500	.245		
		6,000	.275		
		6,500	.295		Dimple On Rear Face
		7,000	.330		
		7,500	.390		
		8,000	.440		
		8,250	.470		
		8,500	.500		
		8,700	.530		
		8,900	.600	.070	Crack Thru
		9,000	.670	.340	
		9,050	.780	.750	Failure

TABLE A-16 FLAW GROWTH RECORD

Specimen No. 353493-2		Type: .008 LAMINATE		ELOX: .023 x .040	
Sharpening Stress: 36 KSI Rate: 5 cps		Growth Stress: 40 KSI Rate: 5 cps			
Cycles	Surface Length, in.	Cycles	Front Face, in.	Front Face, in.	Remarks
0	.040 (ELOX)	0	.070		
9,000	.065	500	.080		
9,500	.070	1,000	.090		
		1,500	.100		
		2,000	.110		
		2,500	.120		
		3,000	.130		
		3,500	.140		
		4,000	.150		
		4,500	.170		
		5,000	.180		
		5,500	.200		
		6,000	.220		
		6,500	.240		
		7,000	.260		
		7,500	.300		
		8,000	.340		Dimple On Rear Face
		8,500	.410		
		9,000	.490	.060	Crack Thru
		9,100	.540	.200	
		9,200	.560	.360	
		9,300	.660	.560	
		9,330	.820	.800	Failure

TABLE A-17 FLAW GROWTH RECORD

Specimen No. 353493-3 ⁽¹⁾ Type: .008 Laminate ELOX: .023 x .040					
Sharpening Stress: 36 KSI Rate: 5 cps		Growth Stress: 40 KSI Rate: 5 cps			
Cycles	Surface Length, in.	Cycles	Front Face, in.	Rear Face, in.	Remarks
0	.040 (ELOX)	0	.070		
10,000	.060	500	.075		
10,500	.065	1500	.090		
11,000	.070	2000	.100		
		2500	.110		
		3000	.120		
		3500	.130		
		4000	.145		
		4500	.160		
		5000	.175		
		5500	.190		
		6000	.205		
		6500	.220		
		7000	.240		
		7500	.270		
		8000	.300		
		8500	.330		
		9000	.360		
		10,000	.440		
		10,200	.490	.080	Leak Detector Indication
		10,500	.560	.360	
		10,700	.800	.760	Failure
(1) Leak Detector Unit Used Throughout Test					

TABLE A-18 FLAW GROWTH RECORD

Specimen No. 353493-4 ⁽¹⁾ Type: .008 Laminate ELOX: .025 x .040					
Sharpening Stress: 36 KSI Rate: 5 cps		Growth Stress: 40 KSI Rate: 5 cps			
Cycles	Surface Length, in.	Cycles	Front Face, in.	Rear Face, in.	Remarks
0	.040 (ELOX)	0	.070		
10,000	.070	500	.080		
		1000	.090		
		1500	.100		
		2000	.110		
		2500	.120		
		3000	.130		
		3500	.140		
		4000	.155		
		4500	.170		
		5000	.180		
		5500	.200		
		6000	.215		
		6500	.230		
		7000	.245		
		7500	.270		
		8000	.300		
		8500	.325		
		9000	.355		
		9500	.400		
		10,000	.445		
		10,500	.490		
		10,688	.530	.08	Leak Detector Indication
		11,000	.610	.370	
		11,100	.810	.800	Failure
(1) Leak Detector Unit Used Throughout Test					

TABLE A-19 FLAW GROWTH RECORD

Specimen No.: 353493-5 ⁽¹⁾ Type: .008 Laminate ELOX: .021 x .040					
Sharpening Stress: 36 KSI Rate: 5 cps		Growth Stress: 40 KSI Rate: cps			
Cycles	Surface Length, in.	Cycles	Front Face, in.	Rear Face, in.	Remarks
0	.040 (ELOX)	0	.070		
10,000	.070	500	.080		
		1000	.085		
		1500	.095		
		2000	.105		
		2500	.120		
		3500	.135		
		4000	.150		
		4500	.170		
		5000	.190		
		5500	.210		
		6000	.225		
		6500	.245		
		7000	.290		
		7500	.340		
		8000	.380		
		8500	.460		
		8750	.510	.080	Leak Detector Indication
		9000	.630	.440	
		9070	.820	.820	Failure
(1) Leak Detector Unit Used Throughout Test					

TABLE A-20 FLAW GROWTH RECORD

Specimen No. 353493-6		Type: .008 LAMINATE		ELOX: .028 x .040	
Sharpening Stress: 36 KSI Rate: 5 cps		Growth Stress: 40 KSI Rate: 5 cps			
Cycles	Surface Length, in.	Cycles	Front Face, in.	Rear Face, in.	Remarks
0	.040 (ELOX)	0	.070		
7,500	.070	1,000	.085		
		2,000	.105		
		2,500	.120		
		3,000	.135		
		3,500	.155		
		4,000	.180		
		4,500	.195		
		5,000	.215		
		5,500	.235		
		6,000	.260		
		6,500	.285		
		7,000	.320		Dimple On Rear Face
		7,500	.365		
		8,000	.440		
		8,500	.570	.200	Crack Thru Failure
		8,585	.620	.580	

TABLE A-21 FLAW GROWTH RECORD

Specimen No. 353494-1 ⁽¹⁾ Type: .012 Laminate ELOX: .024 x .040					
Sharpening Stress: 36 KSI Rate: 5 cps		Growth Stress: 40 KSI Rate: 5 cps			
Cycles	Surface Length, in.	Cycles	Front Face, in.	Rear Face, in.	Remarks
0	.040 (ELOX)	0	.070		
9200	.070	500	.085		
		1000	.105		
		1500	.120		
		2000	.130		
		2500	.145		
		3000	.160		
		3500	.180		
		4000	.200		
		4500	.220		
		5000	.245		
		5500	.300		
		6000	.360		
		6312	.460	.080	Leak Detector Indication
		6500	.540	.370	
		6585	.700	.700	Failure
(1) Vacuum Leak Detector Unit Used Throughout Test					

TABLE A-22 FLAW GROWTH RECORD

Specimen No. 353494-2		Type: .012 LAMINATE		ELOX: .023 x .040	
Sharpening Stress: 36 KSI Rate: 5 cps		Growth Stress: 40 KSI Rate: 5 cps			
Cycles	Surface Length, in.	Cycles	Front Face, in.	Rear Face, in.	Remarks
0	.040 (ELOX)	0	.070		
9,250	.070	500	.080		
		1,000	.090		
		1,500	.110		
		2,000	.125		
		2,500	.140		
		3,000	.155		
		3,500	.175		
		4,000	.195		
		4,500	.215		
		5,000	.240		
		5,500	.265		
		6,000	.300		Dimple On Rear Face
		6,500	.350		
		7,000	.460		
		7,061	.460	.080	Crack Thru
		7,164	.510	.280	
		7,200	.520	.340	
		7,300	.640	.640	Failure

TABLE A-23 FLAW GROWTH RECORD

Specimen No. 353494-3 ⁽¹⁾ Type: .012 Laminate ELOX: .022 x .040					
Sharpening Stress: 36 KSI Rate: 5 cps		Growth Stress: 40 KSI Rate: 5 cps			
Cycles	Surface length, in.	Cycles	Front Face, in.	Rear Face, in.	Remarks
0	.040 (ELOX)	0	.080		
10,250	.060	500	.085		
10,750	.065	1000	.095		
11,050	.080	1500	.115		
		2000	.130		
		2500	.150		
		3000	.165		
		3500	.185		
		4000	.210		
		4500	.230		
		5000	.275		
		5500	.335		
		6000	.415		
		6068	.435	.090	Leak Detector Indication Failure
		6348	.670	.780	
(1) Vacuum Leak Detector Used Throughout Test					

TABLE A-24 FLAW GROWTH RECORD

Specimen No. 353494-4		Type: .012 LAMINATE		ELOX: .023 x .040	
Sharpening Stress: 36 KSI Rate: 5 cps		Growth Stress: 40 KSI Rate: 5 cps			
Cycles	Surface Length, in.	Cycles	Front Face, in.	Rear Face, in.	Remarks
0	.040 (ELOX)	0	.070		
5,000	.055	1,000	.090		
6,000	.065	2,000	.135		
6,300	.070	2,500	.145		
		3,000	.175		
		3,500	.190		
		4,000	.225		
		4,500	.250		Dimple On Rear Face
		5,000	.290		
		5,500	.370		
		6,000	.510	.100	Crack Thru Failure
		6,145	.700	.700	

TABLE A-25 FLAW GROWTH RECORD

Specimen No. 353494-5

Type: .012

ELOX: .022 x .040

SPECIMEN ACCIDENTALLY OVERLOADED TO FAILURE AFTER
5000 CYCLES AT 36 KSI

TABLE A-26 FLAW GROWTH RECORD

Specimen No. 353494-6		Type: .012 LAMINATE		ELOX: .016 x .040	
Sharpening Stress: 36 KSI Rate: 5 cps		Growth Stress: 40 KSI Rate: 5 cps			
Cycles	Surface Length, in.	Cycles	Front Face, in.	Rear Face, in.	Remarks
0	.040 (ELOX)	0	.070		
7,000	.070	500	.080		
		1,000	.090		
		1,500	.110		
		2,500	.160		
		3,000	.190		
		3,500	.210		
		4,000	.240		
		4,500	.270		
		5,000	.340		Dimple On Rear Face
		5,500	.400		
		6,000	.530	.300	Crack Thru Failure
		6.150	.660	.630	

Appendix A (Continued)

PHASE II SPECIMENS

TABLE A-27 FLAW GROWTH RECORD

Specimen No.: 2		Type: MONOLITHIC		ELOX: .020 X .040	
Sharpening Stress: 36 Rate: 5		Growth Stress: 40 KSI Rate: 5 CPS			
Cycles	Surface Length, in.	Cycles	Front Face, in.	Rear Face, in.	Remarks
0	.040 (ELOX)	0	.135		
12000	.050	1000	.140		
19000	.110	1500	.150		
19200	.125	2000	.170		
19250	.130	2500	.190		
19300	.135 (1)	3000	.220		
		3500	.250		
		4000	.310		
		4019	.310	.08	Crack on Rear Face
		4500	.410	.280	
		4972	.820	.820	Failed

Notes 1. Specimen was dye marked at this time.

TABLE A-28 FLAW GROWTH RECORD

Specimen No.: 4		Type: Monolithic		ELOX: .022' X .040	
Sharpening Stress: 36 Rate: 5 CPS		Growth Stress: 40 KSI Rate: 5 CPS			
Cycles	Surface Length, in.	Cycles	Front Face, in.	Rear Face, in.	Remarks
0	.040 (ELOX)	0	.135		
11,000	Possible Start	500	.150		
12,000	.060	1000	.165		
13,000	.070	1500	.190		
15,000	.090	2000	.210		
16,000	.095	2500	.250		
17,000	.100	3000	.290		
18,500	.107	3078	.300	.06	Crack on Rear Face
19,000	.115	3500	.380	.28	
19,200	.120	3985	.800	.800	Failed
19,400	.122				
19,600	.129				
19,800	.127				
20,000	.130				
20,300	.135 (1)				

Note: 1. Specimen was dye marked at this time.

TABLE A-29 FLAW GROWTH RECORD

SPECIMEN #6		TYPE: MONOLITHIC		ELOX: .023 x .040	
SHARPENING STRESS: 36 KSI RATE: 5CPS // GROWTH STRESS: 40 KSI RATE: 5CPS					
CYCLES	SURFACE LENGTH	CYCLES	FRONT FACE	REAR FACE	REMARKS
0	.040 (ELOX)	0	.135		
10,000	.060	500	.150		
12,000	.070	1000	.175		
14,000	.085	1500	.200		
16,000	.100	1658	.205		SLIGHT DIMPLE
17,000	.115	2000	.230		
17,500	.120	2500	.270		DECIDED DIMPLE
17,700	.125	2700	.300		
18,000	.130	2740	.305	.040	CRACK THRU
18,250	.135	2900	.325	.150	
		3100	.410	.230	
		3200	.430	.300	
		3300	.465	.380	
		3400	.530	.480	
		3500	.670	.680	
		3521	.740	.740	FAILURE

TABLE A-30 FLAW GROWTH RECORD

Specimen #8		Type: MONOLITHIC		ELOX: .023 x .040	
Sharpening Stress: 36 KSI Rate: 5 cps		Growth Stress: 40 KSI Rate: 5 cps			
Cycles	Surface Length, in.	Cycles	Front Face, in.	Rear Face, in.	Remarks
0	.040 (ELOX)	0	.135		
10,000	.045	500	.140		
11,000	.055	1000	.160		
12,000	.060	1500	.190		Slight Dimple
13,000	.070				On Rear Face
14,000	.085	2000	.220		
15,000	.090	2500	.260		Decided Dimple
16,000	.095	2745	.285	.050	Crack Thru
17,000	.100	3000	.320	.180	
17,500	.110	3200	.365	.300	
18,000	.120	3400	.450	.440	
18,400	.131	3500	.540	.500	
18,450	.135	3575	.620	.600	
		3645	.820	.820	Failure

TABLE A-31 FLAW GROWTH RECORD

Specimen No.: 10		Type: Monolithic		ELOX: .024 X .040	
Sharpening Stress: 36 KSI Rate: 5 CPS		Growth Stress: 40 KSI Rate: 5 CPS			
Cycles	Surface Length, in.	Cycles	Front Face, in.	Rear Face, in.	Remarks
0	.040 (ELOX)	0	.135		
12,000	.070	500	.150		
14,000	.190	1000	.170		
16,000	.105	1500	.195		
18,000	.120	2000	.215		
18,500	.135 (1)	2500	.260		
		2700	.285		
		2769	.290	.040	Crack on Rear Face
		3000	.330	.120	
		3250	.380	.280	
		3500	.500	.440	
		3680	.800	.800	Failed

Note: 1 Specimen was dye marked at this time.

TABLE A-32 FLAW GROWTH RECORD

Specimen No.: 12		Type: Monolithic		ELOX: .024 X .040	
Sharpening Stress: 36 KSI Rate: 5 CPS		Growth Stress: 40 KSI Rate: 5 CPS			
Cycles	Surface Length, in.	Cycles	Front Face, in.	Rear Face, in.	Remarks
0	.040 (ELOX)	0	.135		
12,000	.020	500	.150		
16,000	.090	1000	.170		
18,000	.110	1500	.190		
20,000	.135	2000	.210		
		2500	.260		
		2786	.300	.08	Crack on Rear Face
		3000	.340	.230	
		3250	.400	.340	
		3500	.600	.600	
		3550	.800	.800	Failed

Notes: 1. Specimen was dye marked at this time.

TABLE A-33 FLAW GROWTH RECORD

Specimen No. 353492-1A		Type: .004 Laminate		ELOX: .018 x .050	
Sharpening Stress: 36 KSI Rate: 5 cps		Growth Stress: 40 KSI Rate: 5 cps			
Cylces	Surface Length, in.	Cycles	Front Face: in.	Rear Face: in.	Remarks
0	.050 (ELOX)	0	.290		
13,700	.080	250	.310		
15,000	.085	500	.320		
16,000	.095	750	.330		
17,000	.105	1000	.340		Dimple on Rear Face
18,000	.120				
19,000	.140	1250	.350		
20,000	.155	1500	.360		
21,000	.170	1750	.380		
22,000	.195	2000	.390		
23,000	.215	2250	.410		
24,000	.240	2500	.410		
25,000	.270	2750	.420		
25,400	.280	3000	.430		
25,500	.280	3250	.450		
25,600	.290	3500	.460		
		3750	.480		
		4000	.500		
		4250	.520		
		4500	.540		
		4750	.540		
		5000	.560		
		5250	.580		
		5500	.600		
		5750	.630		
		6000	.660		
		6250	.700		
		6500	.730		
		6750	.770		
		7000	.840	.360	
		7040	.920	.690	Crack Thru Failure Dye did not penetrate crack

TABLE A-34 FLAW GROWTH RECORD

Specimen No. 353492-2A		Type: .004 Laminate		ELOX: .016 x .050	
Sharpening Stress: 36 KSI Rate: 5 cps		Growth Stress: 40 KSI Rate: 5 cps			
Cycles	Surface Length, in.	Cycles	Front Face: in.	Rear Face: in.	Remarks
0	.050 (ELOX)	0	.290		
11,000	.060	500	.330		
12,000	.065	1000	.395		Dimple on Rear Face
13,000	.075				
14,000	.085	1500	.495		
15,000	.095	2000	.660		
16,000	.110	2250	.780		
17,000	.125	2350	.820		
18,000	.140	2400	.850		
19,000	.155	2450	.890		
20,000	.185	2500	.940		
21,000	.215	2550	.970		
22,000	.255	2600	1.030		
23,000	.280	2650	1.080		
23,200	.290	2750	1.350		Failure, Separation between 2nd & 3rd layers Dye penetrated to third layer

TABLE A-35 FLAW GROWTH RECORD

Specimen No.: 353492-3A ⁽¹⁾ Type: Laminate ELOX: .110 X .053					
Sharpening Stress: 36 KSI Rate: 5 CPS		Growth Stress: 40 KSI Rate: 5 CPS			
Cycles	Surface Length, in.	Cycles	Front Face, in.	Rear Face, in.	Remarks
0	.110	0	.145		
3,100	.145 (2)	1000	.195		
		2200	.280		
		2500	.315		
		3200	.400		
		3500	.450		
		3750	.500		
		4000	.560		
		4180	.640	.200	Crack Thru Leak Detection
		4250	.670	.340	
		4300	.750	.530	Failure (3)
Notes: 1. Vacuum leak detector used throughout test. 2. Specimen was dye marked at this time. 3. Dye did not penetrate crack.					

TABLE A-36 FLAW GROWTH RECORD

Specimen No.: 353492-1A ⁽¹⁾ Type: Laminate		ELOX: .110 X .053			
Sharpening Stress: 36 KSI Rate: 5 CPS		Growth Stress: 40 KSI Rate: 5 CPS			
Cycles	Surface Length, in.	Cycles	Front Face, in.	Rear Face, in.	Remarks
0	.110	0	.145		Penetrate
3150	.145 (2)	1000	.195		
		2000	.245		
		3000	.320		
		3500	.365		
		4000	.450		
		4250	.500		
		4500	.560		
		4690	.590	.100	Crack thru Leak Detection
		4800	.680	.320	
		4900	.720	.650	
		4930	.800	.720	Failure ⁽³⁾
Notes: 1. Vacuum leak detector used throughout test 2. Specimen was dye marked at this time 3. Dye did not penetrate crack					

TABLE A-37 FLAW GROWTH RECORD

Specimen No.: 353492-5A ⁽¹⁾ Type: Laminate ELOX: .110 X .048 .004 Diffusion Line					
Sharpening Stress: 36 KSI Rate: 5 CPS		Growth Stress: 40 KSI Rate: 5 CPS			
Cycles	Surface Length, in.	Cycles	Front Face, in.	Rear Face, in.	Remarks
0	.110	0	.145		
3300	.145 (2)	1000	.180		
		2000	.220		
		3000	.275		
		3500	.310		
		4000	.355		
		4500	.405		
		4750	.440		
		5000	.475		
		5250	.525		
		5500	.580		
		5685	.620	.110	Crack thru Leak Detection
		5750	.650	.240	
		5850	.700	.440	
		5930	.780	.700	Failure
Notes: 1. Vacuum leak detector used throughout test 2. Specimen was dye marked at this time					

TABLE A-38 FLAW GROWTH RECORD

Specimen No.: 353492-6A ⁽¹⁾ Type: Laminate ELOX: .110 X .059 .004 Diffusion Line					
Sharpening Stress: 36 KSI Rate: 5 CPS		Growth Stress: 40 KSI Rate: 5 CPS			
Cycles	Surface Length, in.	Cycles	Front Face, in.	Rear Face, in.	Remarks
0	.110	0	.150		
2600	.150 (2)	1000	.205		
		2000	.295		
		2500	.355		
		3000	.420		
		3500	.520		
		3750	.580		
		4000	.670		
		4130	.710	.100	Crack thru Leak Detection
		4200	.760	.220	
		4235	.820	.540	Failure
Notes: 1. Vacuum leak detector used throughout test 2. Specimen was dye marked at this time					

Appendix A (Continued)

PHASE III SPECIMENS

TABLE A-39 FLAW GROWTH RECORD

Specimen #13		Type: MONOLITHIC		ELOX: .025 x .040	
Sharpening Stress: 36 KSI Rate: 5 cps		Growth Stress: 48 KSI Rate: 5 cps			
Cycles	Surface Length, in.	Cycles	Front Face, in.	Rear Face, in.	Remarks
0	.040 (ELOX)	0	.090		
11,000	.050	500	.105		
12,000	.055	1000	.120		
13,000	.060	1500	.135		
14,000	.065	2000	.200		Slight Dimple
15,000	.075	2250	.230		
15,750	.080	2500	.290		
16,000	.0825	2572	.305	.070	Crack Thru
16,500	.089	2700	.345	.240	
16,600	.090	2800	.480	.440	
		2810	.500	.450	Failure

TABLE A-40 FLAW GROWTH RECORD

Specimen No.: 14		Type: Monolithic		ELOX: .025 X .040	
Sharpening Stress: 36 KSI Rate: 5 CPS		Growth Stress: 48 KSI Rate: 5 CPS			
Cycles	Surface Length, in.	Cycles	Front Face, in.	Rear Face, in.	Remarks
0	.040 (Elox)	0	.135		Ultrasonic Reading Dimple on Rear Face
10,000	.075	250	.150		
12,000	.085	500	.170		
14,000	.100	750	.190		
15,000	.115	1000	.220		
15,500	.120	1250	.280		Crack on Rear Face Failed
16,000	.125	1500	.420	.380	
16,350	.135	1520	.460	.440	

TABLE A-41 FLAW GROWTH RECORD

Specimen No.: 15		Type: Monolithic		ELOX:.025 X .040	
Sharpening Stress: 36 KSI Rate: '5 CPS		Growth Stress: 48 KSI Rate: '5 CPS			
Cycles	Surface Length, in.	Cycles	Front Face, in.	Rear Face, in.	Remarks
0	.040 (Elox)	0	.070		
10,300	.070	500	.080		
		1000	.090		
		1500	.100		
		2000	.110		
		2500	.115		
		3000	.150		
		3500	.210		
		4000	.350	.08	Dimple on Rear Face
		4130	.490	.430	Crack on Rear Face
					Failure

TABLE A-42 FLAW GROWTH RECORD

Specimen No.: 16		Type: Monolithic		ELOX: .025 X .040	
Sharpening Stress: 36 KSI Rate: 5 CPS		Growth Stress: 48 KSI Rate: 5 CPS			
Cycles	Surface Length, in.	Cycles	Front Face, in.	Rear Face, in.	Remarks
0	.040 (Elox)	0	.135		
10,000	.080	700	.170		
13,500	.135	1000	.230		Dimple on Rear Surface
		1250	.280		
		1350	.310	.100	Crack on Rear Face
		1450	.385	.320	
		1530	.470	.430	Failure

TABLE A-43 FLAW GROWTH RECORD

Specimen No.: 17		Type: Monolithic		ELOX: .027 X .040	
Sharpening Stress: 36 KSI Rate: 5 CPS		Growth Stress: 48 KSI Rate: 5 CPS			
Cycles	Surface Length, in.	Cycles	Front Face, in.	Rear Face, in.	Remarks
0	.040 (Elox)	0	.070		
9500	.065	250	.080		
10000	.070	500	.090		
		750	.095		
		1000	.100		
		1250	.105		
		1500	.110		
		1750	.120		
		2000	.125		
		2250	.140		
		2500	.155		
		2750	.170		
		3000	.195		
		3250	.230		
		3500	.275		
		3683	.335	.070	Crack on Rear Face
		3750	.400	.260	
		3800	.490	.470	Failed

TABLE A-44 FLAW GROWTH RECORD

Specimen No.: 18		Type: Monolithic		ELOX: .029 X .040	
Sharpening Stress: 36 KSI Rate: 5 CPS		Growth Stress: 48 KSI Rate: 5 CPS			
Cycles	Surface Length, in.	Cycles	Front Face, in.	Rear Face, in.	Remarks
0	.040 (Elox)	0	.135		
12,000	.070	250	.160		
14,500	.100	500	.190		
14,000	.110	750	.230		
16,000	.135	1000	.280		
		1100	.300		
		1200	.330		
		1241	.340	.080	Crack on Rear Face
		1300	.380	.220	
		1350	.480	.480	Failed

TABLE A-45 FLAW GROWTH RECORD

Specimen No.: 353492-7A		Type: Laminate		ELOX: .016 X .050	
Sharpening Stress: 36 KSI Rate: 5 CPS		Growth Stress: 48 KSI Rate: 5 CPS			
Cycles	Surface Length, in.	Cycles	Front Face, in.	Rear Face, in.	Remarks
0	.055	0	.070		
9000	.065	1000	.096		
9500	.070 (1)	2000	.135		
		3000	.180		
		3500	.210		
		4000	.245		
		4500	.295		
		5000	.335		
		5500	.375		
		6000	.430		
		6500	.480		
		6750	.550		
		7000	.560		
		7250	.590		
		7500	.620		
		7750	.680		
		8000	.770		
		8175	.890	.150	Failure (2)

Notes: 1. Specimen was dye marked at this time
2. Dye did not penetrate crack

TABLE A-46 FLAW GROWTH RECORD

Specimen No. 353492-8A		Type: .004 Laminate		ELOX: .018 x .050	
Sharpening Stress: 36 KSI Rate: 5 cps		Growth Stress: 48 KSI Rate: 5 cps			
Cycles	Surface Length, in.	Cycles	Front Face: in.	Rear Face: in.	Remarks
0	.050 (ELOX)	0	.070		
14,500	.070	250	.080		
		500	.090		
		750	.100		
		1000	.105		
		1250	.110		
		1500	.120		
		1750	.135		
		2000	.150		
		2250	.160		
		2500	.180		
		2750	.190		
		3000	.210		
		3250	.230		
		3500	.240		
		3750	.260		
		4000	.280		
		4150	.290		
		4250	.300		Dimple on Rear Face
		4500	.320		
		4750	.340		
		5000	.360		
		5250	.380		
		5500	.400		
		5750	.430		
		6000	.460		
		6250	.480		
		6500	.510		
		6750	.540		
		7000	.580		
		7250	.620		
		7500	.680		
		7750	.840	.140	Failure, Dye penetrated first layer only

TABLE A-47 FLAW GROWTH RECORD

Specimen No.: 353492-9A		Type: LAMINATE		ELOX: .015 X .050	
Sharpening Stress: 36 KSI Rate: 5 CPS		Growth Stress: 48 KSI Rate: 5 CPS			
Cycles	Surface Length, in.	Cycles	Front Face, in.	Rear Face, in.	Remarks
0	.050	0	.070		
10,500	.070 (1)	1000	.100		
		2000	.130		
		3000	.175		
		4000	.230		
		4500	.270		
		5000	.305		
		5500	.360		Slight Dimple on Rear Face
		6000	.410		
		6500	.465		
		7000	.550		
		7250	.580		
		7500	.670		
		7750	.620		
		8000	.740		
		8200	.850		
		8230	.940		Failure (2)

Notes: 1. Specimen was dye marked at this time
2. Dye did not penetrate crack

TABLE A-48 FLAW GROWTH RECORD

Specimen No. 353492-10A		Type: .004 Laminate		ELOX: .020 x .050	
Sharpening Stress: 36 KSI Rate: 5 cps		Growth Stress: 48 KSI Rate: 5 cps			
Cycles	Surface Length, in.	Cycles	Front Face: in.	Rear Face: in.	Remarks
0	.050 (ELOX)	0	.320		
14,000	.090	250	.380		Dimple on Rear Face
15,000	.100				
16,000	.110	500	.465		
18,000	.150	600	.580	.100	Failure
20,000	.190				
22,000	.240				Dye penetrated to third layer
23,000	.270				
24,000	.310				
24,200	.320				

TABLE A-49 FLAW GROWTH RECORD

Specimen No.: 353492-11A Type: Laminate .004 ELOX: Diffusion Line					
Sharpening Stress: 36 KSI Rate: 5 CPS		Growth Stress: 48 KSI Rate: 5 CPS			
Cycles	Surface Length, in.	Cycles	Front Face, in.	Rear Face, in.	Remarks
0 3150	.110 .145 (1)	0 500 1000 1500 1750 2000 2050	.145 .190 .245 .350 .420 .570 .660		Failure
Note: 1. Specimen was dye marked at this time					

TABLE A-50 FLAW GROWTH RECORD

Specimen No.: 353492-12A		Type: LAMINATE		ELOX: 110 X .054	
Sharpening Stress: 36 KSI Rate: 5 CPS		Growth Stress: 48 KSI Rate: 5 CPS			
Cycles	Surface Length, in.	Cycles	Front Face, in.	Rear Face, in.	Remarks
0	.110	0	.145		
3000	.145 (1)	500	.200		
		1000	.275		
		1500	.450		
		1700	.600		
		1725	.650		Failure
Note: 1. Specimen was dye marked at this point					

Appendix A (Continued)
ADHESIVE BONDED SPECIMENS

TABLE A-51 FLAW GROWTH RECORD

Specimen No.: 1		Type: Adhesive Bond		ELOX: .026 X .048	
Sharpening Stress: 36 KSI Rate: 5 CPS		Growth Stress: 40 KSI Rate: 5 CPS			
Cycles	Surface Length, in.	Cycles	Front Face, in.	Rear Face, in.	Remarks
0	.048 (Elox)	0	.080		
10,150	.080	500	.090		
		1000	.100		
		1500	.120		
		2000	.140		
		2500	.165		
		3000	.190		
		3500	.220		
		4000	.260		
		4500	.320		
		5000	.340		
		5500	.390		
		6000	.440		
		6500	.500		
		7000	.560		
		7500	.600		
		8000	.700		
		8500	.800		
		9500	.940		
		10000	1.080		
		10500	1.240		
		11000	1.430		
		11500	1.680		
		12000	2.080		
		12500	2.500		
		16875			First Layer Failed Second and Third Layers Failed

TABLE A-52 FLAW GROWTH RECORD

Specimen No.: 2		Type: ADHESIVE BONDED		ELOX: .020 X .046	
Sharpening Stress: 36 KSI Rate: 05		Growth Stress: 40 KSI Rate: 5 CPS			
Cycles	Surface Length, in.	Cycles	Front Face, in.	Rear Face, in.	Remarks
0	.046 (Elox)	0	.070		
9100	.060	500	.075		
10,600	.070	1000	.080		
		1500	.090		
		2000	.105		
		2500	.120		
		3000	.135		
		3500	.150		
		4000	.175		
		4500	.200		
		5000	.230		
		5500	.260		
		6000	.300		
		6500	.350		
		7000	.400		
		7500	.460		
		8000	.520		
		8500	.600		
		9000	.680		
		9500	.750		
		10000	.900		
		10500	1.020		
		11000	1.200		
		11500	1.380		
		12000	1.680		
		12500	2.440		
		12600	2.500		
		18830			First Layer Failed Second and Third Layers Failed

TABLE A-53 FLAW GROWTH RECORD

Specimen No.: 3		Type: Adhesive Bonded ELOX: .018 X .047			
Sharpening Stress: 36 KSI Rate: 5 CPS		Growth Stress: 40 KSI Rate: 5 CPS			
Cycles	Surface Length, in.	Cycles	Front Face, in.	Rear Face, in.	Remarks
0	.047 (Elox)	0	.070		
11,000	.060	500	.075		
11,500	.070	1000	.080		
		1500	.090		
		2000	.100		
		2500	.110		
		3000	.130		
		3500	.140		
		4000	.160		
		4500	.180		
		5000	.200		
		5500	.230		
		6000	.270		
		6500	.300		
		7000	.340		
		7500	.380		
		8000	.410		
		8500	.460		
		9000	.500		
		9500	.560		
		10000	.620		
		10500	.720		
		11000	.800		
		11500	.900		
		12000	1.010		
		12500	1.120		
		13000	1.280		
		13,500	1.480		
		14,000	1.770		
		14,500	2.360		
		14,550	2.500		
		16,630			First Layer Failed Second and Third Layers Failed

TABLE A-54 FLAW GROWTH RECORD

Specimen No.: 4		Type: ADHESIVE BOND		ELOX: .024 X .050	
Sharpening Stress: 36 KSI Rate: '5 CPS		Growth Stress: 48 KSI Rate: '5 CPS			
Cycles	Surface Length, in.	Cycles	Front Face, in.	Rear Face, in.	Remarks
0 8250	.050 (Elox) .070	0 500 1000 1500 2000 2500 3000 3500 4000 4500 5000 5100 5135	.070 .090 .110 .140 .185 .240 .310 .420 .540 .760 1.170 2.500		First Layer Failed Second and Third Layers Failed

TABLE A-55 FLAW GROWTH RECORD

Specimen No.: 5		Type: ADHESIVE BOND		ELOX: .026 X .046	
Sharpening Stress: 36 KSI Rate: 5 CPS		Growth Stress: 48 KSI Rate: 5 CPS			
Cycles	Surface Length, in.	Cycles	Front Face, in.	Rear Face, in.	Remarks
0	.046 (Elox)	0	.080		
9000	.080	500	.100		
		1000	.130		
		1500	.160		
		2000	.230		
		2500	.300		
		3000	.400		
		3500	.560		
		3750	.630		
		4000	.720		
		4250	.840		
		4500	1.010		
		4750	1.310		
		4880	2.500		First Layer Failed
		4980			Second and Third Layers Failed

TABLE A-56 FLAW GROWTH RECORD (Continued)

Specimen No.: 6		Type: ADHESIVE BOND		ELOX: .027 X .045	
Sharpening Stress: 36 KSI Rate: 5 CPS		Growth Stress: 48 KSI Rate: 5 CPS			
Cycles	Surface Length, in.	Cycles	Front Face, in.	Rear Face, in.	Remarks
0	.045 (Elox)	0	.080		
3000	.080	500	.100		
		1000	.140		
		1500	.180		
		2000	.240		
		2500	.300		
		3000	.390		
		3500	.520		
		3750	.590		
		4000	.630		
		4500	1.340		
		4555	2.500		First Layer Failed
		4575			Second and Third Layers Failed

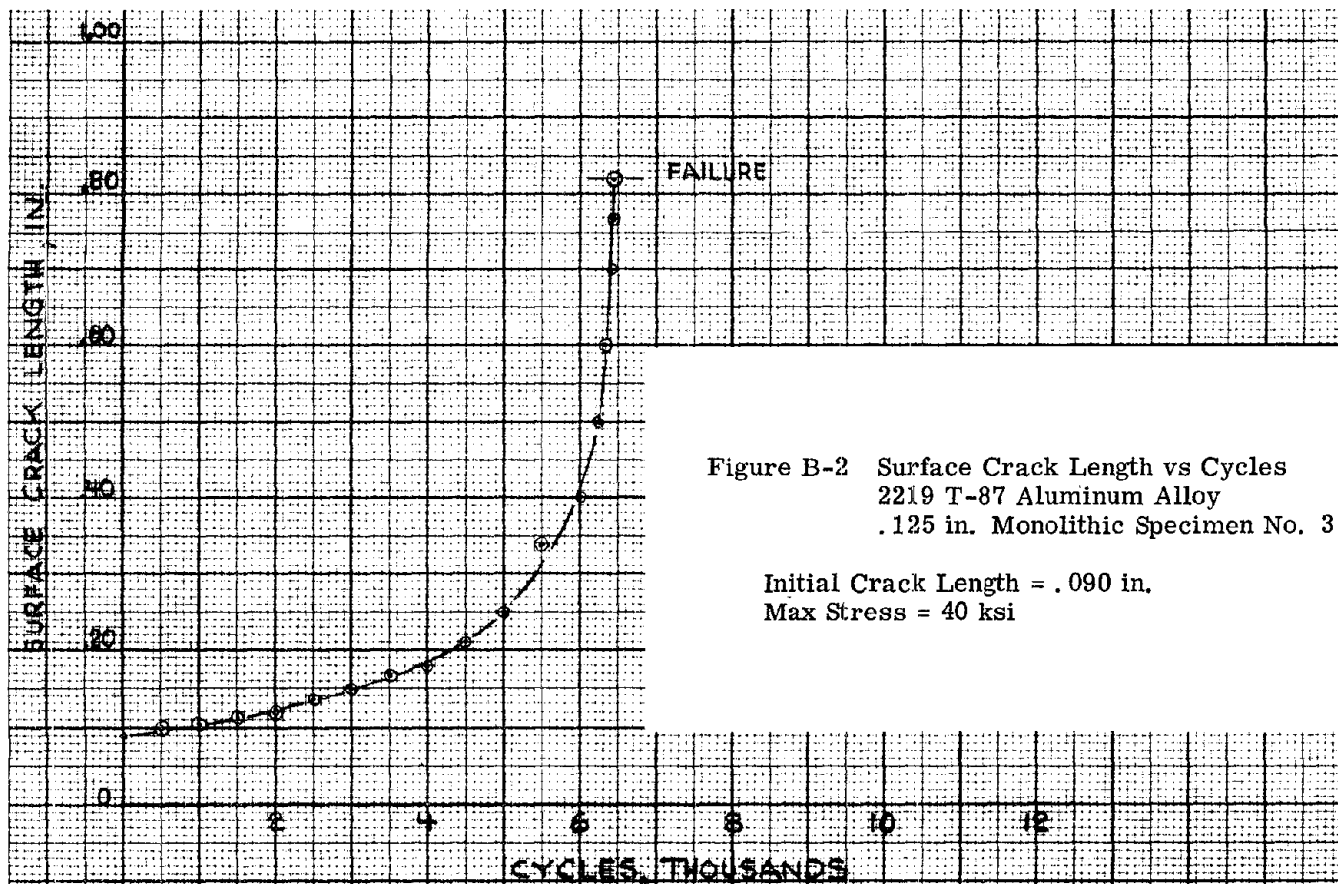
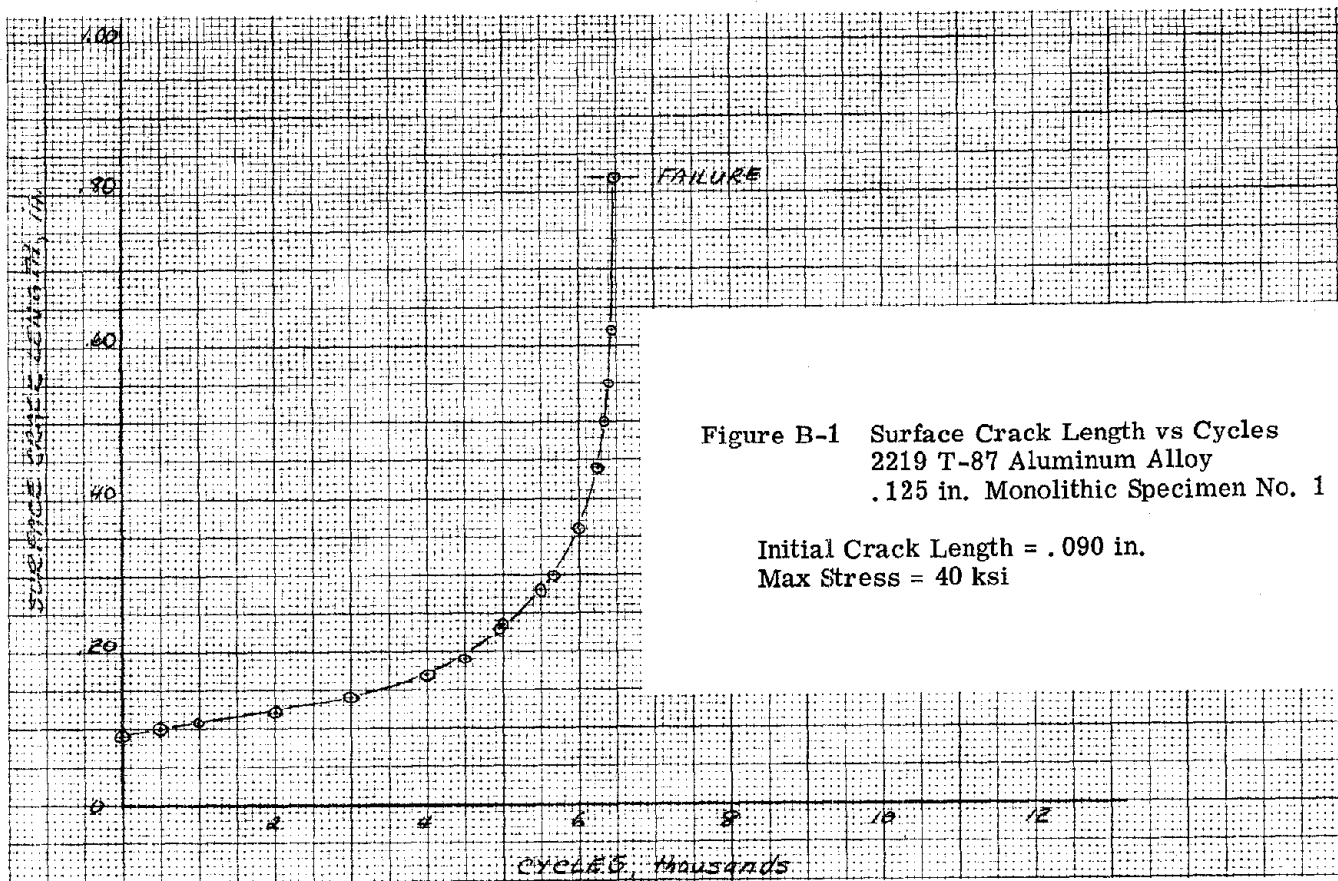
Appendix B

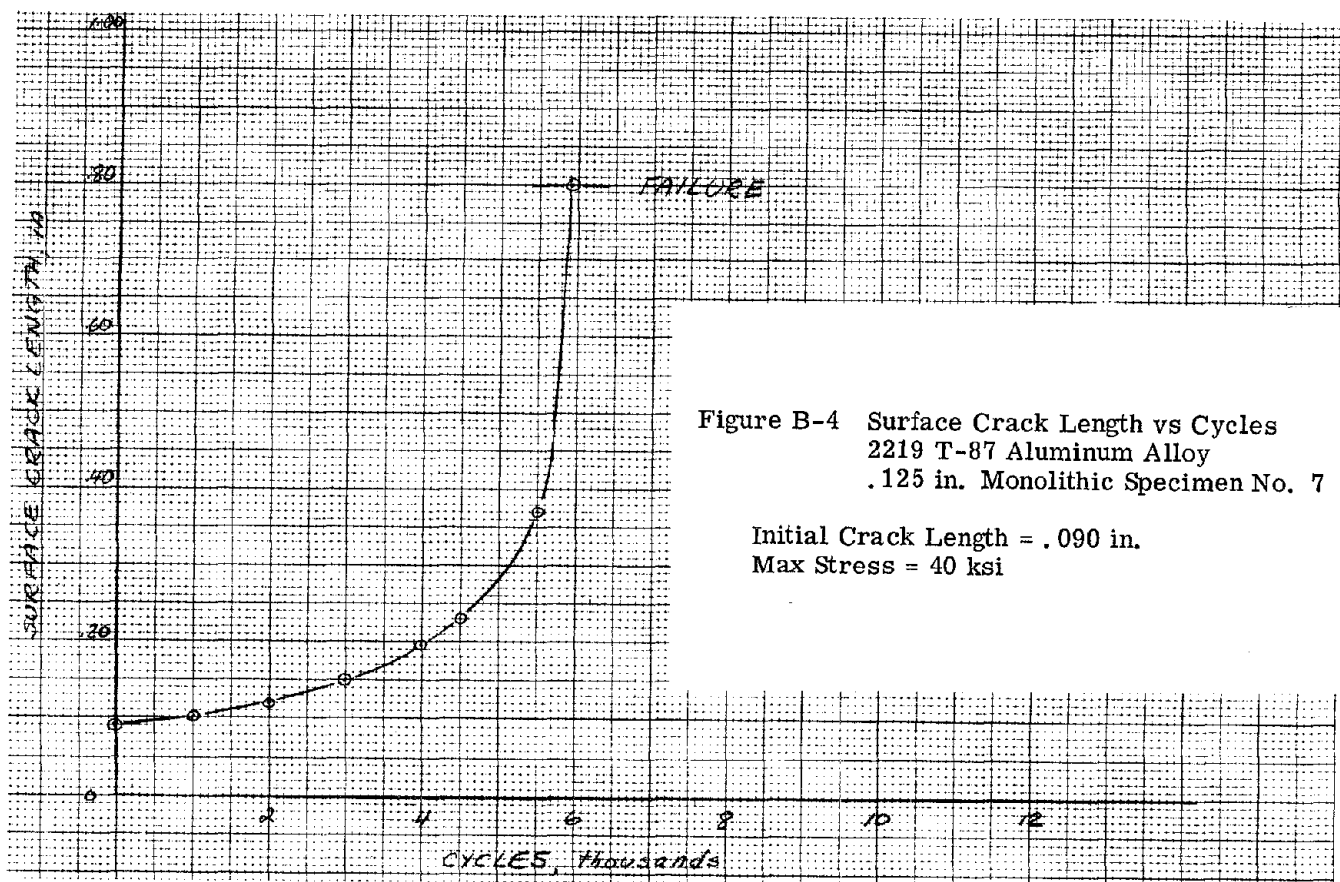
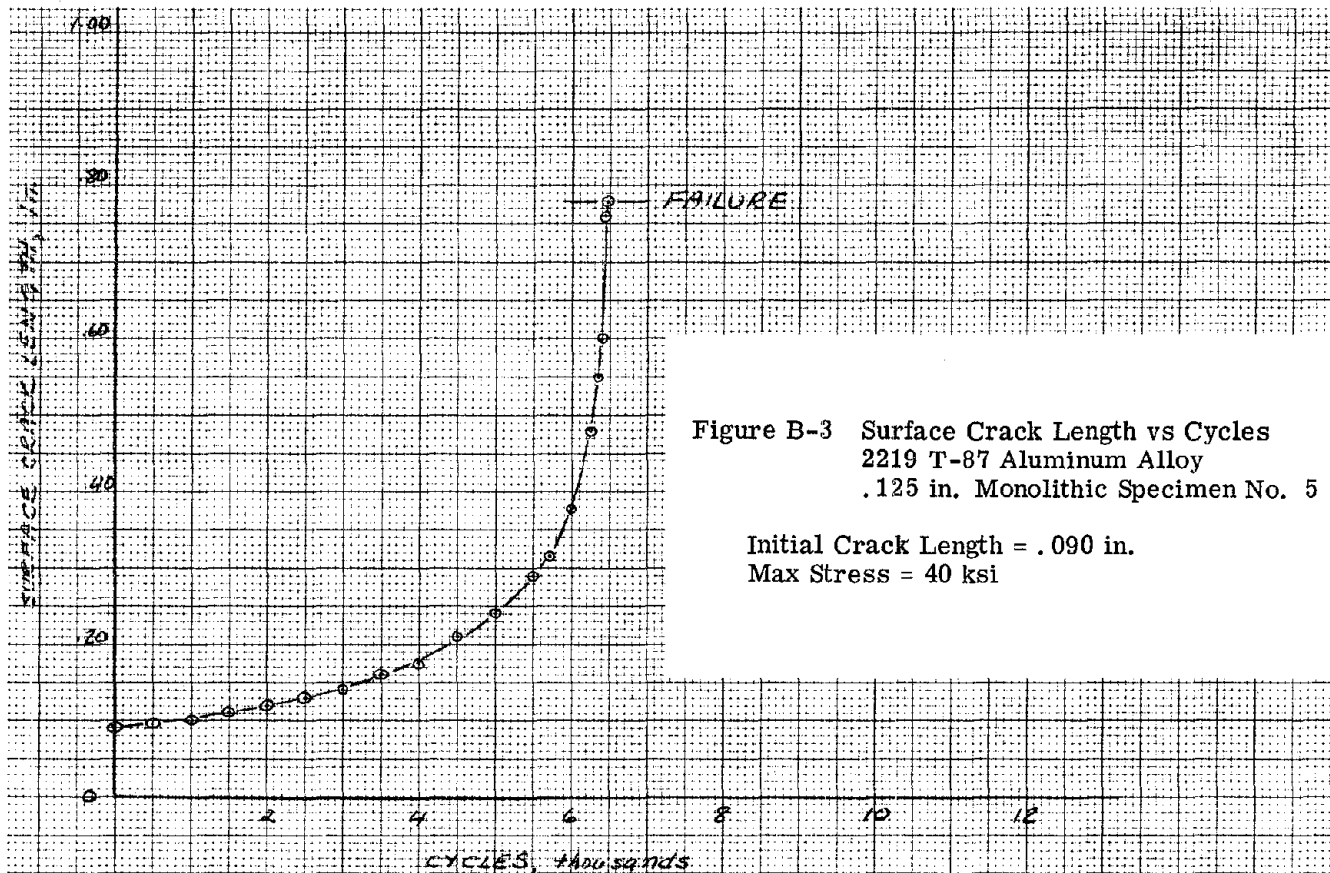
CURVES OF SPECIMEN SURFACE FLAW WIDTH VERSUS CYCLES

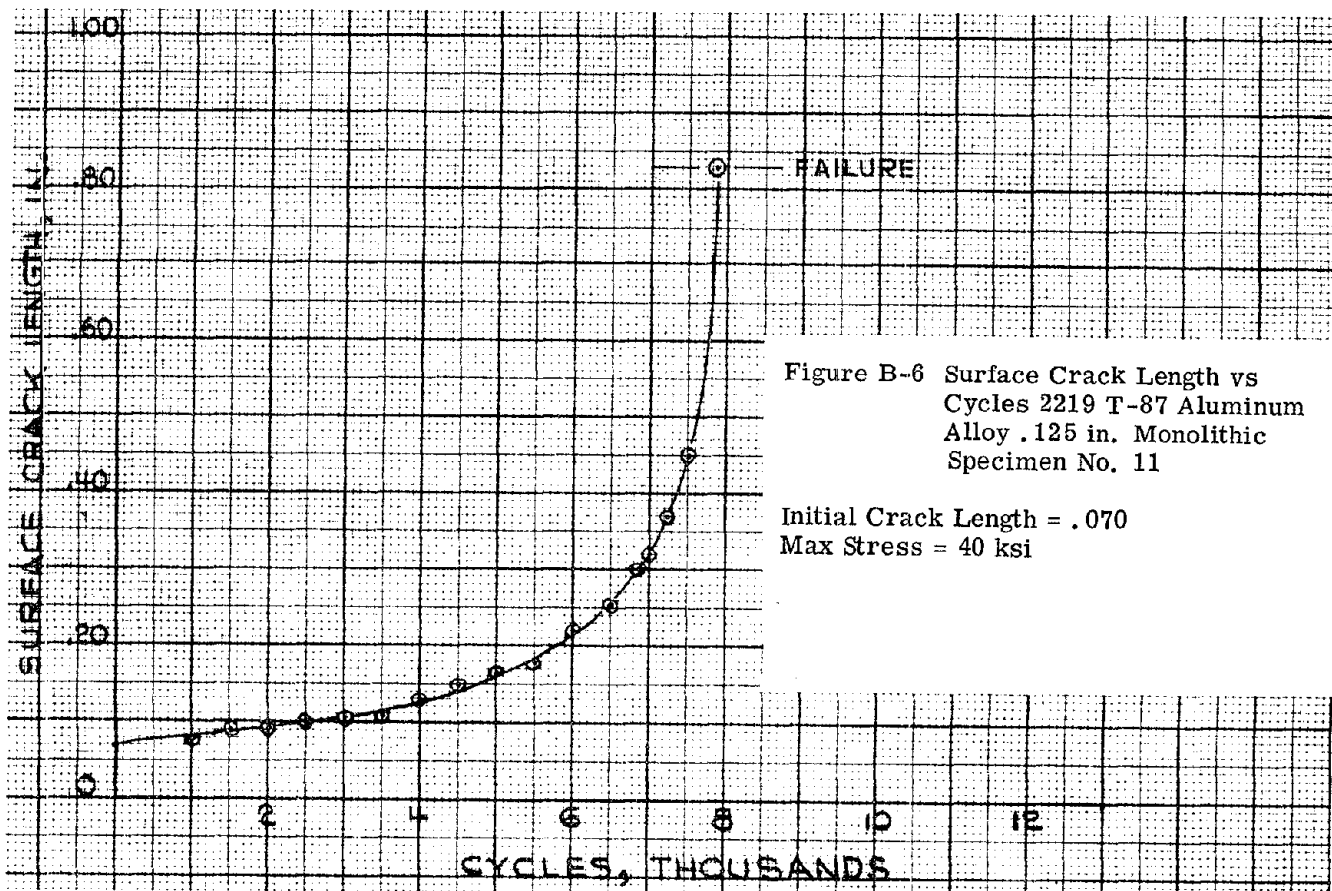
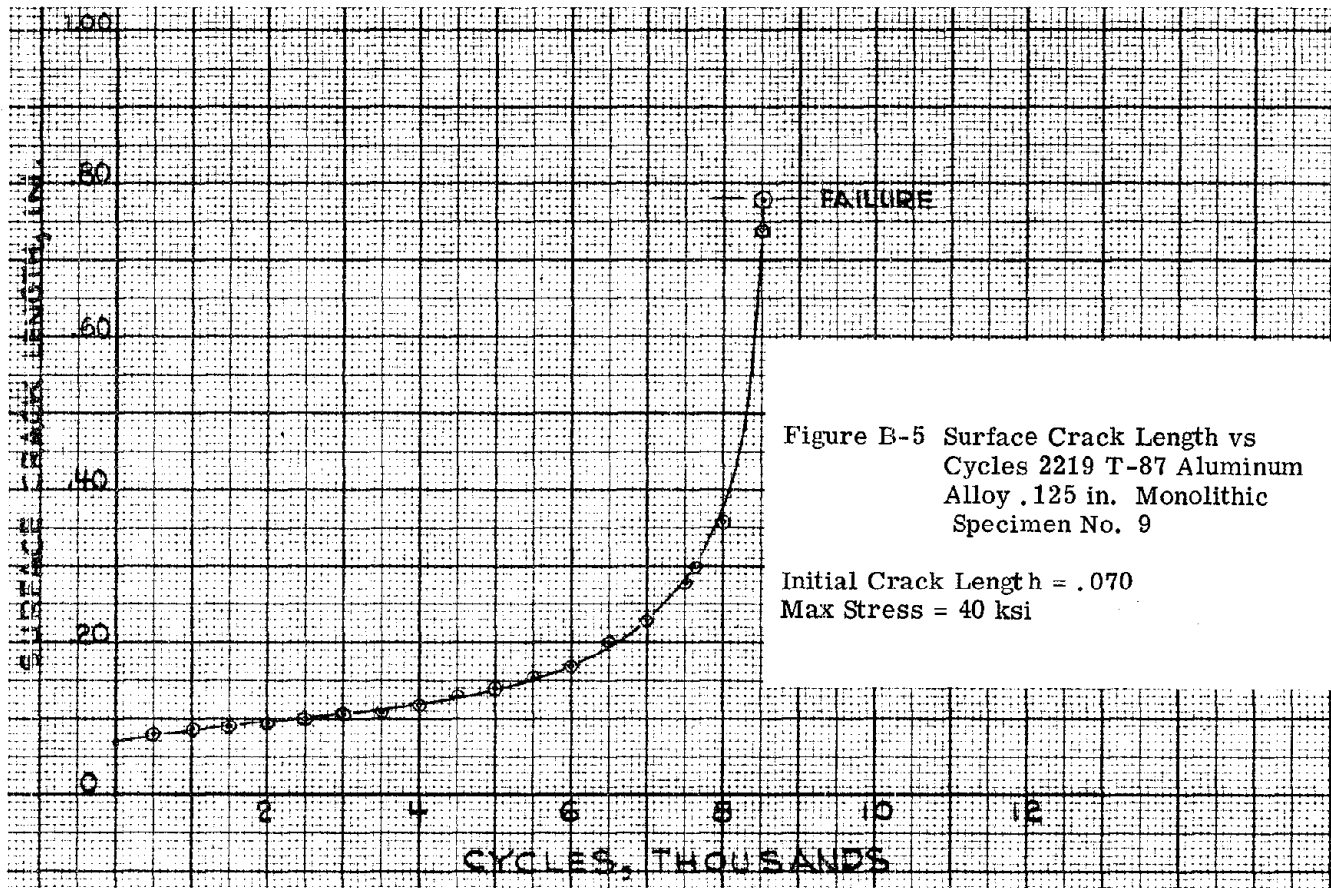
Surface flaw width versus cycles curves for each program test specimen are presented in this Appendix. The specimen curves are in the same order as the tabular records of Appendix A, that is, Phase I, Phase II, Phase III and Adhesive Bonded.

Appendix B (Continued)

PHASE I SPECIMENS







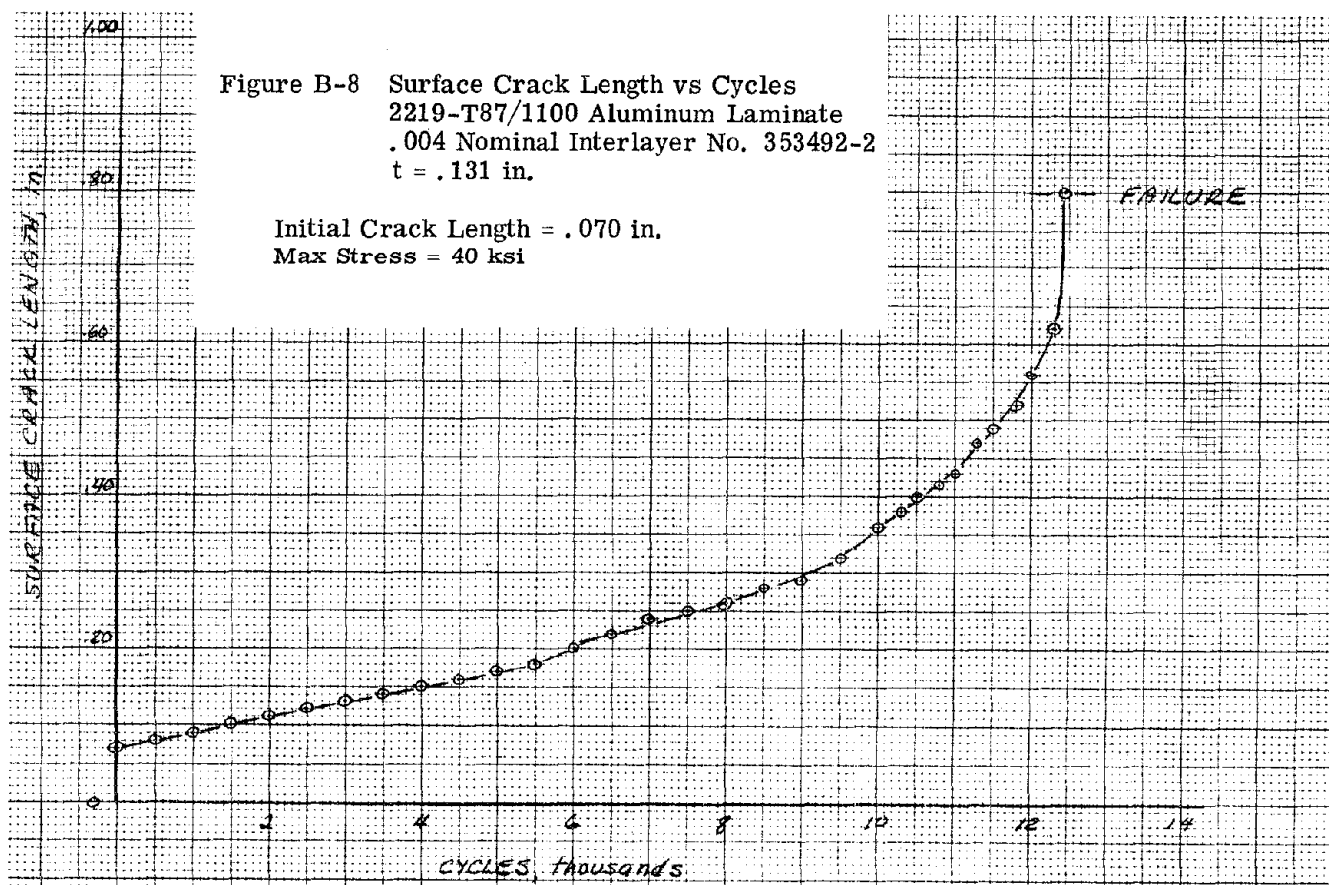
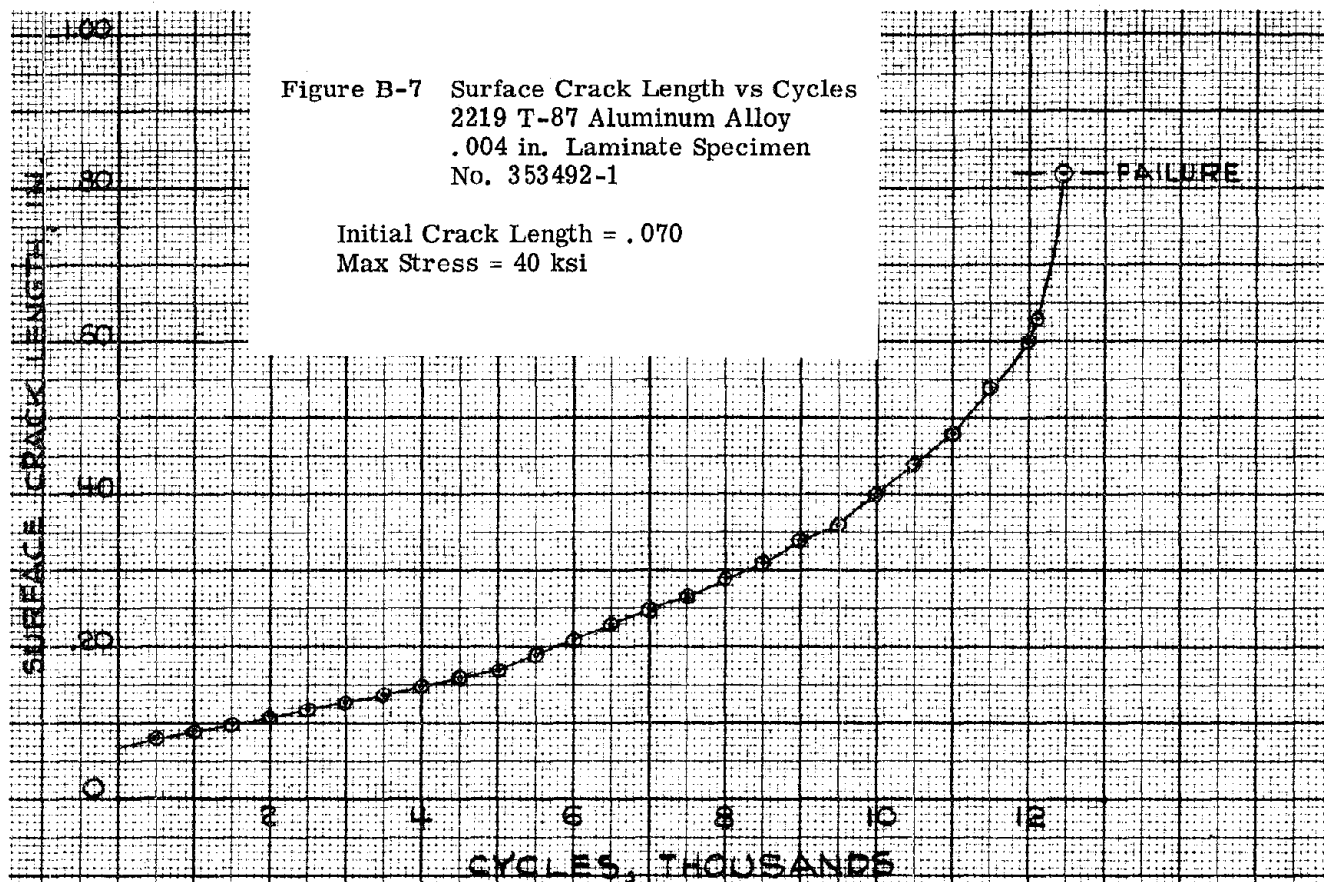


Figure B-9 Surface Crack Length vs Cycles
 2219 T-87 Aluminum Alloy
 .004 in. Laminate Specimen
 No. 353492-3

Initial Crack Length = .070
 Max Stress = 40 ksi

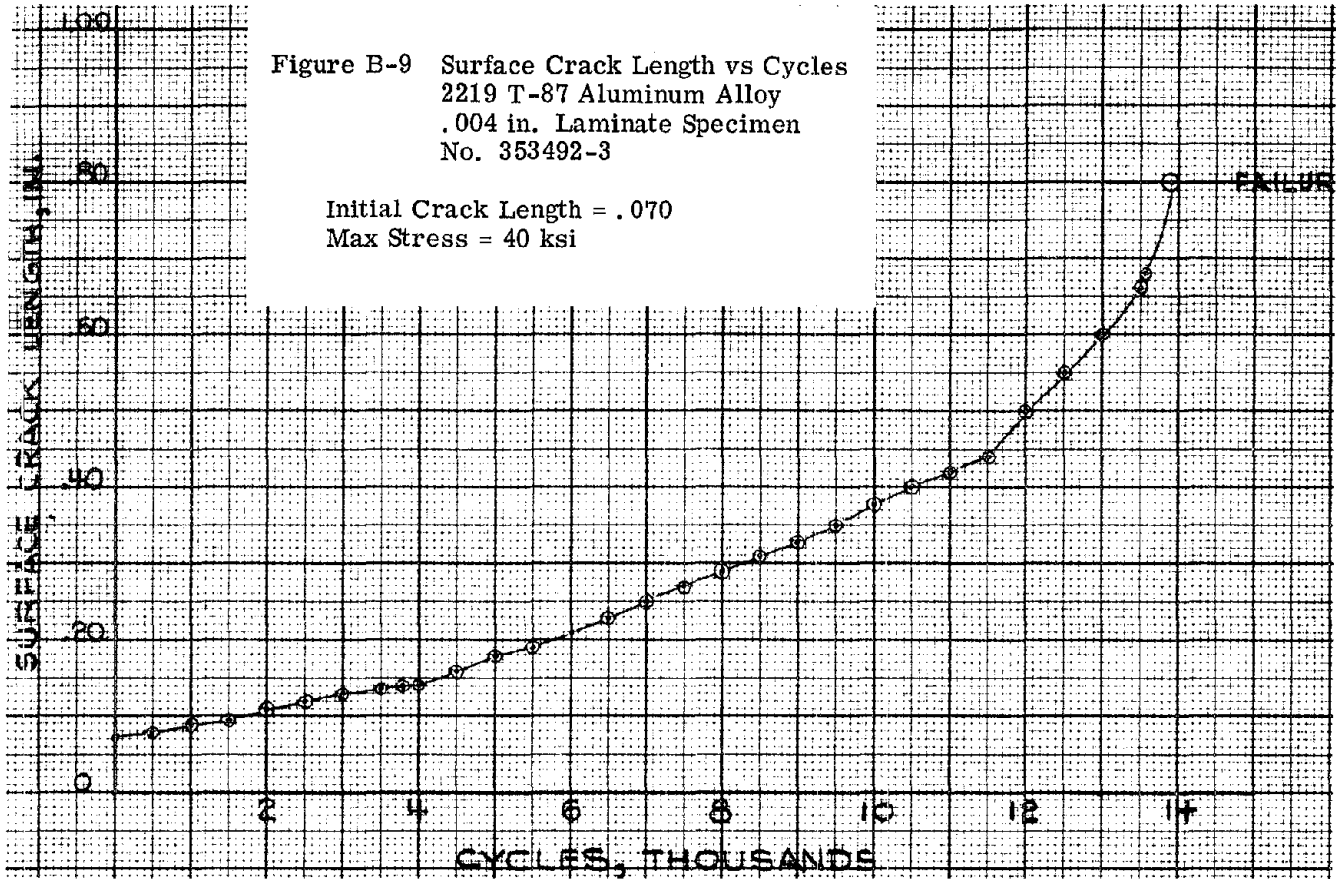
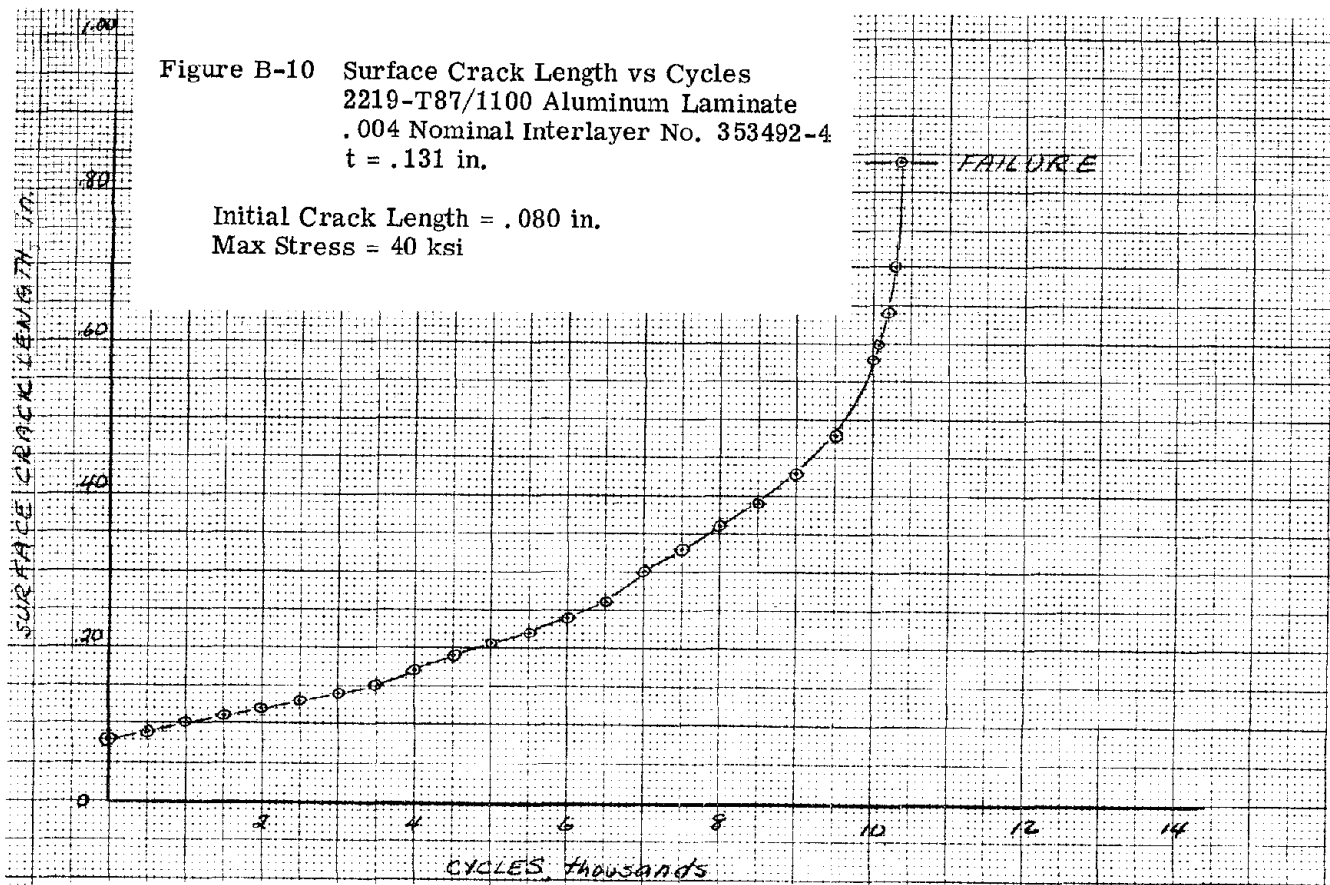
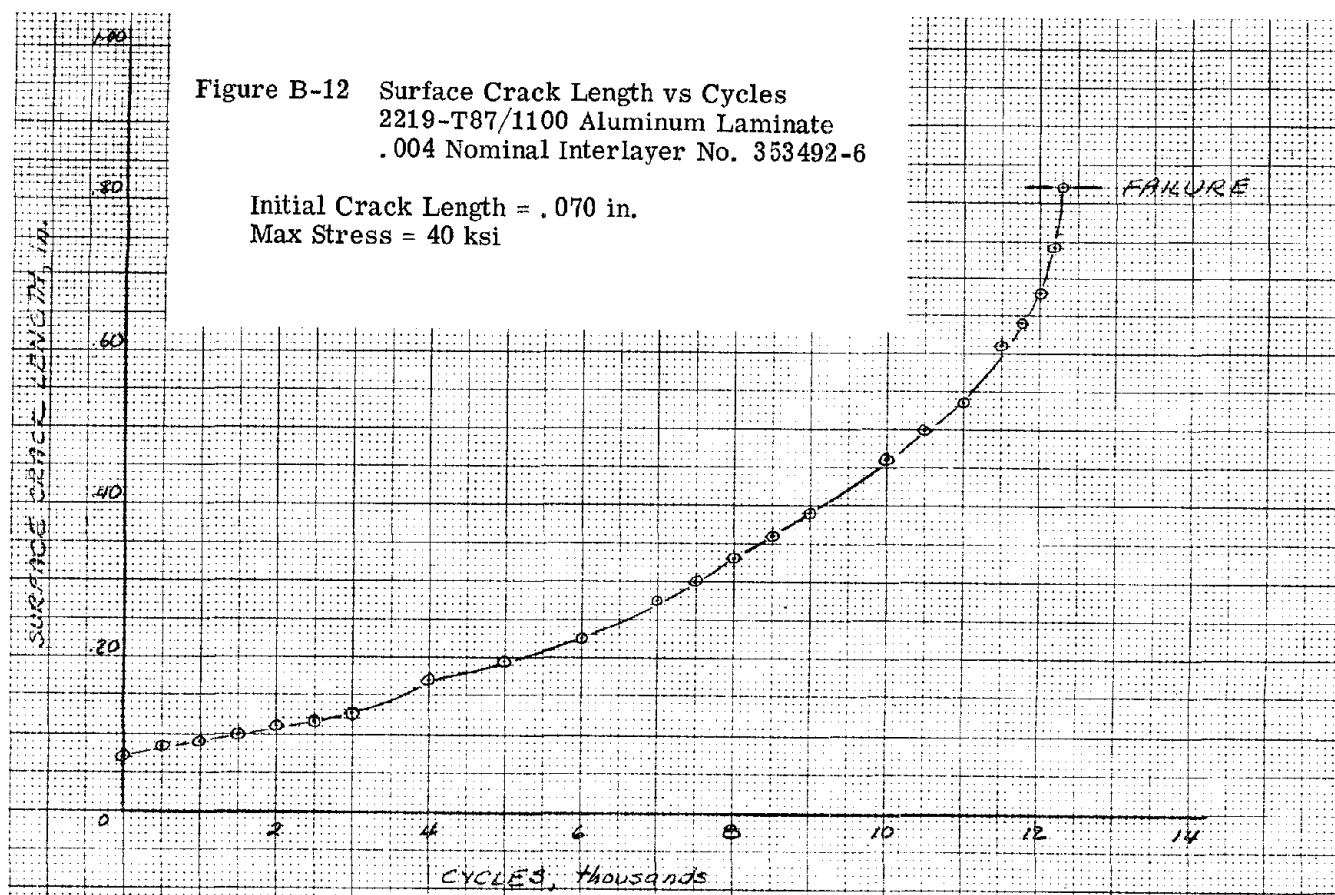
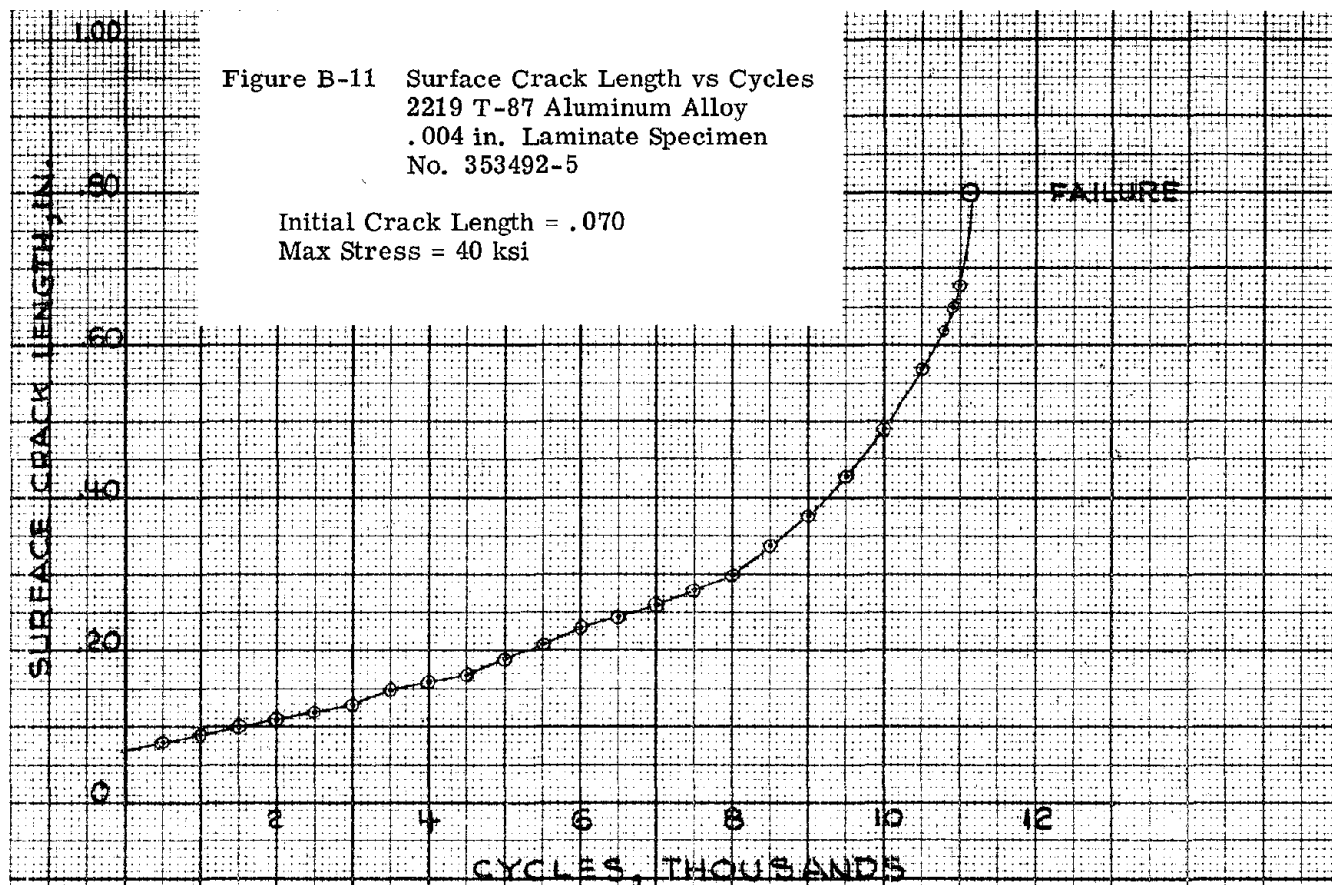
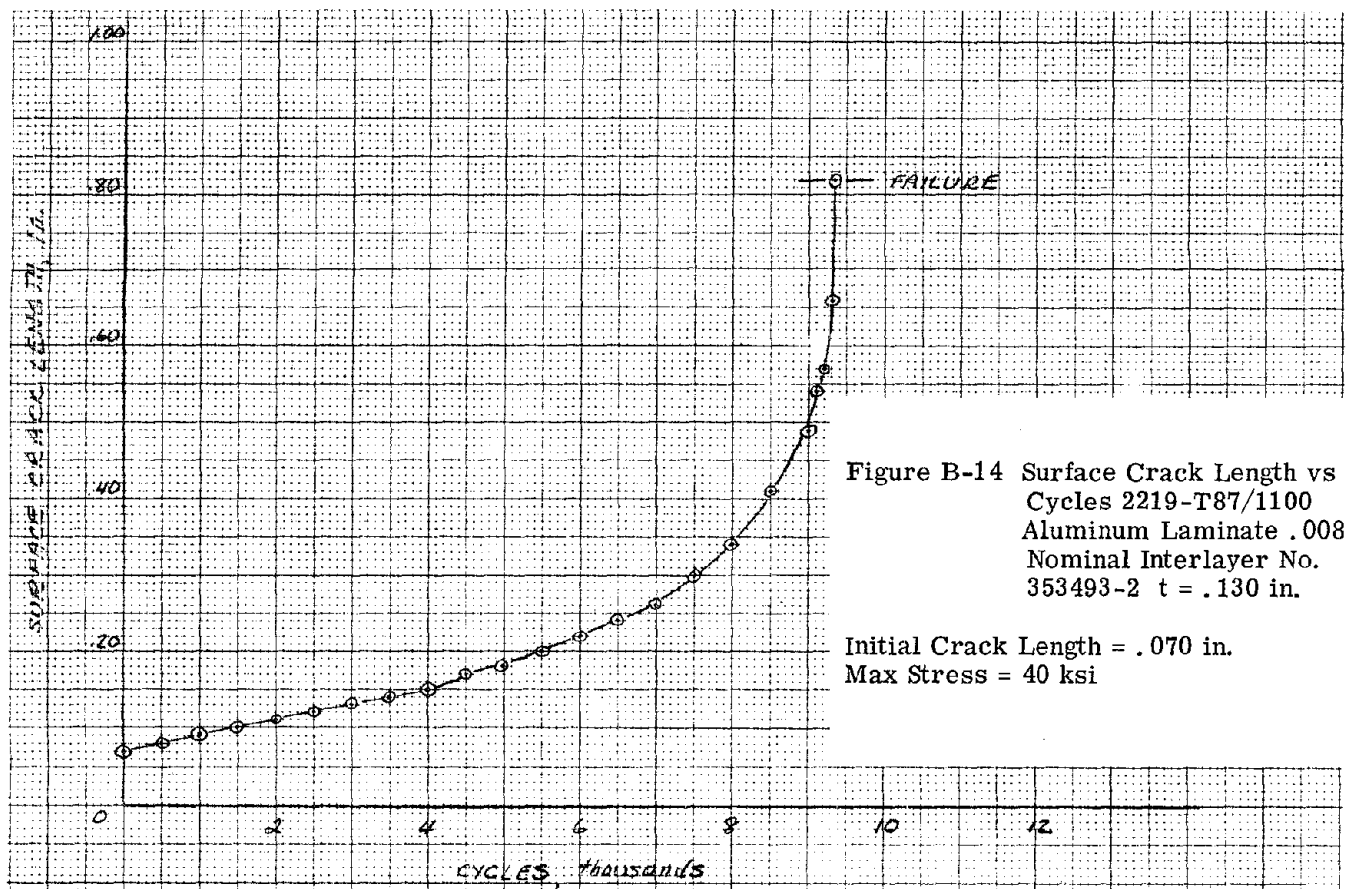
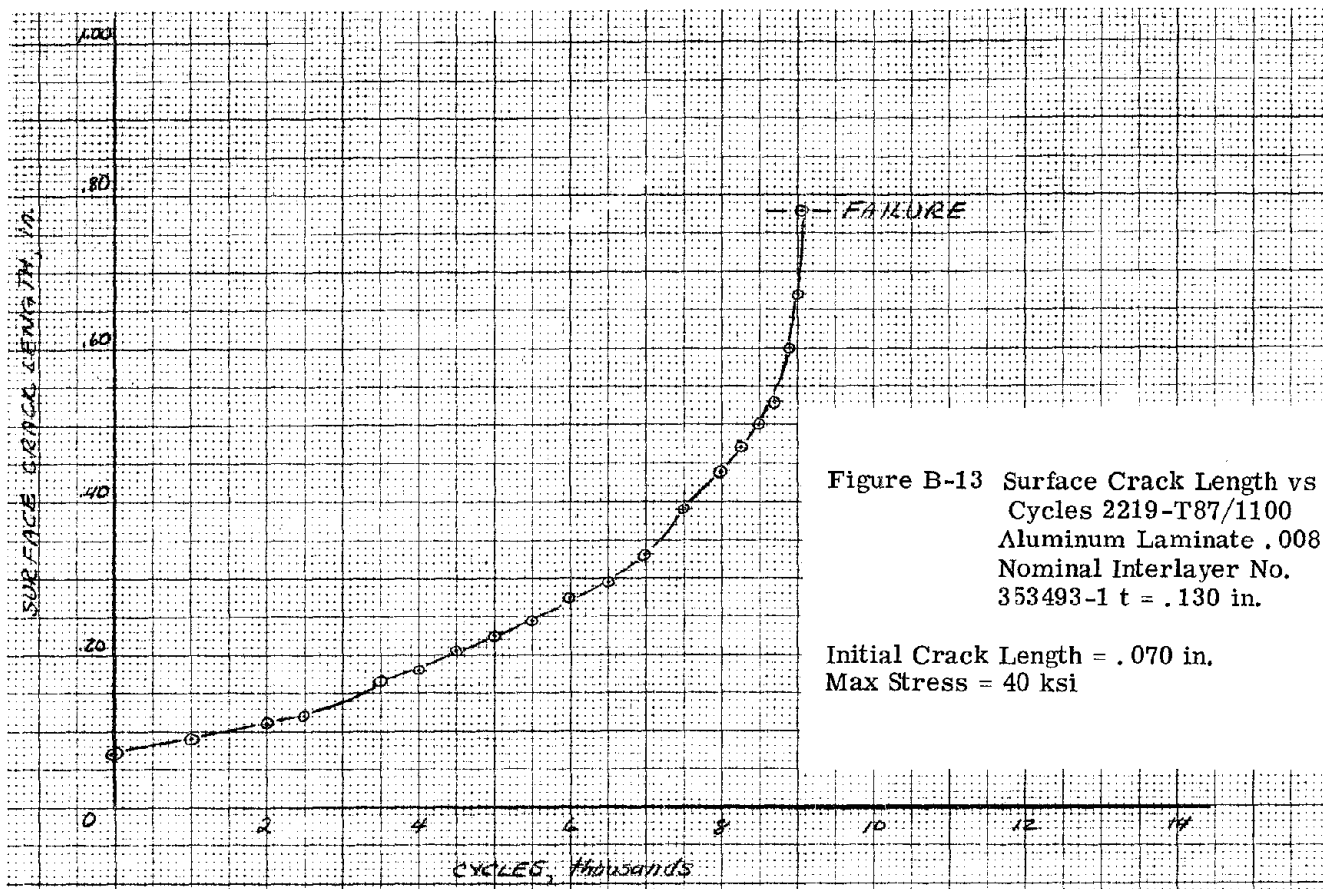


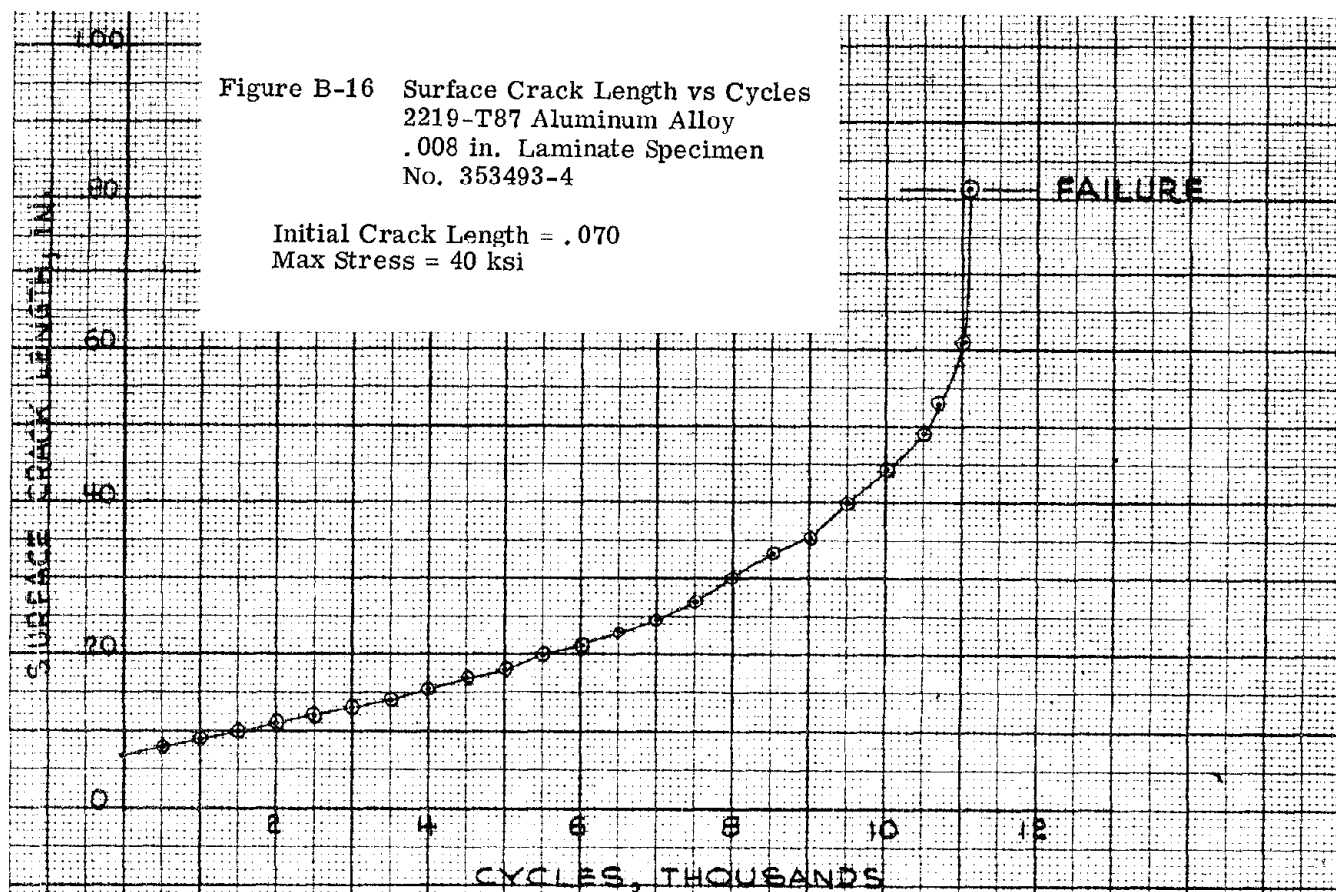
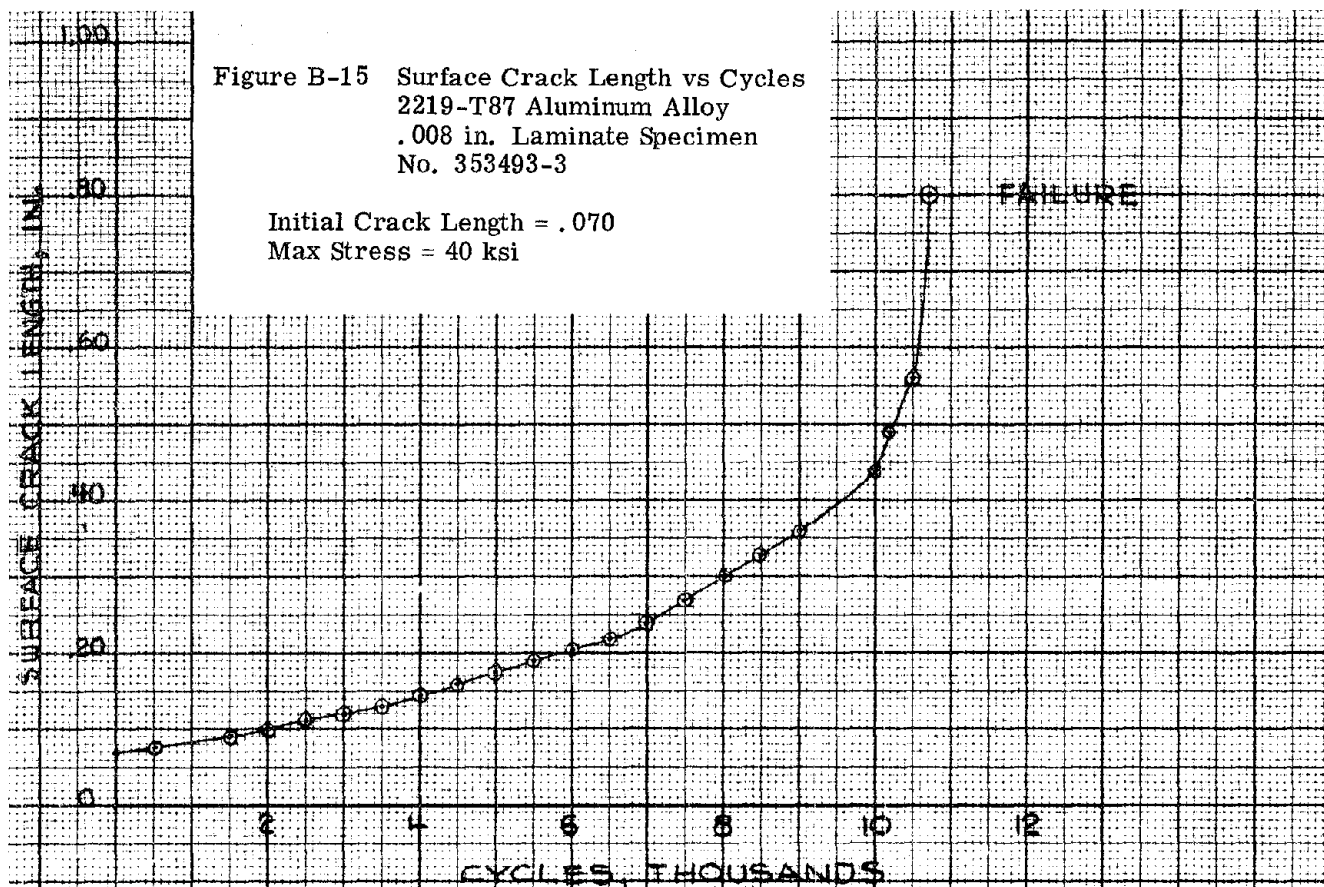
Figure B-10 Surface Crack Length vs Cycles
 2219-T87/1100 Aluminum Laminate
 .004 Nominal Interlayer No. 353492-4
 $t = .131$ in.

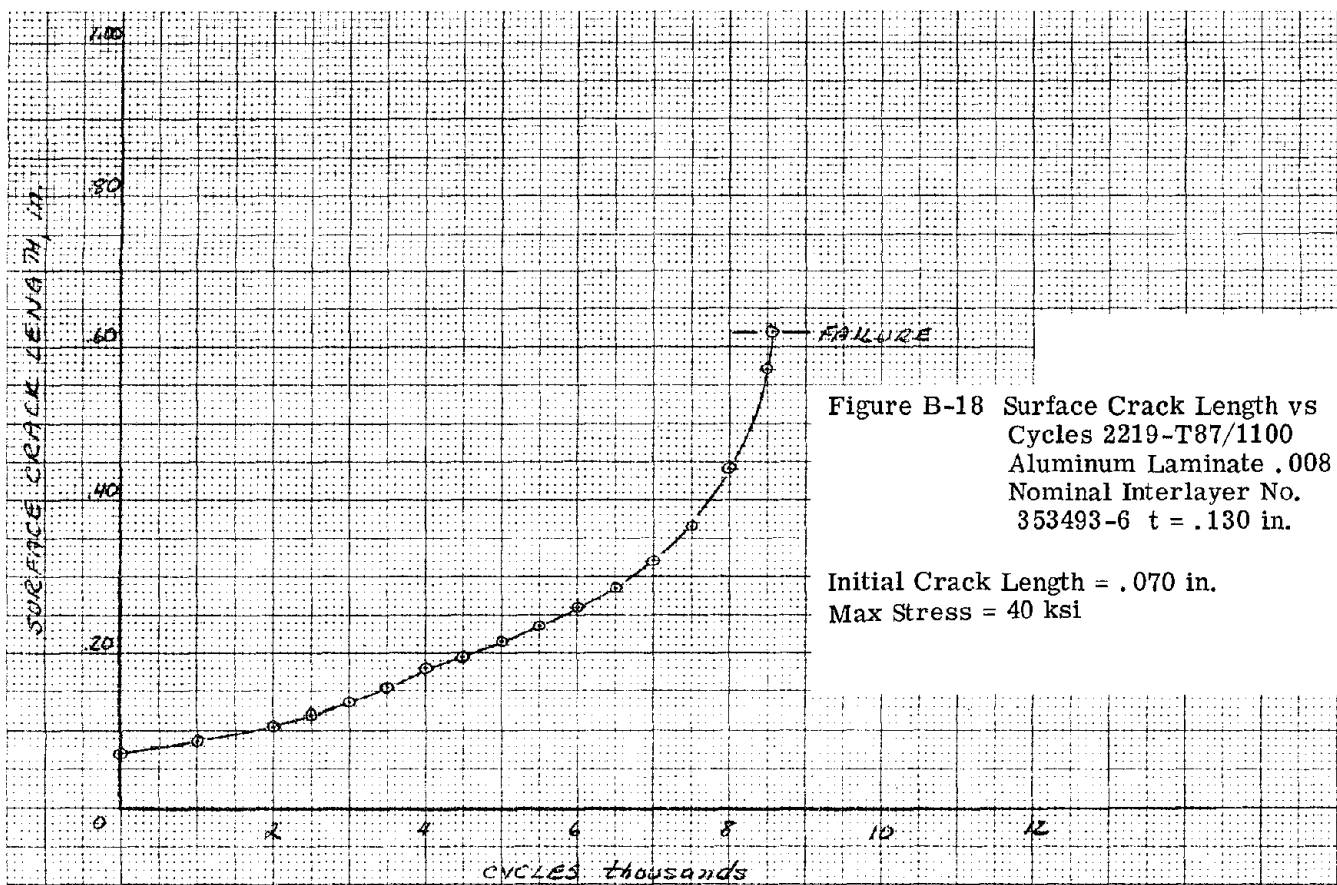
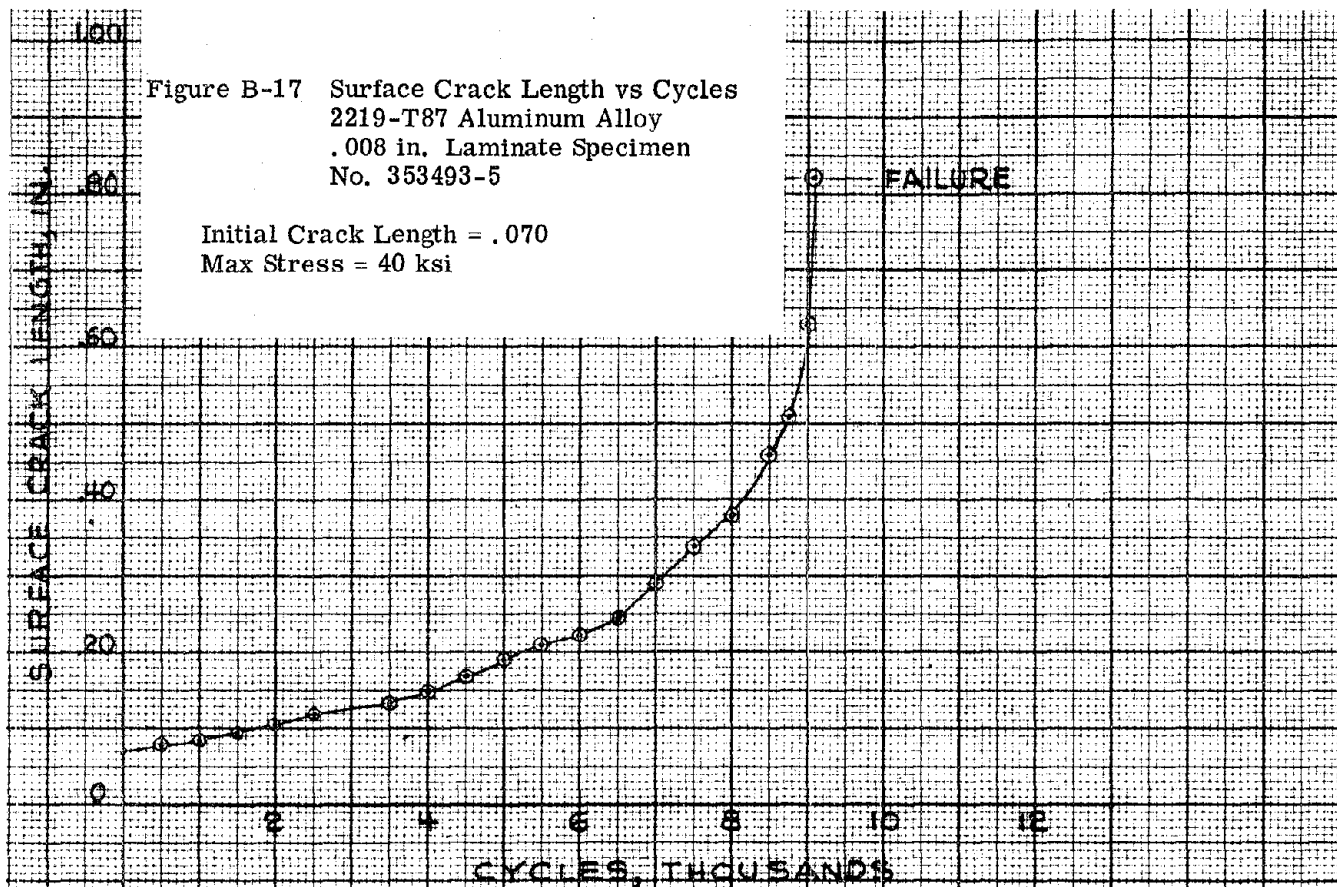
Initial Crack Length = .080 in.
 Max Stress = 40 ksi

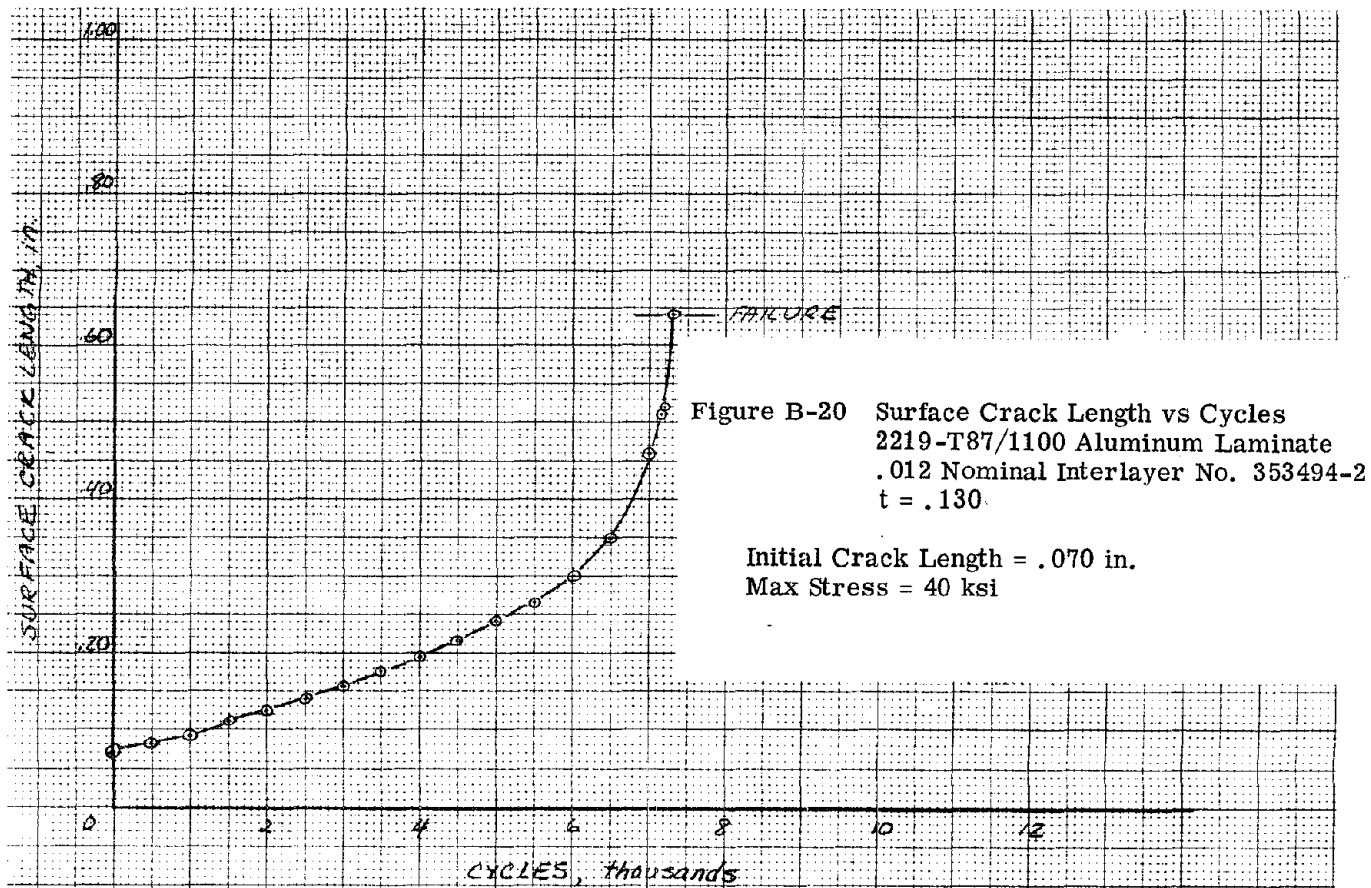
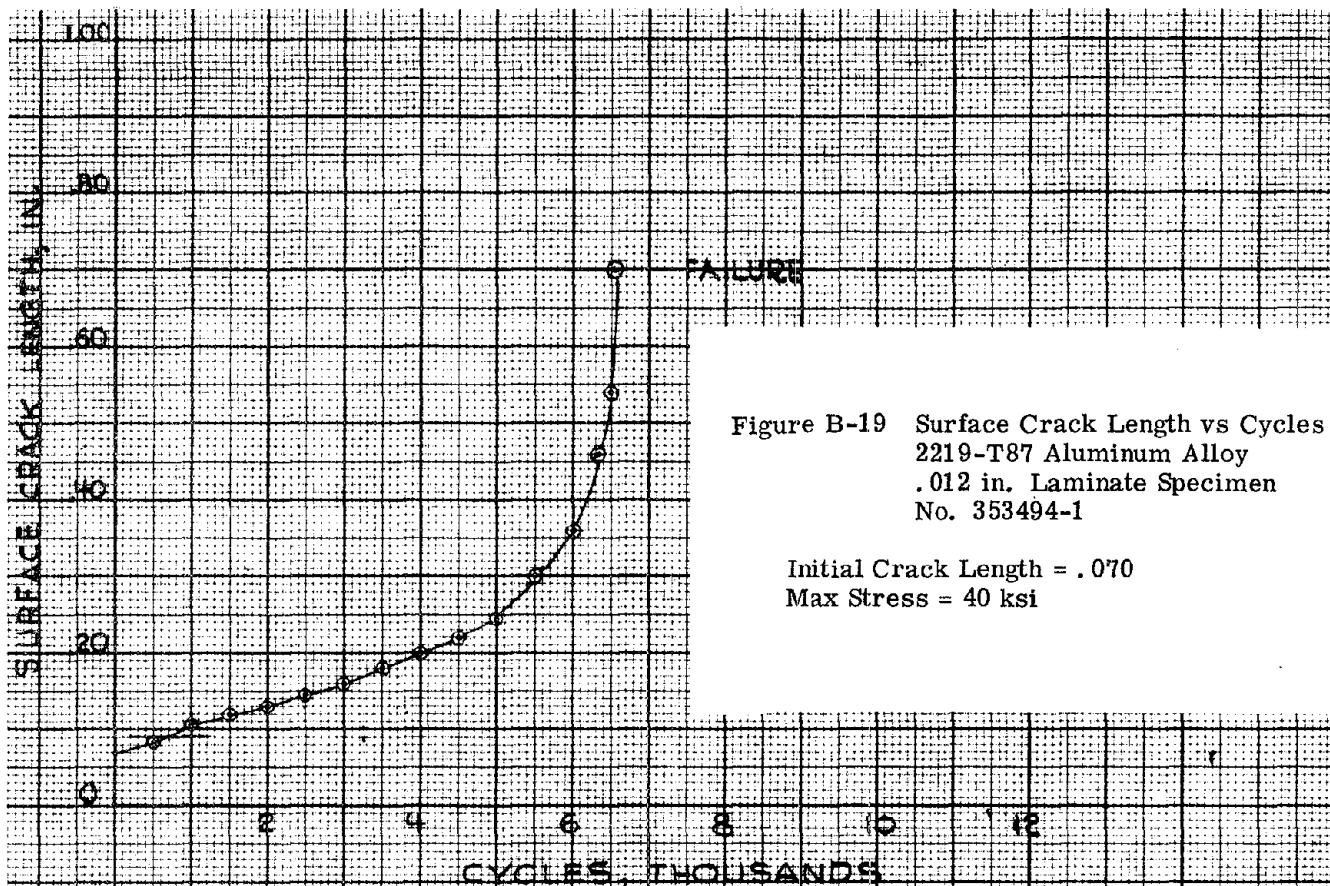


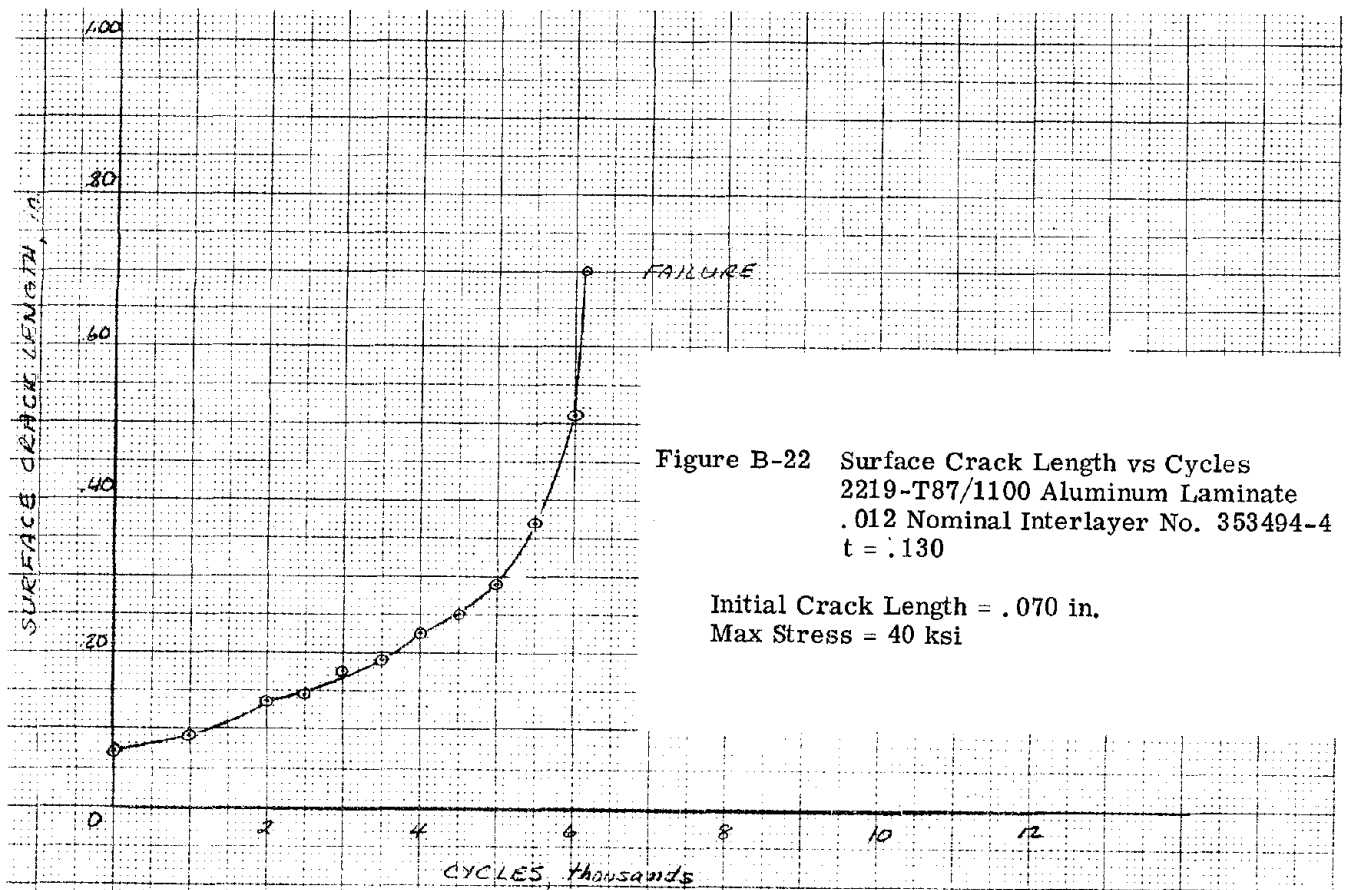
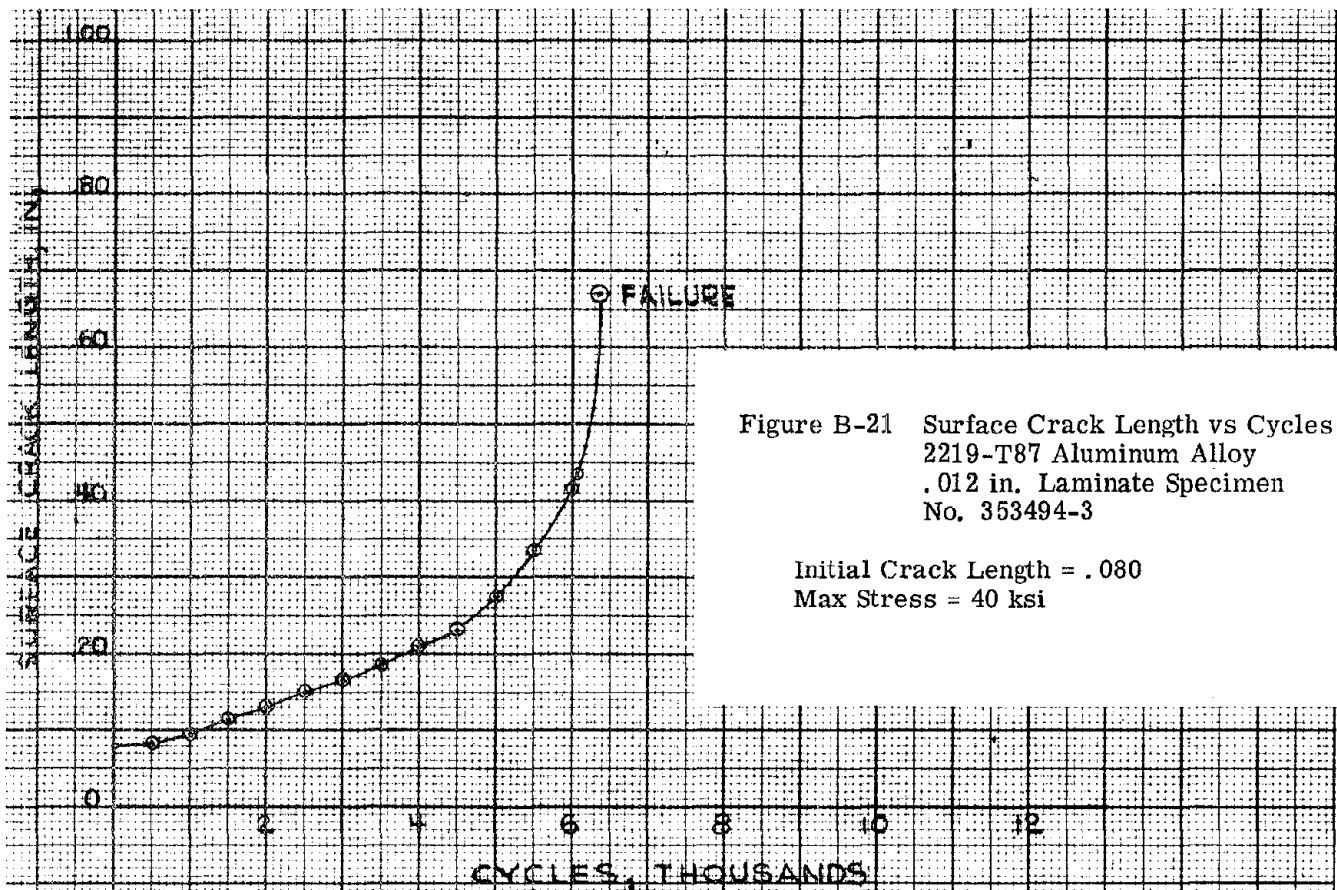


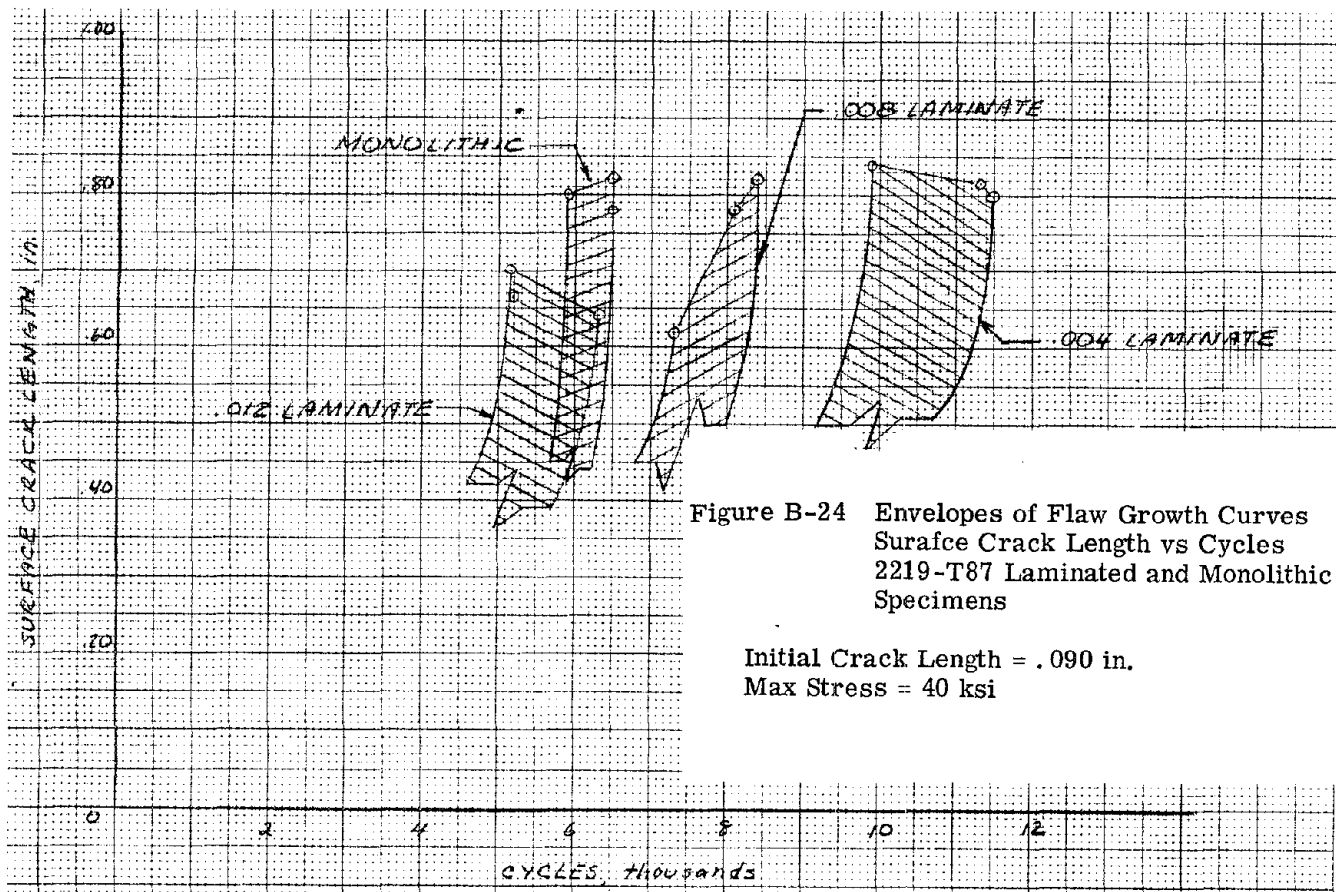
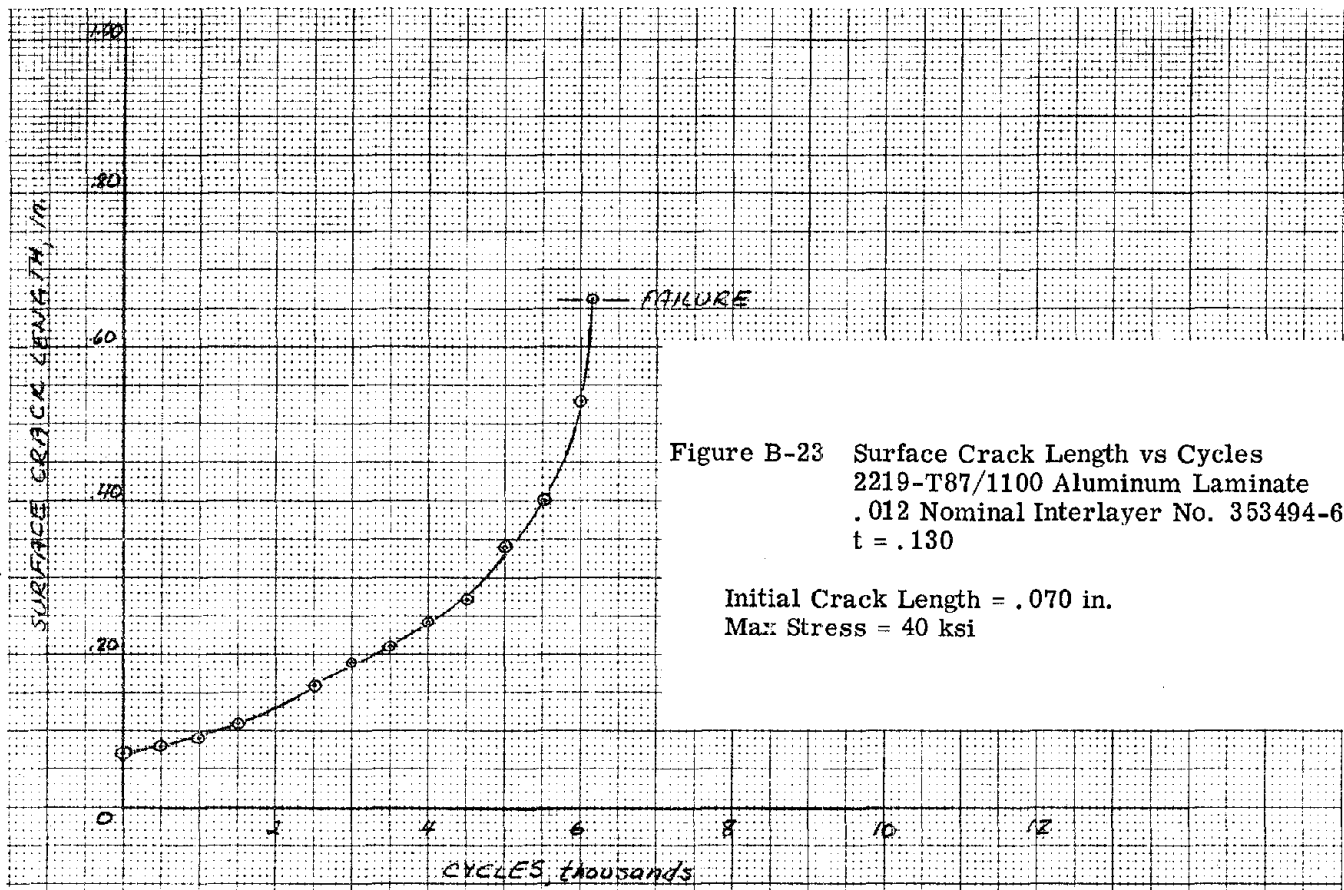






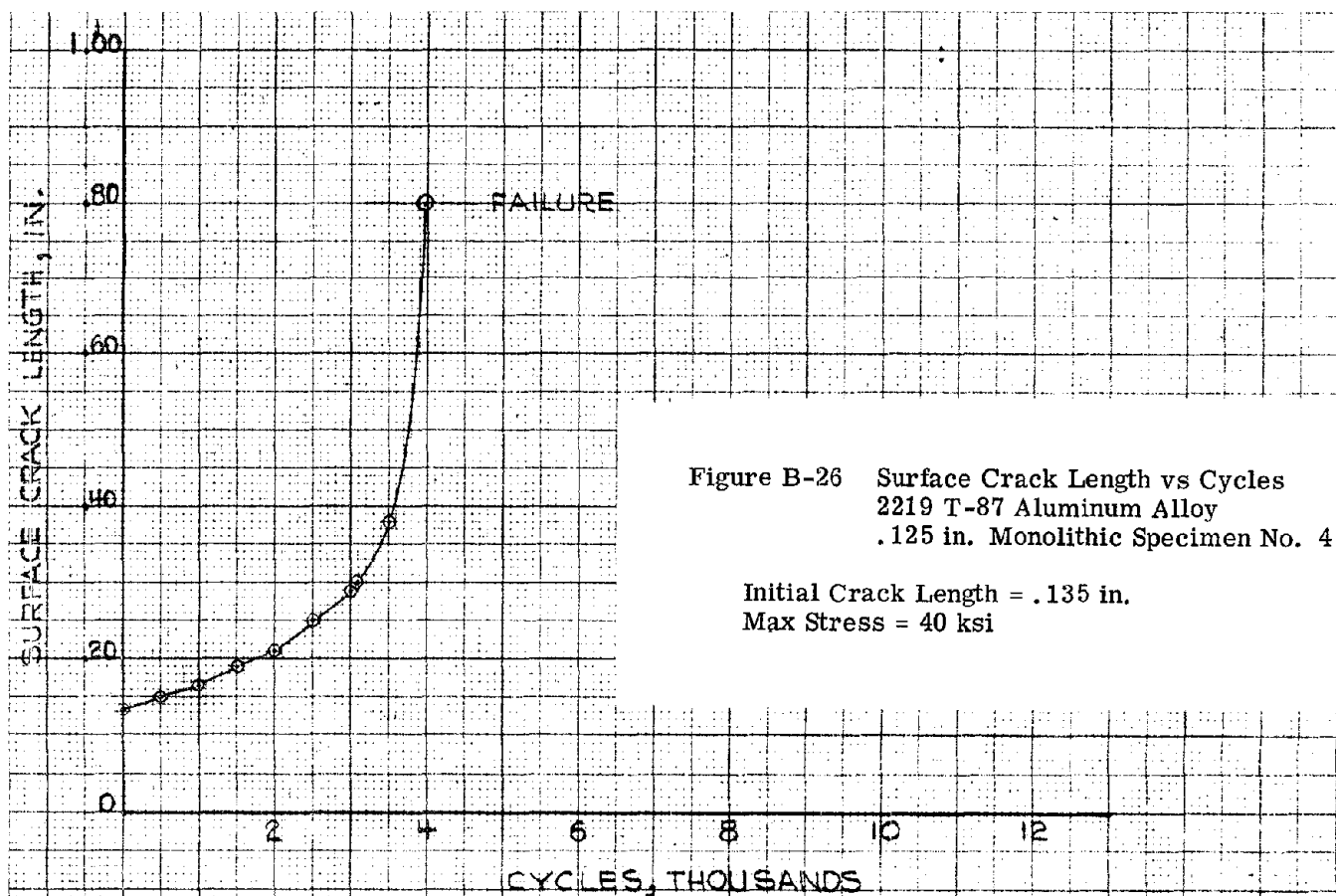
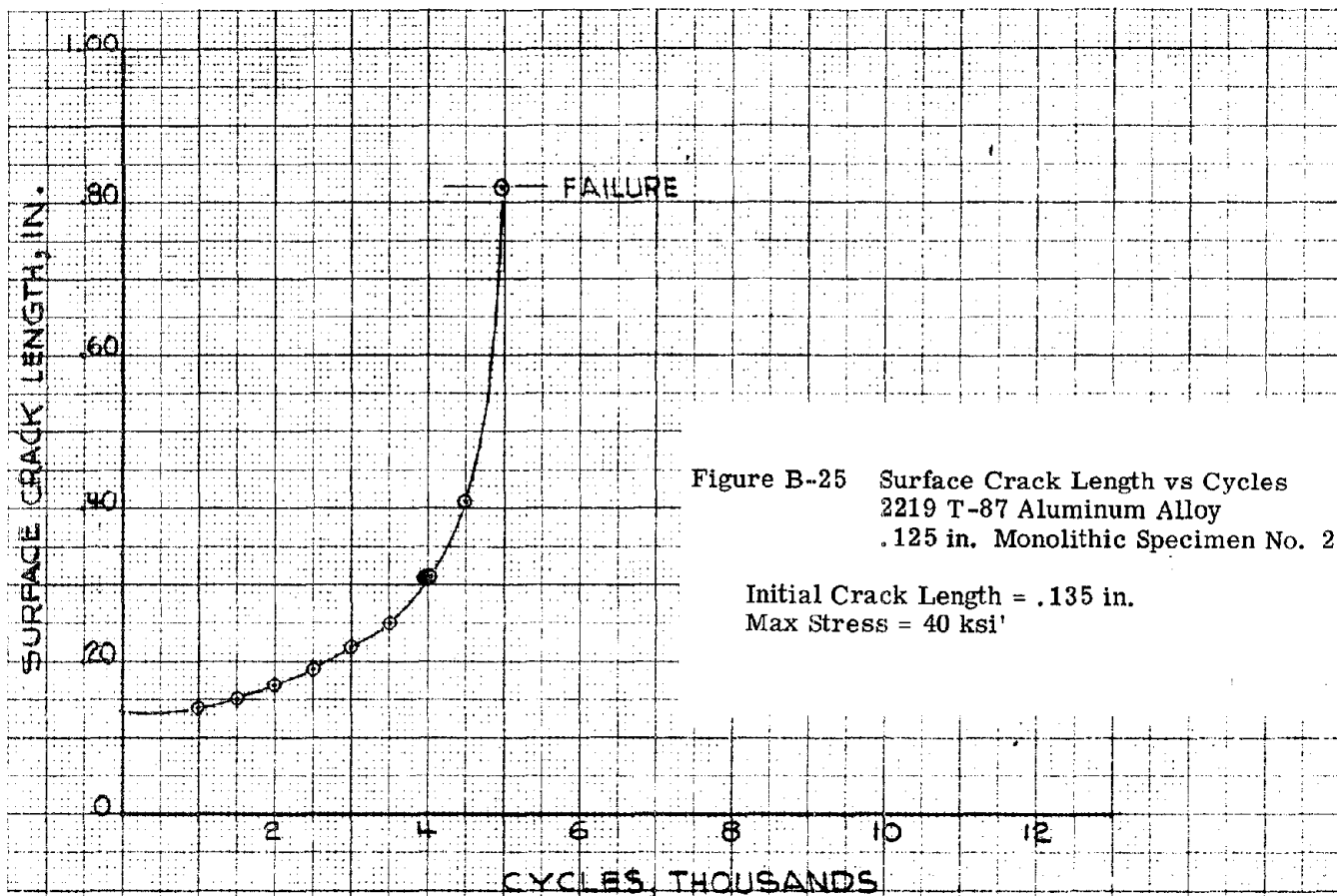


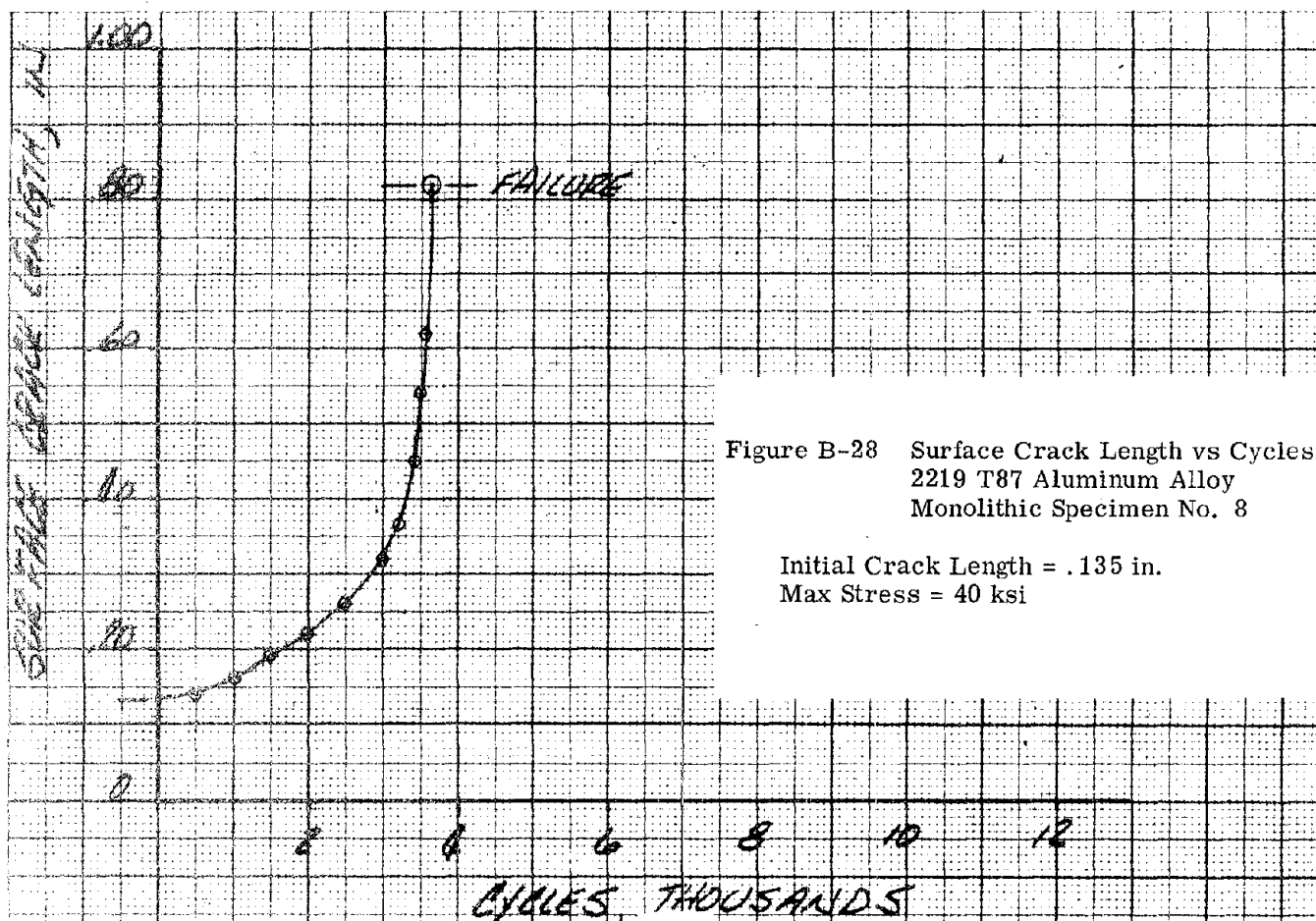
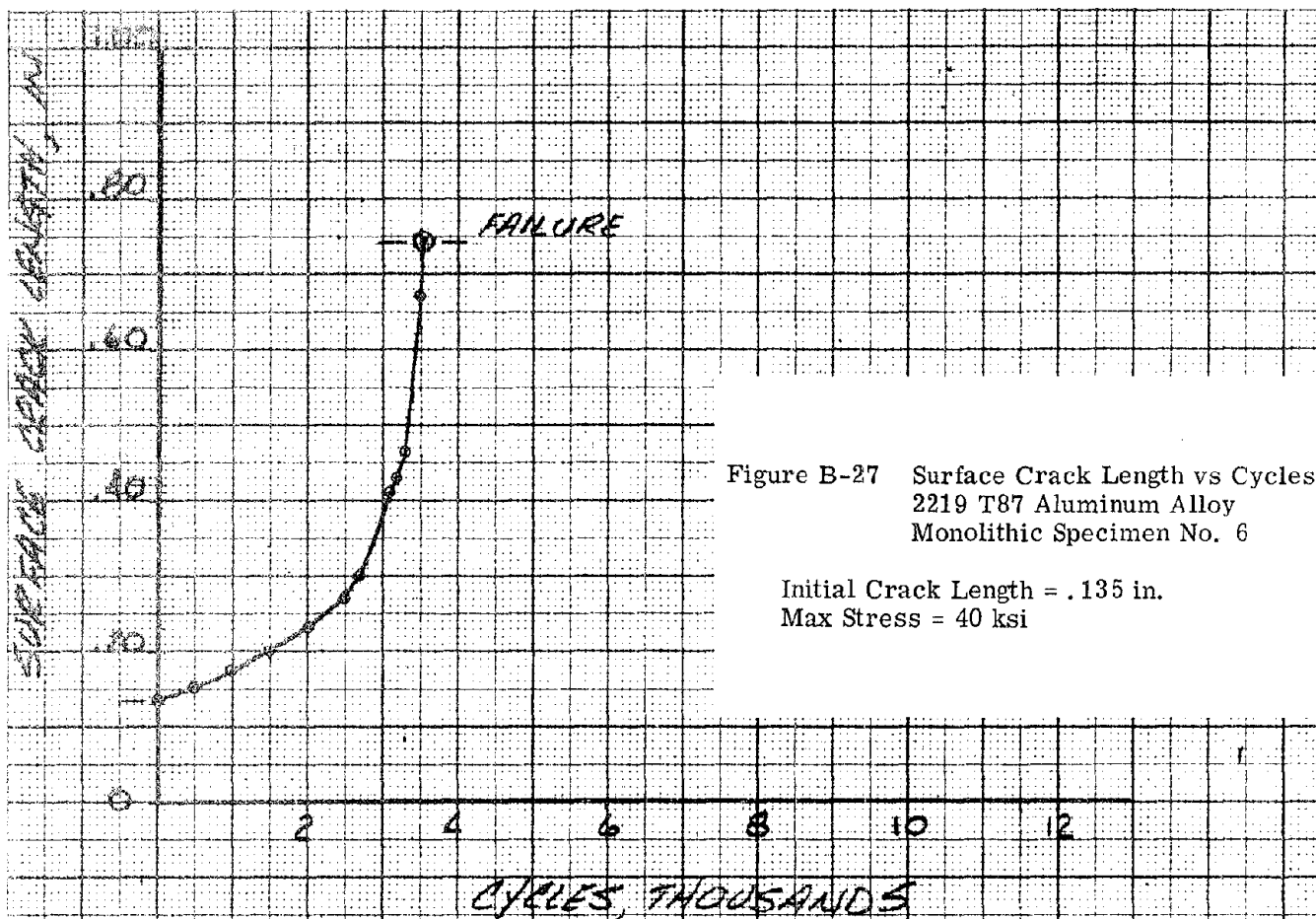


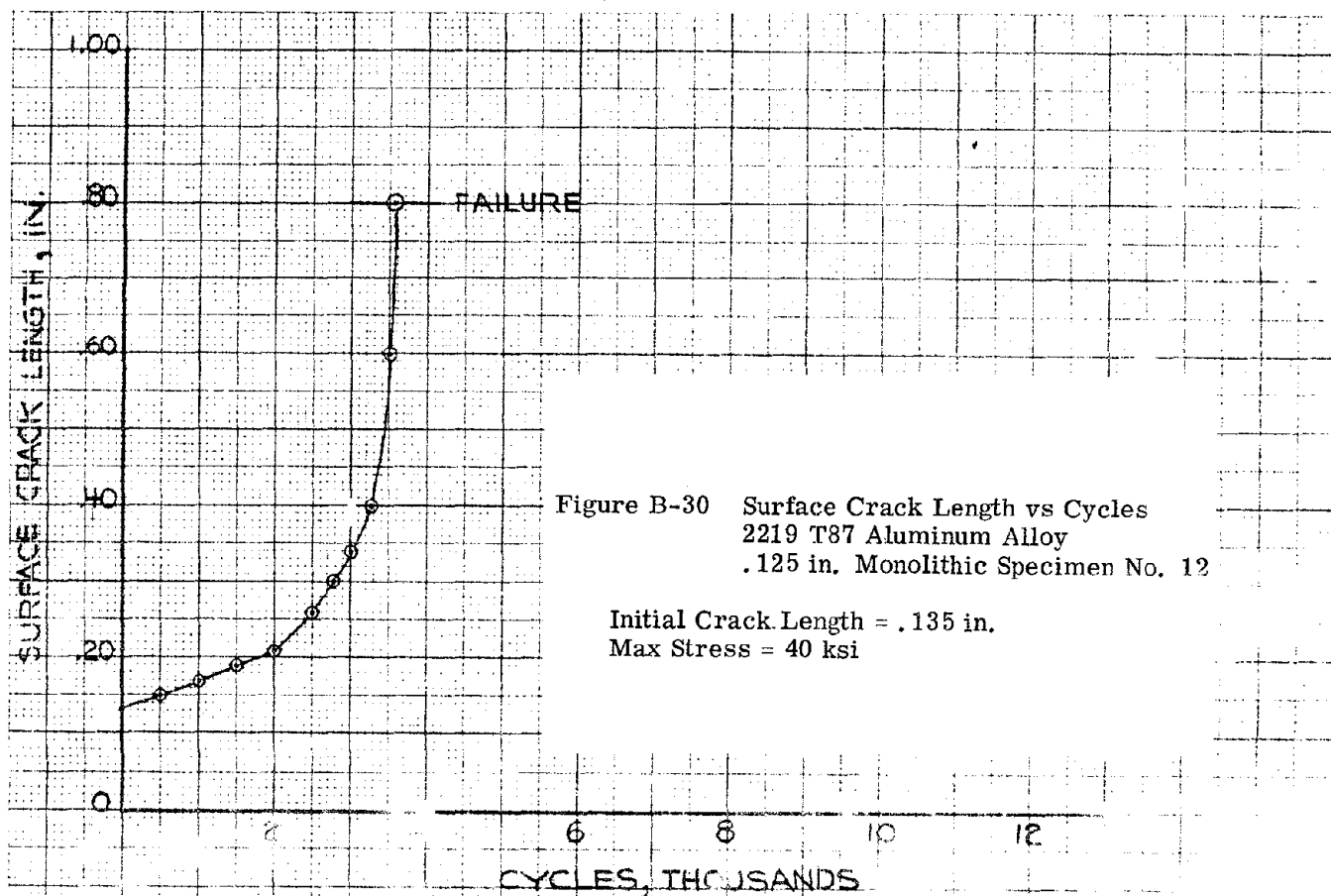
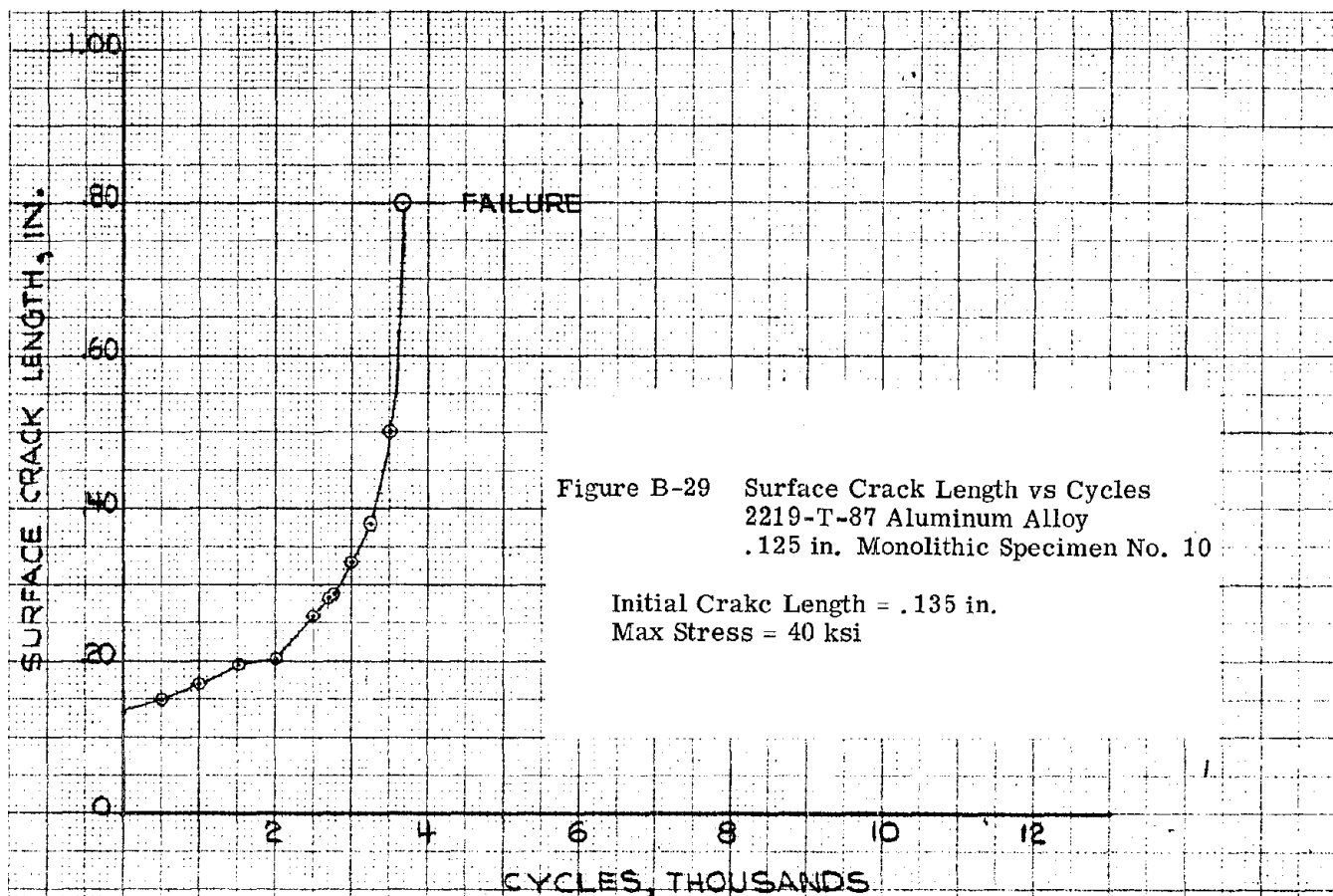


Appendix B (Continued)

PHASE II SPECIMENS

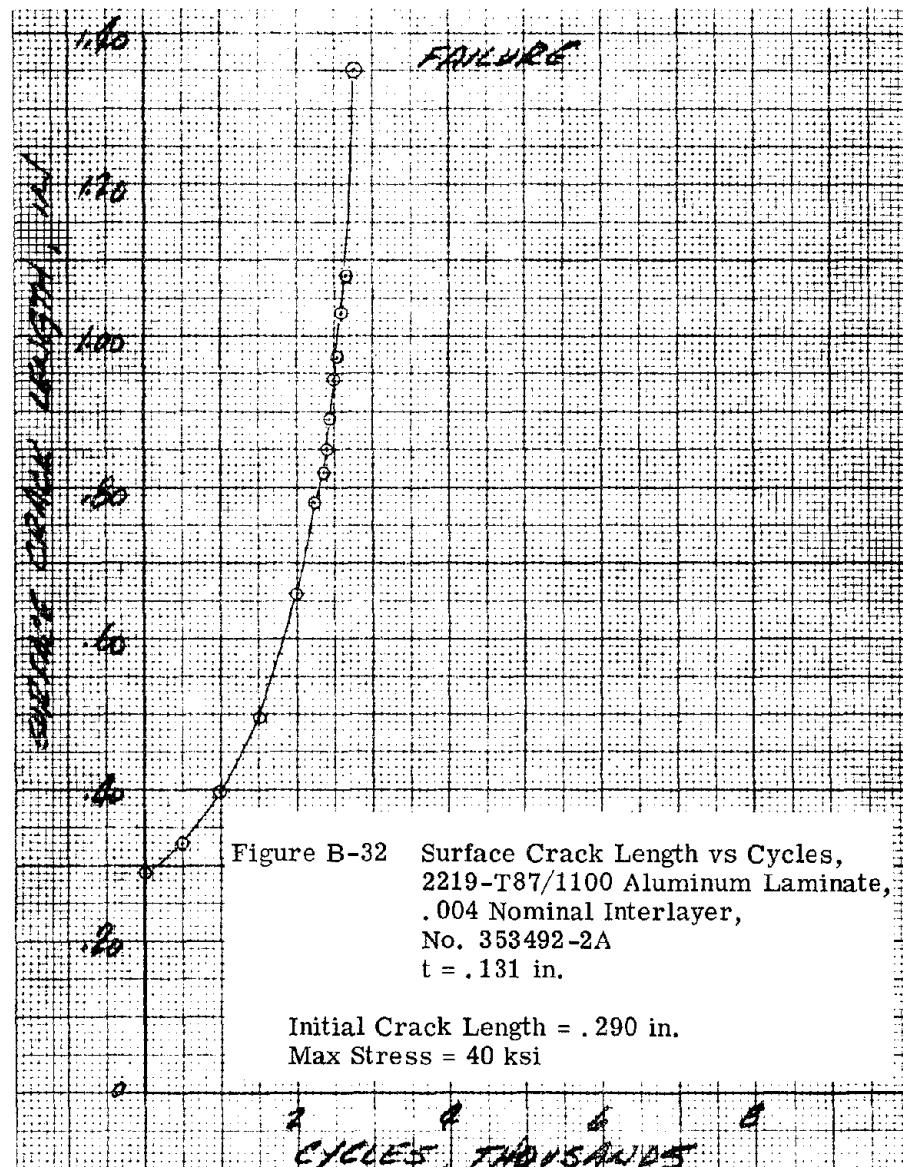
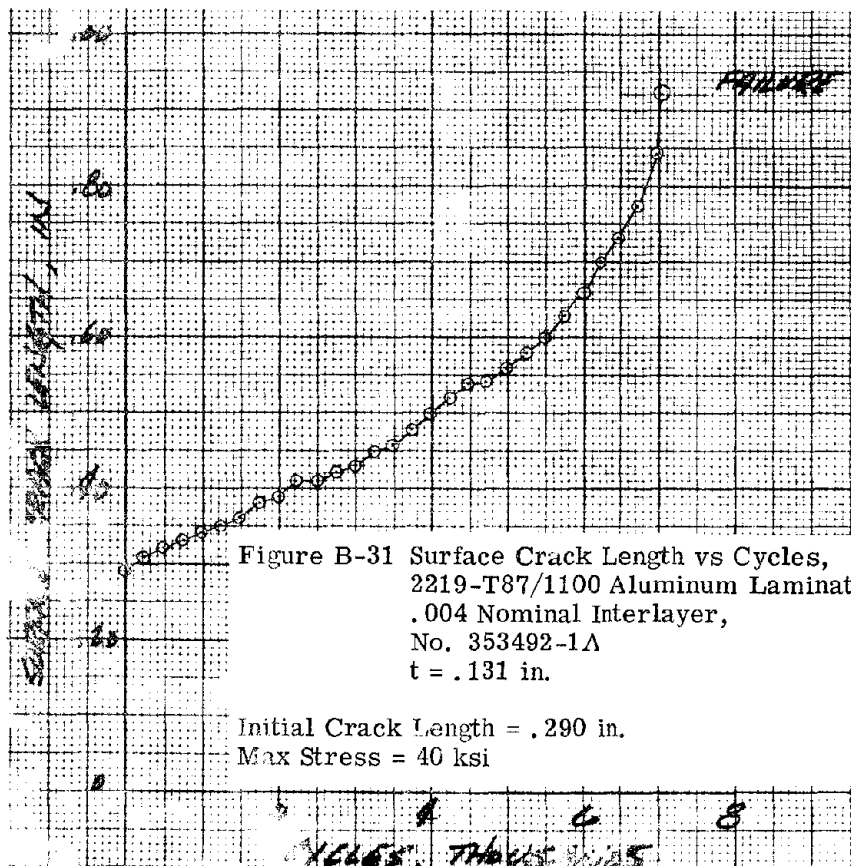


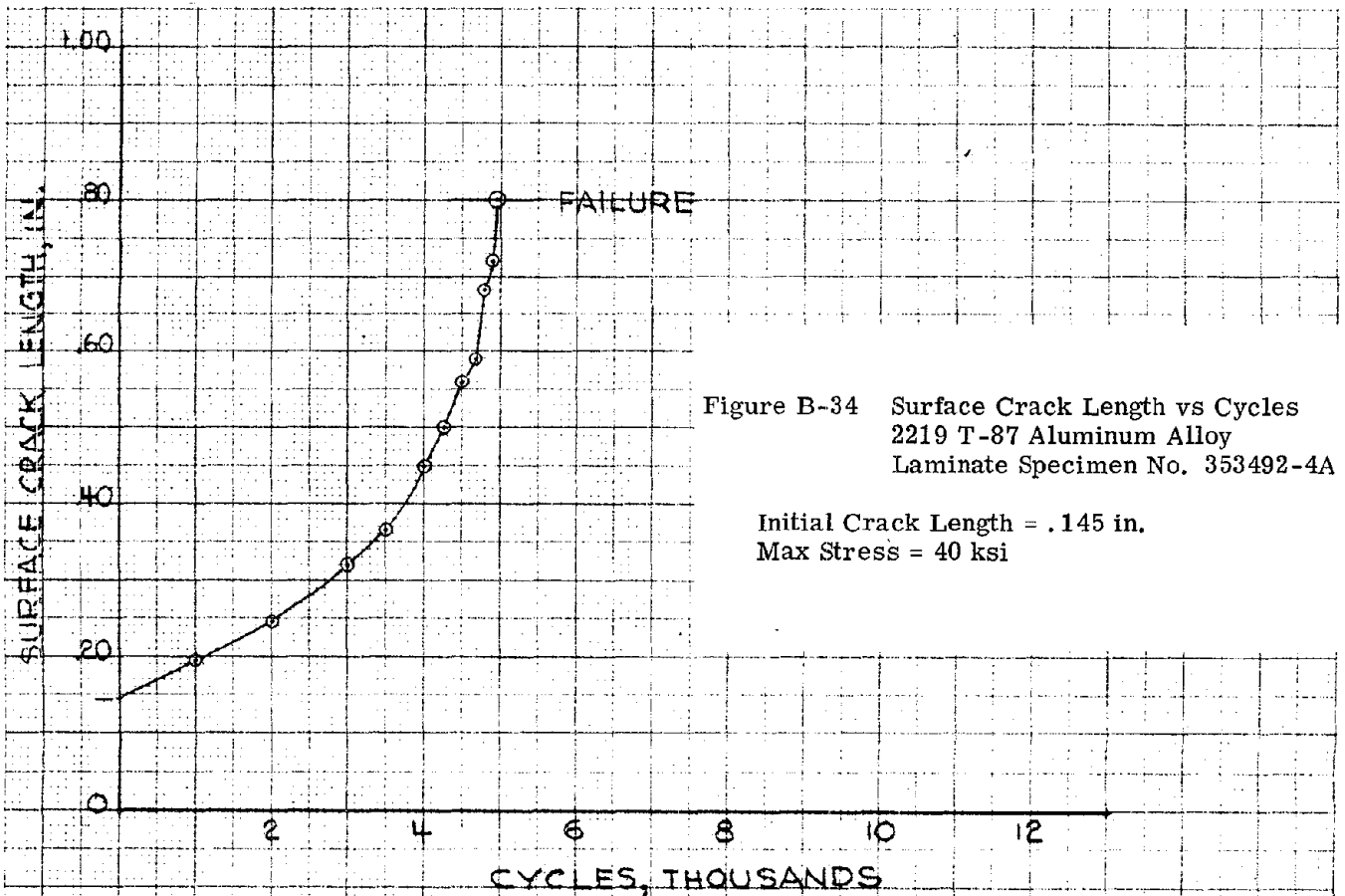
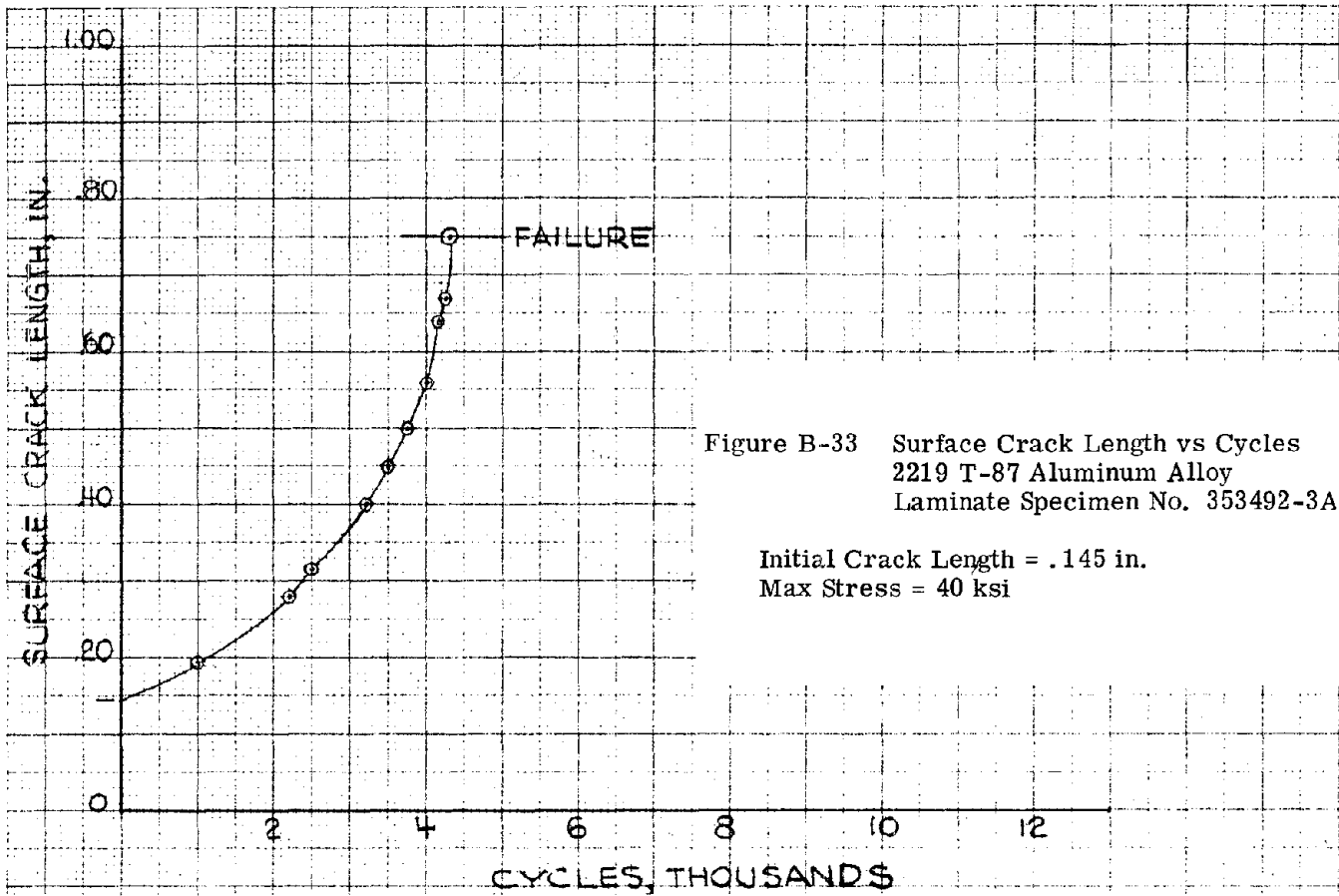


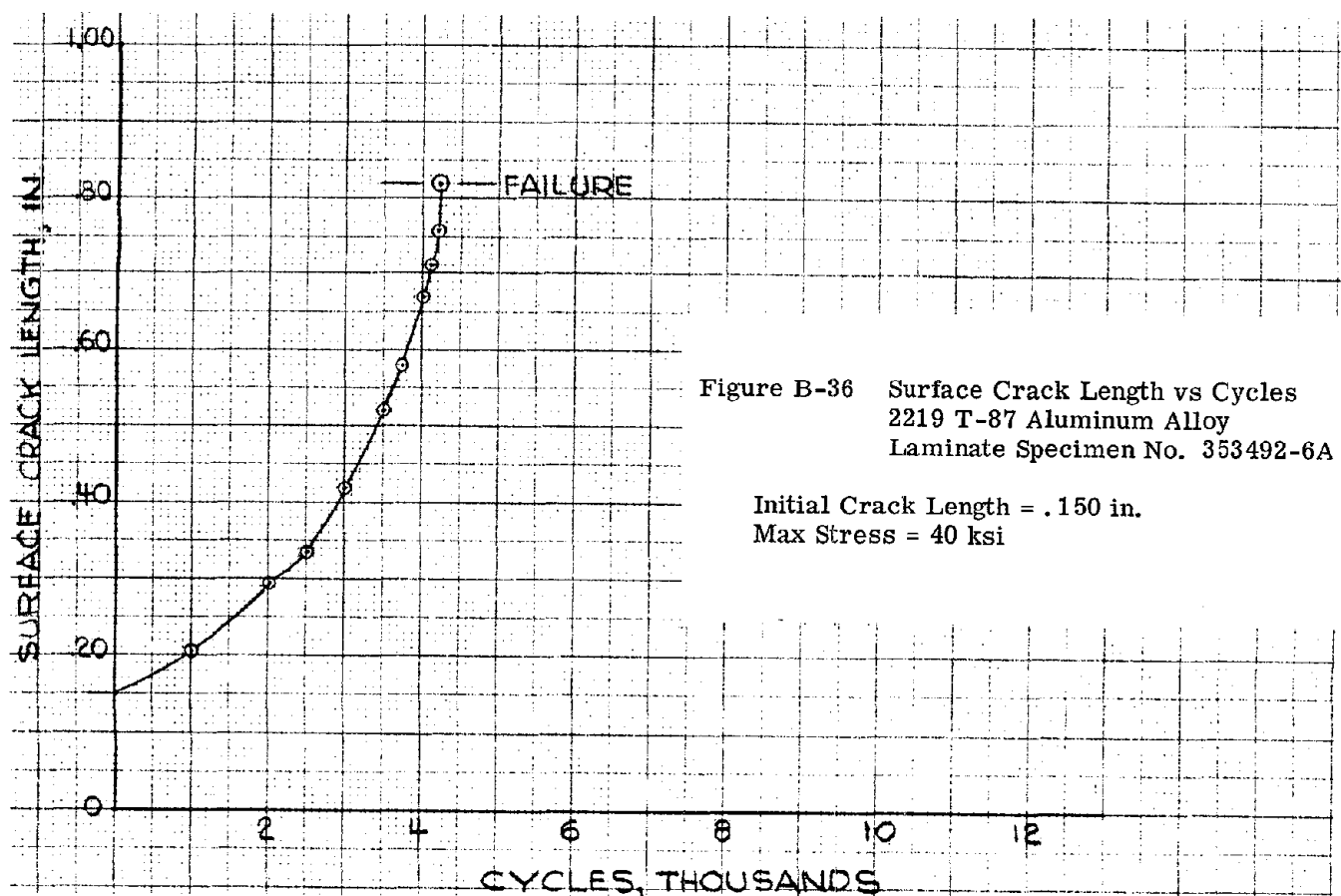
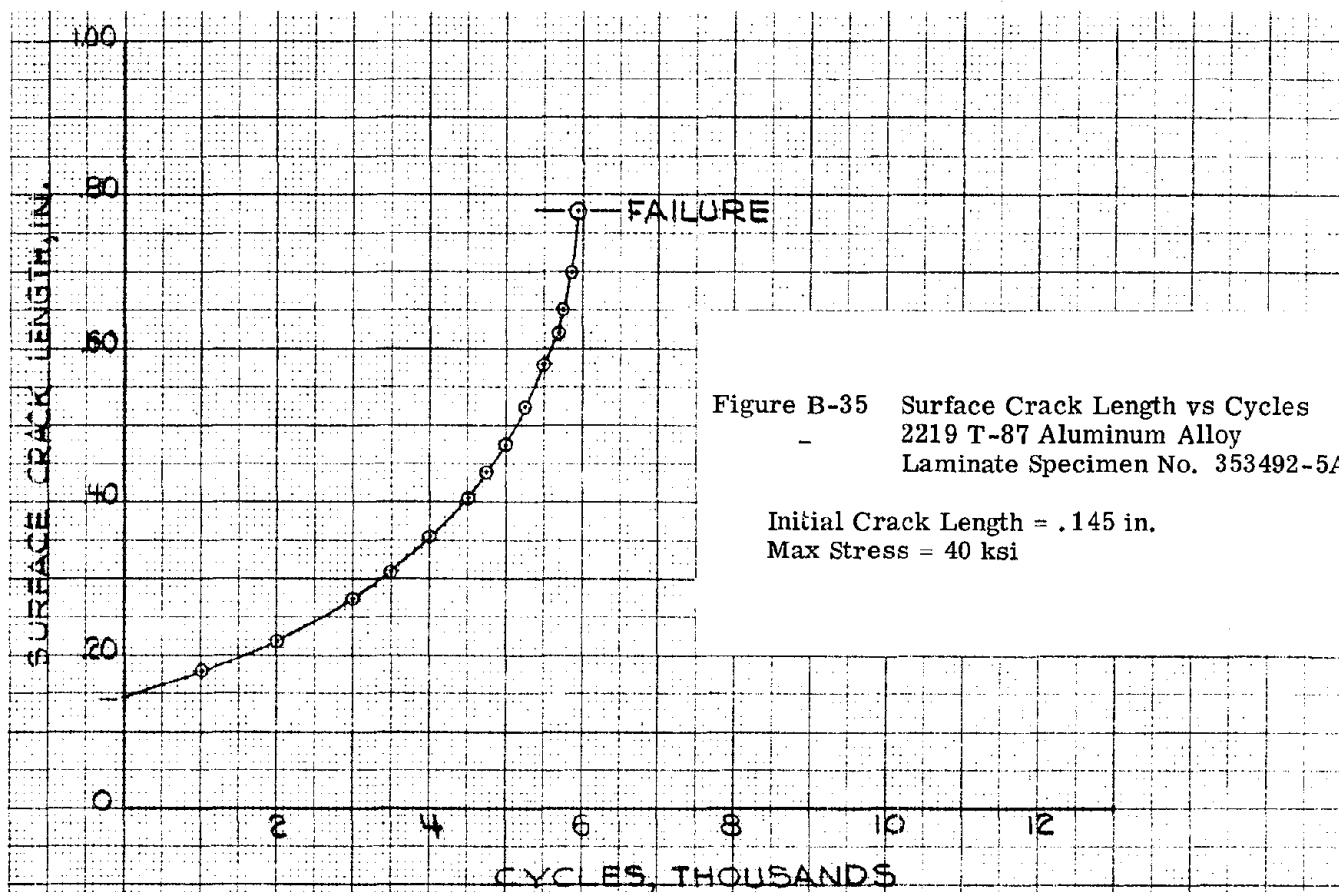


Reproduced from
best available copy.

B-19

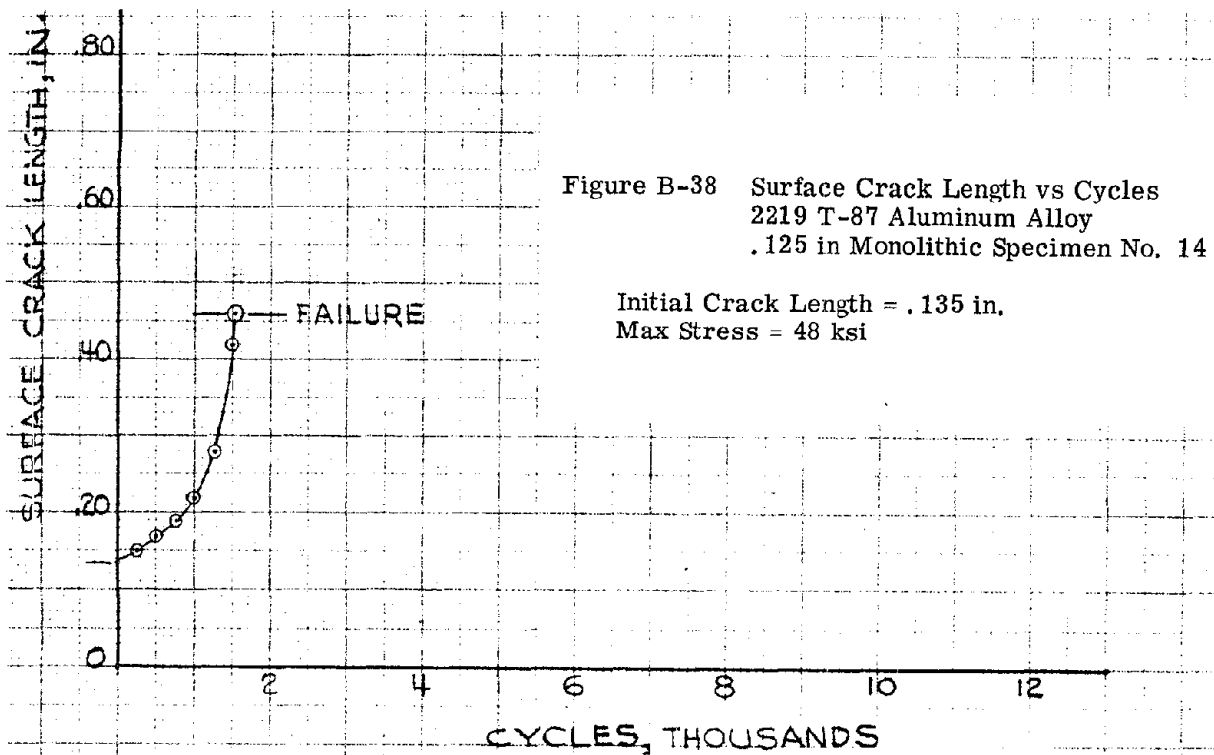
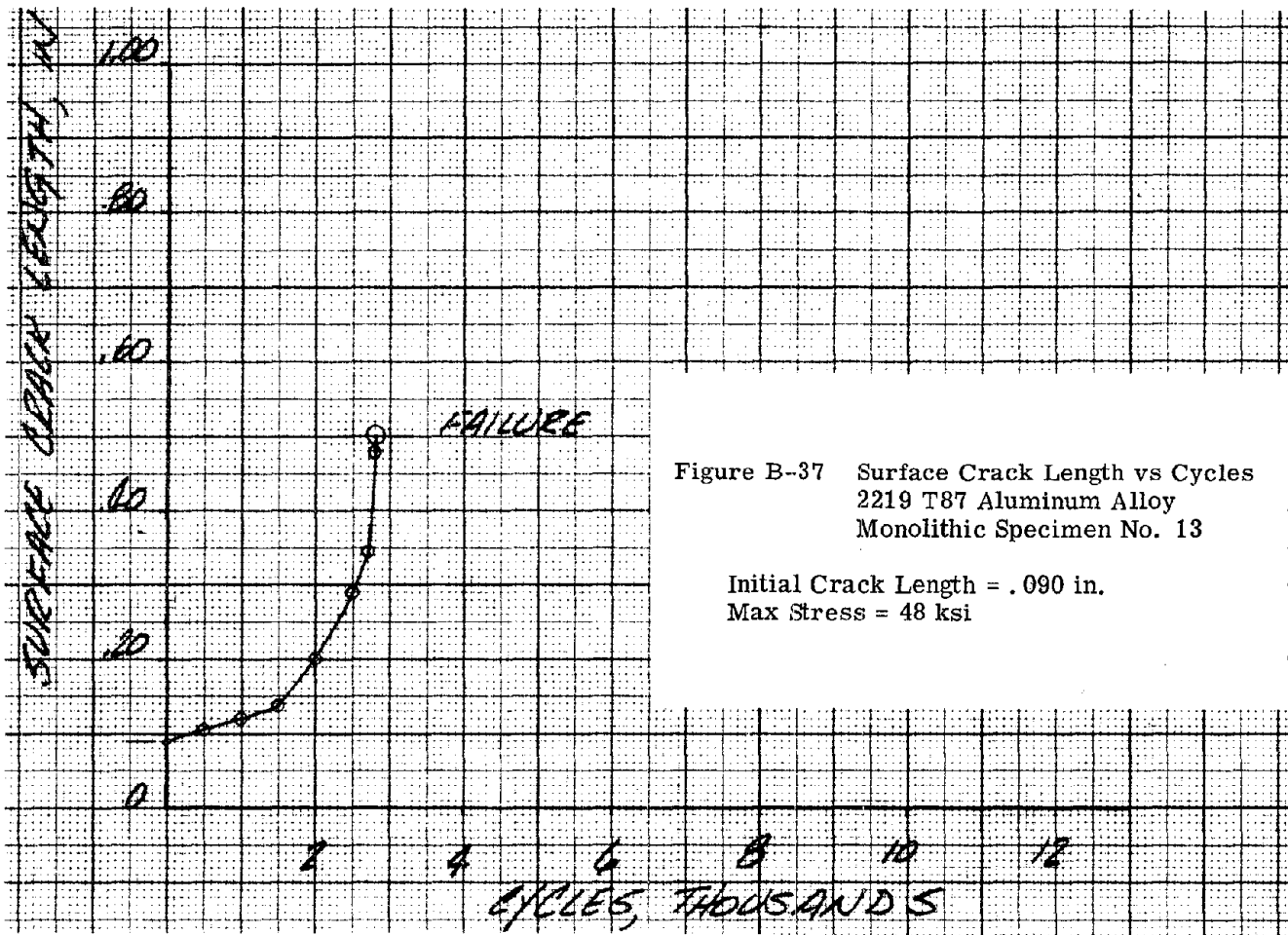


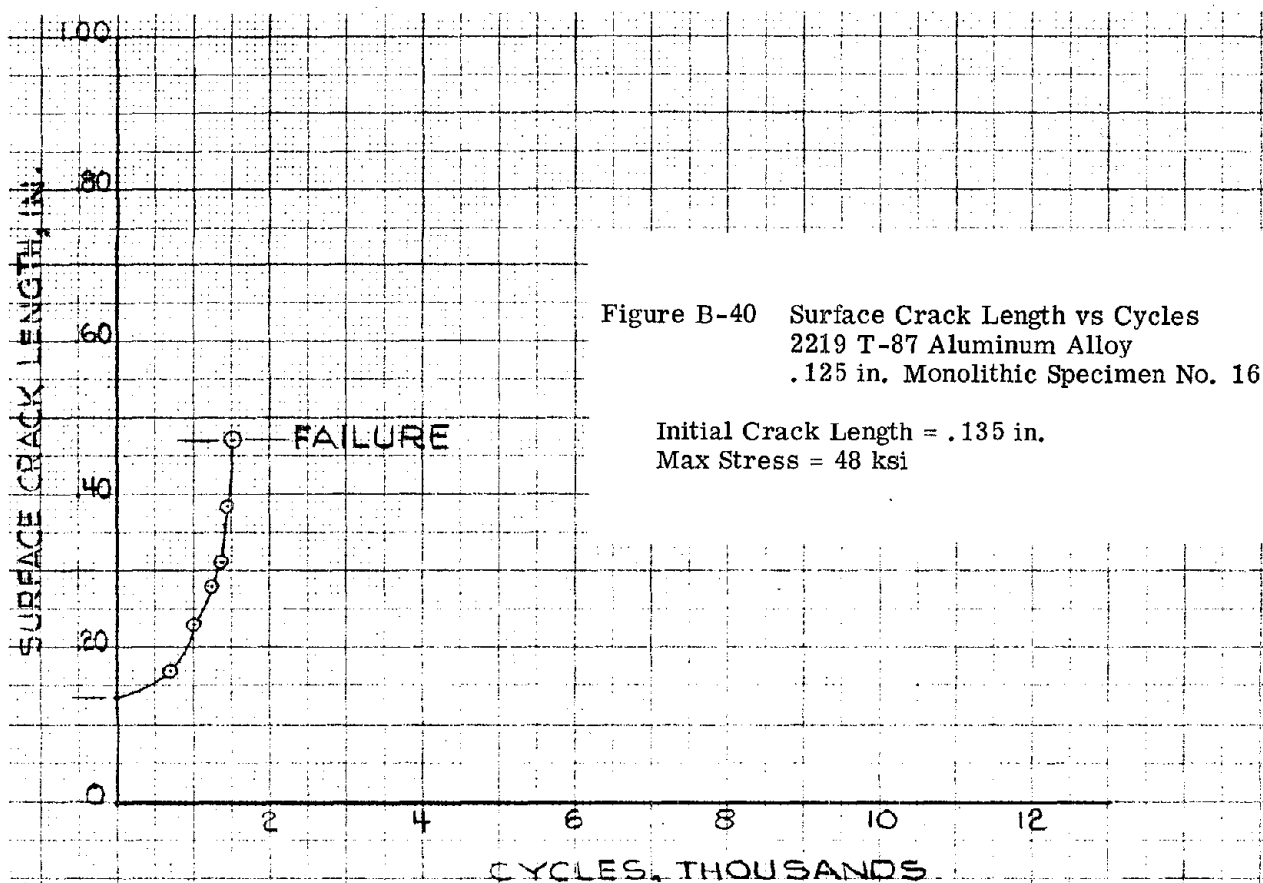
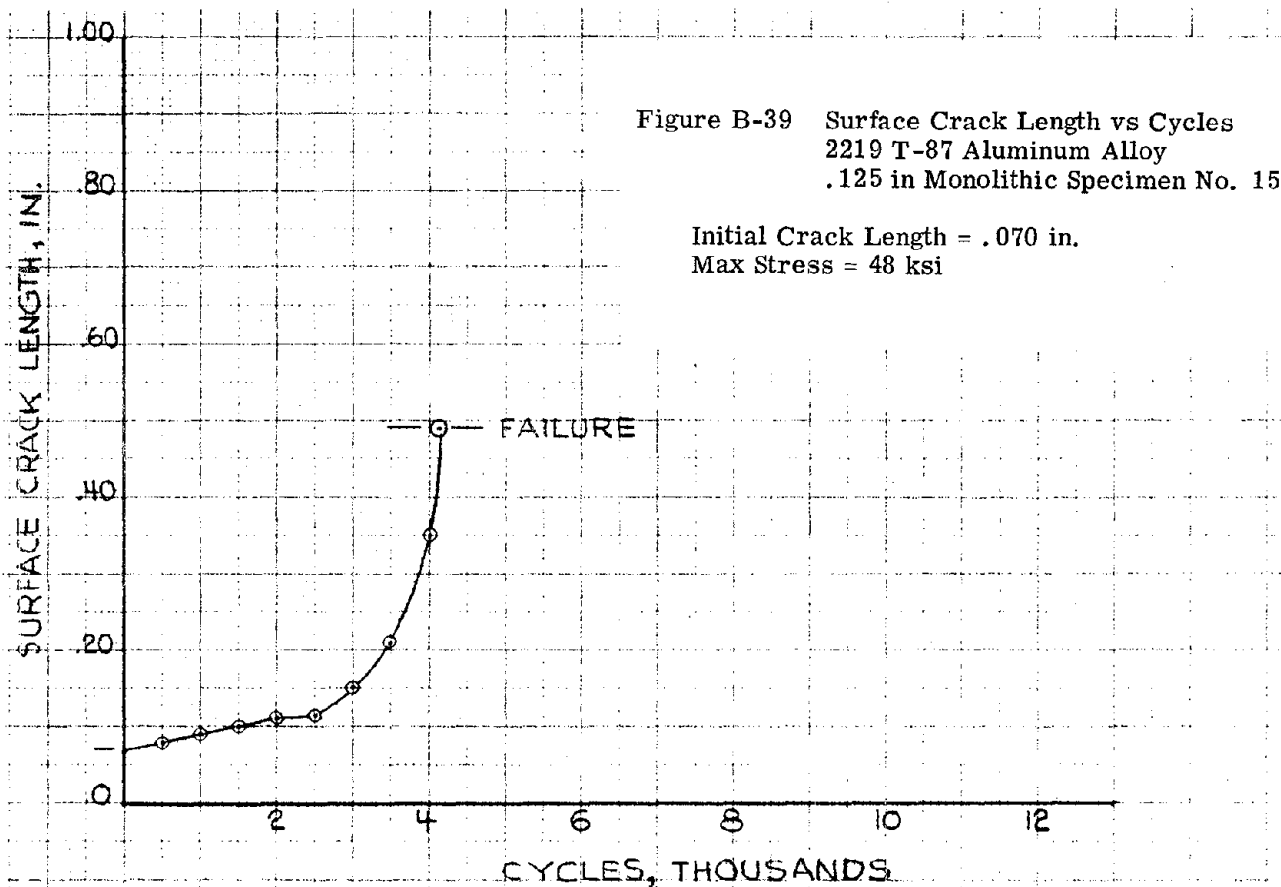




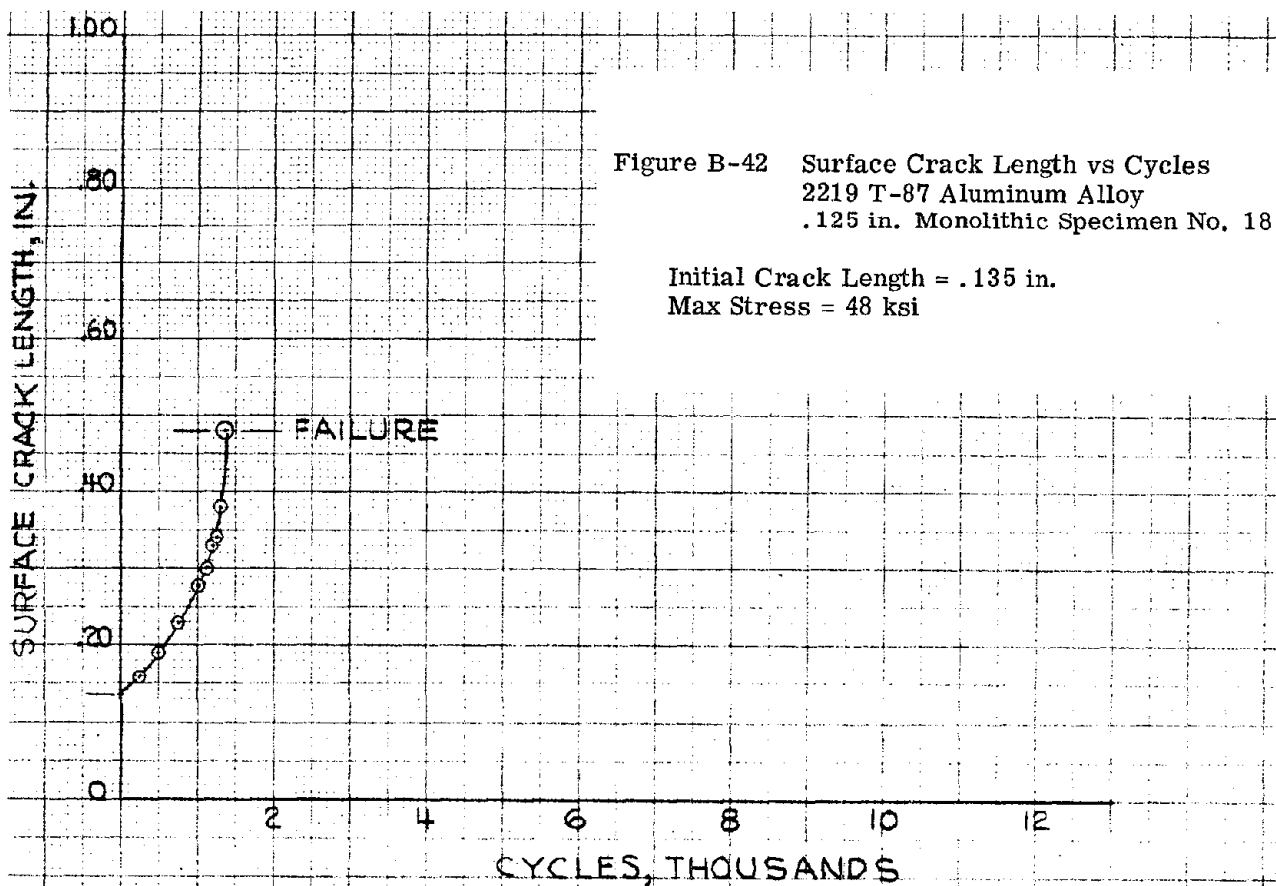
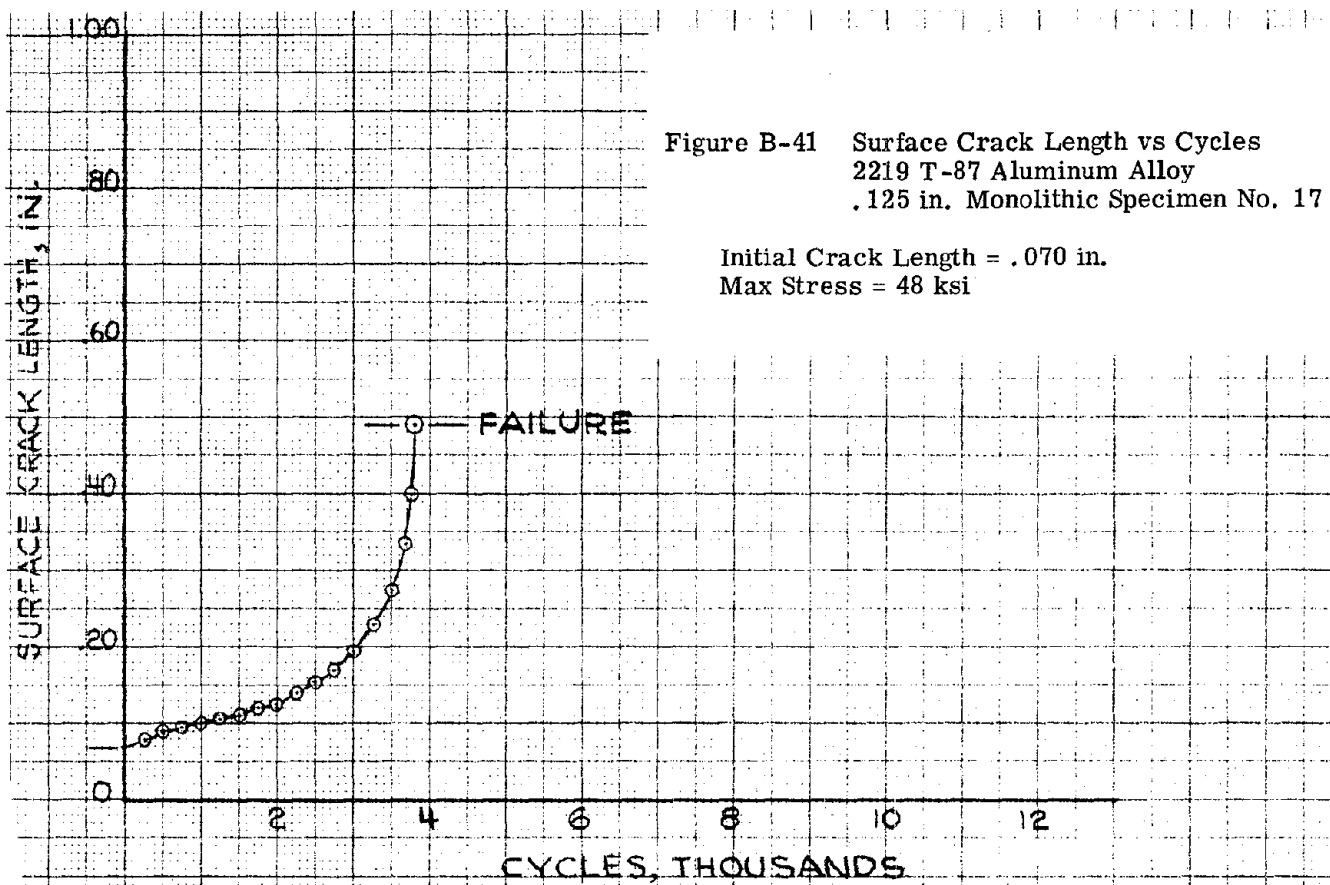
Appendix B (Continued)

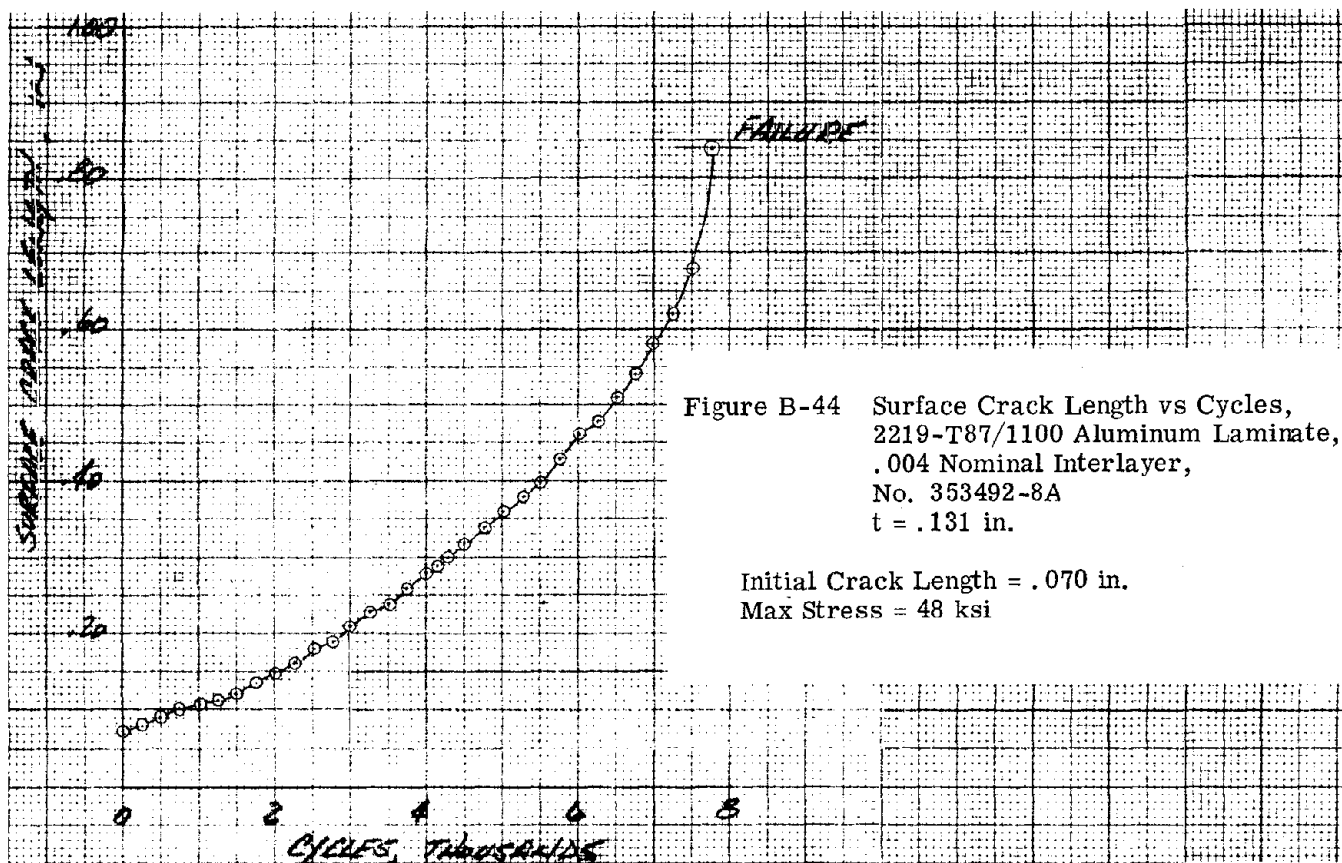
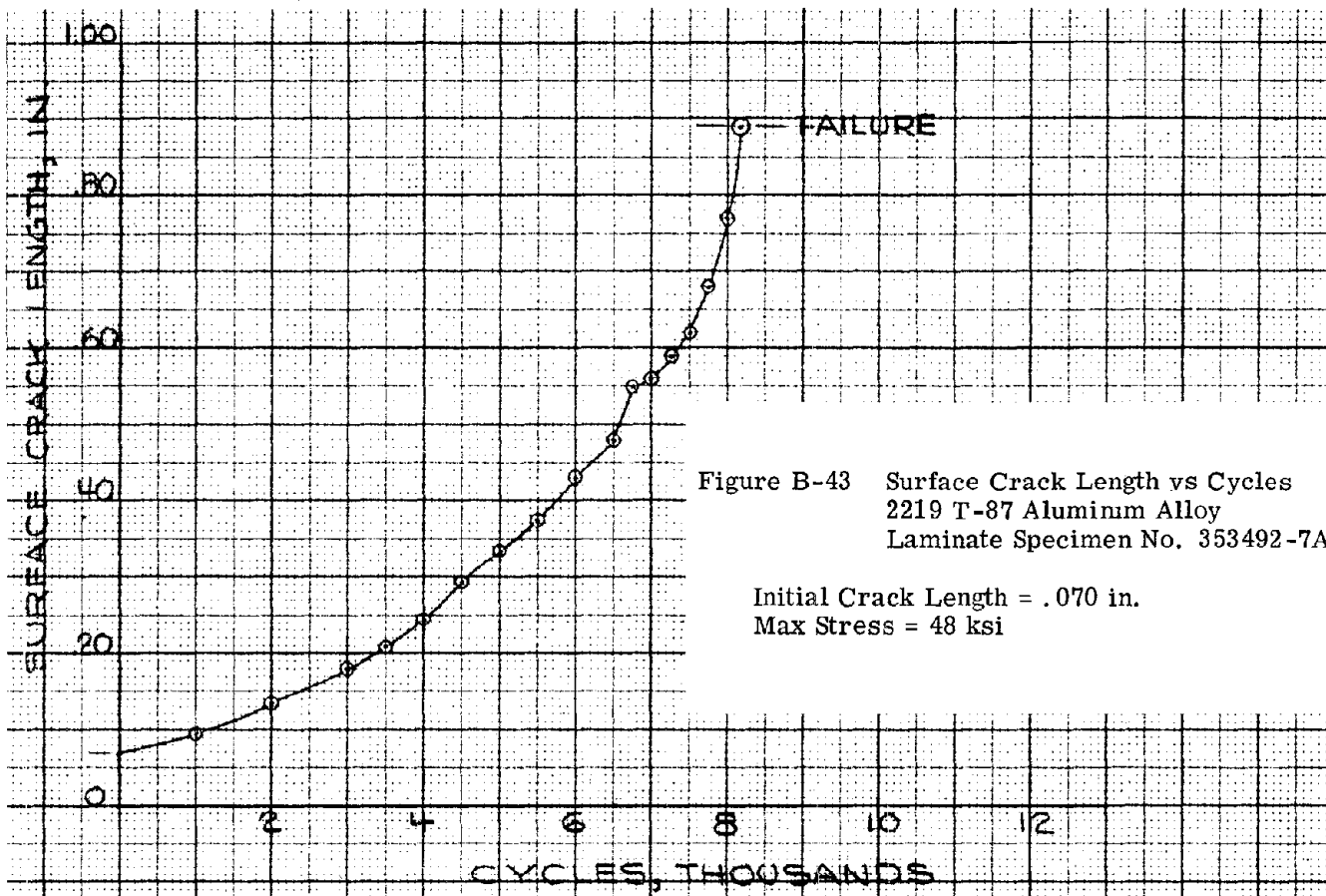
PHASE III SPECIMENS

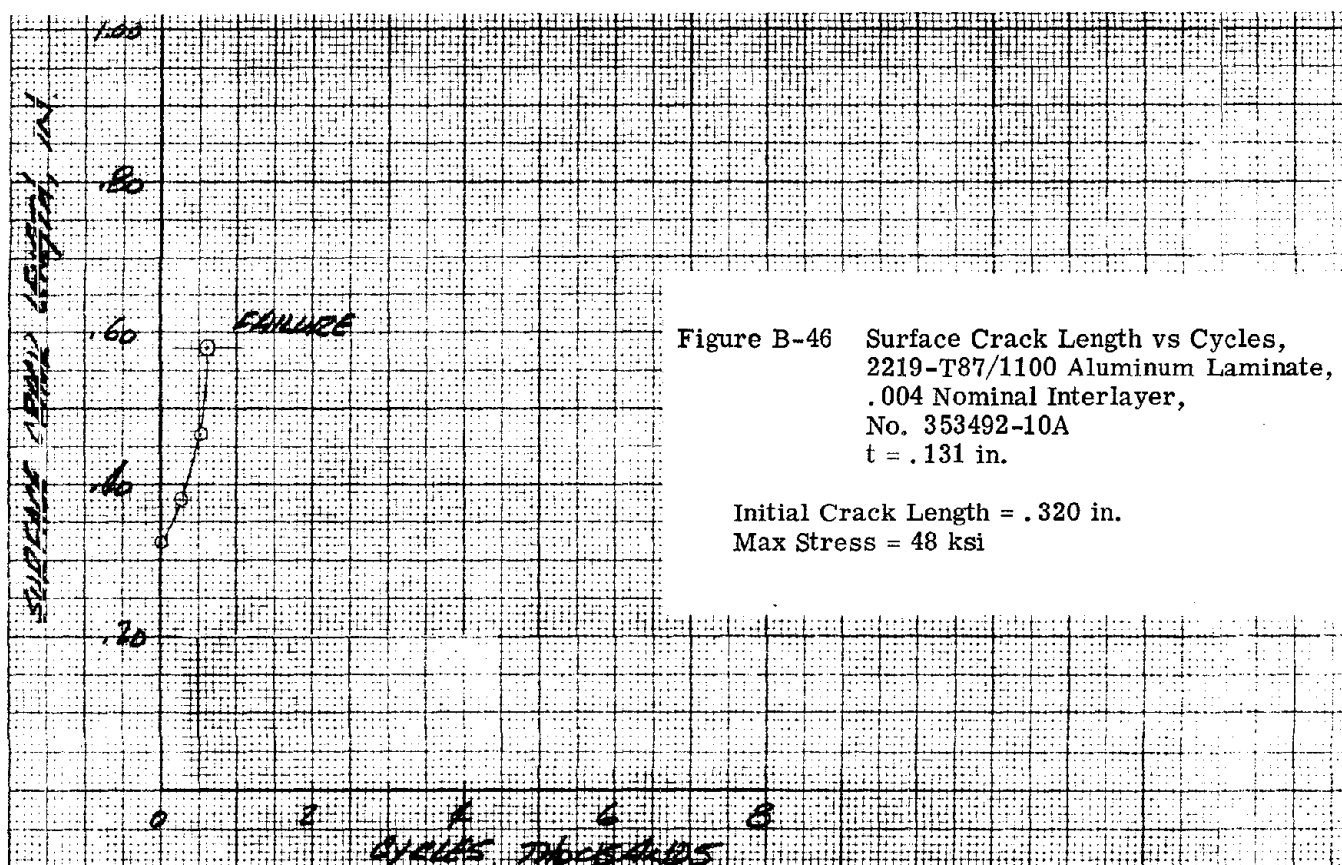
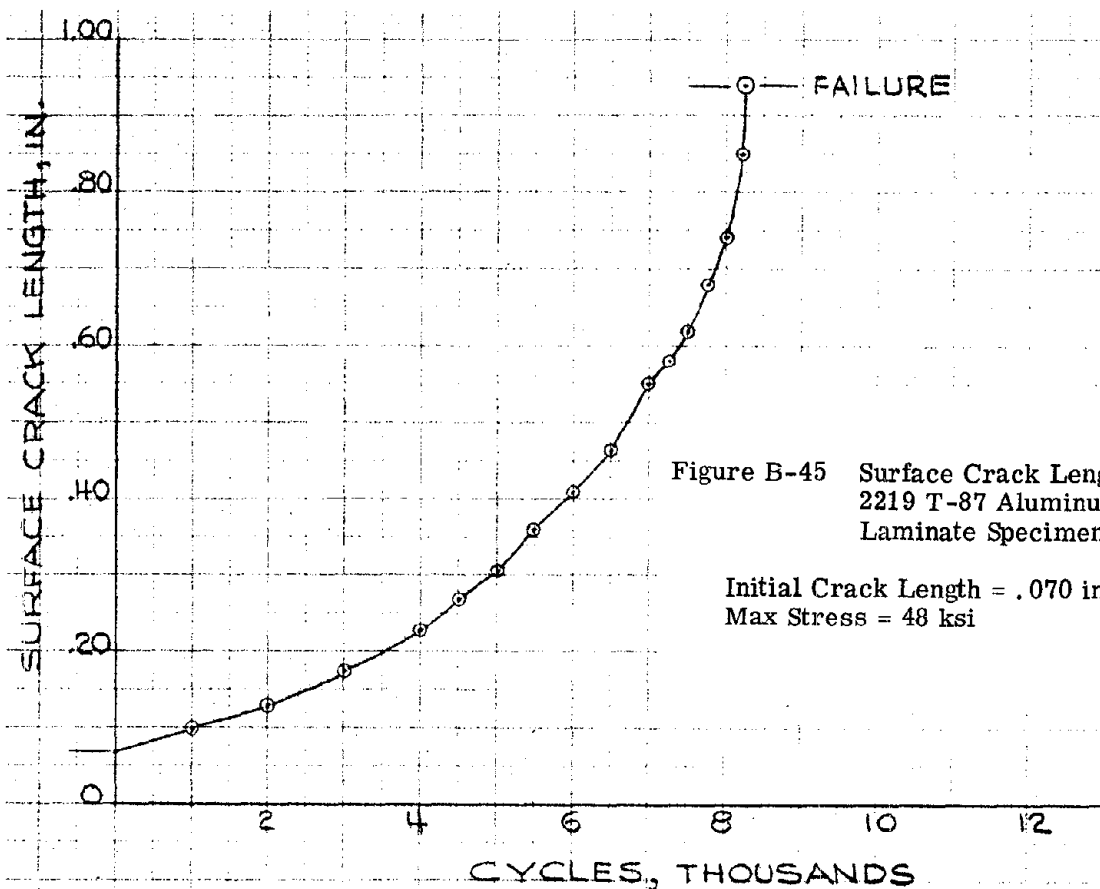


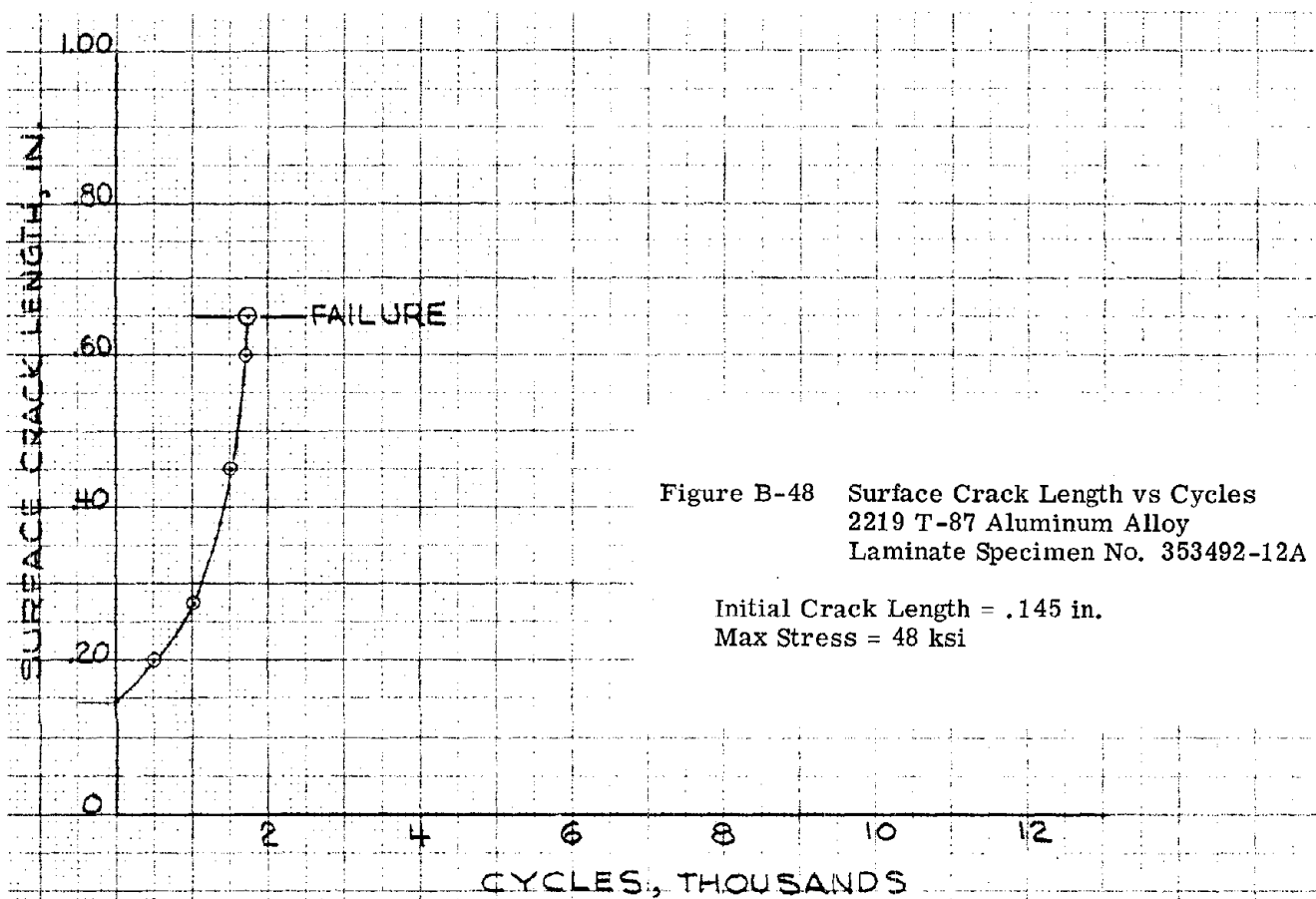
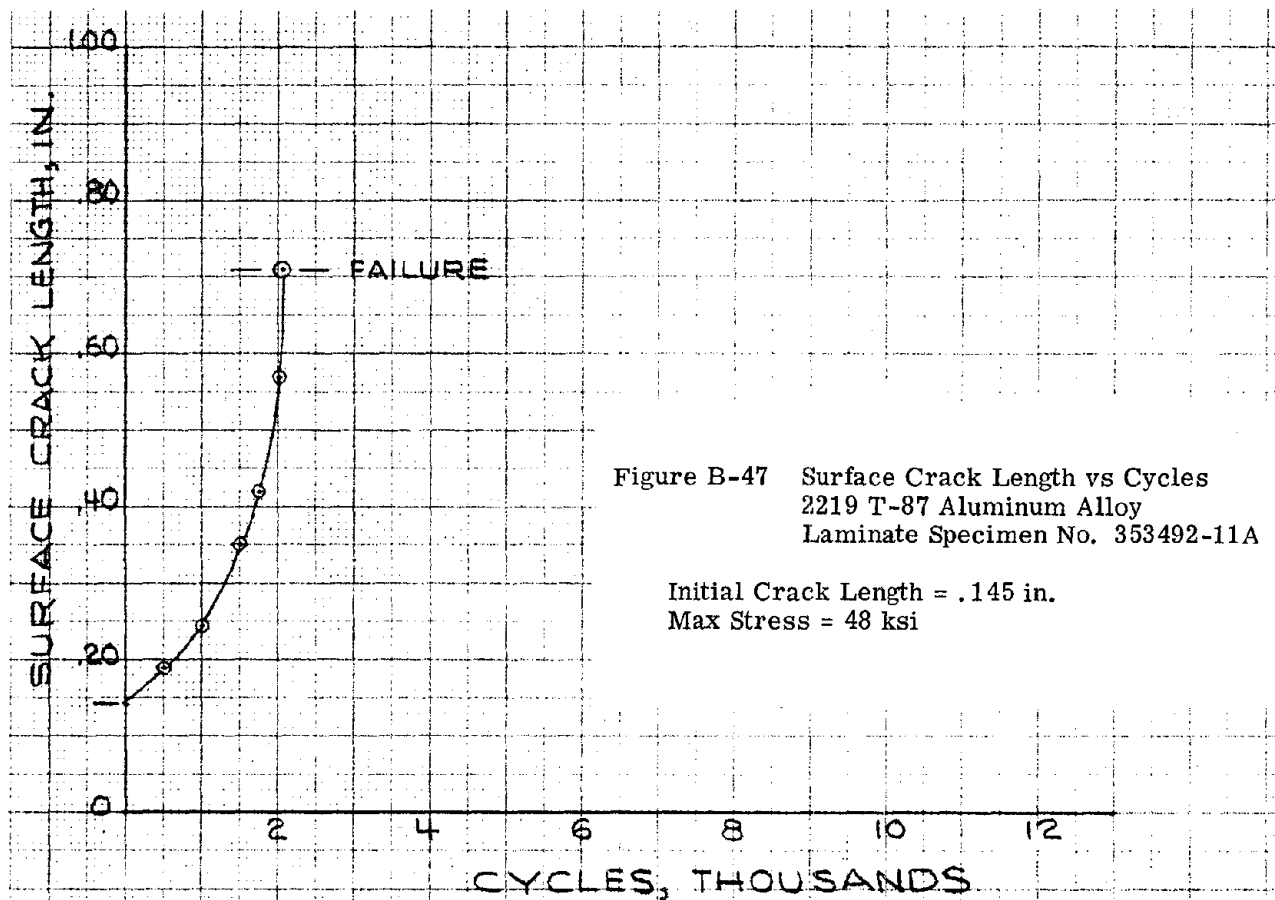


B



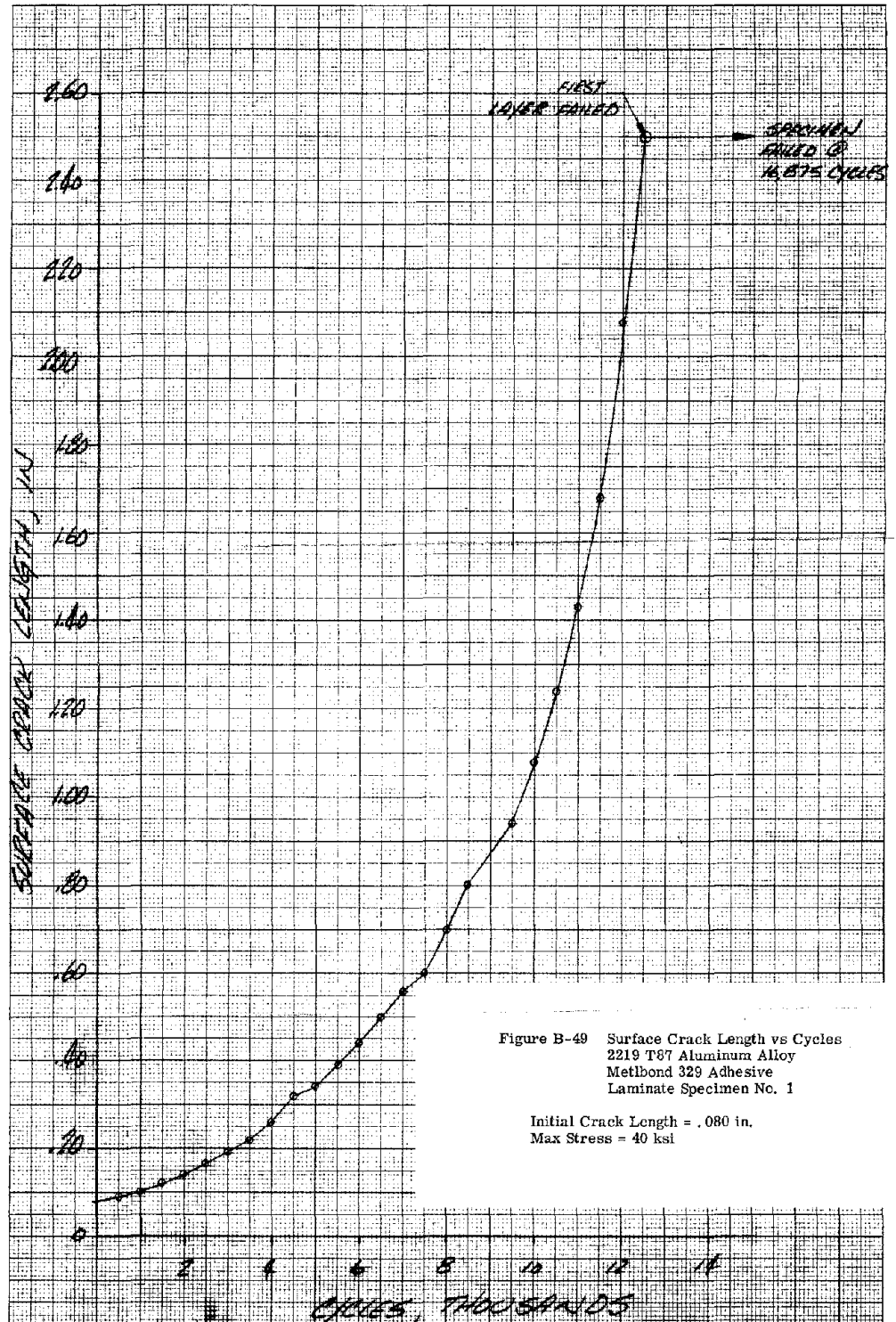






Appendix B (Continued)
ADHESIVE BONDED SPECIMENS

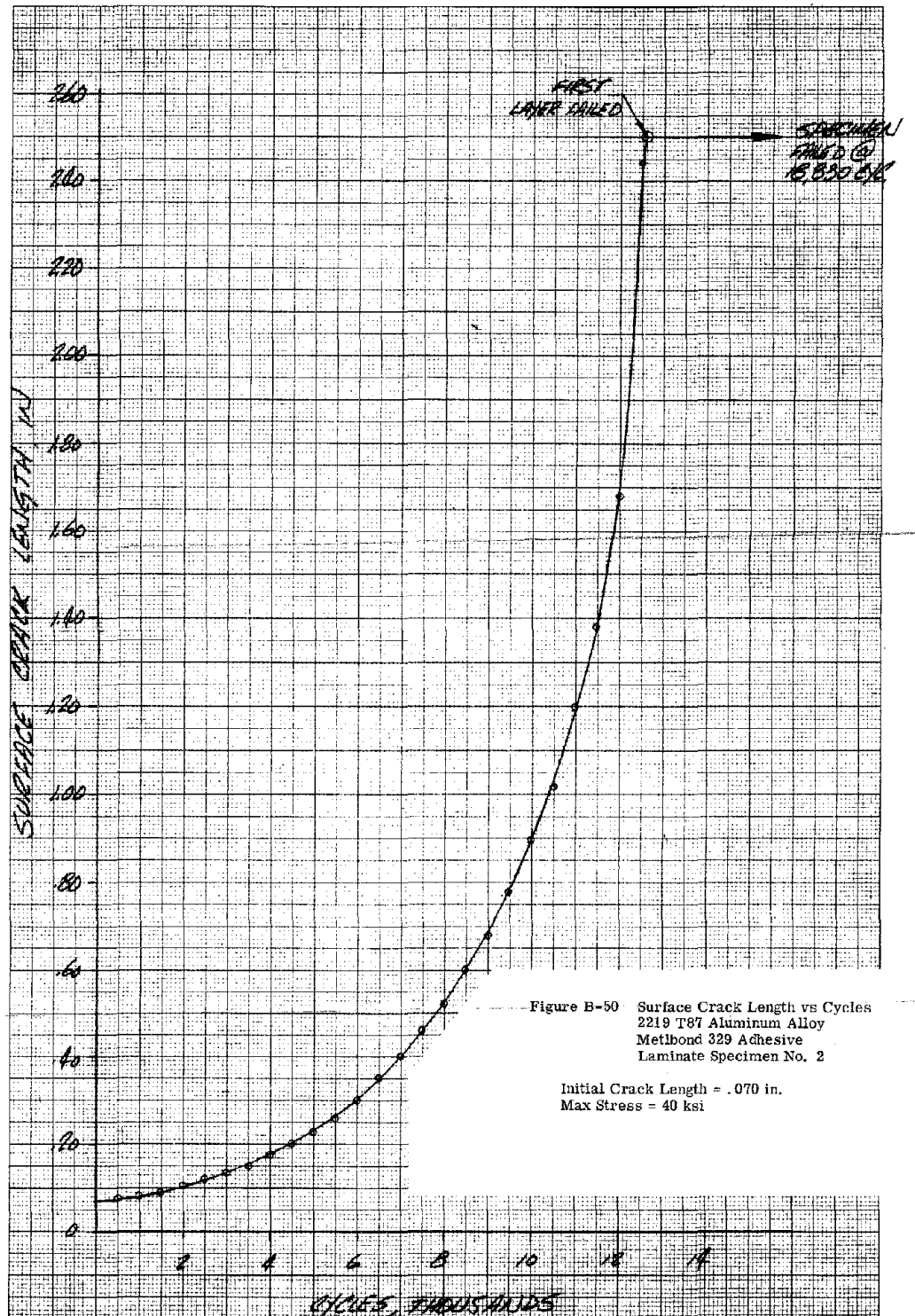
FOLODOUT FRAME 1



B-30

FOLODOUT FRAME 2

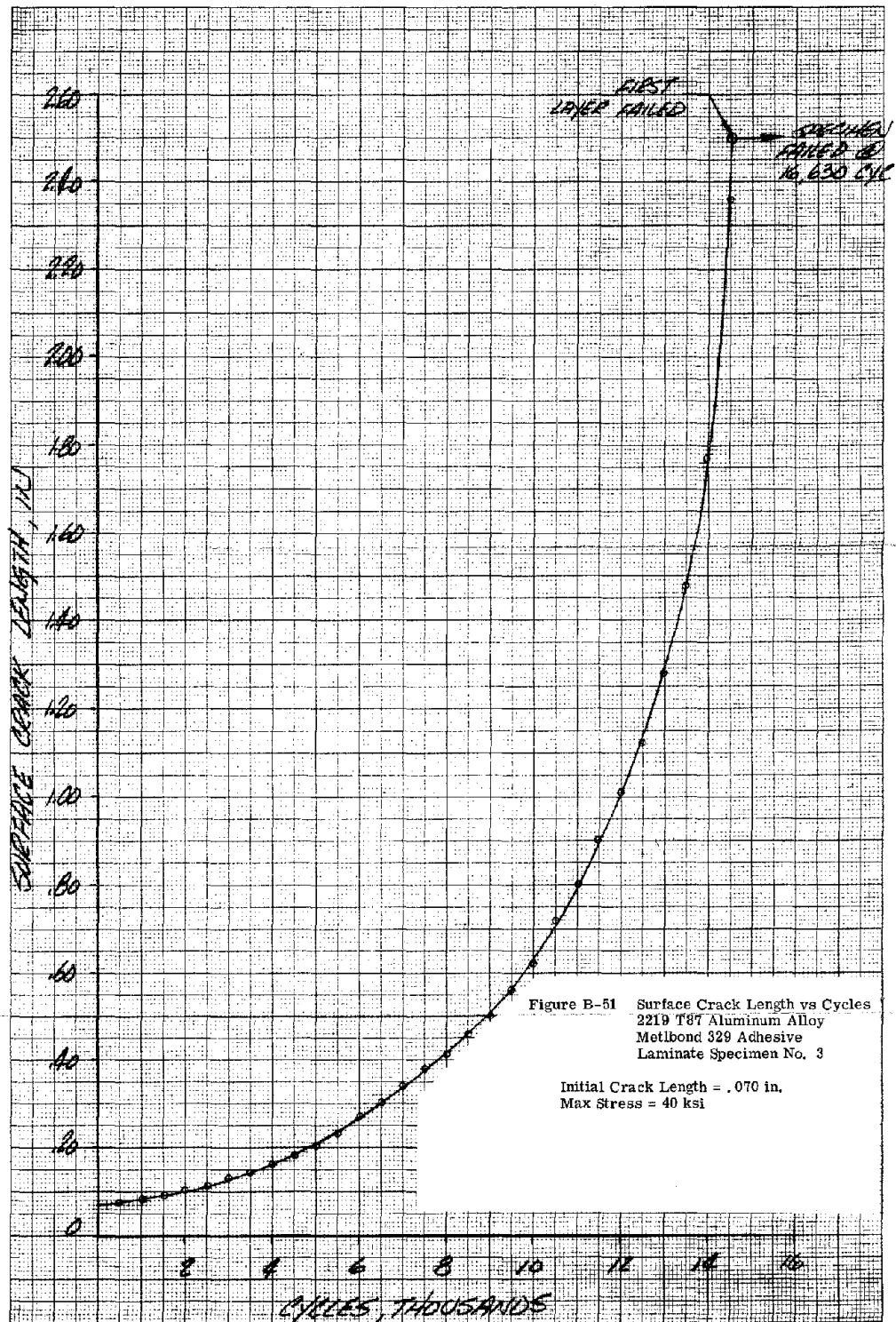
FOLDOUT FRAME /



B-31

FOLDOUT FRAME 2

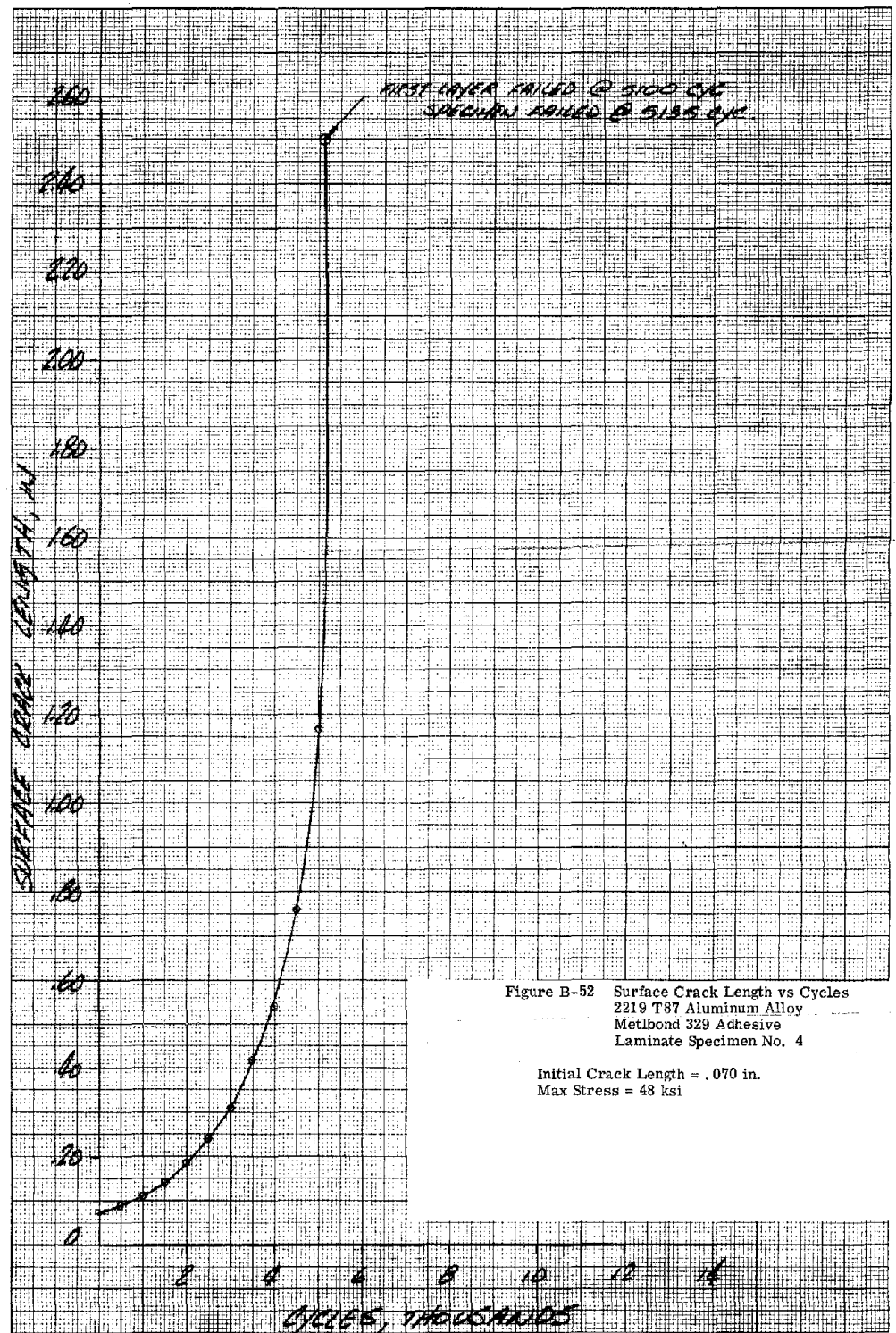
FOLOOUT FRAME 1



B-32

FOLOOUT FRAME 2

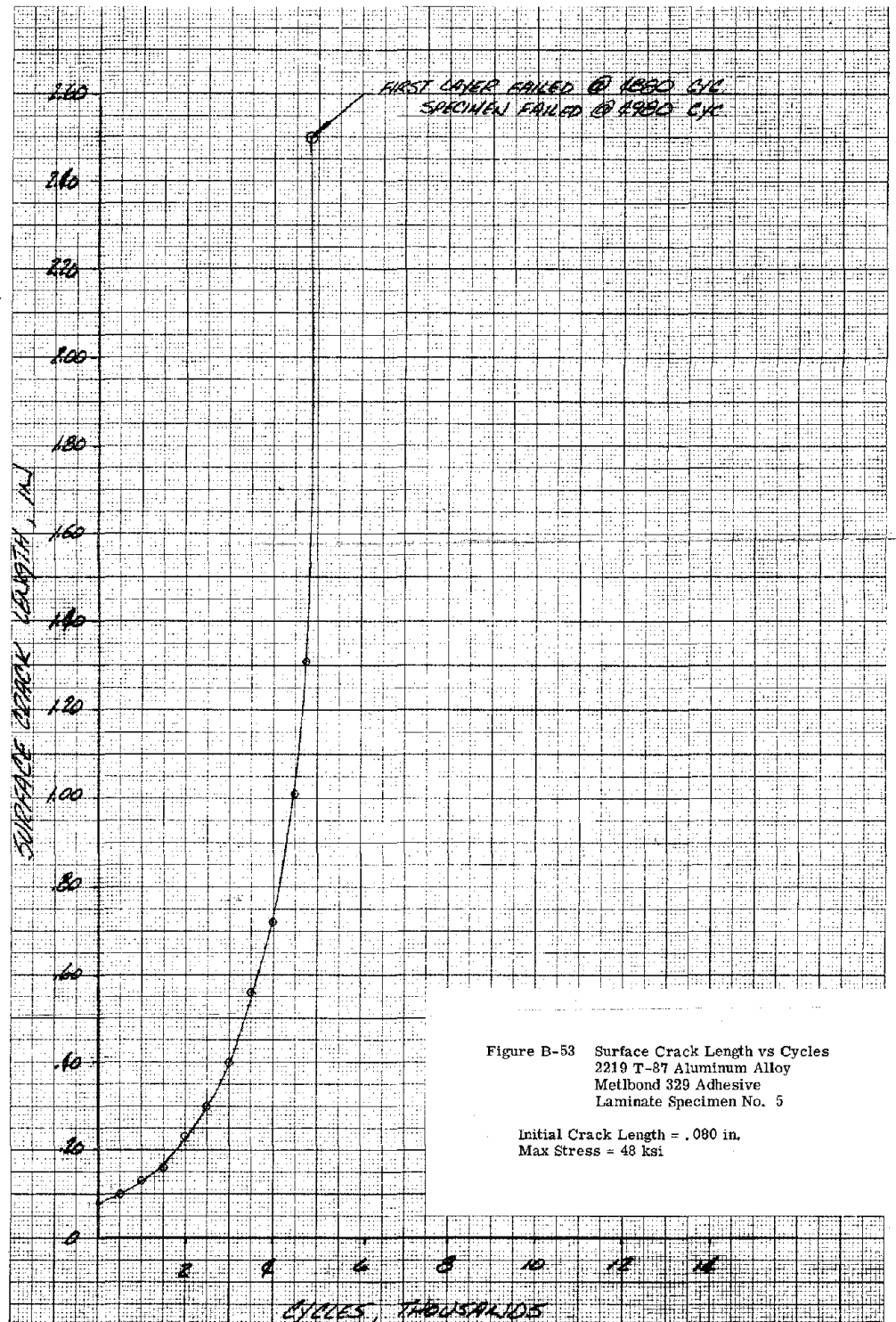
POLOUT FRAME /



B-33

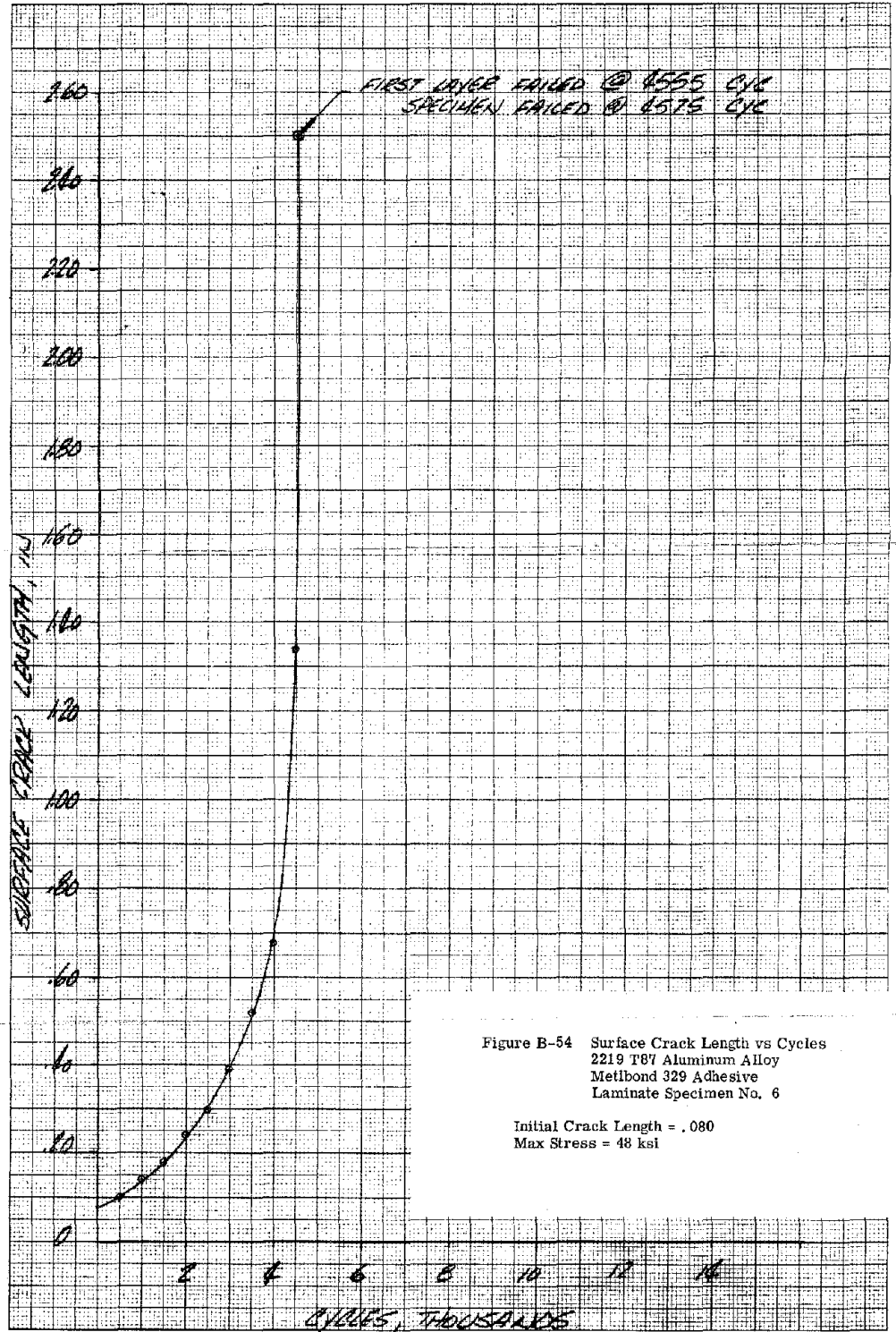
POLOUT FRAME /

FOLOOUT FRAM /



FOLOOUT FRAM

FOLDOUT FRAME



B-35

FOLDOUT FRAME